

CRC Report No. E-88-2

**TRANSPORTATION FUEL
LIFE CYCLE ANALYSIS**
**A Review of Indirect Land Use Change
and Agricultural N₂O Emissions**

January, 2012



COORDINATING RESEARCH COUNCIL, INC.

3650 MANSELL ROAD·SUITE 140·ALPHARETTA, GA 30022

The Coordinating Research Council, Inc. (CRC) is a non-profit corporation supported by the petroleum and automotive equipment industries. CRC operates through the committees made up of technical experts from industry and government who voluntarily participate. The four main areas of research within CRC are : air pollution (atmospheric and engineering studies); aviation fuels, lubricants, and equipment performance, heavy-duty vehicle fuels, lubricants, and equipment performance (e.g., diesel trucks); and light-duty vehicle fuels, lubricants, and equipment performance (e.g., passenger cars). CRC's function is to provide the mechanism for joint research conducted by the two industries that will help in determining the optimum combination of petroleum products and automotive equipment. CRC's work is limited to research that is mutually beneficial to the two industries involved, and all information is available to the public.

CRC makes no warranty expressed or implied on the application of information contained in this report. In formulating and approving reports, the appropriate committee of the Coordinating Research Council, Inc. has not investigated or considered patents which may apply to the subject matter. Prospective users of the report are responsible for protecting themselves against liability for infringement of patents.

CRC Project No. E-88-2

FINAL REPORT

TRANSPORTATION FUELLIFE CYCLE ANALYSIS
A Review of Indirect Land Use Change and Agricultural N₂O
Emissions

Prepared by:

Amber Broch

S. Kent Hoekman



Desert Research Institute

Reno, NV 89512

Stefan Unnasch



Life Cycle Associates

Portola Valley, CA 94028

January, 2012

TABLE OF CONTENTS

Table of Contents	i
Table of Figures	iv
Table of Tables	vii
Executive Summary	ix
Indirect Land Use Change Modeling	ix
Time Accounting.....	xii
Agricultural N ₂ O Emissions.....	xiv
List of Acronyms	xvii
1 Introduction and Background.....	1
1.1 Life Cycle Assessments in Policy	1
1.2 Life Cycle Analysis of Fuels.....	2
1.2.1 Co-products	3
1.2.2 Agricultural Emissions	5
1.2.3 Land Use Changes	6
1.3 Previous CRC E-88 Work	6
2 Land Use Change Impacts.....	8
2.1 GHG from Land Use Changes: The Carbon Cycle.....	10
2.1.1 Soil Organic Carbon (SOC).....	11
2.2 Modeling Indirect Land Use Changes- General Methodologies.....	12
2.3 Agro-Economic Models	13
2.3.1 GTAP.....	14
2.3.2 FASOM	16
2.3.3 FAPRI-CARD	17
2.4 Emission Factor Databases.....	18
2.4.1 Woods Hole	19
2.4.2 Winrock Carbon Stock Database.....	24
2.5 LUC Application and Approaches in Policies	31
2.5.1 EPA – Renewable Fuel Standard (RFS2).....	31
2.5.1.1 International Land Use Change.....	33
2.5.1.2 Domestic Land Use Changes	38
2.5.2 California Air Resources Board- Low Carbon Fuel Standard.....	39

2.5.2.1	Current CARB Methodology	41
2.5.2.2	Updates to CARB ILUC Analysis in 2011	43
2.5.3	European Union- Renewable Energy Directive	45
2.5.3.1	EU Study to Assess Existing Modeling Activities.....	46
2.5.3.2	Study Using AGRI/ OECD Partial Equilibrium Model	46
2.5.3.3	EU Literature review of LUC studies	47
2.5.3.4	IFPRI ILUC GHG Assessment	47
	Model and database description.....	47
	Model approach.....	47
	Results.....	48
2.5.4	Other Models	50
2.5.4.1	Searchinger.....	50
2.5.4.2	Tyner – GTAP Bio-ADV	51
2.6	Comparison of LUC Model Results.....	53
2.6.1	Land Use Changes	55
2.6.2	Greenhouse gas emissions from land use changes	57
2.6.3	Type of Land Use Change	59
2.6.4	Comparison of Emission Factors from Key Studies	60
2.7	Comparison Of Emission Factor Databases.....	62
2.7.1	Comparison of C-Stock Data from Woods Hole and Winrock Databases.....	64
2.7.1.1	Above/ Below Ground Carbon.....	64
2.7.1.2	Soil Carbon.....	65
2.7.1.3	Non-CO ₂ / Combustion Emissions.....	67
3	Time Accounting Practices	68
3.1	Annualization	69
3.1.1	Analytical Horizon	70
3.1.2	Discount Rate	71
3.1.3	Land Reversion.....	74
3.2	Cumulative Radiative Forcing & Fuel Warming Potentials	74
3.2.1	Fuel Warming Potential.....	75
3.2.2	Time Correction Factor	78
3.3	Other Methodologies.....	78
3.3.1	Baseline Time Accounting	78
3.3.2	Simplified Time Accounting	78
3.4	Social Cost of carbon	79
4	N ₂ O Emissions From Agricultural Activites.....	80
4.1	Background/Introduction	80

4.2	N ₂ O Occurrence and Inventories.....	81
4.3	N ₂ O Formation Mechanisms.....	86
4.4	Modeling Approaches for Agricultural N ₂ O Emissions Inventories	88
4.4.1	IPCC Modeling Approach.....	88
4.4.1.1	IPCC 1995 Methodology	89
4.4.1.2	IPCC 1997 Approach	89
	Direct soil emissions	90
	Direct N ₂ O from animal production activities	91
	Indirect N ₂ O emissions from agricultural activities.....	92
	Summary of IPCC 1997.....	94
4.4.1.3	IPCC 2006 Methodology	97
	Direct N ₂ O Emissions	98
	Indirect N ₂ O Emissions.....	101
	Summary of IPCC 2006 Methodology	104
4.4.1.4	Comparison of IPCC Estimates with Field Measurements.....	105
4.4.2	Process-Based Models for Estimating N ₂ O Emissions.....	107
4.4.2.1	Development of DAYCENT.....	108
4.4.2.2	Validation of DAYCENT.....	110
4.4.3	U.S. Approach for Agricultural N ₂ O Emissions Inventories.....	110
4.4.4	Comparison of DAYCENT and IPCC N ₂ O Estimates.....	111
4.5	Effects of N ₂ O Emissions on Life-Cycle GHG Emissions of Biofuels	114
4.5.1	CARB/ GREET Approach.....	114
4.5.2	EPA’s Approach in the RFS2.....	115
4.5.3	JRC/ Biograce Approach in EU- Renewable Energy Directive	116
4.5.4	Comparison of N ₂ O Estimates from different modeling systems	117
4.5.5	Other Considerations	118
4.6	Mitigation of N ₂ O Emissions	120
5	Summary and Recommendations.....	122
5.1	Indirect Land Use Changes	122
5.2	Time Accounting.....	125
5.3	Agricultural Emissions.....	125
5.4	Recommendations for future work.....	127
6	References	129

TABLE OF FIGURES

Figure 1-1: Biodiesel from soybean pathway. From Reference [17].....	2
Figure 2-1: GHG Emission from Corn and Wheat Ethanol from LCA modeling and reports. Source CRC-E88 Final Report [4]	9
Figure 2-2. The Global Carbon Cycle (Adopted from IPCC 2001, 2007 [53,54]).....	11
Figure 2-3: Modeling flow to predict total biofuel lifecycle carbon intensity including ILUC. ..	12
Figure 2-4: 30-year emission factors (in Mg CO ₂ ha ⁻¹) for Searchinger, CARB and Tyner for conversion from A) forest and B) grassland.	24
Figure 2-5: Data sources used for estimating forest carbon stocks in Winrock emission factor analysis. Source [55].....	25
Figure 2-6: Spatially averaged forest carbon stocks in above- and belowground biomass (in t CO ₂ ha ⁻¹) used in the Winrock emission factor analysis. Source [55].....	26
Figure 2-7: Soil carbon stocks in the top 30 cm of soil for each country and/or administrative unit as calculated by Winrock from the World Harmonized Soil Database v.1.1. (Units in tons CO ₂ ha ⁻¹). Source: [55]	26
Figure 2-8: Grassland carbon stock estimates used in the Winrock emission factor analysis by country and administrative unit. For savanna, multiply by 1.8. For shrubland, multiply by 3.4. Units in t CO ₂ ha ⁻¹ . Source:[55].....	28
Figure 2-9: 30-year emission factors for conversion and reversion for each land category type for Buenos Aires, Argentina. (Source: Winrock EF Database, 2009)	29
Figure 2-10: System boundaries and modeling flow chart for biofuel LCA in EPA RFS2. [2]...	32
Figure 2-11: Flow chart of model linkage and calculation flows for international ILUC modeling in the EPA RFS2. The calculations within the stochastic model are shown within the dotted line.	37
Figure 2-12: Changes in domestic land use by type for RFS2, 2022. Source:[2] p 358.....	39
Figure 2-13: Schematic of CARB ILUC modeling database flow.	42
Figure 2-14: GTAP Regions combined with AEZs result in 203 unique regions. Source: [87] ..	44
Figure 2-15: AEZ-EF model to combine LUC results from GTAP with carbon stock data to predict total GHG emissions from LUC. Source: [87]	45
Figure 2-16: ILUC emissions and direct savings for different EU mandate levels in the EU-IFPRI Study.	49

Figure 2-17: Land Use Changes (A) and GHG from ILUC (B) from alternative fuel policies in the EU (modeled by IFPRI) the U.S. (modeled by Searchinger and EPA) and California (modeled by CARB and Tyner). WH= Woods Hole.....	58
Figure 2-18: ILUC classification, normalized by billion BTU for each study for A) Corn Ethanol, and B) Soy Biodiesel. IFPRI study shown in A is for complete policy with a blend of fuels.....	59
Figure 2-19: Total 30-year emission factors for key studies for corn ethanol, corresponding to Woods Hole regions. Note: The IFPRI study is based on the complete policy, with a blend of fuels. Author’s calculations.	61
Figure 2-20: Contribution of C sources to EFs from Winrock and Woods Hole for Latin America and Southeast Asia.	63
Figure 2-21: Comparison of C stock data for above- and below- ground C in vegetation in Woods Hole regions and corresponding Winrock regions for forestlands (A), and grasslands (B).	64
Figure 2-22: Carbon soil stock data from Woods Hole and Winrock.	66
Figure 3-1: Emission flows over time. (Adapted from[95]).....	69
Figure 3-2: ILUC emissions of corn ethanol (EPA analysis) with 0% and 5% discount rates and 30 year time horizon.	72
Figure 3-3: CO ₂ abundance resulting from ILUC and direct emissions of ethanol (25 years at 60 g CO _{2,eq} MJ ⁻¹) and gasoline (25 years at 94 g CO _{2,eq} MJ ⁻¹) (From [11,105]).....	76
Figure 3-4: Fuel warming intensity (g CO _{2,eq} MJ ⁻¹) vs. analytical horizon (From [11,105]).	77
Figure 4-1: Radiative forcing of climate between 1750 and 2005. (Taken from IPCC-2007 [54])	80
Figure 4-2: Concentrations of long-lived GHGs over the past 2000 years. (Taken from IPCC-2007 [54]).....	81
Figure 4-3: Total U.S. Anthropogenic N ₂ O Emissions Inventories, Tg CO _{2,eq} . (Data from U.S. EPA [13])......	82
Figure 4-4: Total GHG Inventories, Tg CO _{2,eq} . (a) U.S. 1990; (b) U.S. 2009; (c) Global 2000. (Data from U.S. EPA [13,112])	83
Figure 4-5: U.S. GHG emissions trends. Emissions from electricity generation are distributed to the relevant economic sectors. (Taken from U.S. EPA [13].)	84
Figure 4-6: Non-CO ₂ GHG emissions from the U.S. agricultural sector. (Data from U.S. EPA [112].).....	84
Figure 4-7: Global non-CO ₂ GHG’s from the Agricultural Sector. (Taken from U.S. EPA [112].)	85

Figure 4-8: N ₂ O Emissions from agricultural soils. (Taken from U.S. EPA [112].).....	86
Figure 4-9: Nitrogen cycle of agricultural soils and its relationship to N ₂ O production. (Taken from Oonk & Kroeze (1998) [118] by permission of John Wiley & Sons, Inc.)	87
Figure 4-10: Global agriculture-related N ₂ O emissions in 1989, Tg N ₂ O-N. Calculated using IPCC 1997 methodology. (Data from Mosier et al. [135].).....	95
Figure 4-11: Global N ₂ O budgets derived using different IPCC methodologies. (Data from Mosier et al. [135].)	96
Figure 4-12: Schematic diagram illustrating sources and pathways of N that result in direct and indirect N ₂ O emissions from soils and waters. (Taken from IPCC 2006 [52])	98
Figure 4-13: Measurement of N ₂ O fluxes on a near-continuous basis. Arrows indicate dates of N fertilization. (Taken from Smith & Dobbie (2001) [164] by permission of John Wiley and Sons.)	105
Figure 4-14: Comparison of direct soil N ₂ O emission estimates from DAYCENT and IPCC (2006). (Taken from U.S.EPA [13])	112
Figure 4-15: Comparison of DAYCENT and IPCC (1997) estimates of N ₂ O emissions from major crops and agricultural regions in the U.S. Results are 10-year mean and standard deviation in units of CO ₂ -C _{eq} . (Taken from Del Grosso et al. [183]. Used by permission of Elsevier.)....	113
Figure 4-16: CARB's assessment of N ₂ O's contribution to direct CI of biofuels. [81,82,79] ...	115
Figure 4-17: Annual N ₂ O emission rates from the RFS2 Analysis. [2].....	116
Figure 4-18: Comparison of Annual N ₂ O emissions from LCA modeling systems.....	118
Figure 4-19: Impact of crop management system on emissions of N ₂ O per unit crop and on the change in GHG emissions compared with fossil fuels. OM is optimized management, CM is conventional management. (Taken from Smeets et al. [219]. Used by permission of publisher)	120

TABLE OF TABLES

Table 1-1: Renewable fuel requirements and GHG Reduction targets for U.S. and E.U. policies.	1
Table 2-1: The models used, their key assumptions and outputs for estimating ILUC.....	12
Table 2-2: Comparison of Agro-Economic models for LUC Analysis. (Modified from Unnasch CRC E-88 report, Table 5.3 [4]).....	14
Table 2-3: FAPRI-CARD Model Description: Source:[64]	18
Table 2-4: World Regions and Ecosystem types for Woods Hole data with corresponding carbon stocks in vegetation and soil. The classification of ecosystems type is designated as (F) for forest or (G) for grassland.....	20
Table 2-5: Application of Woods Hole database in Searchinger, CARB and Tyner.	23
Table 2-6: Winrock Emission Factor Database carbon stock and conversion/ reversion categories.	25
Table 2-7: Fuel Volume Scenarios Considered in RFS2 in billions of gallons (From Table 2.3-1 of EPA [2]).....	31
Table 2-8: Conversion categories and groupings from FAPRI, Winrock and MODIS.....	36
Table 2-9: International ILUC and GHG results from each fuel scenario modeled in the RFS2.	37
Table 2-10: EPA RFS2 2022 Fuel Volumes modeled with FASOM for each fuel scenario (in billions of gallons) Source: EPA- RFS2 Table 2.4-1 [2].....	38
Table 2-11: Change in total domestic cropland used for production by scenario in the RFS2 in 2022 and resulting GHG emissions. Source: [2] p 356 and p 367.....	39
Table 2-12: GTAP regions and their corresponding Woods Hole Regions in CARB.....	41
Table 2-13: LUC and CI results from CARB’s LCFS.....	43
Table 2-14: Comparison of revised CARB model to predict ILUC to original approach. Source: [87].....	45
Table 2-15: ILUC and resulting indirect emissions from EU-IFPRI Study [8].....	48
Table 2-16: Marginal indirect ILUC results from the EU-IFPRI study, $g\ CO_{2,eq}\ MJ^{-1}\ yr^{-1}$. (20- year life cycle). Source: [8].....	49
Table 2-17: Corn ethanol and Soy biodiesel ILUC and resulting emissions from Searchinger. [1,6].....	51
Table 2-18: Simulated global ILUC due to U.S. ethanol production. Source: p 28 of [5].....	52
Table 2-19: Annual marginal and average estimated ILUC emissions due to U.S ethanol production from Simulation 2. Source p 40 of [5].....	52

Table 2-20: Comparison of 30-year ILUC results (IFPRI is for 20 years) from different studies. Units are g CO _{2,eq} MJ ⁻¹ fuel.....	53
Table 2-21: ILUC modeling inputs and results.....	55
Table 2-22: Land Use Factors for Soil Emissions in Winrock	66
Table 2-23: Fire and combustion factors for land conversion to crops in Winrock database.	67
Table 3-1: Advantages and Disadvantages for applying short or long time frames in GHG time accounting.	71
Table 3-2: Arguments for and against discounting ILUC emissions.....	73
Table 3-3: Lifetimes, radiative efficiencies and direct GWPs relative to CO ₂ . [104] Note: data taken from IPCC/ TEAP 2005.	75
Table 4-1: Estimated Uncertainty in U.S. GHG Inventory (From U.S. EPA [13]).....	86
Table 4-2: Default Emission Factors to Estimate Direct N ₂ O Emissions from Managed Soils .	101
Table 4-3: Default Emissions, Volatilization and Leaching Factors for Indirect Soil N ₂ O Emissions	104
Table 4-4: Default N ₂ O Emission Factors used in GREET	114

EXECUTIVE SUMMARY

Renewable fuels are beginning to take on a more significant role in transportation with the implementation of legislation such as the 2007 Energy Independence and Security Act (EISA), which requires 36 billion gallons of renewable fuels to be used annually in the U.S. by 2022. These fuels must meet greenhouse gas (GHG) reduction targets, set by the EPA Renewable Fuel Standard (RFS2), which are measured relative to conventional petroleum fuels through life cycle assessments (LCA). Other state regulations, such as California Air Resources Board's (CARB) Low Carbon Fuel Standard (LCFS) also set local GHG reduction targets.

Established fuel LCA models such as GREET (Greenhouse Gas, Regulated Emissions, and Energy use in Transportation) have long been used to estimate the well-to-wheels GHG emissions and energy use of transportation fuels. However, there are still many uncertainties associated with LCAs related to biofuels. For example, the contribution of N₂O emissions from agricultural operations to the overall carbon intensity (CI) of a biofuel is significant given its high global warming potential (GWP). In addition, the effects of land use change (LUC) and how it is included and modeled in LCA has been the area of much debate. LUC is initiated as more crops such as corn and soy are required to meet the feedstock needs of a growing biofuel sector. The increased demand for crops ultimately results in conversion of new lands for agriculture. Traditional LCA models do not typically have the capability to model the global supply and demand changes that result, requiring inputs from additional models to determine how much land is necessary, which type of land is converted and how much GHG emissions result from the conversion.

As shown in Figure ES-1, LUC emissions (white hashed bar) and agricultural emissions (green bar) contribute substantially to the overall CI of a fuel. However, both are primary areas of uncertainty for the determination of the GHG benefits of alternative fuels with respect to conventional fuels for policy. In this work, we examined the assumptions and methodologies surrounding these two highly controversial areas. We also investigated different approaches to time accounting for LUC.

INDIRECT LAND USE CHANGE MODELING

Searchinger was one of the first to call attention to the potentially significant impacts of indirect land use change (ILUC) to GHG of biofuels. [1] Subsequently, government agencies have tended to incorporate the effects of ILUC in alternative- biofuels policies: EPA calculates ILUC in its RFS2, as does CARB in its LCFS. [2,3] Because modeling ILUC is outside the scope of many LCA models, links are made between agro-economic models, which predict the amount and location of ILUC, and land-cover GHG emission factor databases. The net emissions occur over time, the length of which must be considered in determining carbon intensity (CI) for the fuel.

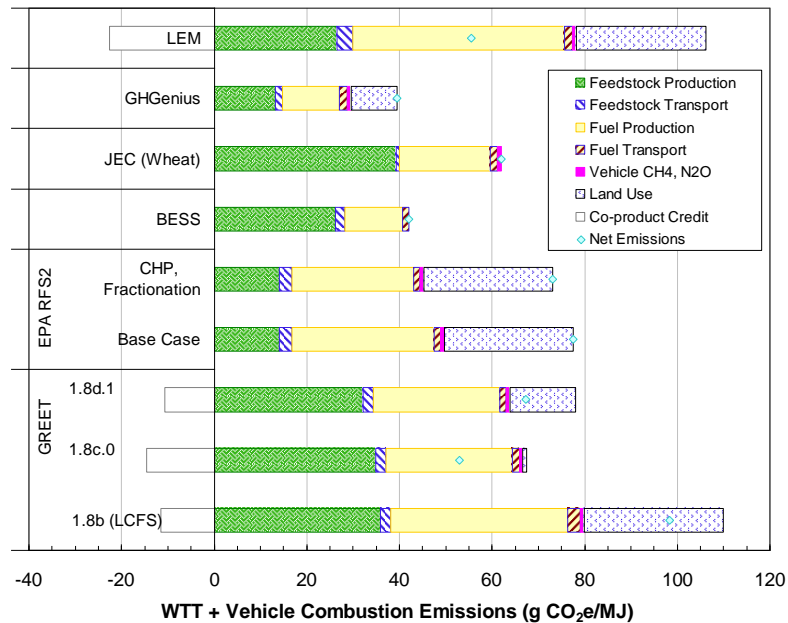


Figure ES-1: GHG Emission from Corn and Wheat Ethanol from LCA modeling and reports. Source CRC-E88 Final Report [4] .

In this work, we have investigated the modeling approaches and linkages between databases used in the RFS2 and LCFS, along with other key LUC studies such as Searchinger and Tyner. [5] We first explored how the agro-economic databases are linked to the emission factor databases to estimate the net GHG emissions. Then we compared the LUC results from each study. Finally, we compared the carbon-stock data in the different emission factor databases used.

The EPA approach is the most complex, using two different modeling pathways to determine domestic LUC and international LUC. Domestic changes are determined through the FASOM economic model. FASOM is linked to the DAYCENT/ CENTURY and FORCARB databases to endogenously determine the net ILUC. Since the databases and detailed results were not available, the methodologies applied could not be compared to other approaches. International ILUC is modeled with the FAPRI model in the RFS2. The land use results from FAPRI are linked to emission factors from the Winrock databases, which are aggregated according to historical land conversions measured through MODIS satellite imagery.

In the LCFS, CARB models LUC with the GTAP model, which is linked to emission factors from the Woods Hole database. A similar approach is used in work by Wally Tyner at Purdue University; however, the GTAP model is updated in this more recent work to include a better estimation of biofuels commodities. [5] The final CI results attributed to ILUC from these studies, along with results from Searchinger and a study for EU policy by the International Food Policy Research Institute (IFPRI) are shown in Table ES-1. Since Searchinger first publically highlighted the topic of ILUC emissions in 2008, databases and modeling practices have been refined, producing lower ILUC emission estimates.

**Table ES-1: Comparison of 30-year ILUC results (IFPRI is for 20 years) from different studies. Units are g CO₂,
eq MJ⁻¹ fuel.**

	Searchinger [1,6]	EPA International[2]	EPA Domestic[2)	CARB[7]	Tyner [5]	IFPRI[8]
Corn Ethanol	106	30	-4	30	18	54
Soy biodiesel	340	40	-8	62		75
Sugarcane Ethanol		4 (incl. domestic)		46		18
Complete Policy with blend of fuel types						17

The amount, location and type of ILUC occurring, which are predicted by the agro-economic models, are significant factors in the final CI of the fuel. They are then linked to emission factors (EF) to determine the total GHGs produced. The ILUC for each study are shown for corn ethanol in Figure ES-2-A, and the resulting GHG emissions (normalized over the time horizon of each study) are shown in Figure ES-2-B. The models predict significantly different amounts and locations of land conversion. For example, both CARB and Tyner use the GTAP model (although an updated version is used in the Tyner study). The LUC results from Tyner are only half of those predicted by CARB, and occur throughout the world, while much of the LUC predicted by CARB occurs in the U.S.

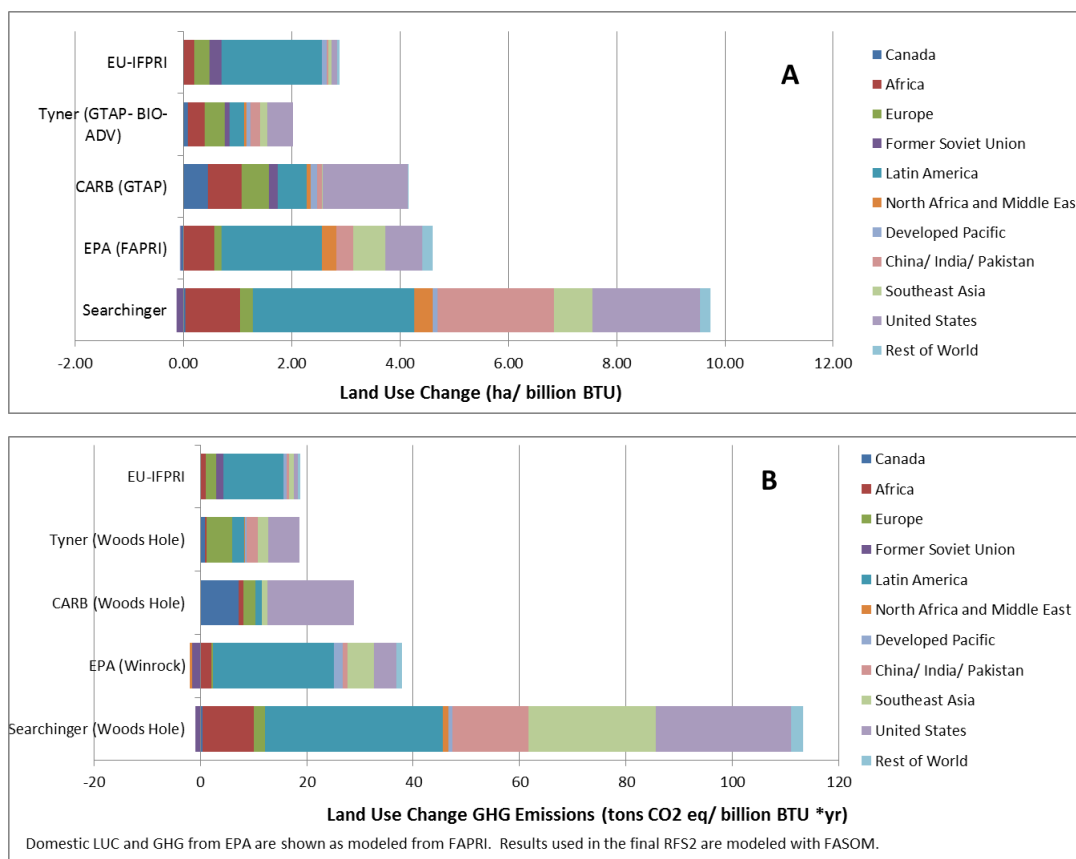


Figure ES-2: ILUC (A) and GHG emissions (B) for corn ethanol from key studies.

The amount of GHGs predicted depends on the Emission Factors applied to the land conversion. In this work, we attempted to compare the carbon-stock data used in the Woods Hole and Winrock emission factor databases. However, a direct comparison between the two is not possible. The differences in the databases are highlighted in Table ES-2. The application of the databases can also be significantly different. For example, CARB, Tyner and Searchinger all use the Woods Hole database, but arrive at different emission factors due to different assumptions applied.

Table ES-2: Differences in Winrock and Woods Hole EF databases.

Emission Factor Step	Winrock	Woods Hole
Regions	755 administrative units	10 world regions
Conversion Categories	47 different conversion/ reversion categories between 8 different land classifications.	Conversion from forests and grasslands only.
Emission Factor Weighting	Historical LUC is predicted through MODIS satellite data to weight different conversion EFs into EFs that correspond to FAPRI.	Regions are divided into ecosystems. CARB and Searchinger weight EFs based on historical data from the 1990's by Houghton[9]. Tyner uses the total land cover of each ecosystem type.
C-Stock for Above- and below-ground C in vegetation	C-stock included for each type of land classification. The change in stocks is calculated as the difference between the original and new land use type.	Stock Change method also used.
Loss of C- in vegetation	All C in vegetation is lost, however database includes a calculation for harvested wood products that could be added at a later date.	Searchinger assumes 100% is lost. CARB assumes 90% is lost. Tyner assumes 75% is lost.
Soil Carbon	Uses Harmonized World Soil Database for top 30 cm of soil. Loss of soil carbon occurs over 20 years, with varying rates (20-80%).	C-stock in top 1 m of soil; 25 % is lost over the time horizon (30 years).
Wetlands	Peat land soils are estimated for Indonesia and Malaysia, occurring over the 30-year time period.	Referenced to IPCC for SE Asia default for peat lands.
Non-CO ₂ emissions	Fire CH ₄ and N ₂ O IPCC defaults included as combustion factors for conversion and reversion. Rice methane combined in direct LCA.	No separate calculation for CH ₄ and N ₂ O emissions from fire.
Reversion Emissions	Reversion factors are the negative of conversion factors, except for forests, which are estimated as the lower of the annual foregone sequestration over 20 years or the initial forest carbon stock.	75% of lost soil carbon is regained (18.75% original soil carbon) in regions where cropland is shrinking (EU and Former Soviet Union).

TIME ACCOUNTING

Time accounting plays a significant role in the overall determination of GHG emissions from ILUC. A large release of GHG emissions occurs in year zero from above and below ground biomass as a result of land conversion. Additionally, soil carbon emissions continue to be released for approximately 20 years, and foregone sequestration is accounted for through the

duration of biofuel production. How long these emissions are accounted for, and how they are allocated over time will affect the final CI value of the fuel.

Although both the EPA and CARB have currently settled on a 30-year time horizon with a 0% discount rate, there is still on-going debate on how to appropriately allocate indirect emissions occurring over a long time period. The factors that have the most impact are the time horizon and the discount rate.

The time horizon is the length of time during which all emissions are accounted for and attributed to the biofuel, allocated over the volume of fuel produced during that time period. There are benefits and drawbacks when considering either a shorter (20-30 year) or longer (100-year) time frame. A shorter time frame emphasizes the importance of near-term emissions, and is more conservative, since predictions grow more and more uncertain further into the future. However, short time frames may truncate potential benefits that occur over time (e.g. if cropland reverts to its natural state after the project lifetime has ended). Longer time frames are more uncertain, and may also reduce the significance of near term emissions changes.

Applying a 100-year time frame treats ILUC emissions on a similar scale as GHGs, whose global warming potentials (GWPs) are expressed as CO₂-eq. based on a 100-year time period. Additionally, a longer time frame allows for consideration of reversion emissions. Some argue, however, that reversion emissions are too uncertain, and should not be included.

The practice of discounting emissions is also an area that lacks consensus. Discount rates are used in economics to determine future value based on today's dollar. They are applied to ILUC emissions to emphasize the significance of near term emissions by giving them more weight than future emissions, since they are likely to cause an earlier compounding effect if they are emitted to the atmosphere earlier. However, applying an economic practice to a physical phenomenon doesn't necessarily have the same meaning since it is difficult to determine if a gram of CO₂ emissions will cause different effects if it is released today or tomorrow. There has been an ongoing effort to attribute a dollar value to CO₂ emissions, named the social cost of carbon, which can then be discounted accordingly. However, many argue about the appropriate discount rate to apply to ILUC emissions. Peer reviewers for the RFS2 suggested discount rates ranging from 0% to 7.9%. [10]

Some argue that 0% is an appropriate discount rate because of the issue of intergenerational equity. Others argue that ILUC emissions are already uncertain, and applying a discount rate amplifies the uncertainty. However, applying a 0% discount rate suggests that future emissions have the same equity as current emissions, implying that there would be no value in avoiding emissions today, since it will be cheaper and easier to do so in the future owing to technology advancements. Additionally, the significance of current emissions is ignored when using a 0% discount rate.

Others have suggested alternative approaches to allocating emissions over time. O'Hare suggests calculating a fuel warming potential (FWP) using calculations for cumulative radiative

forcing (CRF), the same methodology that is applied in assigning a global warming potential (GWP) to GHGs. [11] The FWP could then be discounted. Kloverpris argues for a baseline time accounting methodology which would measure LUC relative to a baseline LUC.[12] Although there is growing support to use FWP methodologies since they utilize similar metrics to those already used to determine GWPs of different GHGs, it is unclear that current policies will adopt a different method in the near future.

AGRICULTURAL N₂O EMISSIONS

Nitrous oxide (N₂O) is an important species in the overall biochemical-geochemical cycling of nitrogen. It is produced naturally in soils by microbial processes. Due to its potent GHG behavior (GWP is 298 times that of CO₂) and its influence by human activities, N₂O is considered an important contributor to anthropogenically-induced radiative forcing of climate change. Globally, approximately 7.5% of total GWP is attributed to N₂O. Methane's contribution to global GWP is twice as large, but only a very small fraction of this is attributable to agricultural activities related to biofuels. Thus, N₂O is the primary GHG of interest in LCAs of biofuels.

N₂O is produced in soils as a by-product of microbial processes involving nitrification and denitrification pathways. Nitrification is an aerobic process, by which nitrogenous species are oxidized to nitrate (NO₃⁻); de-nitrification is an anaerobic process, by which nitrate is reduced to molecular nitrogen (N₂). The balance between aerobic and anaerobic conditions is affected by numerous factors -- particularly soil type, tillage practice, and moisture level. Other important factors influencing nitrification and denitrification include soil nitrogen inputs, temperature, pH level, and soil organic matter (SOM) content.

Major inputs of nitrogen to the soil include synthetic fertilizers, organic fertilizers, crop residues, and animal wastes. Besides direct formation in soils, indirect N₂O is produced by two main pathways: (1) volatilization of ammonia and NO from soils, followed by deposition onto lands and waterways, and (2) runoff and leaching of nitrate from soils, followed by nitrification/denitrification in waterways. A complete accounting of N₂O emissions impacts from biofuels requires assessments of both direct and indirect sources of N₂O.

A variety of modeling approaches have been developed and applied to estimate N₂O emissions from agricultural activities. Among the most widely used are approaches developed by IPCC. Because of IPCC's interest in quantifying and monitoring GHG emissions on a consistent, country-wide basis, their methodologies for determining N₂O emission inventories are relatively simple, and rely upon readily-available data inputs, such as total fertilizer use and crop production within a given country.

IPCC's approach has evolved over the years, as understanding of N₂O processes has improved and more experimental data have been acquired for testing and validating the models. The most recent IPCC guidelines, published in 2006, outline a 3-tiered hierarchical approach for estimating N₂O emissions. The choice of which tier to employ is based upon availability (and reliability) of

inventory information at hand. Tier 1 is the simplest approach, requiring the least data inputs. This is also the approach which seems to be most widely used in LCA studies of biofuels.

When using the GREET model to assess life-cycle GHG emissions for biofuels, it appears that most modelers apply simple Tier 1 default values for all emission factor terms (EFs), fraction of soil nitrogen that is volatilized, and fraction of soil nitrogen that is lost due to runoff and/or leaching. A clear explanation of nitrogen input terms is often not provided, though it seems that nitrogen from fertilizer applications is the only term used in some cases. Use of such defaults leads to an overall “Tier 1 N₂O emission factor” of 0.0133 kg N₂O-N/kg soil-N input. The derivation of this value is shown in Table ES-3, which also indicates the wide uncertainty range that applies to each component of this emission factor.

Table ES-3. Default N₂O Emission Factors used in GREET

N₂O Emissions Component	Factor, kg N₂O-N/kg soil-N inputs	Uncertainty Range, kg N₂O-N/kg soil-N inputs
Direct N ₂ O from soil	0.0100	0.0030 – 0.0300
Indirect N ₂ O from volatilized and re-deposited N	0.0010	0.0001 – 0.0055
Indirect N ₂ O from nitrate leaching and runoff	0.0023	0.0004 – 0.0088
Total	0.0133	0.0058 – 0.0348 *

***Total estimated range is derived assuming the individual IPCC ranges are log normal. Standard propagation of error routines are applied to lower and upper standard deviations.**

Tier 3 of IPCC-2006 defines use of process-based modeling approaches to determine N₂O emissions inventories. Process-based biogeochemical models simulate fluxes of C and N among the atmosphere, vegetation, and soil; and determine global budgets for these species. These models require extensive parameterization to represent the physical, chemical, and biological processes influencing N₂O formation. Thus, they require data inputs regarding crop type, soil type, nutrient supply, temperature, pH, precipitation, tillage practices, and other parameters.

The U.S. EPA and USDA have adopted a Tier 3 approach to determining the direct N₂O emissions component of the total U.S. agricultural GHG inventory for major crop species. (Simpler emission factor approaches are still used for minor crops and for indirect N₂O emissions components.) For this purpose, a biogeochemical model called DAYCENT is employed.

Application of a Tier 3, process model-based method for determining N₂O emissions inventories would be expected to provide more reliable results than a simple Tier 1 approach – provided sufficient inputs of high quality are available to run the model. However, direct comparisons of Tier 1 and Tier 3 approaches are difficult to perform, partly because of inconsistencies in spatial and temporal scales. The IPCC Tier 1 methodology is intended to estimate annual average N₂O emissions on a large spatial scale – typically country-wide. In contrast, process-based models are generally applied to smaller regions, but with higher temporal resolution.

In their description of the U.S. GHG inventory process, EPA presented a comparison of direct N₂O emission estimates provided by DAYCENT and the IPCC-2006 Tier 1 approach. Published field measurement studies from 12 North American sites were considered, representing several combinations of crop type, fertilizer treatment, and cultivation practices. All N₂O emission values were expressed on a common basis of g N₂O-N/ha-day. The results shown in Figure ES-3 are taken directly from the EPA document. This figure shows that in nearly every case, the DAYCENT estimates were closer to measured values than were the IPCC estimates. In general, the IPCC Tier 1 methodology over-estimated emissions when the observed values were low, and under-estimated emissions when the observed values were high. In comparison, the DAYCENT estimates are less biased. The improved performance of DAYCENT is expected, because this model accounts for site-specific factors (such as weather, soil type, and crop type) that influence N₂O emissions, while the IPCC methodology does not.

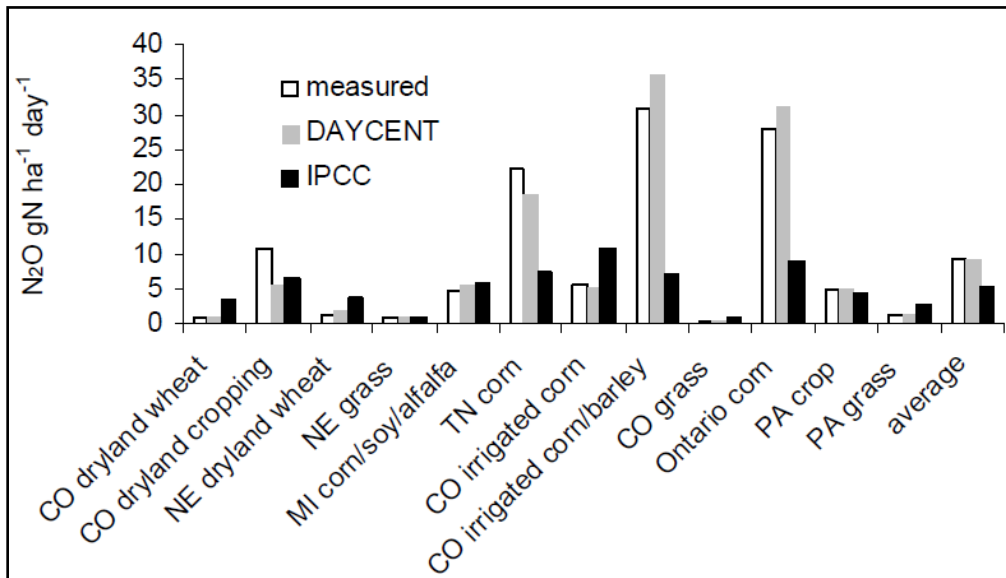


Figure ES-3. Comparison of direct soil N₂O emission estimates from DAYCENT and IPCC Tier 1 (2006)(Taken from U.S. EPA [13]).

LIST OF ACRONYMS

AEZ	Agro-economic zone
AFOLU	Agriculture, Forestry and Land Use
ANPV	Annual net present value
ASM	Agricultural Sector Model
AWMS	Animal waste management system
b BTU	billion BTU
BEES	Building for Environmental and Economic Sustainability
BESS	Biofuel Energy Systems Simulator
BG	billion gallons
C	Carbon
CARB	California Air Resources Board
CENTURY	Biogeochemical model of plant-soil nutrient cycling
CEPII	Centre d' Etudes Prospectives et d' Informations Internationales
CES	Constant Elasticity of Supply
CET	Constant Elasticity of Transformation
CGE	Computational General-Equilibrium
CH ₄	Methane
CI	Carbon Intensity
CO ₂	Carbon Dioxide
CO _{2,eq}	Mass of a specified GHG expressed as a mass of CO ₂ having equivalent GWP
CP	Cropland Pasture
CRC	Coordinating Research Council
CRF	Cumulative Radiative Forcing
CRP	Conservation Reserve Program
DAYCENT	Daily time-step version of CENTURY biogeochemical model
DDGS	Dried distillers grain with solubles
DGS	Distillers grain with solubles
DNDC	De-Nitrification De-Composition (model for N ₂ O emissions)
EBAMM	ERG Biofuels Analysis Meta-Model
EC	European Commission
EF	Emission Factor
EIO-LCA	Economic Input-Output- Life Cycle Assessment Model
EISA	Energy Independence and Security Act
EPA	Environmental Protection Agency
EU	European Union
FAO	Food and Agricultural Organization
FAPRI	The Food and Agricultural Policy Research Institute; FAPRI-CARD is at Center for Agricultural and Rural Development
FASOM	The Forest and Agricultural Sector Optimization Model
FORCARB	U.S. Forest Carbon Budget Model
FQD	Fuel Quality Directive

FSU	Former Soviet Union
FWI	Fuel Warming Intensity
FWP	Fuel Warming Potential
g CO _{2,eq} MJ ⁻¹	grams of CO ₂ , equivalents per MJ of fuel
Gg	Gigagram = 10 ⁹ grams = one thousand metric tonnes
GHG	Greenhouse Gas
GREET	Greenhouse Gases, Regulated Emissions, and Energy Use in Transportation Model
GTAP	Global Trade and Analysis Project
GWP	Global Warming Potential
ha	hectare
HWSD	Harmonized World Soil Database
IEA	International Energy Agency
IFPRI	International Food Policy Research Institute
ILUC	Indirect Land Use Changes
IPCC	International Panel on Climate Change
ISO	International Organization for Standardization
JEC	JRC, EUCAR and CONCAWE
JRC	Joint Research Center
kg	kilogram
LCA	Life Cycle Assessment
LCFS	Low Carbon Fuel Standard
LCI	Life Cycle Inventory
LEM	Life Cycle Emissions Model
LUC	Land use change
MIRAGE	Modeling International Relationships in Applied General Equilibrium
MODIS	Moderate Resolution Imaging Spectroradiometer
MOVES	Motor Vehicle Emission Simulator
M ton	Million tons
Mg	Mega-grams = 10 ⁶ grams= 1 metric tonne
MJ	Mega joule = 10 ⁶ joule
mmBTU	million BTU
Mtoe	Million tons of oil equivalent
N	Nitrogen
N ₂ O	Nitrous Oxide
NO	Nitric Oxide
NOAA	National Oceanic and Atmospheric Administration
NOE	Nitrous Oxide Emissions (model for N ₂ O emissions)
NPV	Net present value
NREL	National Renewable Energy Laboratory
ODS	Ozone depleting substance
OECD	Organization of Economic Cooperation and Development
Pg	Petagram (10 ¹⁵ grams)

RED	Renewable Energy Directive
RF	Radiative Forcing
RFS2	Renewable Fuel Standard
RIA	Regulatory Impact Analysis
RTFO	Renewable Transport Fuel Obligation
SBM	Soy Bean Meal
SCC	Social Cost of Carbon
SOC	Soil Organic Carbon
SOM	Soil Organic Matter
t C	ton of Carbon
TCF	Time Correction Factor
Tg	Teragram = 10^{12} grams= one million metric tons
TH	Time Horizon
UK	United Kingdom
UNFCCC	U.N. Framework Convention on Climate Change
USDA	U.S. Department of Agriculture
WFPS	Water-filled pore space
WH	Woods Hole
WTT	Well-to-Tank
WTW	Well-to-Wheel

1 INTRODUCTION AND BACKGROUND

1.1 LIFE CYCLE ASSESSMENTS IN POLICY

Interest in measuring greenhouse gas emissions (GHG) from transportation fuels is increasing as alternative fuel policies are being implemented to address concerns regarding energy security and global climate change. Policies such as California’s Low Carbon Fuel Standard (LCFS), the EPA’s Renewable Fuel Standard (RFS2), the EU’s Renewable Energy Directive (RED), and the UK’s Renewable Transport Fuel Obligation (RTFO), among others, require GHG reduction targets be met through the use of alternative fuels, as shown in Table 1-1.[2,3,14,15] The GHG emissions are determined through life cycle assessments (LCA), which are employed as a means to estimate the cradle-to-grave GHG emissions (among other environmental impacts) of a fuel. The GHG reductions are measured through comparison of LCA results of an alternative fuel to its conventional counterpart (such as gasoline or diesel). The net GHG is determined in terms of a carbon intensity (CI), which includes all GHG emissions, measured in CO_{2,eq}.

Table 1-1: Renewable fuel requirements and GHG Reduction targets for U.S. and E.U. policies.

Policy	Volume Requirement	GHG Reduction Target
EPA - RFS2 (EISA)	36 billion gallons by 2022	Renewable Fuel- 20% Advanced Fuel – 50% Biomass-based diesel- 50% Cellulosic Biofuel- 60%
CARB - LCFS	Weighted blending requirement based on carbon intensity.	10 % by 2020
EU- RED	10% of renewable energy in transport fuels by 2020.	6% reduction in life-cycle GHGs from biofuels by 2020.
UK- RTFO	10% of renewable energy in transport fuels by 2020.	35% reduction by 2020 (40% recommended)

A fuel LCA is performed by accounting for all energy and emission flows during the life of the fuel, from the cradle to the grave. This includes all phases of production, processing, transportation and use. This accounting practice requires numerous data inputs and assumptions and clear definition of boundaries. The results of LCA can be highly variable and dependent on these inputs. Because of their importance in policy, LCA methodologies and data have been under critical review, with each assumption, definition, data input, etc., being evaluated by stakeholders and experts in an effort to ensure that the life-cycle GHG emissions of transportation fuels are justly represented. The assumptions that generate the greatest uncertainties and yet have the largest impacts in LCA of a biofuel are those regarding co-product allocation, agricultural emissions (particularly N₂O emissions) and indirect land use changes (ILUC).

1.2 LIFE CYCLE ANALYSIS OF FUELS

Life cycle analyses are being applied to determine the carbon intensity (CI) of various alternative fuels to compare to the CI of conventional fuels. The CI of a fuel is typically determined as mass of $\text{CO}_{2,\text{eq}}$ emissions per energy content of the fuel ($\text{g CO}_{2,\text{eq}} \text{MJ}^{-1}$), but can also be compared per volume of fuel or per distance driven (e.g., $\text{g CO}_{2,\text{eq}} \text{L}^{-1}$ or $\text{g CO}_{2,\text{eq}} \text{km}^{-1}$).

A full-fuel LCA includes all emissions flows (and/ or other environmental impacts such as energy use, eutrophication, or acidification) starting with raw material extraction and ending with fuel consumption.[16] For a biofuel, this includes all inputs and requirements for feedstock growth, harvesting, fuel production, distribution and combustion as well as intermediate transportation steps. Figure 1-1 shows a typical pathway for biodiesel production from soybeans, which includes all direct emissions typically associated with the production and use of soy biodiesel. The production phase of the soybean includes all agricultural inputs necessary to grow and harvest the crop, including the energy and emissions from farm equipment, production and use of fertilizers, and any intermediate transportation steps. Co-products such as soybean-meal and glycerin are generated during oil extraction and biodiesel production phases. The emissions produced during the use of the biofuel are dependent on the type and efficiency of the vehicle. A common assumption is that the carbon released from the fuel during combustion is offset by the biogenic carbon from plant growth. Other non- CO_2 emissions such as NO_x , however, are typically included in the combustion emissions.

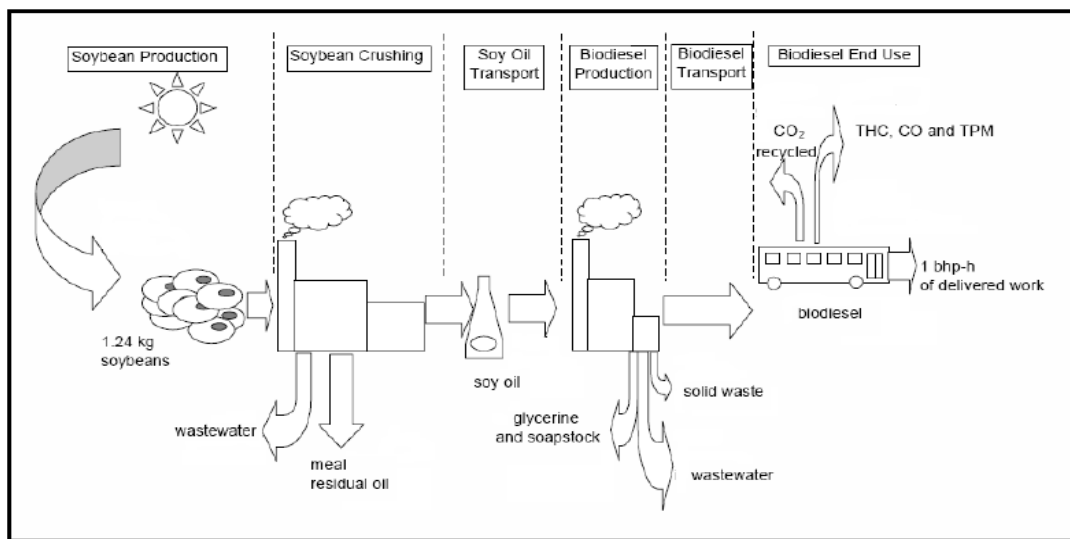


Figure 1-1: Biodiesel from soybean pathway. From Reference [17]

LCAs require numerous assumptions, clear definitions of boundaries, and detailed data. Numerous modeling tools and databases have been constructed to support fuel LCA. Some of the models used include BEES, BESS, EBAMM, EcoIndicator, EIO-LCA, LEM, GaBi, GHGenius, GREET, GEMIS, and SimaPro. Commonly used databases include NREL's US LCI Database and EcoInvent. The GREET model, developed by Argonne National Laboratory, offers

over 200 specific pathways for alternative fuels and vehicles. It is among the most prevalent models in the U.S. and is used by the EPA for the Renewable Fuel Standard (RFS2). In addition, California has updated the GREET model with its state and regionally specific data to produce the California-GREET model, which the California Air Resources Board (CARB) is using in support of its Low Carbon Fuel Standard (LCFS). Similar models have been used in support of other policies: GHGenius is used in support of Canadian policy, and SimaPro is used for many European studies.

LCAs are typically conducted to assess the relative attractiveness of various transportation fuels, and are becoming a common aid in determining the most desirable options for sustainable fuel and energy processes. They are increasingly used in alternative fuel policies to compute the benefits (or dis-benefits) of alternative fuels with respect to conventional fuels. Many LCAs conducted for biofuels show a relative GHG reduction compared to petroleum counterparts.[18,19,20,21] However, most studies have not included the effects of indirect land use changes (ILUC). ILUC is of increasing concern because of its potentially dramatic impacts on the carbon intensity (CI) of biofuels.

Traditional LCA models, however, have limited or no capabilities to model indirect effects such as ILUC, which requires the consideration of market effects. This requires expanding the system boundaries, in what is termed a consequential approach, to determine how supply and demand changes affect the broader markets. This approach requires economic models to simulate market behavior.

Even when models implement similar data or databases, they are likely to produce differing results because numerous assumptions differ from model to model (or modeler to modeler). Some of the key assumptions affecting the results include the following:

- definition of the boundaries
- scale of production
- farming energy and chemical requirements
- amount of nitrogen fertilizer for plant growth
- conversion of nitrogen fertilizer to N₂O
- crop yields
- energy use and efficiencies from biofuel processing plants
- credits given to co-products
- LUC impacts

While some of these assumptions are simply minor variations in practices and methodologies, others can generate significant differences in the final results. Three of the most influential assumptions that also have the largest uncertainties are discussed below.

1.2.1 CO-PRODUCTS

Several by-products are produced during the production of biofuels. Dried distillers grain with solubles (DDGS) is a useful by-product of ethanol production, which can be used as animal feed. During biodiesel production, animal feed meal is also produced during the oil extraction process,

and glycerin is produced during transesterification. Other co-products such as naphtha or propane may be produced in 2nd Generation biodiesel manufacturing involving hydroprocessing. [22] Common practice in LCA modeling is to allocate some of the energy and emissions produced during the fuel life-cycle to these co-products since they can replace other similar products in the market. Several different methods of co-product treatment are commonly used. [20,23,24] These are described below in more detail.

- ♦ **Physical Allocation**—Environmental impacts are allocated to each by-product and the biofuel based upon a common physical parameter such as mass (kg) or energy (MJ). A drawback of this method is that it does not consider the environmental impacts that have been offset by replacing other products.
- ♦ **Economic Allocation**—Calculations are performed on the basis of the economic value of the biofuel and other valuable by-products. The economic allocation method has similar drawbacks to the physical allocation method in that it does not consider changes to environmental impacts from replacement of other materials.
- ♦ **Displacement/ Substitution**—A co-product that replaces an existing product also displaces the existing product's emissions stream. The environmental impacts of the replaced product must also be assessed through LCA, and are then subtracted from the total fuel pathway being analyzed. Changes in assumptions, however, can have significant effects on the results, and more data are required for the analysis. This method is also referred to as the “system expansion” method.
- ♦ **No Co-Product Allocation**—All energy and emissions incurred in the lifecycle are attributed to the final biofuel product. While perhaps the easiest approach to use, failing to allocate any energy or environmental impacts to co-products is clearly an oversimplification of reality.

The choice of allocation method may significantly affect the final results of the LCA. Several studies have examined the effects that different allocation methods have on the results. Bernesson, et al. studied the effects of all four allocation methods listed above on soy biodiesel, as well as a range of production plant sizes. [25] They found that differences in plant size were almost negligible in some cases, but the allocation method had significant impacts, reducing CI by a factor of 2 to 3 compared to no allocation, and possibly resulting in the process becoming a net-supplier of energy for the expanded allocation method. A quick scan of LCA methodology by Guinee and Heijungs found that different allocation methods could result in up to a 250-fold difference in extreme cases. [24] Numerous other studies included cases for one allocation method compared to no allocation, which generally produced large differences in LCA results. [26]

Co-product allocation also plays an important role in the quantification of ILUC, since some biofuels produce a large amount of co-products which can be used as an animal feed and replace crops that would have otherwise been grown. A literature review conducted by the EU summarized LUC studies that looked at land requirements with and without consideration of co-products. [27] Many of the studies were consistent in that co-products reduced the land

requirements by significant amounts: between 23% and 94%, with a median overall reduction around 36%.

Although there are still several choices of allocation methodologies, ISO recommends the system expansion method, which may produce distorted results, particularly when co-products are a main product. [26] Co-product methodologies have been reviewed in the previous CRC E-88 report, and are outside the scope of this work, so will not be discussed in detail.[4]

1.2.2 AGRICULTURAL EMISSIONS

Emissions occurring during the growth of the biofuel crop contribute substantially to the total carbon intensity of the fuel. This is largely due to the emissions of N_2O and CH_4 which have high global warming potentials (GWP). Using the IPCC 100-year GWP, a single gram of N_2O or CH_4 equates to 298 or 25 grams of CO_2 , respectively. Therefore, small fluctuations in either gas can result in large consequences for the biofuel.

In particular, because of their large GWP, N_2O emissions can have a significant impact on the final CI of a biofuel. N_2O emissions typically evolve from Nitrogen fertilizers that are applied during the growth of the biofuel feedstock, therefore, it is crucial to account for all N inputs and outputs from cultivation of land to grow biomass – including crop residues, fertilizer, N fixation, manure, deposition, gaseous losses, crop output, runoff, N transfer between co-rotated crops, and others. It is also important to know how these factors change over time.[28]

In many LCA studies, the N_2O emissions resulting from the agricultural phase are dependent on the total amount of N-fertilizer applied and an N_2O conversion factor. The most commonly used conversion factor is the IPCC default factor of 1.325%, which determines the relative amount of N_2O formed from each gram of N fertilizer applied. The IPCC includes assumptions about direct emissions and indirect emissions from leaching and deposition; however, there is large variability in N_2O conversion factors (even the variability associated with the IPCC default factor ranges from 0.003 to 0.03) and dissenting opinions on which factors should be applied. The GREET model uses the IPCC value[29] and the GHGenius model uses a factor of 1.125%.[17] However, Crutzen et al.[30] concluded that the IPCC emission factor for N_2O was seriously underestimated, and recommended a conversion value equivalent to an IPCC factor of 2.24-3.74.[29]

N_2O emissions are also dependent on the region, climate, temperature, amount of precipitation, fertilizer type, soil type, soil moisture, and soil temperature, among other things. A single conversion factor does not accurately capture these differences. Process-based models such as the DAYCENT/CENTURY model have been developed to account for these factors affecting N_2O emissions. However, process-based models are not widely applied in fuel LCA studies.

The methodologies to model N_2O and agricultural emissions are discussed in more detail in Chapter 4.

1.2.3 LAND USE CHANGES

Emissions from land use change (LUC) have been shown to have potentially significant effects when considered in a biofuel LCA. LUC effects may occur as the demand for energy crops increases as a result of increased biofuel requirements. Because of international trade of agricultural commodities, fluctuations in supply and demand have global implications. The increased need for biofuel crops will ultimately lead to the expansion of cropland, which can occur elsewhere in the world (indirect land use changes- ILUC). Depending on the location and type of land converted, significant GHG emissions may result. Carbon stored in vegetation and soils will be released as vegetation is cleared by burning or left to decompose and soils are disturbed. Additionally, there may be a loss of carbon sequestration potential from clearing forests. Since these types of emissions are a response to increased biofuel use, some argue that they should be attributed to the biofuel and accounted for in the biofuel's CI. Although ILUC effects are difficult to quantify, because of their potentially irreversible impacts ILUC modeling is being included in biofuel LCA used for regulatory compliance. However, modeling LUC is beyond the capabilities of many traditional LCA models, and must be done through complex linkage to additional models and databases. Agro-economic models are used to forecast the price response to supply and demand changes and predict the location and type of ILUC. The land requirements are then linked to databases containing information about the carbon-stock of the land to calculate the resulting GHG emissions. This consequential approach is more complex and requires more expansive boundaries and additional models and assumptions. However, biofuel policy is trending toward taking the consequential approach to incorporate ILUC effects over the more traditional attributional approach, in which only direct environmental impacts are quantified.

The uncertainties associated with LUC are significant, and its determination requires detailed input and assumptions and additional modeling efforts not typically included in a traditional LCA. This work will describe how ILUC is modeled in policy-related studies and investigate the carbon stock databases in Chapter 2.

1.3 PREVIOUS CRC E-88 WORK

This work is a follow-on to CRC Project No. E-88, in which an assessment of existing life cycle analyses of transportation fuels was performed. [4]E-88 included a review of methodologies, analytical tools and models. The review focused on published studies which have received the greatest attention for policy.

The E-88 study provided a detailed review of different LCA models and their key attributes. The models reviewed include: GREET, CA-GREET, JRC/ EUCAR/ CONCAWE, LEM, and BESS, detailing the key assumptions and inputs for each model. The review compared outputs of the results of different fuel pathways from each of the studies to illustrate how inputs affect each stage of the fuel life-cycle. The report also detailed key assumptions affecting LCA results,

describing how co-product allocation assumptions, agricultural emissions and ILUC impact the results.

The methodologies used to determine the ILUC effect of biofuels were also described. The descriptions included background on different agro-economic models used and a comparison of the results of these models. Additionally, comparisons of the emission factor databases and the carbon stock data applied were provided.

In the present work, we build upon CRC E-88 and further investigate the uncertainties surrounding both ILUC and agricultural N₂O emissions, two of the most influential factors in determining the CI of a biofuel.

The uncertainties associated with assessments of ILUC are significant, and its estimation is not always transparent. ILUC is dependent on how much land is converted, the type of land that is converted, the emission factors applied, and the time horizon that is selected. In this work, we focus on the estimation of ILUC in the EPA's RFS2 and CARB's LCFS, as well as other influential studies, in an attempt to clarify the approaches taken and the assumptions made. This involves describing the models and databases used and their key assumptions, and tracing the quantification of LUC and GHG emissions resulting from biofuel policies. The estimation of how much land is needed to meet biofuel crop production requirements, as well as the type of land that will be converted, is generally predicted through the use of agro-economic models such as GTAP, FAPRI, or FASOM. A thorough investigation of economic models is outside the scope of this work, however, key assumptions are highlighted and results from policy-related work will be described. The linkage between the economic models and emission factor databases will be described, and a comparison of the carbon stock data used to determine the emission factors will be made. The time accounting practices applied and alternative methods will also be described.

The estimation of agricultural emissions in all biofuel LCA is also highly uncertain. The N₂O emissions in particular can have a substantial impact to the overall CI of a biofuel given its high GWP. Although it is common practice to apply a single conversion factor, such as the IPCC factor of 1.325 % g N₂O/ g N applied, the conversion of N₂O from agricultural fertilizers depends on many factors including the climate and soil properties. In this work, we will describe the significance of N₂O emissions in a biofuel LCA, as well as their significance to overall global GHG emissions. The development of the IPCC approaches from 1997 to 2006 will be described. Process-based models such as DAYCENT/CENTURY model will also be described and compared to the IPCC approach.

2 LAND USE CHANGE IMPACTS

As biofuel production expands due to policy changes, crop production of biofuel feedstocks must be increased to meet the demand. These increases can occur from increased yields through intensification, from displacement of existing crops, or from expansion into new lands. All three methods, however, result in fluctuations of GHG emissions, while the second two result in land use changes (LUC), either directly or indirectly. Direct LUC impacts are those that can be traced directly to the production of biofuel, e.g. those that are occurring as a direct expansion of biofuel production into new lands. Indirect land use changes (ILUC) are those that occur from market responses as crops or croplands are diverted to biofuels. The effects of LUC and how it is considered (or not considered) in fuel LCA has drawn considerable attention. In particular, the area of ILUC has been the focus of much debate since there is potential for significant emissions from the loss of carbon in vegetation (i.e., forests or grasslands) or soils, as well as the loss of on-going carbon sequestration that would have occurred had the land remained in its original state [6].

Searchinger was one of the first to introduce the concept of ILUC, and predicted that its consideration would have detrimental impacts on the overall CI of biofuels, resulting in a carbon payback of 167 years for corn ethanol. [1] However, some argue that current practices for modeling ILUC result in an unacceptable range of uncertainty, so should not be included until the data are more scientifically robust. [31,32] Others argue that including ILUC unfairly singles out biofuels, making producers responsible for activities outside of their control. [33,34] Yet, some argue that ILUC likely has a non-zero impact and should not be ignored. For example, Liska and Perrin argue that a conservative overestimation of biofuel CI is less costly since an underestimation will lead to more rapid adoption and higher initial investments and infrastructure. [35] Regardless of the debate, policies are trending toward inclusion of ILUC in LCA estimates for biofuels: RFS2 includes a detailed assessment of ILUC within its biofuel LCA; CARB determines an ILUC “adder” for each biofuel; and, the European Commission is working to understand ILUC issues to include in its RED.

There have been several attempts to model ILUC, and results of studies are highly variable and uncertain. [2,3] Initial estimates by Searchinger showed that the GHG impacts of corn ethanol were more than doubled when ILUC is considered. Subsequent work has been done to refine the analysis, and the inclusion of ILUC in policies which undergo rigorous peer review have resulted in a more acceptable estimation of ILUC. All have shown, however, that the ILUC is potentially one of the primary sources of GHGs for a biofuel CI. More recently, others have suggested that the effects of ILUC are even less severe [5], or perhaps irrelevant [36]. Many agree that ILUC will likely have some impact, and should be given a non-zero value [2,31,33,37].

Results from various LCA models and reports for corn or wheat ethanol are given in Figure 2-1. Many of the studies include an estimation of ILUC (shown as the white hashed bar). The figure

illustrates that effects of ILUC are not insignificant, and can have dramatic impacts on the final CI value of a fuel as modeled by LCA.

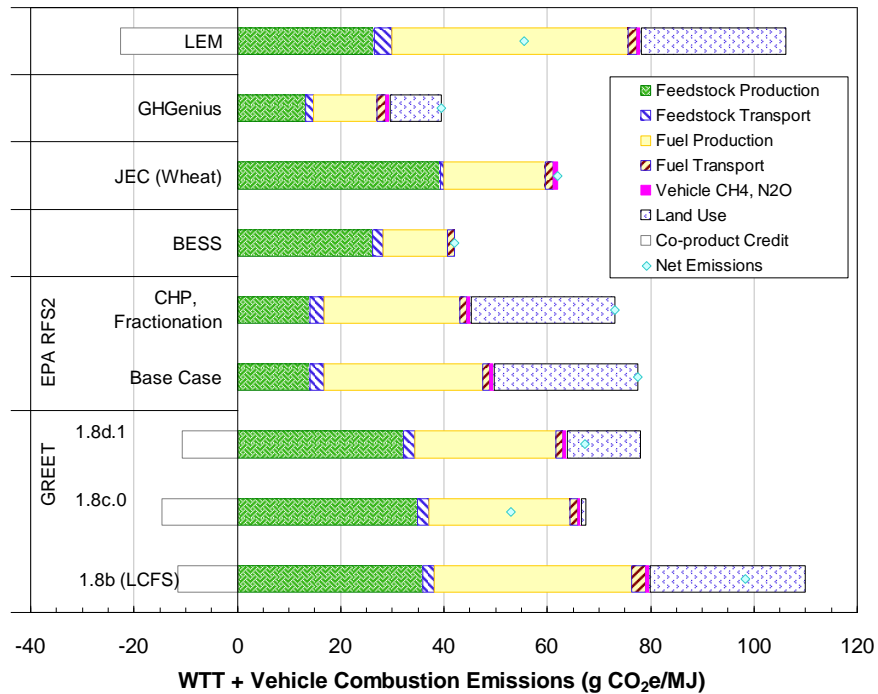


Figure 2-1: GHG Emission from Corn and Wheat Ethanol from LCA modeling and reports. Source CRC-E88 Final Report [4].

The effects of ILUC are significant, but the uncertainties associated with its estimation are also large. Therefore, it is important to understand the modeling process, data, and assumptions that affect the results. ILUC is not generally predicted by conventional fuel LCA models such as GREET or BESS. Determination of ILUC is complex and requires knowledge of price fluctuations occurring in response to supply and demand changes of crops. This requires linking several models to predict how and where ILUC will occur: generally an agro-economic model is used in conjunction with an emission factor database to determine how much land is impacted, where the LUC will occur and on which type of land, and how much GHGs will result.

In this section of the report, we will first describe why LUC is significant and what contributes to the determination of LUC, and then describe the general approaches to model ILUC. Since ILUC is quantified to determine compliance with certain fuel regulations, we will describe the methodologies that CARB and EPA follow to predict ILUC, and introduce the approach evaluated by the EC. We will then give an introduction to the models and databases used for each policy and provide comparisons between them. Finally, we will use the results of various modeling efforts by the EPA and CARB to make comparisons between the databases and methodologies followed.

2.1 GHG FROM LAND USE CHANGES: THE CARBON CYCLE¹

As the demand for biofuel crops increases, more and more croplands will be required to satisfy the feedstock requirements as well as traditional food and feed crop requirements. This demand necessitates that lands be converted from their current use. Land conversion, such as converting from forests to cropland, results in the removal of biomass and vegetation which can store large amounts of carbon. If the vegetation is burned or left to decompose, the carbon will be emitted to the atmosphere as a GHG.

The terrestrial biosphere can act as both a source and a sink for carbon. The carbon cycle is the mass transfer of carbon by natural geological, physical, biological, and chemical processes between the biosphere, hydrosphere, and the atmosphere. [38] Biogenic greenhouse gas (GHG) fluxes associated with agriculture include the storage of atmospheric carbon in plant biomass due to photosynthesis, respiration, decomposition, and the uptake or release of carbon into roots, soil, or back to the atmosphere. Non-CO₂ emissions (CH₄, N₂O) from agricultural practices vary depending on the management practice employed. The atmospheric uptake of CO₂ into plant material is considered a credit against the biogenic carbon in the fuel. However, the biogenic components of feedstock production and land use are important elements of a biofuel's life cycle impact, and these emissions should include changes in soil carbon and aboveground flora and belowground soil and biomass.

Land conversion also results in a flux of soil carbon. [39] Conversion of forest to cropland releases large quantities of soil carbon. However, reduced tillage practice or crop residues re-incorporated back into the agricultural system can lessen this effect and provide the benefit of improved soil quality. [40,41,42] In addition, if existing cropland is tilled, much of the soil carbon (over 25%) is released over time. [43] No-till practices can help to build up soil carbon and perennial crops will add to soil carbon mass in variable quantity and over time. [44] The effect of tillage practice remains uncertain. [45,46]

Converting cropland or Conservation Reserve Program (CRP) land to pasture or forest generally results in increased storage of carbon. [47,9,35,48] Spatial and temporal relationships between agricultural patterns and practices and the net amount of carbon stored have not, to date, been adequately quantified.

Direct LUC can be defined as the type of activity being carried out on a unit of land. [49] The IPCC has updated guidelines for Land-use, Land-use Change and Forestry which have set default values for above-ground LUC. [50] The land categories are a combination of land cover (the type of vegetation covering the earth's surface) and land-use classes. [50] Six top-level land categories for greenhouse gas (GHG) inventory reporting are specified. These categories include forest land, cropland, grassland, wetlands, settlements, and other land.

¹ This section is taken from CRC-E-88 [4]

IPCC estimates that ~1.5 billion tons of carbon are emitted to the atmosphere each year from forest and grassland clearing, which accounts for 20% of annual CO₂ emissions [51,52].

2.1.1 SOIL ORGANIC CARBON (SOC)

Global soil organic carbon (SOC) estimates are 2,300 Pg C (Pg = 10¹⁵ g) as shown in Figure 2-2. This is three times the estimated 760 Pg in the atmosphere. Yet this soil organic carbon sink is also one of the major sources of atmospheric CO₂, as also shown in Figure 2-2. Soil naturally acts as a carbon sink, the magnitude of which is affected by a combination of factors such as soil moisture, pH, salinity, texture, and the presence of microbes and plants that live in and above the earth. Natural and anthropogenic external factors such as seasonal change, tillage, and fertilizer and water inputs also have a strong effect on the CO₂ cycle.

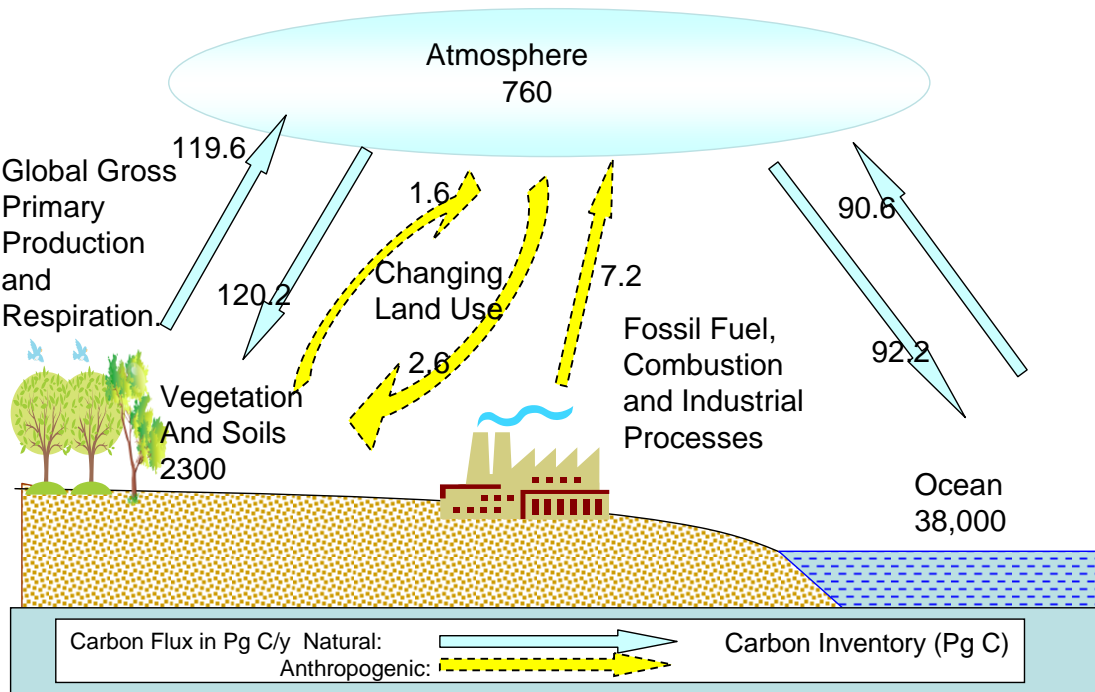


Figure 2-2. The Global Carbon Cycle (Adopted from IPCC 2001, 2007[53,54])

SOC mapping is highly variable in terms of total carbon estimates stored in vegetation vs. in the soil and root systems. The highest stores are found in the boreal and tropical regions. Peat lands are especially high in soil carbon in the boreal areas, and yet often lumped together in estimates from tropical peat land areas as ‘forest’, for example. [55]

2.2 MODELING INDIRECT LAND USE CHANGES- GENERAL METHODOLOGIES

Modeling GHGs resulting from ILUC requires quantifying how much land will be required, where LUC are occurring, and what the carbon stocks of the land types are. This requires detailed data on historical and future trends in crop growth and LUC patterns, economic market and price fluctuations, and estimations of carbon stocks of converted lands. It typically requires linking agro-economic models and emission factor databases to the outputs of more traditional LCA models such as GREET or BESS, as shown in Figure 2-3. Agro-economic models use data about agricultural trends to predict the amount and type of LUC that will occur and the land types they occur on. Those results are linked to emission factor databases to quantify the amount of GHG that will be released from the vegetation, soil, and from foregone sequestration. Additionally, some type of time allocation is necessary. The models and databases available for ILUC modeling are highlighted in Table 2-1. Each of the input models will be discussed further as noted by Section in the table.

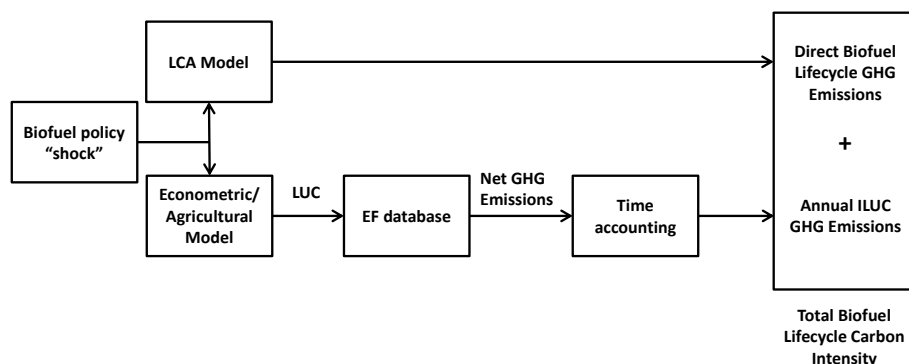


Figure 2-3: Modeling flow to predict total biofuel lifecycle carbon intensity including ILUC.

Table 2-1: The models used, their key assumptions and outputs for estimating ILUC.

Type of Model	Section of Report	Models/ Methods	Outputs	Key Inputs/ Assumptions
Econometric/ Agricultural Models	Section 2.3	GTAP, FASOM, FAPRI	Amount of LUC Type of LUC conversions Location of LUC	<ul style="list-style-type: none"> Amount of biofuel "shock" Yield elasticity Price elasticity Co-products
Emission Factor Databases	Section 2.4	Woods Hole, Winrock/ MODIS	How much GHGs are released per LUC location over a period of time	<ul style="list-style-type: none"> Carbon Stock data Historical LUC trends
Time accounting practices	Chapter 3	Amortization Fuel Warming Potential	Allocation of one time plus continuing emissions over time	<ul style="list-style-type: none"> Time horizon Discount Rate

An introduction to the agro-economic models and emission factor databases will be presented first. Particular attention is made to models used in U.S. policies. In the following section, the model implementation and linkage between databases will be described for each policy scenario (EPA and LCFS). The results of the policies will then be compared, which will be used to highlight differences between the modeling efforts, where possible. Time accounting practices will be discussed in Chapter 3.

2.3 AGRO-ECONOMIC MODELS

In ILUC analysis, economic models can be used to predict how supply and demand changes of energy crops affect global markets. Economic models represent economic equilibrium in which supply equals demand. A change in the supply or demand of commodities moves the model out of equilibrium, so the model adjusts new prices, and supply and demand to establish a new economic equilibrium. There are two types of equilibrium modeling: general equilibrium, in which equilibrium is sought for the whole economy with many interacting markets; and partial equilibrium, which only analyzes a single market. In ILUC analysis, agro-economic models such as the Global Trade and Analysis Project (GTAP) by Purdue University, the Forest and Agricultural Sector Optimization Model (FASOM), and the Food and Agricultural Policy Research Institute- Center for Agricultural and Rural Development (FAPRI-CARD), among others, are used. These models have long been in use to analyze global agricultural economics and resulting LUC, and have recently been adapted to predict ILUC for GHG analysis in LCA. Changes in biofuel production volumes are input to predict how much land will be required to compensate for the crop that has been displaced by the production of biofuels. The models can predict the amount and type of land required, and are spatially aggregated into different regions to predict the location of LUC. The resulting LUC can be used in conjunction with emission factor databases to determine the resulting GHGs.

Agro-economic models require numerous input assumptions. Key input parameters such as crop yields, price elasticities and transformation elasticities are used to predict price fluctuations of agricultural commodities, and how those price changes influence ILUC internationally. Assumptions regarding crop yields and yield changes are critical to estimate the LUC. It is expected that some of the increased demand for crops can be met through intensification of existing croplands, i.e., by increasing the yields. This can be accomplished through advancements in technology or application of additional fertilizers, which would have an effect on resulting ILUC emissions. Additionally, as lands expand, the yields of new lands are expected to be less than existing croplands (termed *marginal lands*, which describes the land brought into production last and abandoned first due to its poor productivity[56]), as we can assume that the highest productivity lands are already in use. The productivity of new croplands in comparison to existing croplands is a critical input factor that influences the amount of land required. Another key input parameter, the transformation elasticity, limits the ease of which one type of land is converted to another, so it affects the total amount of land required, as well as the type. The market response to price changes (price elasticities) also strongly influences the economic

modeling results. Comparisons of the agro-economic models used in U.S. policies along with inputs to several key assumptions are highlighted in Table 2-2. Each of these models is discussed further.

Table 2-2: Comparison of Agro-Economic models for LUC Analysis. (Modified from Unnasch CRC E-88 report, Table 5.3[4])

Model	GTAP	FAPRI	FASOM
Application	CARB-LCFS	EPA RFS2	EPA RFS2
Type:	Global computational general equilibrium model (CGE) with explicit treatment of land.	Global partial equilibrium model of agricultural sector.	Partial equilibrium model of U.S. forestry and agriculture incorporating GHG emissions
Regions	18 international AEZs	54 International regions	11 U.S. Regions
Fuel demand	Biofuel shock with surrogate petroleum tax subsidy.	Demand for feedstock modeling of blend wall price effects.	Demand for feedstock on agricultural system
Price/ yield response	0.2-0.3 price/ yield elasticity plus exogenous yield multiplier	0.074 long run price/ yield elasticity	No price response
Area/ yield response	0.66-0.75 area expansion multiplier	0.977 area expansion multiplier	Yield projections for new land in U.S.
Co-product treatment	Feed co-product is subtracted from bio-fuel feedstock requirements	DGS and SBM are treated as separate agricultural commodities	DGS and SBM are treated as separate agricultural commodities
Co-product power	New power for ag and biorefineries included in GREET calculations with regional specific emission factors	Credit for power export from biorefineries using GREET emission factors	U.S. agricultural system power modeled by FASOM with addition of new power consumption from biorefineries
Carbon Accounting	Emission factors from Woods Hole database.	MODIS satellite data combined with Winrock analysis of land conversion factors	Endogenous, direct emission factors comparable to GREET. Land emissions from CENTURY

A thorough review of the agro-economic models is outside the scope of this work. However, some of the underlying assumptions, inputs and outputs of the models are described below to provide a basic understanding of their general capabilities and how they affect the overall ILUC results. Additional details on the models were provided in CRC E-88. [4]

2.3.1 GTAP

The Global Trade Analysis Project (GTAP) is a computable general equilibrium model (CGE) developed at Purdue University. The model uses a database containing global data describing bilateral trade patterns, production, consumption and intermediate use of commodities and

services. It constrains primary production factors such as capital, labor and land to model the global economy.

Since its application in biofuel LCA, the model has been continually updated to more accurately model biofuel and biofuel crop markets. The most recent database for LUC modeling is the GTAP Version 7 Land Use Database, which includes land cover data by land type and agro-ecological zone (AEZ) for the year 2004. The GTAP model has also been improved for the treatment of biofuels and by products, called GTAP-BIO.[57] The database has been modified to include data on production, consumption and trade of biofuels including grain based ethanol, sugarcane ethanol, and biodiesel from oilseeds. Tyner has updated the GTAP-BIO model (GTAP-BIO-ADV) for recent work to improve the analysis of corn ethanol.[5]

GTAP uses a Constant Elasticity of Transformation (CET) supply function to estimate the supply of land across cropland, forestry, and grazing land. [58]The CET function used in GTAP is based entirely on U.S. data, but is applied to all the world regions.

The input parameters to GTAP for modeling LUC include:

- Baseline year
- Fuel production increase
- Land use analysis: the change in biofuel production expected in response to policy.
- Crop yield elasticity: which defines how much a crop yield will increase in response to a price increase (as prices increase, farmers have more incentive to intensify production of their existing crops). A higher elasticity means a greater yield increase in response to a price increase.
- Elasticity of crop yields with respect to area expansion: yields on newly converted land will be lower than corresponding yields on existing crop land.
- Elasticity of harvested acreage response: the extent to which land cost changes affect changes of cropping patterns on existing agricultural lands.
- Elasticity of land transformation across cropland, pasture and forest land: the extent of which types of lands change.
- Trade elasticity of crops: expresses the likelihood of substitution among imports from all available exporters.

GTAP can be used to predict LUC in 18 agricultural economic zones (AEZ) and 19 regions worldwide. The CET function is used to predict how much land is transferred between forests, pastures and croplands, and its LUC outputs are the area of land converted under each category.

It has been noted that because GTAP simulates a land scarcity regime, in which biofuel demand results in new land to be cleared (rather than a net land surplus regime in which increased demand for biofuels would result in less land reversion), the methodology is flawed, and should instead be able to account for the possibility of a net reduction in total agricultural lands[59]. However, historic patterns show that demand for biofuel crops has outpaced yield improvements, so corn and soybean production are likely to be in the land scarcity regime in the near term.

GTAP is used by CARB to model ILUC as part of its LCFS, and results of these modeling efforts will be discussed further in Section 2.6. Since its use in CARB analysis, Tyner and others at Purdue University have been working to update the models to more accurately reflect biofuels markets. [5,60] These revisions to the GTAP model and the resulting ILUC estimates will be discussed in Section 2.5.4.2.

2.3.2 FASOM

The Forest and Agricultural Sector Optimization Model (FASOM) is a dynamic, nonlinear programming model of the forest and agriculture sectors in the United States. It is a partial equilibrium model that accounts for land competition and response to changing prices, and simulates land use interactions to predict the types of land converted in the U.S. FASOM utilizes data about crop inputs to build crop budgets which include data on yields, fertilizer, chemicals and energy use needed to grow crops in each of 11 market regions and 63 sub-regions. The use of FASOM enables determination of secondary impacts such as crop switching, movements between cropland and pasture, movements between agricultural land and forestland, and reductions in equilibrium quantities of agricultural and forest commodities due to higher prices. It also accounts for changes in primary GHGs (CO₂, CH₄, and N₂O) from agricultural activities and tracks carbon sequestration and losses over time. [61]

FASOM simulates a dynamic baseline and changes from that baseline in response to policy. It covers the 48 contiguous States, broken into 63 sub regions for agricultural production and 11 market regions, and tracks over 2,000 production possibilities for field crops, livestock and renewable fuel. All cropland, pastureland, rangeland and private timberland throughout the conterminous U.S. are included, and land is allowed to move between categories with some limited restrictions. FASOM includes a representation of seven different land use categories including:

- Cropland- actively managed cropland used for traditional (corn and soy) and dedicated energy crops.
- Cropland-pasture (CP) –managed pasture land used for livestock production, but which can also be converted to cropland production.
- Forestland- includes a number of subcategories, and in which the number of acres of reforested, afforested and total area on public land is continually tracked.
- Forest-pasture- unmanaged pasture with varying amounts of tree cover that can be used for livestock or timber harvest.
- Rangeland- unmanaged land that can be used *only* for livestock grazing.
- Developed land- high-value urban land.
- Acres enrolled in the Conservation Reserve Program (CRP)-generally marginal cropland retired from production and converted to vegetative cover.

The output of the model includes changes in total domestic (U.S.) agricultural sector fertilizer, energy use, and livestock (due to changes in animal-feed prices), as well as changes to land. The

FASOM model is endogenously linked to other models such as DAYCENT/ CENTURY and FORCARB models.

The DAYCENT/ CENTURY model simulates the fluxes of C and N among the atmosphere, vegetation and soil. It can be used to predict daily N-gas fluxes (N_2O , NO_x , N_2), CO_2 flux from soil respiration, soil organic C and N, net primary production of plants, H_2O and NO_3 leaching, and other environmental parameters. [62]

FORCARB is a simulation model used to estimate carbon budgets in the U.S. forest system. It produces national carbon inventories, partitioned into forest soils, trees, understory and forest floor vegetation, and C in harvested products. [63]

FASOM utilizes both of these models to endogenously estimate GHGs from its simulated LUC. The total GHGs from LUC are dependent on the changes to agricultural soil carbon and N_2O determined, and changes to above- and below-ground and soil carbon stock in the forestry sector.

The agricultural soil GHGs are estimated through the DAYCENT/ CENTURY model, which is based on factors for different types of crops, management practices and conversion effects. Carbon soil storage is based on the intensity of agricultural tillage, the irrigation status, relative abundance of grasslands, and the mix of annual versus perennial crops. The model also yields changes from N_2O in pastureland and cropped soil.

Forest carbon changes are estimated within FASOM's forestry module, which follows the FORCARB model by the U.S. Forest Service. The module tracks changes in above- and below-ground C in both continuous and afforested forestlands, as well as in forest products. The evaluation of GHG emissions from domestic forests includes tree carbon, soil carbon, forest floor carbon, understory vegetation, and carbon in harvested logs.

FASOM is used in the EPA-RFS2 LUC analyses to predict the ILUC occurring within the U.S. Additional results and discussion of the modeling is given in Section 2.5.1.2.

2.3.3 FAPRI-CARD

The FAPRI-CARD model is a global agricultural model that can be used to examine land use fluctuations in response to renewable fuel policies. It is a system of econometric models including multi-market, partial equilibrium, and non-spatial econometric models that cover all major temperate crops, sugar, ethanol, dairy and livestock and meat products for all major producing and consuming countries [64]. It projects how policy or economic shocks will affect agricultural commodity markets and land areas used to produce those agricultural goods.

FAPRI accounts for several key parameters that affect the amount of ILUC including: crop yield growth rates over time, price induced crop yield changes, crop yields on marginal/ new lands, the efficiency of renewable fuel co-products over time, supply and demand in the livestock sector, and other variables.

Determination of the location of LUC is a critical factor in ILUC since that carbon stored in vegetation and soil, and therefore GHG emissions, can vary significantly by region. The FAPRI-CARD model predicts changes in both annual and perennial cropland as well as changes to pastureland for 54 regions (shown in Appendix A). The inputs and outputs of the model are shown in Table 2-3 and include changes in crop acres. FAPRI includes both an international and a U.S. domestic module.

Table 2-3: FAPRI-CARD Model Description: Source:[64]

Exogenous Variables	Population, GDP, GDP Deflators, Exchange Rates, Policy Variables
Endogenous Variables	Production, Consumption, Exports, Imports, Stocks, World and Domestic Prices
Commodity Coverage	Grains: Corn, Wheat, Sorghum, Barley, Oats, and Other Grains Oilseeds: Soybeans, Rapeseed, Sunflower, Palm, and Other Oilseeds Livestock: Beef, Pork, Poultry, and Other Livestock Products Dairy: Milk, Cheese, Butter, and Other Dairy Products Sugar Biofuels: Ethanol, Biodiesel
Major Countries/Regions	North America: United States, Canada, Mexico South America: Argentina, Brazil, etc. Asia: China, Japan, India, Malaysia, etc. Africa: South Africa, Egypt, Nigeria, etc. Europe: European Union, Russia, Ukraine, etc. Oceania: Australia, New Zealand
Output by Commodity and Country	World Prices, Domestic Prices, Production, Consumption, Net Trade, Stocks, Area Harvested, Yield

FAPRI is used in the EPA RFS2 analysis to predict international ILUC in both crop and pasture land for each fuel scenario (i.e. corn ethanol, soy biodiesel, sugarcane ethanol, or switch grass ethanol). Only the results from the international module are used in the EPA RFS2. Domestic LUC is predicted by FASOM. In the RFS2, the changes in crop and pasture acreage from FAPRI are used in conjunction with the Winrock EF database to predict the international LUC. FAPRI results are also used to predict other “direct” emissions, such as international livestock emissions, and international rice methane emissions. The linkage between other models in the RFS2 and results from modeling efforts are discussed in Sections 2.5.1.1 and 2.6.

2.4 EMISSION FACTOR DATABASES

As lands are converted from one use to another, a large release of GHG emissions can occur for carbon contained in vegetation that is removed or from soil that is disturbed. Additionally, there may be lost opportunity of carbon sequestration that would have been provided by growing vegetation. The area of LUC predicted by the economic models can be linked to emission factors to determine the net release of GHGs associated with the land conversion. In U.S. policy analysis, CARB uses the GTAP model linked to the Woods Hole emission factor databases to

predict ILUC emissions. The EPA uses the FAPRI model linked to the Winrock carbon stock database to predict international ILUC emissions, and uses the FASOM model, which contains a DAYCENT/ CENTURY module, to determine domestic ILUC emissions.

The amount of GHG emissions from land conversions depends heavily on the location of the land, as well as the beginning and ending land types. Emission factor databases, such as Woods Hole Emission Factor database and the Winrock Carbon Stock, contain relevant carbon stock data that, along with the land use conversion types predicted by the agro-economic models, allow for the quantification of GHGs from LUC. These two primary databases are described in more detail in this section. Additional details on how these emission factor databases are linked to the econometric models within each policy model are described in Section 2.5.

The emissions associated with LUC can continue to be released over a period of time, which must also be considered when determining emission factors. The time allocation of ILUC emissions are discussed in more detail in Chapter 3. However, the time period selected also affects the emission factor. Since both CARB and EPA have settled on a 30-year emission factor, that time frame will be discussed below.

2.4.1 WOODS HOLE

The Woods Hole emission factor database as presented by Searchinger [1] is based on research done by R.A. Houghton at the Woods Hole Oceanographic Institute [65,66,9]. The data discussed herein are presented in Searchinger supplemental materials and have been revised into Excel™ tables by CARB in their ILUC analysis. [1,67] The data are from Houghton's research on carbon flux due to LUC based on historical trends from 1850-1990 [68]. Carbon fluxes in $C\ ha^{-1}$ due to anthropogenic activities are presented for vegetation, soils and lost sequestration for multiple ecosystem types within 10 world regions as shown in Table 2-4. The carbon flux data are converted to emission factors, given in $g\ CO_{2,eq}\ ha^{-1}$ by the ratio of the mass CO_2 per gram of Carbon (44/12). A weighted 30-year emission factor is then calculated based on the following data contained within the database:

Historical Land Use Clearing by Ecosystem Type

For each ecosystem type within each of the 10 regions, the amount of historical land clearing (in hectares) in the 1990's as analyzed by Houghton is given. [66,9] The analysis of land conversions included clearing of natural ecosystems for croplands and pasture, and the abandonment of cleared lands followed by recovery of original vegetation and soils. Both the EU and the Former Soviet Union (FSU) experienced a decline in cropland in the 1990's, while the remaining regions experienced an increase in croplands. The total land clearing in a region is used to calculate a weighted average emission from each of the ecosystem types for each region. Additionally, the ecosystems are classified as either forests or grasslands (as indicated in Table 2-4), so the total clearing by land type can be summed to give a weighting factor for either conversion from forests or grasslands.

Carbon in Vegetation

The ecosystems within each region have corresponding data about how much carbon is stored in live vegetation, as shown in Table 2-4. The data presented in the Table are ranges of global and regional vegetation. The values include both above- and below-ground live biomass of trees and ground cover.[66]

Table 2-4: World Regions and Ecosystem types for Woods Hole data with corresponding carbon stocks in vegetation and soil. The classification of ecosystems type is designated as (F) for forest or (G) for grassland.

World Wide Region	Ecosystem Type	Carbon in Vegetation Mg C/ha	Soil Carbon Mg c/ ha
1. Europe	Boreal Forest (F)	90	206
2. Pacific Developed	Broadleaf Forest (F)	150	150
3. Former Soviet Union	Chaparral (G)	40	80
4. N. Africa/ Middle East	Coniferous Mountain forest (F)	150	100
5. Canada	Coniferous Pacific Forest (F)	200	160
6. United States	Desert (G)	6	58
7. Latin America	Desert Scrub (G)	3	58
8. South and SE Asia	Grassland (G)	10	42-80
9. Africa	Mixed Forest (F)	170	160
10. India/ China/ Pakistan	Montane Forest (F)	80	100
	Open Forest (F)	60	50
	Shrubland (G)	5	30
	Temperate Deciduous Forest (F)	120-135	134
	Temperate Evergreen Forest (F)	160	134
	Temperate Grassland (G)	7	189
	Temperate Seasonal Forest (F)	100	134
	Temperate Woodland (F)	27	69
	Tropical Dry Forest (F)	13	70
	Tropical Evergreen Forest (F)	160-200	98-134
	Tropical Grassland (G)	18	42
	Tropical Moist Forest (F)	60-250	115-120
	Tropical Open Forest (F)	55	69
	Tropical Rain Forest (F)	127	190
	Tropical Seasonal Forest (F)	140-150	80-98
	Tropical Woodland (F)	27	69
	Tundra (N/A)	5	165
	Woodland (F)	90	90

Soil carbon

Soil carbon data provided in the Woods Hole database also corresponds to ecosystem type as shown in Table 2-4. The soil carbon provided is the initial carbon stock measured to 1 m depth for each ecosystem type. [66] It is estimated that about 25% of the carbon is lost to the atmosphere with cultivation, although the rate of loss depends on the ecosystem (based on research in [69,70,71]).

Foregone Sequestration in Forests

There are two types of foregone sequestration considered in the Woods Hole database: (1) the lost opportunity for CO₂ uptake by existing forests once they are converted to other uses (uptake of existing forests), and (2) the lost opportunity from re-growing forests in lands in which cropland is retracting (uptake of re-growing forests), which is considered for the EU and the FSU.

To determine the foregone emissions, the database includes both the total land area cover of growing forests (in ha), land area cover of re-growing forests (in ha) of a particular ecosystem type, and emission factors (EF-given in Mg C year⁻¹) for each type of ecosystem. The annual emissions from foregone sequestration are then the EF divided by the total area of forest. This is then multiplied by the number of years of foregone sequestration (30 years for a 30-year EF).

Other issues with the database are described in [66]. One error includes information about the soil carbon, which in previous reports was significantly higher due primarily to the fact that 50% of the soil carbon was assumed to be lost in the earlier estimate versus approximately 25-30% in the later estimate. The article states that 50% loss generally applies to the upper 20-30 cm of the

Scheme 2-1: General equations to calculate 30-year EF from Woods Hole database

The 30 year emission factor from Woods Hole database is the sum of the carbon contained in the above and below ground vegetation, the carbon lost from the soil, and the number of years of foregone sequestration, weighted for each ecosystem within a region as shown in the equation below:

$$EF_{30_year} = \sum_i F_i * (x * C_{veg,i} + y * C_{soil,i} + N * C_{foregone,i}) * (44/12)$$

i	each ecosystem within a region
EF _{30_year}	30-year emission factor (in Mg CO _{2,eq} / ha)
F _i	Weighting factor for each ecosystem within the region.
C _{veg}	Carbon in above and below ground vegetation (Mg C/ha)
x	% of C in vegetation lost during land conversion
C _{soil}	Carbon in soil (Mg C/ha)
y	Loss of Carbon contained in the soil.
C _{foregone}	Foregone sequestration (Mg C/ha yr)
N	number of uptake years (30 for a 30-year emission factor)
44/12	gram CO ₂ / gram C

soil carbon, but 25% loss applies to soil carbon at a 1m depth.

The sum of the emissions from carbon in vegetation, lost soil carbon and foregone sequestration are taken to give an emission factor for each ecosystem type within each region. The historical LUC data are then used to weight the contribution of each into a single emission factor per region. The emission factor in g C ha^{-1} is converted into $\text{g CO}_2 \text{ ha}^{-1}$ by multiplying by 44/12 (the ratio of the mass of CO_2 to C). However, the Woods Hole database is applied differently by Searchinger, CARB, and Tyner, with each using the data to calculate a slightly different emission factor. The general equation is shown in Scheme 2-1, and the application of the equation is described for each of the studies in Table 2-5.

As described in Table 2-5, CARB takes a similar approach to calculating 30-year emission factors as Searchinger. The primary differences are (1) CARB uses the historical land use clearing patterns to determine two EFs (one for conversion from forests, one from conversion from grasslands), while Searchinger calculates a single weighted EF for each region; and, (2) CARB assumes that 90% of the carbon in vegetation is released upon land clearing, while Searchinger assumes that 100 % is released.

Tyner, however, has taken a fairly different approach in applying the Woods Hole database. Similar to CARB, Tyner also determines two weighted emission factors for conversion from forests and grasslands. However, he weights the data using the total forested area data, rather than historical land clearing. Also, Tyner makes no assumption that the EU and FSU have retracting croplands, and so applies the basic approach to soil carbon (only 25%) and foregone sequestration as uptake avoided by existing forests. Additionally, he assumes only 75% of the carbon in vegetation is lost during land conversion, and that the remaining 25% is stored in wood products.

The Figure 2-4 shows how these assumptions affect the 30-year EFs for each region for conversion from forests (Figure 2-4-A) and grasslands (Figure 2-4-B). Although Searchinger calculates a single weighted EF for each region, enough data are provided to determine EFs for conversion from forest and grassland to compare with those of CARB and Tyner. Figure 2-4 shows that within each region, conversion from forest has a much higher emission factor than conversion from grassland (note the differences in scale between Figure 2-4-A and Figure 2-4-B).

CARB generally uses slightly lower EFs than Searchinger, due to the assumed lower percentage of carbon emitted from vegetation. The EFs for EU and FSU are identical for Searchinger and CARB.

Table 2-5: Application of Woods Hole database in Searchinger, CARB and Tyner.

EF Component	Searchinger (2008)	CARB- LCFS (2009)	Tyner (2010)
Weighting by Ecosystem type (F _i)	A single EF is calculated for each region based on the historical land clearing data from the 1990's. The % of each type of ecosystem cleared within the region is used to weight the final emission factor.	Two EFs are calculated: one for conversion from forests and one from grasslands. The historical land clearing data from the 1990's are used to determine the weighting factors from the total area of grassland and total area of forestland cleared.	Two EFs are calculated: one for conversion from forests and one from grasslands. The total forested land area is used to develop the weighting factors for each land type classification.
Carbon in Vegetation (x)	100% of the above and below ground carbon is emitted. A correction factor for Harvested Wood Products is included, but not used.	90 % is emitted CARB cites IPCC defaults, Searchinger, Guo, [47] and D. Murty[72]	75% is emitted No reference provided
Carbon in Soil (y)	For cropland expansion: 25% of carbon in soil is assumed to be lost. For cropland retraction (in the EU and FSU): the carbon gain is calculated as 75% of the original 25% carbon lost from the initial conversion (i.e. 18.75%).	For cropland expansion: 25% of carbon in soil is assumed to be lost. For cropland retraction (in the EU and FSU): the carbon gain is calculated as 75% of the original 25% carbon lost from the initial conversion (i.e. 18.75%).	25% of soil carbon in all regions.
Time Period of Foregone Sequestration	30 years	30 years	30 years
Foregone Sequestration (C _{foregone})	For cropland expansion: the uptake per forest area (Mg C ha ⁻¹ yr ⁻¹) is calculated by the gross uptake/ forested area (or grassland). For cropland retraction (in the EU and FSU): the uptake from re-growing forests is calculated by the gross uptake/ area of regrowing forests (or grassland).	For cropland expansion: the uptake per forest area (Mg C ha ⁻¹ yr ⁻¹) is calculated by the gross uptake/ forested area (or grassland). For cropland retraction (in the EU and FSU): the uptake from re-growing forests is calculated by the gross uptake/ area of regrowing forests (or grassland).	Uptake per forest area (Mg C ha ⁻¹ yr ⁻¹) is calculated by the gross uptake/ forested area (or grassland).

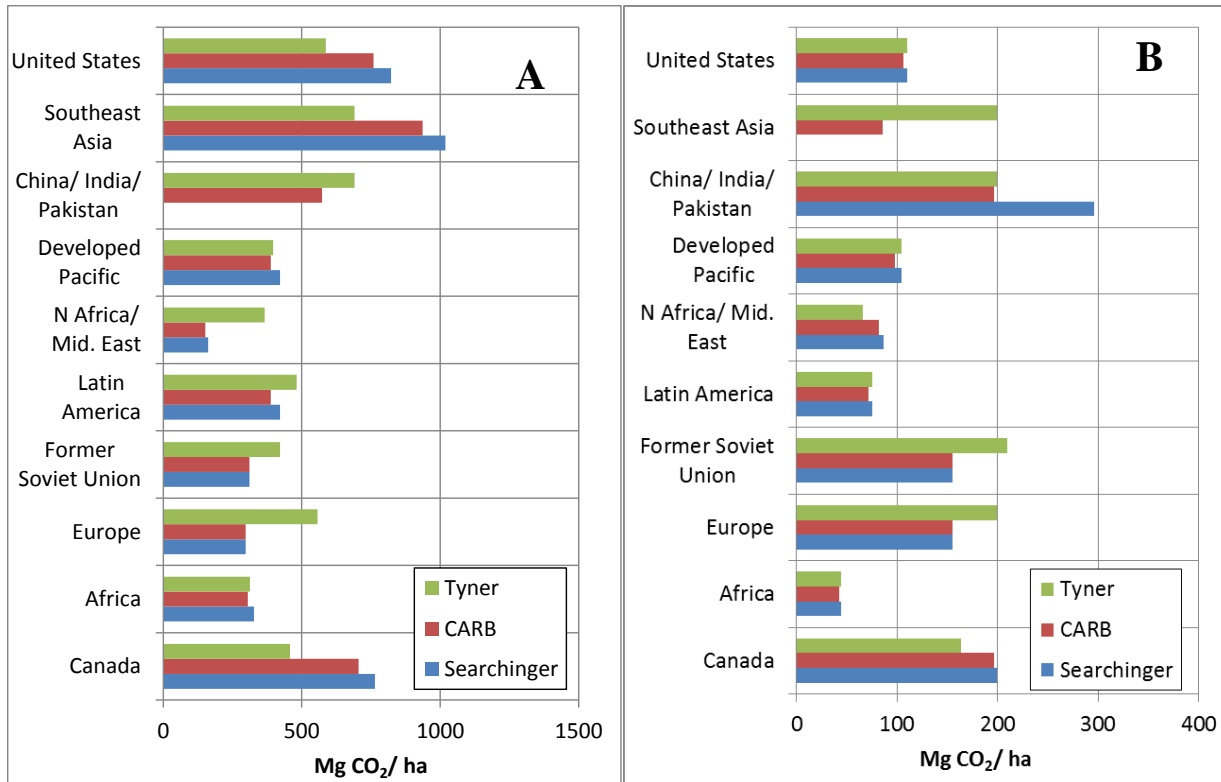


Figure 2-4: 30-year emission factors (in Mg CO₂ha⁻¹) for Searchinger, CARB and Tyner for conversion from A) forest and B) grassland.

Tyner, however, uses quite different EFs. In many cases, the forest conversion EF is actually higher than the EF from Searchinger, particularly for the EU and the FSU due to the differences in foregone sequestration calculation and differences in weighting. However, applications of results from the Tyner study produce even more significant differences, as will be discussed further in Section 2.6.

2.4.2 WINROCK CARBON STOCK DATABASE

The Winrock emission factor database is an ExcelTM workbook that can be used to calculate emission factors for conversion or reversion factors from multiple land categories. The database is much more expansive than the Woods Hole database, containing carbon stock data for 8 land classification categories for 755 administrative units in 160 countries [73]. The carbon stock data for each of the 8 categories, which include forest, soil, grassland, cropland, savanna, shrub, wetland, perennial and mixed, are given in tons CO_{2, eq}ha⁻¹. 47 unique emission factors for each of the 755 regions can be calculated from the spreadsheet for either conversion or reversion of land classifications as shown in Table 2-6. (Note: some land conversion combinations are repeated in this matrix, which are excluded in the count. However, same category conversions such as grass to grass are included, resulting in 47 EFs.)

Table 2-6: Winrock Emission Factor Database carbon stock and conversion/ reversion categories.

From	→	To
Forest	←	Crop
Grass		Grass
Savanna		Savanna
Shrub		Perennial
Wetland		
Perennial		
Mixed		

The carbon stock data for 8 land classification categories contained in the spreadsheet are described below.

1. Forest Carbon Stocks

Carbon stocks for above-ground carbon in biomass are based on spatial maps of forest carbon stocks compiled by Winrock International from several different data sources as shown in Figure 2-5. In cases where below-ground carbon (i.e. contained in live roots) was not included, Winrock estimated it to be about 25% of the aboveground biomass. Spatially averaged forest carbon stocks for above and below ground carbon is shown in Figure 2-6.

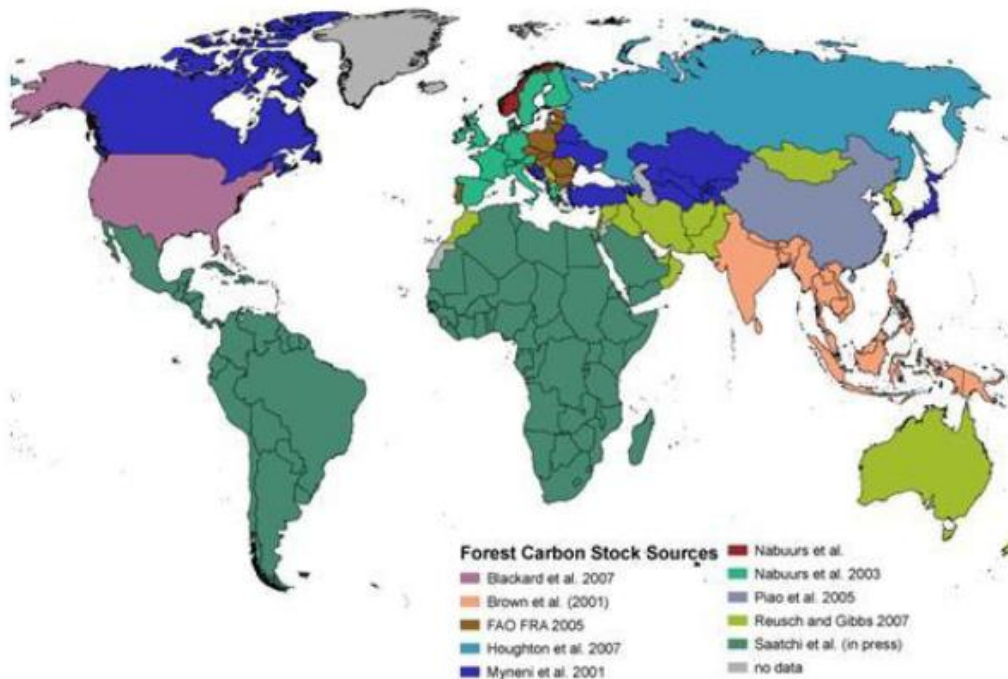


Figure 2-5: Data sources used for estimating forest carbon stocks in Winrock emission factor analysis. Source [55]

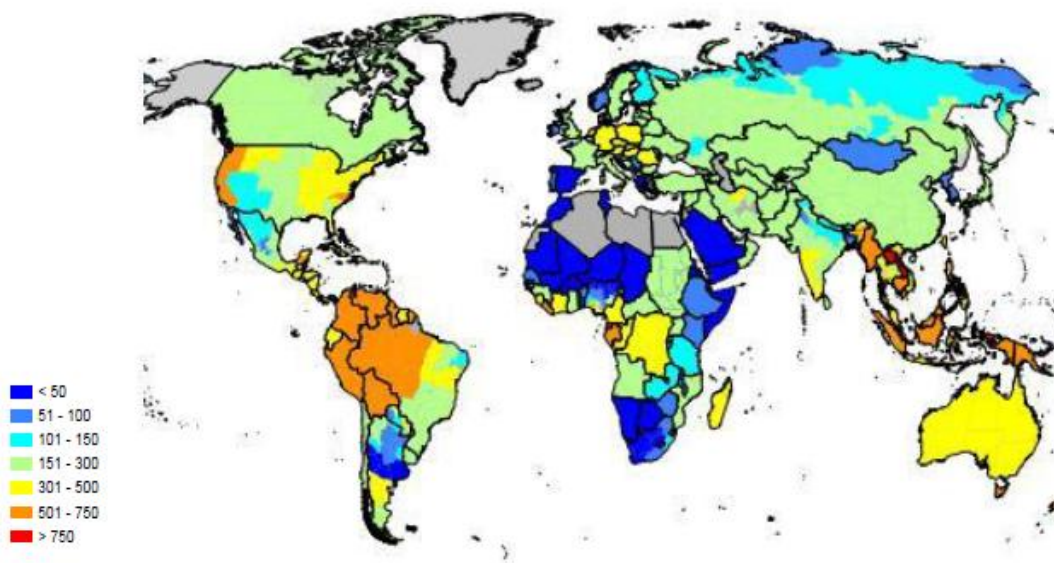


Figure 2-6: Spatially averaged forest carbon stocks in above- and belowground biomass (in $t\ CO_2\ ha^{-1}$) used in the Winrock emission factor analysis. Source [55]

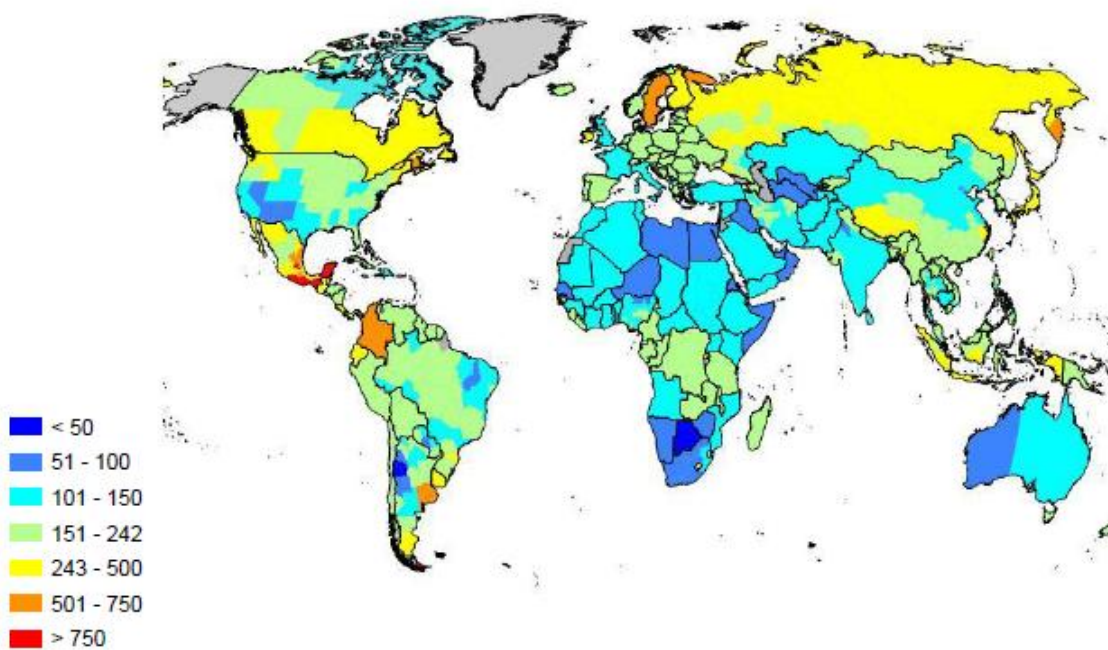


Figure 2-7: Soil carbon stocks in the top 30 cm of soil for each country and/or administrative unit as calculated by Winrock from the World Harmonized Soil Database v.1.1. (Units in $tons\ CO_2\ ha^{-1}$). Source: [55]

2. Soil Carbon Stocks

Soil carbon stocks data in the Winrock emission factor database are based on the Harmonized Soil Map of the World, V.1.1. that was released in March, 2009. The map has 1-km resolution grid cells and includes bulk density (g cm^{-3}) and carbon content (%C) in both the top 30 cm and top meter of soil. Winrock determined carbon stocks in the top 30 cm of soil by multiplying the volume of soil in a given hectare ($3,000\text{m}^3$) by the bulk density and then by the carbon content to derive an average soil carbon stock per hectare (t C ha^{-1}). Soil carbon stocks by country or administrative unit are illustrated in Figure 2-7.

3. Cropland Carbon Stocks

Two types of cropland are included in the Winrock emission factor database, annual cropland (named cropland) and perennial cropland (named perennial).

Perennial crops include sugarcane and oil palm only. Perennial crops in Malaysia and Indonesia are assumed to be oil palm, which are assigned a carbon stock of $15 \text{ t CO}_2 \text{ ha}^{-1}$. All other countries are assumed to be sugarcane with a carbon stock of $44 \text{ t CO}_2 \text{ ha}^{-1}$.

All annual cropland in all regions are assigned a carbon stock of 5 t C ha^{-1} ($18 \text{ t CO}_2 \text{ ha}^{-1}$) based on Table 5.9 of IPCC Agriculture, Forestry and Land Use (AFOLU).

4. Grassland, Savanna and Shrubland

Carbon stocks for above and belowground biomass in grasslands, savanna and shrubland were estimated from Table 6.4 from IPCC AFOLU, except Brazil, which is estimated from a variety of literature sources. A proportional approach was used to estimate savanna and shrubland based on the Brazil dataset, which indicated that crop stocks trends from grassland, savanna, to shrubland in a ratio of 1 to 1.8 to 3.4. Grassland data used in the Winrock database are shown in Figure 2-8.

5. Wetland, Barren and Mixed Carbon Stocks

Wetland carbon stocks are calculated as the average of shrubland and grassland categories. Barren lands are not included in the database, but are included in the corresponding MODIS satellite data, so are assigned a value of $0 \text{ t CO}_2 \text{ ha}^{-1}$. The mixed land cover category is an average of carbon stocks in forest, shrubland, grassland, and cropland.

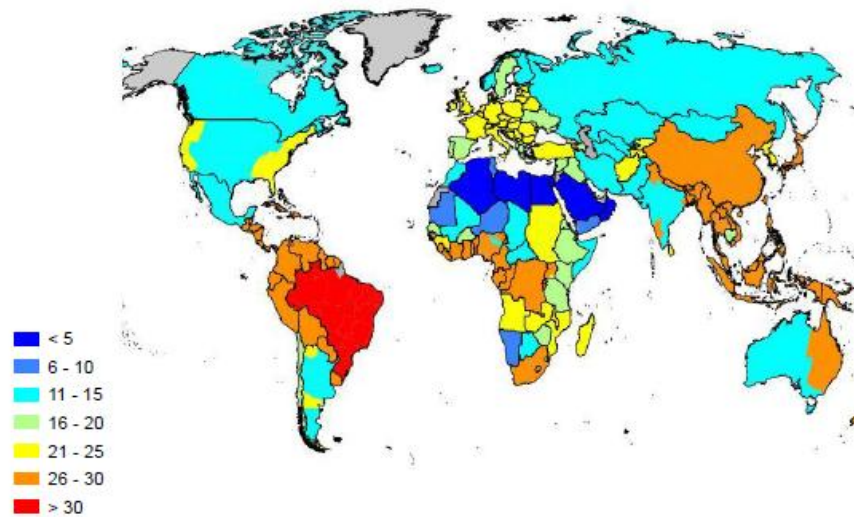


Figure 2-8: Grassland carbon stock estimates used in the Winrock emission factor analysis by country and administrative unit. For savanna, multiply by 1.8. For shrubland, multiply by 3.4. Units in $t\ CO_2\ ha^{-1}$. Source:[55]

Emission factors are calculated within the database by the sum of changes in above- and belowground biomass carbon stocks, annual changes in soil carbon stocks on mineral soils, annual emissions from peat drainage on peat soils cleared for agriculture, annual foregone forest sequestration, and non- CO_2 emissions resulting from land clearing by fire (N_2O and CH_4) following IPCC recommendations. [55] In addition to the carbon stock data described above, the database includes numerous flags and factors for calculation of soil carbon emissions, fire emissions from burning to clear the land, peat drainage emissions, and foregone sequestration emissions. The calculations for each of these contributions to the emission factor are described in Scheme 2-2.

The changes in carbon stocks from conversion or reversion of land categories are calculated to determine emission factors, which are estimated for year 0, years 1-19, and years 20-80. These annual factors are then used to determine a 30-year emission factor for each administrative unit in each conversion category.

The spreadsheet can be used to determine emission factors for 47 land conversion or reversion types in each of the administrative units (Table 2-6). Reversion factors indicate the carbon uptake that occurs when land is abandoned and left to revert to its original state. The data are used in reverse to calculate the reversion emissions, with the exception of reversion to forests.

Forest reversion emissions are estimated to be the lower of the annual foregone sequestration over 20 years or the initial forest carbon stock. An example of the emission factors for the admin unit Buenos Aires in Argentina is given in Figure 2-9. (Note: same category conversions are excluded. These conversions include grass to grass, savanna to savanna and perennial to perennial, so 44 EFs are shown.) In all cases except forest EFs, the reversion EFs are estimated as the reverse of the conversion EFs, where increase in biomass stocks occur in year 1, and soil carbon stocks on abandoned cropland are recovered over 20 years. For reversion of forests, it is assumed biomass accumulates over the entire 30-year period at a rate equal to the foregone sequestration rate.

The database yields 35,485 (47*755) EFs by land conversion and

worldwide region. Therefore, it is critical to understand which types and how much of each type of land is converted or reverted in each administrative region in order to estimate a single weighted emission factor. Additionally, since many countries are disaggregated into several administrative regions, the land use conversion amounts and types must be applied to determine a weighted emission factor for each country or region.

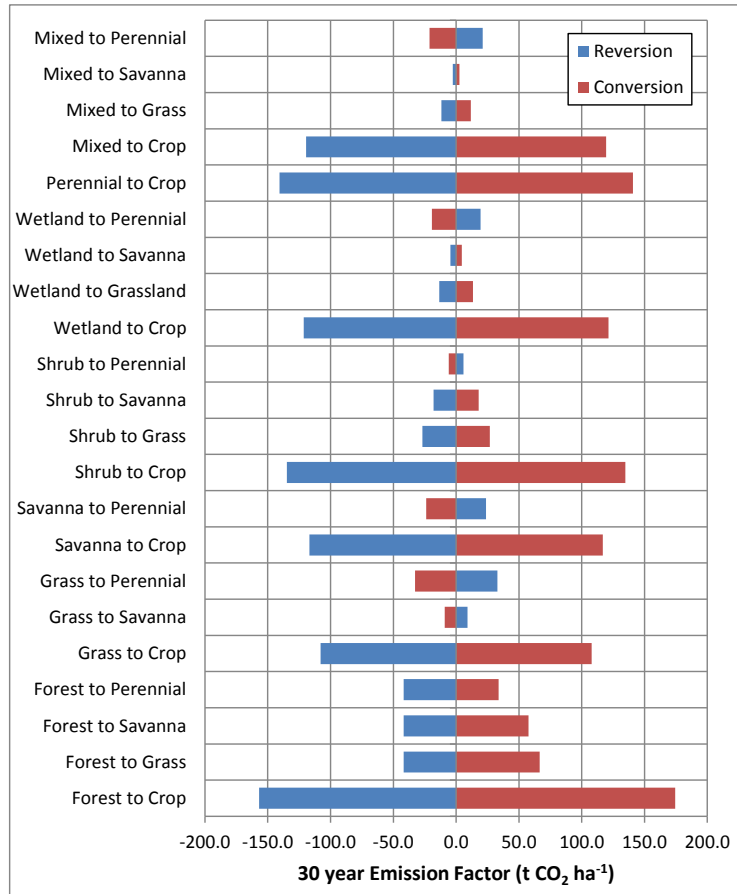


Figure 2-9: 30-year emission factors for conversion and reversion for each land category type for Buenos Aires, Argentina. (Source: Winrock EF Database, 2009)

Scheme 2-2

Winrock calculations for 30-year emission factors for each administrative unit

The 30-year EF is calculated from EFs from year 0, year 1-19, and years 20-80 as:

$$EF_{30\text{ year}} = EF_{\text{year } 0} + 19 * EF_{\text{year } 1-19} + 10 * EF_{\text{year } 20-80}$$

Where:

$$EF_{\text{year } 0} = \Delta C_{\text{biomass}} + \Delta C_{\text{soil}} + \Delta C_{\text{peat}} + \Delta C_{\text{sequestration}} + \Delta C_{\text{fire}}$$

$$EF_{\text{year } 1-19} = \Delta C_{\text{soil}} + \Delta C_{\text{peat}} + \Delta C_{\text{sequestration}}$$

$$EF_{\text{year } 20-80} = \Delta C_{\text{peat}} + \Delta C_{\text{sequestration}}$$

Where,

$EF_{30\text{ year}}$ 30-year emission factor [t CO₂ ha⁻¹]

$EF_{\text{year } 0}$ EF for emission occurring in year 0 from land transformation [t CO₂ ha⁻¹]

$EF_{\text{year } 1-19}$ EF for emissions occurring in years 1 through 19 after land transformation [t CO₂ ha⁻¹]

$EF_{\text{year } 20-80}$ EF for emissions occurring in years 20 through 80 after land transformation [t CO₂ha⁻¹]

$\Delta C_{\text{biomass}}$ *Change in above and below ground carbon* stocks from the initial and final land category. If forest land is being converted, the starting carbon stock is reduced by the percentage of harvested wood products (HWP) removed (this allows for consideration of HWP, although no data are currently included for % of HWP from any land.) [t CO₂ha⁻¹ yr⁻¹]

ΔC_{soil} *Annual Soil Flux*, which occurs only for *conversion to cropland*, is determined as follows]:

$$\Delta C_{\text{soil}} = \frac{C_{\text{soil, initial}} \cdot (1 - FLU \cdot FI)}{20\text{ years}} \cdot (1 - \% \text{ peatlands}) \text{ [t CO}_2\text{ / ha yr]}$$

FLU land use factor, which reflects the soil stock changes associated with conversion to cropland, and ranges from 0.48 to 0.8 based on IPCC default values for different management activities.

FI input factor, which represents different levels of C input to soil for cropland, and is set to 1 for all cases.

% peatlands is a value given for Indonesia and Malaysia only.

ΔC_{peat} *Annual Peat Emissions* are calculated only if a flag in the database indicates that the region has peatlands (only Indonesia and Malaysia). These countries include a peat emission factor in t CO_{2,eq} ha⁻¹ yr⁻¹ and a % of peat land. The peat emission factor is the product of these two. [t CO₂ha⁻¹ yr⁻¹]

$\Delta C_{\text{sequestration}}$ *Lost forest sequestration* is a constant value for each region ranging from 0 to 8.2 t CO₂ ha⁻¹ yr⁻¹, and is only applied when forests are being converted.

ΔC_{fire} *Fire emissions from burning to clear land* are applied only if land is converted to cropland, and fire is used to clear land. A flag in the database indicates if fire is used or not. If fire is used, the total emissions are the sum of CH₄ and N₂O emissions, which are each calculated by multiplying the initial above ground biomass carbon store (which is indicative of the total amount of biomass) by the fire combustion factor (F_{fire}) specific to the type of land converted, and the fire CH₄ or N₂O emission factor (CH₄_{EF}, or N₂O_{EF}). That value is then converted to of CO_{2,eq} based on the IPCC 100-year global warming potential (21 and 310, respectively- Note that IPCC 1996 GWP values are used) to give total emissions due to burning in tons of CO_{2,eq} ha⁻¹. Fire combustion factors, CH₄ and N₂O emission factors are given in Table 2-23 and are discussed in more detail in Section 2.7.1.3.

$$\Delta C_{\text{fire}} = C_{\text{stock}} * F_{\text{fire}} * (310 * N_2O_{\text{EF}} + 21 * CH_4_{\text{EF}})$$

The Winrock database is used in conjunction with MODIS satellite data imagery to determine emission factors for the EPA RFS2. Images from MODIS Version 5 land cover dataset from 2001-2007 with a 500 km resolution are used to determine historical LUC for 79 land conversion categories (which includes same category conversion such as grassland to grassland) for over 755 administration units. The calculations to link the two databases are complex and are described in more detail in Section 2.5.1.1.

2.5 LUC APPLICATION AND APPROACHES IN POLICIES

2.5.1 EPA – RENEWABLE FUEL STANDARD (RFS2)

The EPA employs an intricate linkage of numerous models and databases to determine the carbon intensity of various fuels under the Renewable Fuel Standard (RFS2). Their approach is illustrated in Figure 2-10. It involves the use of two different agro-economic models to predict both international and domestic ILUC. Each is linked to its own series of EF databases to determine resulting emissions. Emission factors from the GREET model are used to determine the cradle-grave LCA emissions, and MOVES is used for tailpipe emissions. The methodologies, data inputs, assumptions, etc. used in the EPA RFS2 analysis underwent substantial peer review to ensure the most accurate results possible. The results of many analyses and modeling efforts, including from the draft regulation and final regulation are docketed and available to the public.² Our analysis is from the information contained in these dockets pertaining to the final regulation.

To determine the ILUC emissions associated with each fuel, the results from a reference case, or the “business as usual scenario”, is compared to the control case which includes the policy volume targets. The change in each fuel volume type is modeled individually to estimate the changes attributable to that fuel. The fuel volume scenarios modeled are shown in Table 2-7.

Table 2-7: Fuel Volume Scenarios Considered in RFS2 in billions of gallons (From Table 2.3-1 of EPA[2])

Biofuel	Reference Case (Low Volume)	Control Case (High Volume)	Change
Corn Ethanol	12.3	15.0	2.7
Switchgrass Cellulosic Ethanol	0	7.9	7.9
Corn Residue Cellulosic Ethanol	0	4.9	4.9
Imported Sugarcane Ethanol	0.6	2.2	1.6
Soybean Oil Biodiesel	0.1	0.6	0.5

² Public docket materials for the RFS2 are available at www.regulations.gov under the Docket ID: EPA-HQ-OAR-2005-0161. Additional updates in 2011 (for canola biodiesel) are also available under Docket ID: EPA-HQ-OAR-2010-0133.

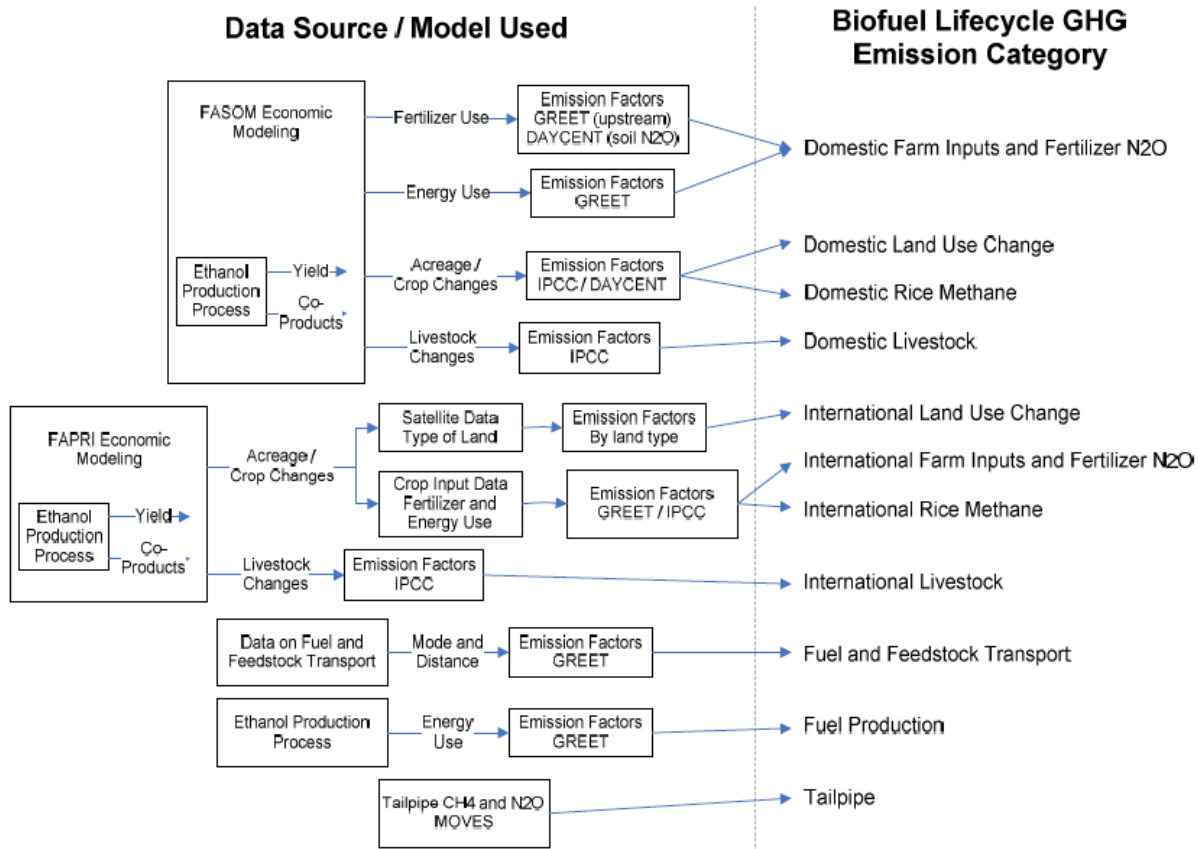


Figure 2-10: System boundaries and modeling flow chart for biofuel LCA in EPA RFS2. [2]

The resulting net carbon intensity of each fuel is the sum of all the outputs listed on the right hand side of Figure 2-10. In this analysis, we focus on the results related to ILUC, which include both domestic and international ILUC. The other “domestic” and “international” categories (including farm inputs and fertilizer N₂O, rice methane and livestock) are considered as part of the direct feedstock production emissions in the RFS2 LCA, so are not included in this analysis.

The domestic and international ILUC are quantified by two separate modeling chains. Domestic ILUC is predicted by FASOM (Forestry and Agricultural Sector Optimization Model), the outputs of which include domestic agricultural sector energy and fertilizer use, changes in number and type of livestock produced, and changes in total land use. This is endogenously linked to IPCC, DAYCENT and FORCARB emission factor databases to predict the total GHG attributed to domestic ILUC.

International ILUC is modeled with the FAPRI-CARD model (Food and Agricultural Policy and Research Institute international model as maintained by the Center for Agricultural and Rural Development at Iowa State University). FAPRI-CARD predicts the global land use and livestock changes and land use types. Its outputs are linked to emission factors generated from Winrock International carbon stock data linked to MODIS satellite data of historical land conversion trends

from 2001-2007. International and domestic ILUC methodologies, databases and results are described separately below.

2.5.1.1 International Land Use Change

Modeling of international ILUC in EPA RFS2 is done through use of the FAPRI agro-economic model linked to the Winrock EF database, which is used in conjunction with MODIS satellite data. The output data from each of the modules are incongruent, so various groupings and weightings are accomplished through the use of a stochastic model by ICF³. [74,75] The stochastic model first applies a Monte Carlo simulation to the MODIS satellite data to assess its uncertainties and produce corrected LUC. ICF uses the results of the simulations to group the satellite data into corresponding Winrock and FAPRI classifications. The linkage between these three models and calculations within the stochastic model are described below.

The FAPRI-CARD international module results are applied in the EPA RFS2 analysis. However, the results for the U.S. are included within the module, so are discussed herein although the U.S. GHG results are replaced by the FASOM modeling results discussed in the next section.

The FAPRI-CARD model predicts changes in crop production acreages for 20 different types of crops within 54 regions. It also determines the changes to units of livestock in each region, which is related to livestock stocking rates to predict the changes to pasture acreage. As shown in Figure 2-10, the crop acreage is linked to fertilizer use to determine international agricultural and rice methane emissions. These emissions are attributed to the agricultural production phase of the feedstock, and are not considered part of the ILUC results. Additionally, the livestock changes are linked to IPCC livestock emission factors to determine emissions from livestock. For this purpose, these will also be considered direct changes and will not be discussed in this section.

ILUC is the change in crop and pasture area (given in ha) predicted by FAPRI for each of the 54 regions. The crop area changes are subsequently broken down into perennial crops (which include sugarcane and palm oil) and annual crops. Therefore, there are three land area classifications (annual, perennial and pasture) for each of the 54 regions (totaling 162 data points). The land area changes are given as either a positive value (indicating an expansion of that land type), or a negative (indicating a retraction of land type).⁴

The land area changes must be linked to the emission factors, which are based on a *conversion*-between land categories. The FAPRI model does not predict changes to forests or natural ecosystems, rather, conversion classifications are done exogenously with the stochastic model

³ Note: it is not clear that the final results from the stochastic model are used for the CI calculations included in the final rule of the RFS2. However, the MODIS data and emission factors are available in the stochastic model to discuss the methodologies that are followed for the weighting of EFs from Winrock.

⁴ FAPRI-CARD results from all scenarios are provided in the EPA public docket at EPA-HQ-OAR-2005-0161-3153

database.⁵ The land conversions are first assumed to be moved within land classifications from FAPRI. For example, if pastureland is declining while annual cropland is increasing, it is assumed that the decrease in pastureland is converted to annual cropland. When there is greater land expansion than retraction, the expansion is met through reduction in natural ecosystems. This systematic approach gives the following different conversions, where a positive number indicates a conversion to, and a negative number indicates a reversion from each category:

- Annual crops to/ from perennial crops
- Pasture to/from Perennial crops
- Pasture to/from Annual crops
- Natural ecosystems to/from Annual Crops
- Natural ecosystems to/from Perennial Crops
- Natural ecosystems to/from Pasture

Therefore, the FAPRI results yield a total of 12 land conversion types for each of the 54 regions (648 data points). This matrix of land area changes (given in ha) must be linked to the appropriate emission factors to calculate the GHGs from LUC.

Winrock data are used to determine the EFs; however, they provide 47 conversion categories for 755 administrative units (yielding 35,485 EFs). These EFs must be aggregated into an identically sized matrix of EFs from the FAPRI output to calculate the net GHG release. The aggregation is done utilizing the MODIS satellite data to appropriately weight the conversion categories and admin units into similar groupings for the FAPRI results. These aggregations are also done within a stochastic model by ICF International [74,75]. A flow chart of the calculations and linkage between FAPRI and Winrock is provided in Figure 2-11, and is described in detail below.

The MODIS data provide 79 different land conversion categories for over 755 administrative units (it includes the additional land categories of barren lands and excluded lands, which are not included in the Winrock database. The EFs from barren lands are assigned $0 \text{ g CO}_2, \text{eq ha}^{-1}$). The Monte Carlo simulation uses a confusion matrix to correct for land classes which tend to be misclassified. The corrected MODIS data are then used to evaluate the types of land affected by the projected land conversions in each scenario.

Conversion categories from MODIS matching those from the Winrock dataset are aggregated to match the 12 conversion categories from the FAPRI model, as shown in Table 2-8. Four additional conversion categories are included for conversion from Barren lands. Additionally, Winrock does not calculate EFs for the reversion to Wetlands, and the conversion category of perennial to perennial is excluded. MODIS data do not distinguish between annual and perennial

⁵ The Stochastic model report and excel spreadsheets are available in the EPA public docket under ID number EPA-HQ-OAR-2005-0161-3152.

cropland, so a default of 95% conversion to annual and 5% conversion to perennial cropland is applied.

To determine a single weighted average conversion factor for each type of conversion within each region, the 755 administrative units of the Winrock data are also aggregated into 54 FAPRI regions (as shown in Appendix A), and the 47 conversion factors are aggregated into corresponding 12 FAPRI conversion factors (Table 2-8). The net land use conversion occurring for one FAPRI classification (i.e. natural to annual) within each individual FAPRI region is summed to determine a land use share factor for each of the Winrock conversion classifications and regions.

This *land use share factor* is then used to weight each of the emission factors from the Winrock data, which can then be summed into a single emission factor for each of the 12 conversion categories and 54 FAPRI regions. The matrix of emission factors is then applied to the output of the FAPRI results to provide an estimate of total GHGs from international ILUC.

The results from each fuel scenario modeled are given in Table 2-9. The results will be discussed in more detail and compared to other modeling results in Section 2.6.

Table 2-8: Conversion categories and groupings from FAPRI, Winrock and MODIS.

Note: Superscripts: M = conversion category in MODIS only (Barren lands); 1 or 2 indicates duplicate categories, 1 indicating its first use, and 2 indicating its second use; S= same category conversion such as grassland to grassland. Excl. Indicates corresponding reversion category to Wetland from Winrock is excluded.

Conversion Categories		Reversion Categories	
FAPRI	Winrock/ MODIS	FAPRI	Winrock/ MODIS
1. Annual to Perennial	Croplands to Perennial	7. Perennial to Annual	Perennial to Croplands
2. Pasture to Perennial	Grasslands to Perennial ¹ Savanna to Perennial ¹	8. Perennial to Pasture	Perennial to Grasslands ¹ Perennial to Savanna ¹
3. Pasture to Annual	Grasslands to Croplands ¹ Savanna to Croplands ¹	9. Annual to Pasture	Croplands to Grasslands ¹ Croplands to Savanna ¹
4. Natural to Annual	Forestland to Croplands Grasslands to Croplands ² Mixed to Croplands Savanna to Croplands ² Shrubland to Croplands Wetland to Croplands Barren to Croplands ^M	10. Annual to Natural	Croplands to Forestland Croplands to Grasslands ² Croplands to Mixed Croplands to Savanna ² Croplands to Shrubland Excl.
5. Natural to Perennial	Forestland to Perennial Grasslands to Perennial ² Mixed to Perennial Savanna to Perennial ² Shrubland to Perennial Wetland to Perennial Barren to Perennial ^M	11. Perennial to Natural	Perennial to Forestland Perennial to Grasslands ² Perennial to Mixed Perennial to Savanna ² Perennial to Shrubland Excl.
6. Natural to Pasture	Forestland to Grassland Grassland to Grassland ^{S,1} Mixed to Grassland Savanna to Grassland ¹ Shrubland to Grassland Wetland to Grassland Barren to Grassland ^M Forestland to Savanna Grassland to Savanna ¹ Mixed to Savanna Savanna to Savanna ^{S,1} Shrubland to Savanna Wetland to Savanna Barren to Savanna ^M	12. Pasture to Natural	Grasslands to Forestland Grassland to Grassland ^{S,2} Grasslands to Mixed Grassland to Savanna ² Grassland to Shrubland Excl. Savanna to Forestland Savanna to Grasslands ² Savanna to Mixed Savanna to Savanna ^{S,2} Savanna to Shrubland Excl.

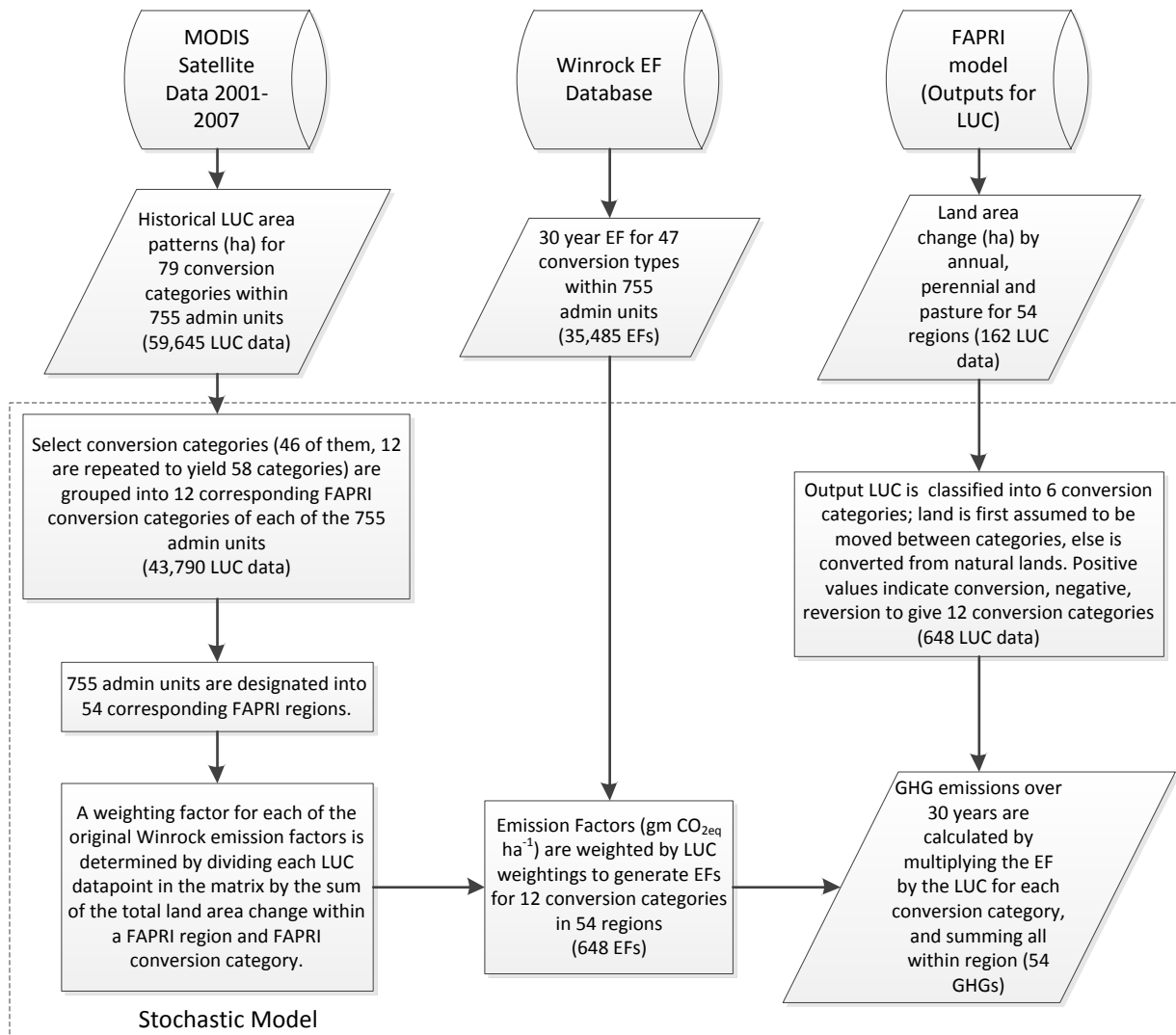


Figure 2-11: Flow chart of model linkage and calculation flows for international ILUC modeling in the EPA RFS2. The calculations within the stochastic model are shown within the dotted line.

Table 2-9: International ILUC and GHG results from each fuel scenario modeled in the RFS2. Source: Table 2.4-29 from [2] and author's calculations. Results from FAPRI do not include ILUC in the U.S.

Scenario	International Crop Area Change (000 ha)	Normalized Crop Area Change (ha bBTU ⁻¹)	30-year annualized GHG from LUC (kg CO _{2,eq} mmBTU ⁻¹ yr ⁻¹)
Corn Ethanol	789	3.94	31.7
Soy-based biodiesel	678	10.65	42.5
Sugarcane Ethanol	430	4.38	4.3
Switchgrass Ethanol	1,358	2.25	15.1

2.5.1.2 Domestic Land Use Changes

The area of domestic ILUC in the EPA RFS2 are predicted by the FASOM model, which is internally linked with data from the DAYCENT/ CENTURY and FORCARB models to predict the LUC-GHGs. Since the LUC effects are interrelated for all fuels, the changes in fuel volumes for the complete policy are modeled simultaneously to determine the total LUC. In order to isolate the incremental impacts of each fuel, the other fuel volumes were held constant, and the volume of the fuel investigated is decreased to its business as usual scenario as shown in Table 2-10. The LUC effects attributed to each fuel are then the difference between the control case and the fuel-specific case.

Table 2-10: EPA RFS2 2022 Fuel Volumes modeled with FASOM for each fuel scenario (in billions of gallons)
Source: EPA- RFS2 Table 2.4-1[2]

Note: the shaded boxes represent the business as usual scenario, without EISA.

	Control Case	Biodiesel Only Case	Corn Ethanol Case	Corn Stover Case	Switchgrass Ethanol Only Case
Soybean Biodiesel	0.6	0.1	0.6	0.6	0.6
Corn Ethanol	15.0	15.0	12.3	15.0	15.0
Corn Stover Ethanol	4.9	4.9	4.9	0.0	4.9
Switchgrass Ethanol	7.9	7.9	7.9	7.9	0.0

In the final RFS2 rule, FASOM was used to model changes in the soil carbon and biomass carbon due to land use conversion between cropland, pasture, forestland and developed land. Carbon sequestration is also considered, and FASOM includes consideration for carbon storage that reaches equilibrium.

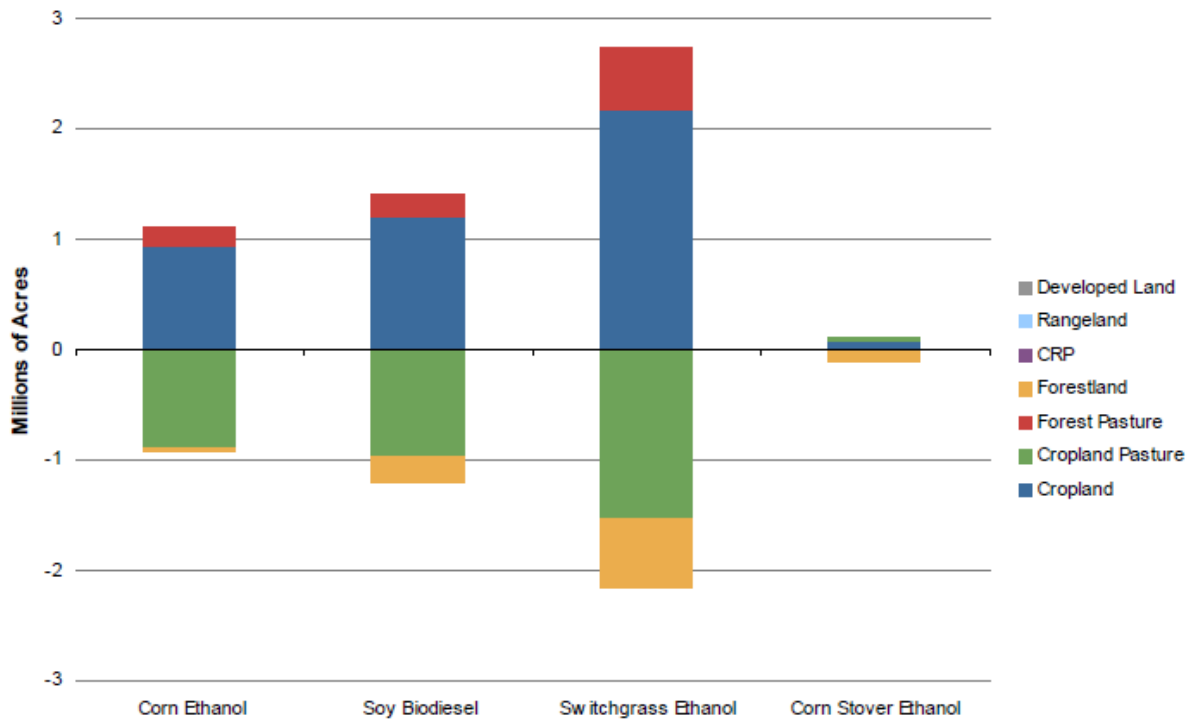
The details and reports from FASOM are also available in the public docket.⁶ Since the GHG modeling is done within the FASOM model, it is difficult to interpret how the calculations are performed. Additionally, the data provided in the reports are difficult to link without a more detailed explanation. For example, the changes in domestic cropland area used for production in the 2022 scenario are provided in Table 2-11. However, the data provided in the table, taken from the RFS2 report (Table 2.4-26 in [2]) do not match the explanation provided in the text, or the following figure, shown in Figure 2-12, which indicates that cropland increases by 0.9 million acres under the corn ethanol scenario, while cropland pasture decreases by 0.9 million acres, forestland decreases by 0.03 million acres and forest pasture increases by 0.2 million acres. The calculation of 30-year annualized GHG emissions for each scenario, also shown in Table 2-11, is negative, indicating that domestic ILUC result in a decrease in GHG emissions. It

⁶ RFS2 Dockets can be accessed at www.regulations.gov. The FASOM Final Technical Report [61] is available under docket ID number EPA-HQ-OAR-2005-0161-3178, and the data from FASOM is available at EPA-HQ-OAR-2005-0161-3179.

is not clear which emission factors are used to produce these results, and there is no explanation for the reason of negative emissions.

Table 2-11: Change in total domestic cropland used for production by scenario in the RFS2 in 2022 and resulting GHG emissions. Source: [2] p 356 and p 367.

Scenario	Total Cropland Increase (million acres)	Normalized Cropland Increase (acres per thousand gallons ethanol equivalent)	Change in GHG due to domestic LUC annualized over 30 years (kg CO ₂ eq mmbTU ⁻¹)
Corn Ethanol	1.4	0.12	-4.0
Soybean Biodiesel	1.9	0.39	-8.9
Switchgrass Ethanol	4.2	0.04	-2.5
Corn Stover Ethanol	0.6	0.06	-10.8



Note: Some of these land use categories are not used in GHG emission calculations

Figure 2-12: Changes in domestic land use by type for RFS2, 2022. Source:[2] p 358.

2.5.2 CALIFORNIA AIR RESOURCES BOARD- LOW CARBON FUEL STANDARD

California’s Low Carbon Fuel Standard (LCFS) was implemented with the Governor’s Executive Order S-01-07 in January, 2007, approved in April 2009, and went into effect in

January, 2010.[76] The LCFS requires a 10% reduction in CI of transportation fuels by 2020. The reduction is measured through LCA, and includes ILUC.

In 2009, CARB developed CI look-up tables for numerous fuel pathways before the regulation went into effect on January 12, 2010. The biofuel pathways include corn ethanol, sugarcane ethanol, and soy biodiesel. The “direct” emissions from the biofuel pathways were modeled with the GREET model adapted for California, and the “indirect” LUC emissions were modeled based on methodologies followed by Searchinger using the GTAP economic model with the Woods Hole database.

An expert workgroup consisting of 30 members was established in February 2010 to review and reflect on the LCFS. In April, 2010, Purdue published a revised GTAP analysis of LUC for Argonne that resulted in $\frac{1}{2}$ to $\frac{1}{3}$ the amount of GHG emissions from ILUC originally predicted by CARB[5]. After review of this work, the expert workgroup recommended that CARB update their ILUC to address the following [76]:

- GTAP model updates by Tyner (Tyner 2010)
- Use a consistent model version and inputs for all biofuel pathways
- Re-evaluate DDGS co-product credit
- Develop a more comprehensive and spatially explicit set of carbon stocks and emission factors
- Gain a better understanding how food consumption is predicted
- Justify or adjust the time accounting methodology
- Improve and update the land pools considered accessible in GTAP
- Address the indirect effects of other transportation fuels.

CARB has since been working with developers of the GTAP model at Purdue University and others to improve the analysis of LUC. The GTAP model has been updated to specifically include biofuels (GTAP-BIO), and researchers have revised inputs to reflect current economic fluctuations. Additionally, CARB is moving away from using the coarse Woods Hole database for emission factors; is working with researchers to develop improved maps of forest, pasture and cropland cover data; and is adopting the Harmonized World Soils Database (HWSD). However, CARB is still in the preliminary and review phases of updating its CI values for LUC, and is working toward having new numbers by the middle of 2012.

In the following sections, the current methodology is described, followed by updates for the targeted methodology.

2.5.2.1 Current CARB Methodology

In the fuel pathways currently published in CARB’s lookup tables⁷, ILUC is modeled through linking the Woods Hole database with LUC predictions from the GTAP economic model.

The GTAP model determines the land changes (in ha) in pasture, cropland and forests within 18 different regions in response to policy changes.⁸ For the ethanol, soy and sugarcane pathways, 15 billion gallons, 995 million gallons, and 2 billion gallons are modeled, respectively. The land area output of the GTAP model is linked to EFs developed from the Woods Hole Database.

CARB uses the Woods Hole database to determine emission factors in Mg CO_{2,eq}ha⁻¹ over a 30-year time periods for the conversion of:

- Forest lost (to crops)
- Forest gained (from pasture)
- Grassland lost (applied to livestock and pasture conversions)

Emissions from cropland are assigned 18 Mg CO_{2,eq}ha⁻¹year⁻¹. The Woods Hole database includes only 10 regions, so are matched to the GTAP AEZs as shown in Table 2-12. The “Rest of World” region in Woods Hole is determined by the weighted average of the 10 regions. The emission factors are multiplied by the land area output from GTAP for a specific type of conversion to determine the net GHGs from ILUC.

Table 2-12: GTAP regions and their corresponding Woods Hole Regions in CARB.

GTAP Region	Woods Hole Region
United States	United States
Canada	Canada
European Union- 27 Rest of Europe	Europe
Brazil Latin American Exporters Rest of Latin America	Latin America
India China and Hong Kong	China India Pakistan
Soviet Union/ Russia	Former Soviet Union
Oceania	Developed Pacific
Middle Eastern and North Africa	North Africa / Mid. East
Sub-Saharan Africa Rest of Africa	Africa
South Asia Rest of Asia	Southeast Asia
Rest of High Income Asia Japan	Rest of World

⁷ Lookup tables for CI values used in the LCFS are published at <http://www.arb.ca.gov/fuels/lcfs/lcfs.htm>. CI values discussed herein were last updated on February 24, 2011.

⁸ GTAP includes 19 regions, yet only 18 of them are reflected in the Woods Hole spreadsheet published by CARB.

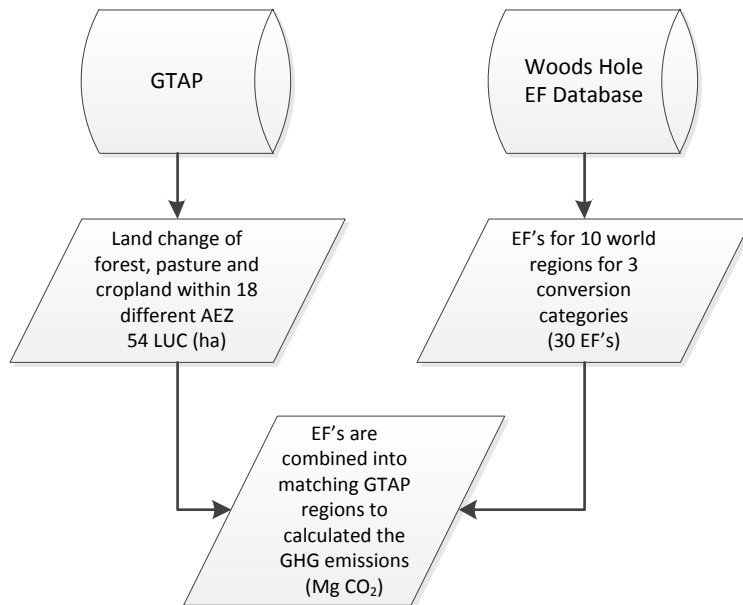


Figure 2-13: Schematic of CARB ILUC modeling database flow.

Although the LCFS underwent peer review, datasets for each fuel pathway are not as detailed as those provided by the EPA. Data and reports are scattered in many locations, including the Staff Report [77] and its appendices [78], as well as documents for each of the individual pathways [79,80,81,82]. However, there have been revisions and updates to individual pathways and new documents have been published for those revisions (for example, updates to ILUC analysis for soy-biodiesel on 01/29/2010 are published on the LCFS website [83]), but the initial staff report has not been updated. Much of the calculations, data and descriptions for ILUC modeling are distributed throughout the documentation, and results from different pathways are presented in different locations. For those reports that are available, the level of detail of the results is minimal. For example, the ILUC modeling for corn ethanol is provided in Chapter IV of the staff report. The documentation provides some key sensitivity analysis inputs and LUC results from each. The LUC is only segregated by forest and pasture converted within the U.S. and total land converted globally. It does not provide detailed results for the international location of LUC. Additionally, the CI values used in the look-up tables for LUC are determined as averages of scenarios in the sensitivity analysis. Details on the distribution of CI are not available (or at least, we cannot find them). To estimate the breakdown of LUC and CI by location for corn ethanol in Section 2.6, results presented in Hertel are used, which is the study that much of the CARB results are based on. [84] Similar studies for other fuel pathways are not available.

It is therefore difficult to trace the calculations to compare the emission factors applied in the ILUC analysis. An ExcelTM spreadsheet of CARB's calculation of EFs from the Woods Hole database is available [67]. The EFs provided in that spreadsheet are used for comparison with other studies. However, without additional information, it is not clear how these EFs are applied to GTAP results. Overall results from each of the fuel pathways for California are provided in Table 2-13 below. The breakdown of results will be discussed in more detail in Section 2.6.

Table 2-13: LUC and CI results from CARB's LCFS.

Fuel Pathway	Volume modeled (billion gallons)	Total LUC (million ha)	ILUC- CI (g CO_{2,eq} MJ⁻¹)
Corn Ethanol [77]	13.25	3.89	30
Sugarcane Ethanol [77]	2	1.09	46
Soy Biodiesel [83]	0.995	0.94	66

2.5.2.2 Updates to CARB ILUC Analysis in 2011

The revisions to CARB's ILUC values were influenced by work done at Purdue University to update the GTAP model to include data specific for biofuels[5]. Tyner's results (discussed in more detail in Section 2.5.4.2) showed that updates to the GTAP model predicted considerably lower ILUC emissions than previously estimated by CARB. Recently, CARB has been working with Tyner and others at Purdue to incorporate the updated GTAP model into the LCFS policy. Additionally, they have been working with others at UC Berkeley (Plevin) and the University of Wisconsin, Madison (Gibbs) to produce a completely new carbon stock database to predict emission factors that are specifically matched to the GTAP output. CARB is working to finalize these changes and get them approved into regulation by mid-2012.

Changes and updates to the GTAP model have continually been made since CARB initially used it to model ILUC for the current CI look-up tables. The revised approach to ILUC still uses the GTAP model to predict the land conversions within the categories of cropland, forest and pastureland. However, they are working to include updates to the model as they were presented in Tyner's report as well as additional updates that Purdue University is working on [5,60]. In the newest version, the GTAP model has been revised with:

- Updated energy elasticities
- Improved treatment of DDGS
- Separation of soy from other seeds and oils
- Modified model structure for livestock sector
- Revised land conversion factor for new cropland
- Incorporate cropland-pasture for US and Brazil and CRP for US (however, CRP is not used)
- Endogenous yield adjustment for cropland pasture
- Greater flexibility in cropland switching

Although the modifications have not yet been adopted into a final CI number for the LCFS lookup tables, CARB has presented a preliminary sensitivity to some of the parameter changes within the GTAP model. [85] Parameter modifications include: yield-price elasticities (changed from 0.25 to 0.10, which results in an increased CI); crop transformation (changed from 0.5 to 0.75, which slightly reduces the CI for all biofuel pathways); cropland pasture yield adjustment

(which reduces the CI for all biofuel pathways); and changing the food constant for the developing world (which increases the CI for all fuel pathways).

The GTAP LUC results will then be linked to updated soil and biomass carbon stock estimates, rather than to the EFs from the Woods Hole Database. Researchers at University of Wisconsin-Madison are working to develop revised geographically explicit carbon stock data that are compatible with GTAP[86]. The database will provide weighted average soil and biomass carbon for 203 unique regions, which are the combination of 19 GTAP regions and 18 AEZs as shown in Figure 2-14.

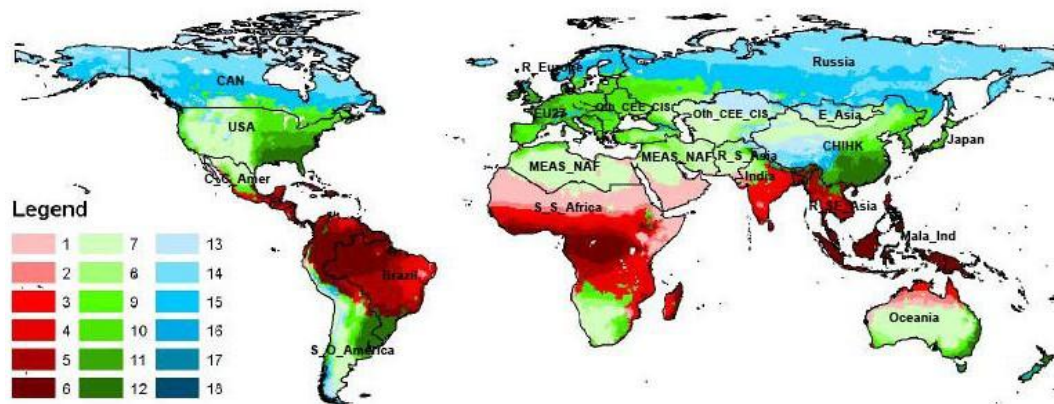


Figure 2-14: GTAP Regions combined with AEZs result in 203 unique regions. Source: [87]

The soil carbon stock data for these regions are based on the Harmonized World Soil Database (HWSD) combined with cropland, forest and pasture maps. The HWSD database provides estimates of soil carbon to both 30 cm depth and 100 cm depths. The analysis of carbon stocks is based on the 30 cm depth dataset to follow IPCC. Additionally, forest biomass carbon stocks are estimated with a combination of datasources. The database considers carbon pools in above- and below-ground biomass, soil carbon, litter, understory, harvested wood products and dead wood[87].

The LUC output from GTAP is combined with the carbon stock data using and AEZ- EF model, as shown Figure 2-15 below.

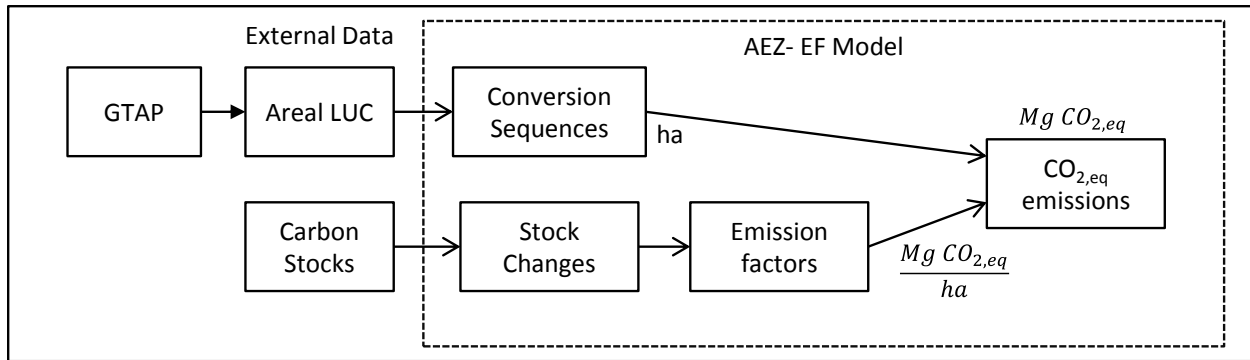


Figure 2-15: AEZ-EF model to combine LUC results from GTAP with carbon stock data to predict total GHG emissions from LUC.Source: [87]

No results have yet been published from this revised CARB work. However, draft reports of the changes are available, along with presentations at the CARB LCFS website.⁹ A summary of the changes in comparison to the previous approach is shown in Table 2-14.

Table 2-14: Comparison of revised CARB model to predict ILUC to original approach. Source: [87]

	Prior Model	New Model
Basis	Searchinger et al. 2008	Newly developed
Carbon Stocks	Woods Hole data for 10 regions	Gibbs & Yui (2011) data for 203 AEZ-region combinations
What's represented	Landcover types at agricultural frontier	Average C stock in each AEZ region combination
Soil emissions	25% of top 100 cm	Variable by regions; IPCC method (30 cm)
Conversion sequences	Forest and grassland to cropland	8 transitions among forest, pasture, cropland and cropland pasture
Other	--	Non- CO ₂ emissions. Peatland in Indonesia/ Malaysia.

2.5.3 EUROPEAN UNION- RENEWABLE ENERGY DIRECTIVE

In 2009, the European Commission adopted the most recent Renewable Energy Directive (RED), which includes a 10% target for renewable energy in transport fuels by 2020. This also includes a minimum rate of direct GHG savings and restrictions on type of land that can be converted to produce biofuel feedstocks. The revised Fuel Quality Directive (FQD), adopted at the same

⁹ The presentations and draft reports to CARB are available at www.arb.ca.gov/fuels/lcfs/lcfs.htm.

time as the RED, includes sustainability criteria and targets a reduction in life-cycle GHGs from biofuels of 6% by 2020.

ILUC have yet not been included in the EU-RED. However, the European Commission launched several studies in order to more fully understand the implications of ILUC and how to include it in sustainability criteria. In 2009, four studies were carried out by the EC regarding ILUC:

1. An assessment of existing modeling activities (JRC) [88]
2. A study using the AGRI/OECD partial equilibrium AgriLink model [89]
3. A literature review [27]
4. A general equilibrium model using GTAP and MIRAGE to determine the impacts on international trade and land use of the EU biofuels policy. [8]

A brief description of each of these studies is provided below. The fourth study is the primary study to assess the GHG impact of ILUC from the EU policy.

2.5.3.1 EU Study to Assess Existing Modeling Activities

The EU commissioned a study to compare ILUC results of marginal increases in biofuel production from different economic models. It compared results from:

- AGLINK-COSIMO (from OECD)
- CARD (from FAPRI)
- IMPACT (from IFPRI)
- GTAP (from Purdue)
- LEI-TAP (from LEI)
- CAPRI (from LEI)

For each of the following scenarios:

- Marginal extra ethanol demand in the EU
- Marginal extra biodiesel demand in the EU
- Marginal extra ethanol demand in the US
- Marginal extra palm oil demand in the EU (for biodiesel or pure plant oil use)

Land area results are compared on a kHa/ Mtoe basis.

2.5.3.2 Study Using AGRI/ OECD Partial Equilibrium Model

As part of the EC assessment of ILUC, the Institute for Prospective Technological Studies (IPTS) carried out an analysis of the results of several agro-economic impact models. The study compares the results from three models: AGLINK-COSIMO, ESIM, and CAPRI. Each of the agro-economic models is a partial-equilibrium model designed for simulating policy changes in the agricultural sector. In each case, the models are used to compare a baseline scenario (in

which the EU biofuel policy for 2020 is in effect) to a “counterfactual” scenario (in which no biofuel policy is in effect to drive supply and demand).

The primary results of the modeling efforts provide a comparison in effects of biofuel and feedstock prices and trading. The simulation results provided in the report estimate land conversions by crop type for each model’s relevant regions. However, the GHGs from the LUC estimates are not predicted, so the modeling results are not discussed in detail.

2.5.3.3 EU Literature review of LUC studies

A comprehensive literature review of ILUC modeling efforts was undertaken by DG Energy for the European Commission. The literature review concentrates on comparing studies’ methodological and data choices, rather than results. Over 20 modeling exercises were reviewed; however, many studies lacked the detail required for extensive comparisons.

2.5.3.4 IFPRI ILUC GHG Assessment

The fourth study is the primary study assessing the impact of EU policy ILUC. It was conducted by IFPRI and CEPII to investigate a 5.6% share of biofuels use in the transport sector under a business-as-usual scenario and under different trade policy scenarios. Results are compared against a baseline scenario which uses the latest energy and economic data from IEA and OECD. The study is used to assess the potential impacts on production and trade under alternative fuel policies, as well as other land use and environmental impacts.

Model and database description

The MIRAGE model is used for the study, which is a CGE model developed at CEPII for trade policy analysis, and modified by IFPRI to address economic and environmental impacts of biofuel policies. It relies on the GTAP 7 database for global economy-wide data. The MIRAGE model allows energy sector modeling, fertilizer modeling, biofuels sector modeling, and co-product and livestock sector modeling. It also includes a land use module which models the decomposition of land into different uses by AEZ.

To determine the land extension coefficients, this study followed Winrock modeling for the preliminary EPA- RFS ruling, which relied on MODIS remote sensing data from 2001-2004.

Model approach

In the IFPRI model, the overall effect of the EU biofuel policy is modeled. The policy target is 5.6% of transportation fuels from alternative fuels, which equates to 17.8 Mtoe of biofuels use in the EU. Two scenarios are modeled and compared to a baseline, in which biofuel consumption is maintained as constant between 2009 and 2020. The scenarios include a “business as usual” scenario, and a full trade liberalization scenario. Additionally, a sensitivity analysis is performed on different mandate levels, which range from 4.6% to 8.6% in 1% increments.

The model is run for the complete fuel policy, which includes use of both ethanol and biodiesel, each from a variety of feedstocks. The ILUC results are not broken down by feedstock or fuel type, but are the influence of the complete policy. (In the US, an ILUC “adder” is determined for each type of biofuel by modeling the contribution of each individually to determine ILUC for a single type of biofuel with respect to the complete policy). However, a marginal approach is taken in evaluating each biofuel to determine those with the lowest impact. This marginal calculation is done by increasing the demand for biofuels in 2020 by an additional 1 million GJ, and allowing the corresponding increase to be met only by a particular fuel type while holding all others constant. This approach provides a CI or LUC number for each fuel type that can be compared to the individual direct emissions set forth in the RED.

ILUC effects considered in the study include emissions from converting forests to other land types, cultivation of new lands, and below-ground carbon stocks of grasslands and meadows using IPCC coefficients for the different ecosystems. Emissions from peatlands are also considered for Indonesia and Malaysia. The study follows the EU recommendation of allocating ILUC emissions over a 20-year period.

Results

The study predicts the overall land use impacts for the entire EU alternative fuel policy. The results are presented by LUC within each region and are also broken down by land type (i.e., cropland, pasture, forest, etc.). The overall results for ILUC and resulting GHG emissions are shown in Table 2-15. These results are described in more detail in Section 2.6.

Table 2-15: ILUC and resulting indirect emissions from EU-IFPRI Study[8].

Scenario	Land Use Change (000 ha)	Percentage LUC	GHG emissions from LUC (million tons CO _{2,eq})	Increase in Biofuel Use (million GJ)	GHG emissions from LUC (CO _{2,eq} MJ ⁻¹ yr ⁻¹)
Data Source in [8]	Table 7	Table 7	Table 9	Table 11	Table 11
Business as Usual	820	0.07%	107.5	300	17.73
Full trade liberalization	973	0.08%	117.7	303	19.45

The results shown in Table 2-15 are for the complete policy. The policy blend of ethanol and biodiesel is shown, as well as the marginal effects for each feedstock, in Table 2-16. The results show that sugarcane and sugarbeet ethanol are the most efficient feedstocks in terms of land use. Under the trading scheme, sugarbeet ethanol ILUC is increased substantially. Corn maize ethanol results in significantly higher ILUC results than other ethanol feedstocks.

Table 2-16: Marginal indirect ILUC results from the EU-IFPRI study, g CO_{2,eq}MJ⁻¹yr⁻¹. (20-year life cycle).
Source: [8]

Note: MEU_BAU is the “business as usual” scenario, and MEU_FT is the full multilateral trade scheme. Figures are provided with and without peatland effects.

	MEU_BAU		MEU_FT	
	Without Peatland effects	With Peatland effect	Without Peatland effect	With Peatland effect
<i>Ethanol</i>	17.74	17.74	19.16	19.18
Ethanol SugarBeet	16.07	16.08	65.48	65.47
Ethanol SugarCane	17.78	17.78	18.86	18.86
Ethanol Maize	54.11	54.12	79.10	79.15
Ethanol Wheat	37.26	37.27	16.04	16.12
<i>Biodiesel</i>	58.67	59.78	54.69	55.76
Palm Oil	46.40	50.13	44.63	48.31
Rapeseed Oil	53.01	53.68	50.60	51.24
Soybean Oil	74.51	75.40	67.01	67.86
Sunflower Oil	59.87	60.53	56.27	56.89

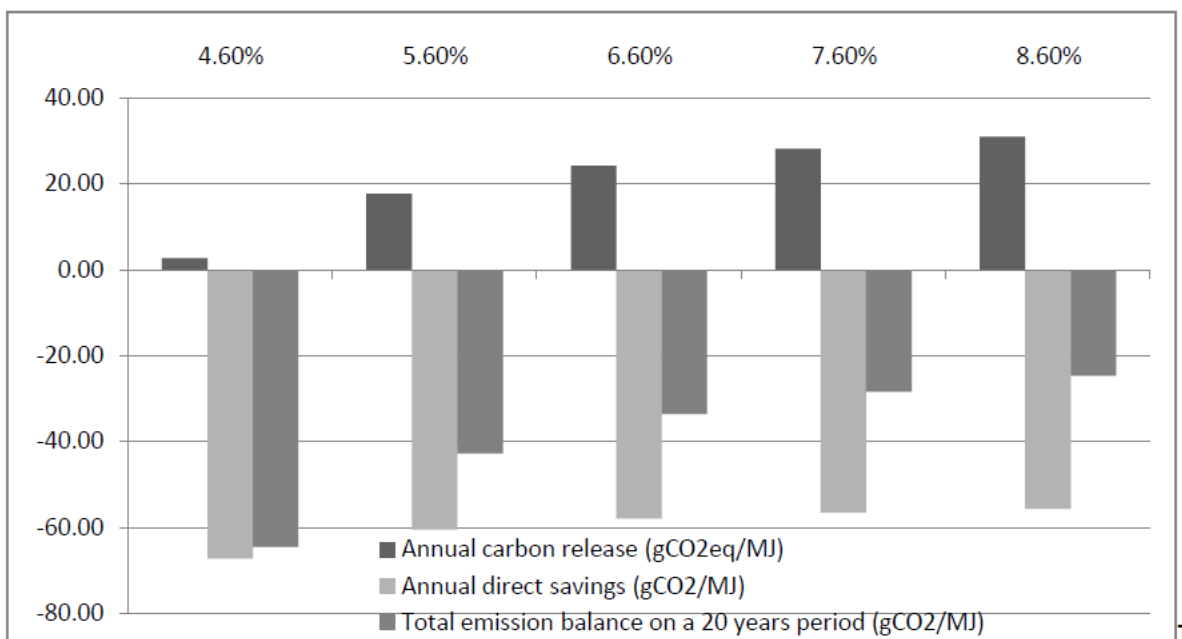


Figure 2-16: ILUC emissions and direct savings for different EU mandate levels in the EU-IFPRI Study.
Note: Scenario is “business as usual” with no change in trade policy. Negative figures represent an emission reduction; positive values represent an emission increase.

Biodiesel feedstocks result in much greater ILUC emissions, and also are adversely affected when peatland emissions are considered. Palm oil is the most efficient biodiesel feedstock, but still has an ILUC much higher than ethanol. Palm is the most efficient for two reasons: it

produces co-products and has a high oil yield (6 times the yield of rapeseed by hectare). Soy biodiesel puts the most pressure on land extension in Brazil, and therefore has the highest ILUC effect.

Figure 2-16 shows results for modeling of different EU mandate levels with no change in trade policy. As the biofuel mandate is increased, the ILUC emissions also increase. Several mechanisms contribute to the non-linear behavior of the ILUC response to different mandate levels as highlighted in the report:

- Land substitution is represented by a CET function, and the marginal productivity of transforming one hectare from one sector to another declines quickly.
- The rigidity of other sectors to reduce consumption of feedstocks, which is defined by a CES function. The propensity to forego units declines with each additional unit.
- The saturation effect on fertilizers.
- The below-average productivity assumed for new units of land.

Direct emissions also increase with increasing biofuels mandate (i.e. result in a decreasing reduction in GHGs with respect to the baseline): increased demand for biofuel production results in use of less efficient feedstocks and production technologies.

The EU27 SAM and GTAP7 databases are used, and the analysis follows IPCC evaluations and factors. However, little or no description is provided to explain these databases and how they are used to derive LUC and GHG results. Results from the complete policy are broken down into contributions to LUC and GHG from each of the regions included in the model. These will be used for comparison in Section 2.6.

2.5.4 OTHER MODELS

2.5.4.1 Searchinger

Searchinger's study was one of the first to question how biofuels policies cause ILUC. To illustrate the potential impacts of LUC on the GHG emissions of biofuels, Searchinger first modeled the impacts of ethanol, using an LUC analysis based on research done by a CARD research team in 2007, which estimated that approximately 10.8 million hectares of cropland would be required globally to meet the demand of 55.9 billion liters of corn ethanol in 2016. [90,1,91] Searchinger used the LUC results from this study in conjunction with the Woods Hole database and the GREET LCA model to predict a carbon payback period of corn ethanol of 167 years. [1] The approach taken to calculate the EFs from the Woods Hole database is described in Section 2.4.1.

Searchinger also applied the same analysis for biodiesel. [6] In this study, several scenarios were investigated for replacement of diverted soybean oil including: replacement solely by soy oil, replacement by soybeans, and replacement by a mix of oils. Each of these scenarios was investigated with and without demand reductions and price-induced yield increases. The results

of the main scenario (which produce the highest LUC emissions) are reported in Table 2-17. Further discussion of the results is provided in Section 2.6.

Table 2-17: Corn ethanol and Soy biodiesel ILUC and resulting emissions from Searchinger. [1,6]

Fuel	Volume Fuel Modeled (billion gallons)	Land Use Change (000 ha)	Total Emissions (million tons CO ₂ eq)	CI (g CO ₂ MJ ⁻¹ annually)
Corn Ethanol	14.772	10,817	3,801	106
Soy Biodiesel	0.264	789	340	340

2.5.4.2 Tyner – GTAP Bio-ADV

Tyner and others performed an assessment of LUC changes associated with U.S. corn ethanol production using the updated GTAP-BIO-ADV model in 2010. [92,5] The updated model included many changes to improve the analysis of corn ethanol. While the group at Purdue is continually working to update the GTAP data and improve biofuels analysis, the significant updates for this study included: addition of a biofuels module, including corn and sugarcane ethanol and biodiesel; addition of cropland pasture in the U.S. and Brazil and Conservation Research Program (CRP) lands; re-estimation of demand and supply elasticities to reflect 2006 reality (more inelastic than previous); addition of DDGS; a restructuring of the livestock sector; econometric estimation of corn yield response to higher prices; and, estimation of productivity on marginal lands based on the ratio of net primary productivity of new cropland to existing cropland in each country and AEZ. [60]

Three simulations were performed in the study: the first used the 2001 database, the second used the updated 2006 database and compared to a baseline of the world economy during 2001-2006, and the third used the 2006 database with the assumption that population and crop yields continue to grow. The data and results from the second simulation are used in this report for comparison to other studies.

The GTAP model is used to predict changes to cropland, forest and pasture within each of the GTAP regions. The marginal impacts of ethanol production are assessed through incremental increases in production from the 2001 level (1.77 billion gallons) until a total production of 15 billion gallons in 2015 (a change of 13.23 billion gallons). The marginal LUC results from the second simulation are shown in Table 2-18.

Table 2-18: Simulated global ILUC due to U.S. ethanol production. Source: p 28 of [5]

Changes in US corn ethanol production	Land use changes (hectares)			Distribution of Land Use changes (%)			Hectares per 1000 gallons
	Within US	Other Regions	World	Within US	Other Regions	World	
3.085 BG (2001 to 2006)	106870	360397	467268	22.9	77.1	100.0	0.15
2.145 BG (2006 to 7 BG)	77989	246464	324452	24.0	76.0	100.0	0.15
2.000 BG (7 to 9 BG)	73308	233222	306529	23.9	76.1	100.0	0.15
2.000 BG (9 to 11 BG)	73754	233992	307746	24.0	76.0	100.0	0.15
2.000 BG (11 to 13 BG)	74717	238378	313094	23.9	76.1	100.0	0.16
2.000 BG (13 to 15 BG)	75731	242685	318416	23.8	76.2	100.0	0.16
13.23 BG (2001 to 15 BG)	482368	1555137	2037506	23.7	76.3	100.0	0.15

The LUC results are then linked to emission factors generated from the Woods Hole database. The emission factors calculated are based on 25% of the soil carbon, 75% of the carbon in the vegetation, and foregone sequestration from existing forests. The EFs are weighted based on the shares of vegetation area in each of the 10 Woods Hole regions. More detailed description of the EF calculation is provided in Section 2.4.1. The marginal emissions from each incremental increase in ethanol production are calculated, as shown in Table 2-19.

Table 2-19: Annual marginal and average estimated ILUC emissions due to U.S ethanol production from Simulation 2. Source p 40 of [5].

Time Segment	Marginal emissions (grams CO ₂ per gallon of ethanol)				Average emissions (grams CO ₂ per gallon of ethanol)			
	Changes in ethanol production	Forest	Grasslands	TOTAL	Total ethanol production	Forests	Grasslands	TOTAL
2001-6	3.085	925	465	1390	3.085	925	465	1390
2006-7	2.145	1019	399	1418	5.23	963	438	1402
2007-9	2.000	1020	406	1427	7.23	979	429	1409
2009-11	2.000	1017	409	1426	9.23	987	425	1412
2011-13	2.000	1027	419	1446	11.23	994	424	1418
2013-15	2.000	1040	427	1467	13.23	1001	424	1426

The results from this study produced significantly lower ILUC estimates than previously used by CARB in their LCFS. The average annual emissions of 1426 g CO_{2,eq} gallon⁻¹ of ethanol equates to about 18 g CO_{2,eq}MJ⁻¹ (for LHV of 76,330 BTU/gal used in CARB), which is nearly half of the 30 g CO_{2,eq}MJ⁻¹ listed in the LCFS lookup tables for corn ethanol. CARB workgroups evaluated this study during review of the earlier LCFS, and suggested that the ILUC modeling be revised to include the updates to the GTAP model. Since then, CARB has worked to incorporate these changes along with updates to the EFs used.

2.6 COMPARISON OF LUC MODEL RESULTS

Results from EPA- RFS2, CARB LCFS, Searchinger, Tyner and EU-IFPRI are compared to highlight the differences in assumptions and application of data in each. The comparison of results, i.e., the differences in ILUC and resulting GHGs predicted, can be used to highlight the differences within the models and application of data, with a particular focus on the C-stock and emission factor databases. These differences will be discussed in the next section.

Table 2-20 provides the final annualized LUC- CI results from each study for various fuel scenarios modeled.

**Table 2-20: Comparison of 30-year ILUC results (IFPRI is for 20 years) from different studies. Units are g CO₂,
eq MJ⁻¹ fuel.**

	Searchinger	EPA International (FAPRI)	EPA Domestic (FASOM)	CARB	Tyner	IFPRI
Corn Ethanol	106	30	-4	30	18	54
Soy biodiesel	340	40	-8	62		75
Sugarcane Ethanol		4 ^A	1 ^A	46		18
Rapeseed Biodiesel						53
Complete Policy with blend of fuel types						17

Note: The U.S. studies annualize ILUC emissions over a 30-year period, while IFPRI follows EU recommendation to annualize over a 20-year period. The results from Searchinger's work are from two different studies, the corn ethanol results are given in [1] and the soy biodiesel results are in [6]. Additionally, the results from the international (FAPRI) and domestic (FASOM) analyses from the EPA are shown separately.

^ABoth domestic and international results for sugarcane ethanol in the RFS2 are modeled with FAPRI. The results are not detailed in the RIA, but can be found in the spreadsheets. It appears that the International total includes GHG estimation in the U.S., but the U.S is again included separately in the domestic emissions.

Influential factors that contribute to the differences in results include how much land is converted, how much GHG the land produces, and what type of land is converted. These results will be compared in the following subsections.

However, it is difficult to directly compare the results from each of the studies due to differences in data availability, input assumptions, and detail of outputs. Reporting differences also make details difficult to obtain and compare. Since the results are not directly comparable between studies, the following data manipulation and caveats apply to subsequent sections:

- Both ILUC and GHG are categorized into the coarsest output for comparison in Figure 2-17 through Figure 2-19 below. Data from all studies are aggregated into the 10 regions of Woods Hole. GHG results from Searchinger and Tyner are already aggregated to the Woods Hole regions. However, the ILUC results from GTAP, and all results from

FAPRI (which has 54 regions) are aggregated into corresponding Woods Hole Regions as shown in Appendix A.

- The results from CARB studies are not spatially explicit, and only provide land classifications for the U.S. and the Rest of the World. Results from Hertel, which influenced the CARB analysis for corn ethanol are used.[84]The CARB analysis for other fuels is only categorized by U.S. and the Rest of the World.
- The volume of fuel modeled also results in differences in the total amount of LUC and GHGs. Therefore, the results are normalized by the energy contained in the fuel (in billion BTU), based on the fuel volume and the lower heating value of the fuel applied in each study. These values are provided in Table 2-21. Note for FASOM modeling results in the EPA study, fuel volumes differ from those applied for the international module.
- Sugarcane ethanol results are calculated in the RFS2 dockets, but are not presented in the final RIA. The results shown in Table 2-21 are from the FAPRI results spreadsheet and the Impacts results spreadsheet.¹⁰ In the final impacts results spreadsheet, the international emissions from ILUC are given as the sum of all FAPRI regions, including the U.S. However, domestic ILUC emissions are also given, which are the U.S emissions resulting from FAPRI analysis. Therefore, it appears that these emissions are double counted. Since the sugarcane ethanol results are not presented in the RIA, there is no additional description or final presentation of the results to verify the calculation.

¹⁰ FAPRI results spreadsheet, which provide the total LUC for RFS2 fuel pathways, can be found under docket ID number EPA-HQ-OAR-2005-0161-3153 for all fuel pathways. Lifecycle GHG final results spreadsheets for each fuel pathway can be found under docket ID EPA-HQ-OAR-2005-0161-3173 at www.regulations.gov

Table 2-21: ILUC modeling inputs and results.

Fuel/ Study	Fuel Volume (bill. gallons)	LHV applied (BTU/gal)	Time Horizon (years)	Total LUC (000 ha)	Total GHG (mil. tons CO _{2,eq})	Final CI ^A (g CO _{2,eq} MJ ⁻¹)
Corn Ethanol						
Searchinger	14.8	76,330	30	10,817	3,801	106
EPA-RFS2	2.7	76,000	30			
FAPRI- International				789	190.9	30
FAPRI- U.S				140	25.0	4
FASOM- U.S	8.2			580	-75.1	-4
CARB-LCFS	13.2	76,330	30	4,200	877	30
Tyner, 2010	13.2	76,330	30	2,037	565	18
Soy Biodiesel						
Searchinger	0.26	119,550	30	789	340	340
EPA-RFS2	0.54	118,000	30			
FAPRI- International				678	81.3	40
FAPRI- U.S				101	-2.5	-1.2
FASOM- U.S	1.5			763	-48	-8.9
CARB-LCFS	0.995	119,550	30	940	230	62
Sugarcane Ethanol						
EPA-RFS2 FAPRI ^D	1.3	76,000	30			
International				395 ^E	12.7 ^F	4
Domestic				35	3.0	1
CARB- LCFS	2.0	76,330	30	1,090	222 ^C	46
EU-IFPRI ^B	--	--	20	820	107	18

^A Final CI value can be calculated from Table using 1055.87 MJ BTU⁻¹

^B IFPRI model is for complete policy with a blend of fuel types with 5.6% share of transport fuels from biofuels. This corresponds to an increase of 300 million GJ or 284,130 billion BTU.

^C Total GHG emissions from CARB Sugarcane scenario is calculated from final CI value.

^D Sugarcane ethanol is only modeled with FAPRI in the RFS2.

^E Land use change results are provided from the FAPRI spreadsheet in the EPA docketed information. Land use is given for the U.S. and as the sum of the rest of the FAPRI regions.

^F In the docketed spreadsheet results for sugarcane ethanol, the international emissions given include the emissions from the U.S. However, the U.S. emissions are *also* accounted separately as domestic emissions. Therefore, the domestic emissions appear to be double counted.

2.6.1 LAND USE CHANGES

The amount of ILUC predicted from each of the models is a key difference which can lead to significantly different final GHG emissions: larger amounts of ILUC bring larger GHG emissions. The ILUC modeling is primarily done through agro-economic models, however, a detailed discussion and comparison of the assumptions in the agro-economic models is outside the scope of this report. Therefore, the differences in LUC predictions from each model are presented without detailed description as to the reasons for the differences. The total projected

LUC, normalized by the fuel energy, in response to each fuel volume are presented in Figure 2-17 A. The LUC from each study is aggregated into regions corresponding to those in the Woods Hole database.

Searchinger's analysis predicts substantially larger ILUC per energy content of fuel than the other studies for both corn ethanol and soy biodiesel. For corn ethanol, the ILUC is distributed around the world, with much of it occurring in Latin America, China/ India/ Pakistan, and the U.S. The total amount of LUC in the Searchinger study is based on results of a study using the FAPRI-CARD model. [91] A study by Dumortier, et al. used a modified version of the FAPRI-CARD model and GreenAgSim (to assess the GHG emissions) to show that differences in assumptions used in the Searchinger study and updates to the FAPRI model resulted in much lower LUC and resulting emissions. [90]

Other ethanol modeling efforts predict ILUC that is less than half of Searchinger's. The results from CARB's analysis using GTAP and EPA's analysis using FAPRI predict similar ILUC acreage, although the locations are quite different. In CARB's corn ethanol analysis, much of the LUC conversion occurs in the U.S., while in the EPA analysis, FAPRI predicts that nearly half of the conversions will occur in Latin American countries. The EPA results shown in Figure 2-17 include both domestic and international ILUC from FASOM and FAPRI. The LUC predicted by FAPRI are shown as solid lavender, and additional LUC predicted by FASOM is shown as dotted lavender bar, so the total resulting LUC is the sum of the two (which is the total from FASOM). FASOM predicts a net increase in domestic croplands of 1.4 million acres (580 thousand hectares) for corn ethanol. However, this number is the area of cropland increase, which is offset by changes in cropland-pasture and other land types. The increase in cropland is also normalized by 8.2 billion gallons of ethanol, an output from the FASOM model. A comparison of the FASOM and FAPRI results is provided in Table 2-21.

The Tyner and CARB corn ethanol studies are both based on the GTAP model; however, Tyner's results are less than half of those predicted by CARB because of updates in the GTAP model. In Tyner's study, the LUC is distributed throughout the world, with no disproportionate changes occurring in any one country. In the CARB study, much of the LUC occurs within the U.S.

Soy biodiesel results in much more ILUC than corn ethanol, due to soy oil's status as a valuable food commodity, which requires that it be replaced by other vegetable oils. CARB, the EPA and Searchinger all present results for soy biodiesel. Again, the ILUC predicted by Searchinger is much larger than other, more recent studies. Much of the ILUC in the Searchinger study occurs in Latin American countries (11.3 ha bBTU⁻¹, occurring in primarily Argentina, followed by Brazil) and Southeast Asia (4.9 ha bBTU⁻¹, occurring in primarily Indonesia and Malaysia). In the EPA study, much of the land conversion occurs in Latin American countries (about 7.6 ha bBTU⁻¹), with limited amounts in Southeast Asia. Again, the results of the FAPRI analysis are shown in the figure; however, the FASOM results for domestic changes are applied in the final rule.

FASOM analysis shows approximately 1.9 million acres of new cropland is required (763 thousand ha), more than the total international LUC. However, the volume modeled in FASOM is 1.5 billion gallons, more than three times the policy volume, resulting in about 4.3 ha bBTU⁻¹ (compared to about 1.6 shown in the figure). This would result in a total LUC of about 15 ha bBTU⁻¹ for biodiesel. The results in the CARB analysis are only provided for the U.S. and the rest of the world. The total ILUC is about half of the total ILUC in the EPA analysis.

The results from the EU- IPFRI study are from *the complete policy*, including combinations of ethanol and biodiesel. The results are not provided in detail to breakout each feedstock or fuel for comparison. The IFPRI study predicts that a large percentage of total LUC from the EU policy will occur in Latin American countries, primarily in Brazil. This is due to the combination of the demand for ethanol (sugarcane) and oilseeds, and the high elasticity of land extension for Brazil.

2.6.2 GREENHOUSE GAS EMISSIONS FROM LAND USE CHANGES

In each study, the location of LUC is tied to corresponding EFs from databases indicated to give the total land-induced emissions shown in Figure 2-17-B. Again, the emissions are aggregated corresponding to the Woods Hole regions for comparison between relative impacts of each region. Both the FAPRI and FASOM results from the EPA analysis are shown. For corn ethanol, the FAPRI analysis predicts an increase in GHG emissions from ILUC in the U.S. (shown as an open purple bar), while the FASOM analysis results in a reduction to GHG emissions even though there is an increase in ILUC in the U.S. For the biodiesel analysis, both FAPRI and FASOM resulted in a net decrease of GHG emissions, with the total reduction represented by both bars.

The Searchinger analysis results in the highest GHG impacts for both corn ethanol and soy biodiesel despite being normalized by energy content. For example, Searchinger predicts just under 10 ha/billion BTU LUC for corn ethanol, but over 100 tons of CO_{2,eq} bBTU⁻¹, indicating an overall emission factor of around 10 tons CO₂ha⁻¹yr⁻¹.

Soy biodiesel results in higher ILUC emissions than corn ethanol. However, the EPA analysis for soy biodiesel predicts fairly significant ILUC, but relatively small resulting GHGs. As explained in the next section, this is because the EPA assumes relatively little conversion of forests.

The analysis for CARB is not provided in enough detail to break out the contributions by region, so is shown as a single bar for “Rest of the World”.

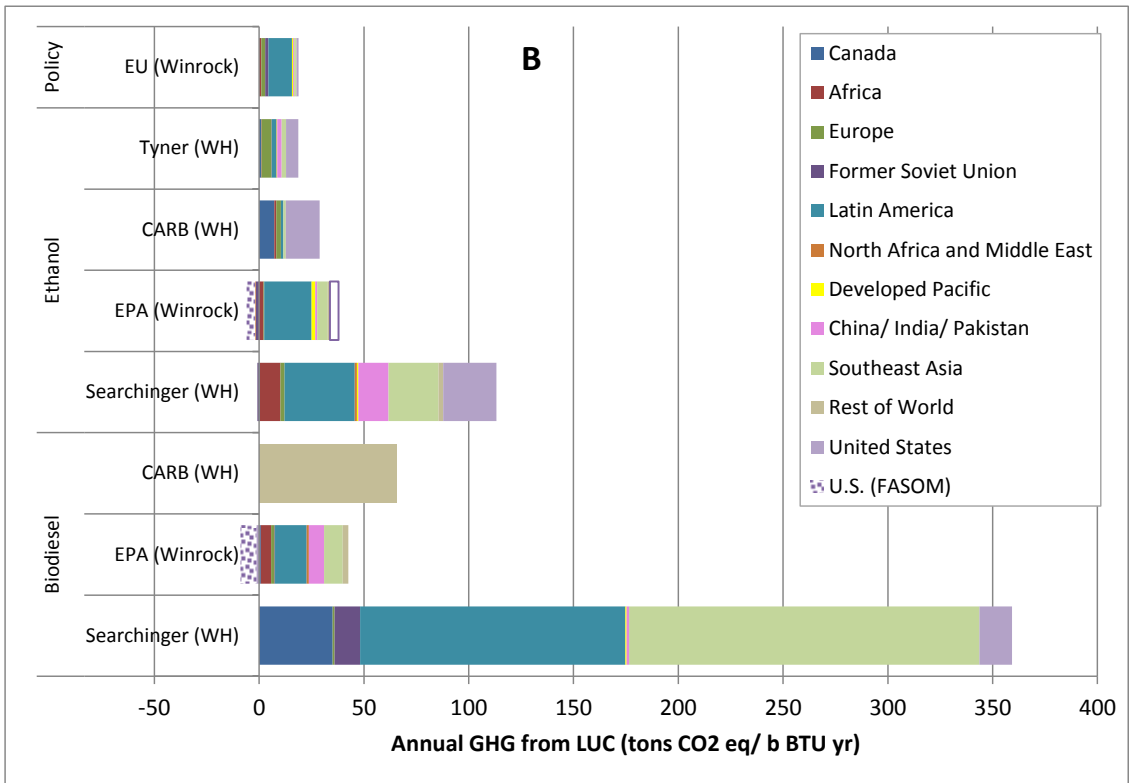
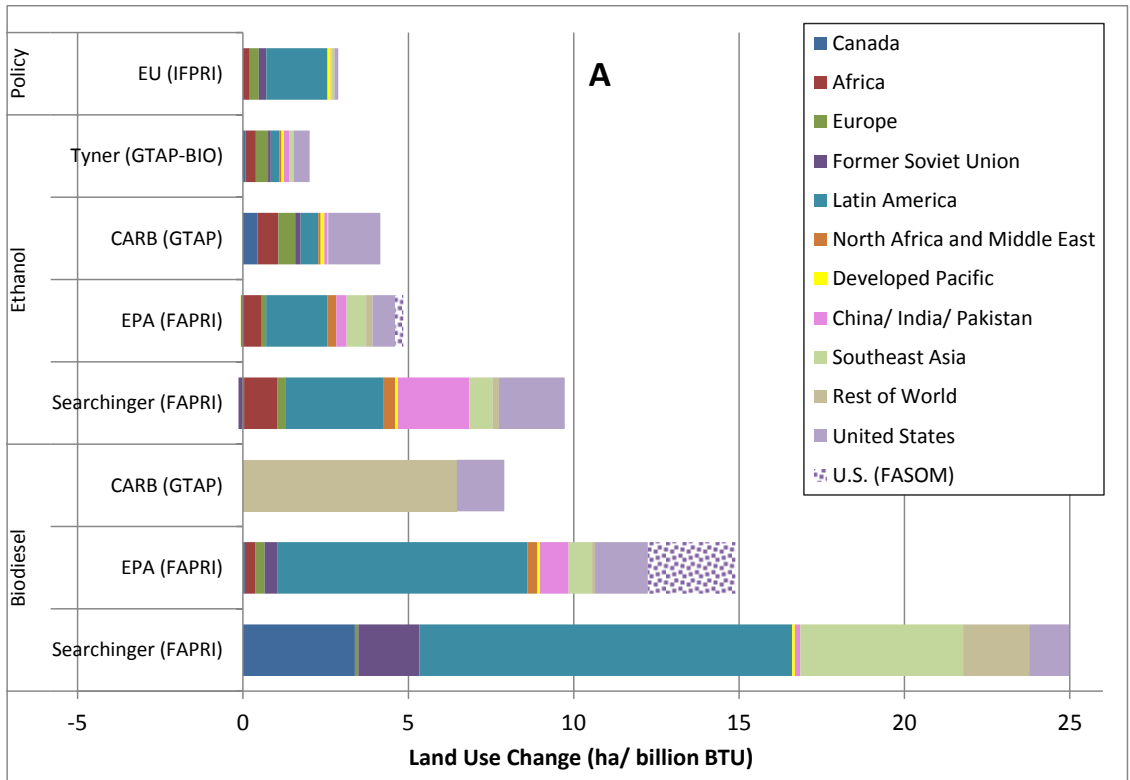


Figure 2-17: Land Use Changes (A) and GHG from ILUC (B) from alternative fuel policies in the EU (modeled by IFPRI) the U.S. (modeled by Searchinger and EPA) and California (modeled by CARB and Tyner). WH= Woods Hole

2.6.3 TYPE OF LAND USE CHANGE

The significant differences between the GHG and LUC results from each study have much to do with the type of land that is assumed to be converted. For example, in Searchinger’s biodiesel scenario, about 20% of the total land conversion occurs in Southeast Asia, which contributes to nearly half of the net GHG emissions, while in the EPA analysis of biodiesel, about 5% of the LUC occurs in Southeast Asia, which results in about 20% of the GHG emissions. Much of the difference in scale has to do with the type of land use conversion. In Searchinger’s analysis, no grasslands are assumed to be converted in Southeast Asia, resulting in a substantially higher EF applied.

The breakdown of total land use conversion classifications from each study is shown for corn ethanol in Figure 2-18-A and for soy biodiesel in Figure 2-18-B, normalized by billion BTU for comparison between studies. The Figure gives the classifications of forest, grassland or pasture, and “other” in total ha/b BTU for each study. The percentage breakdown is also noted on the figure. For the EPA analysis “other” refers to perennial crops, while in the IFPRI analysis, “other” is not specified.

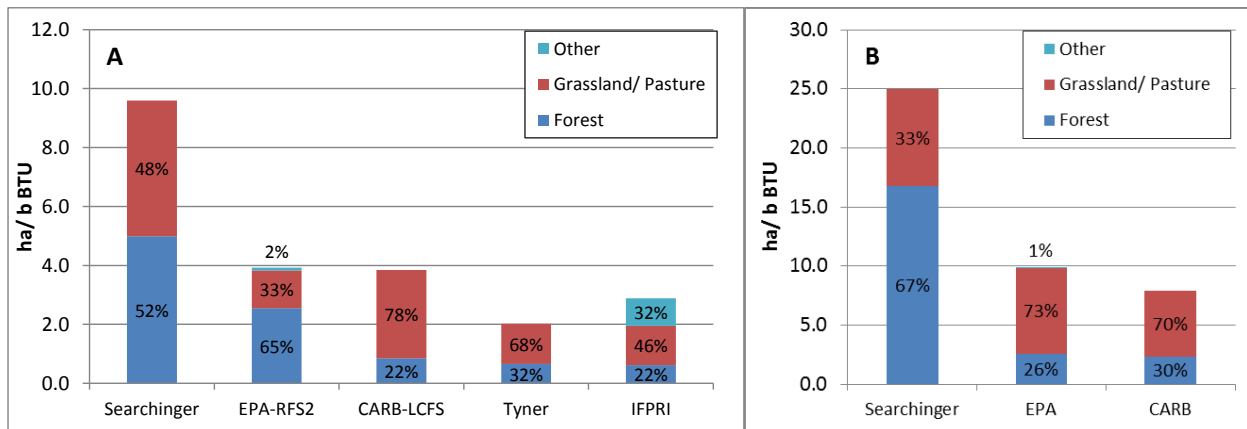


Figure 2-18: ILUC classification, normalized by billion BTU for each study for A) Corn Ethanol, and B) Soy Biodiesel. IFPRI study shown in A is for complete policy with a blend of fuels.

NOTE: The results from Searchinger studies are determined by the percentage of grassland and forests in each region, and the percentage of land conversion occurring in each region.

The EPA-RFS2 results are interpreted from the FAPRI international results (U.S. results are excluded) for conversion TO annual crops only. The classification for “forest” in the EPA analysis is for conversion from “natural to annual” crops. “Natural” categories include conversion from grassland, shrubland, savannah, mixed categories, barren and woodland. Results from the stochastic model indicate breakdown from natural to annual conversion as follows: 13% forests, 60% from grassland, savannah, and shrubland, 24% from mixed category and 3% from barren and wetland. This indicates that less than 10% (13% x 65%) of the land conversion is estimated to come from forests in the ethanol case and less than 5% is from forests in the soy biodiesel case (compared to 65% and 26%, respectively).

This classification of land use has substantial impacts on the overall GHG calculations, since EFs from forests are considerably larger than EFs from grasslands (See carbon stock and EF data in Figure 2-20). In both Searchinger studies, the bulk of land conversion is from forests, particularly for soy biodiesel. This is primarily due to the assumptions that much of the land conversion occurs in Southeast Asia, which has no conversion from grassland. More recent reports predict less conversion of land from forests, from 20 to 30%. (Note: in the EPA analysis, the distribution in the figure for “forests” includes conversion from natural lands. Actual conversion from forests is around 13% in the corn ethanol case).

The low conversion of forests in EPA’s soy biodiesel study explains why lower GHG emissions are predicted for significantly more LUC in comparison to the ethanol study.

2.6.4 COMPARISON OF EMISSION FACTORS FROM KEY STUDIES

Based on the data presented in the reports discussed and their corresponding databases, it is not possible to make a direct comparison between the emission factors from Woods Hole and Winrock databases. The EFs from the Winrock database are weighted into different conversion categories for each of the regions corresponding to the FAPRI regions. They are not weighted into a single EF for each region. Therefore, the final EF is dependent on how much of each type of land is converted within each region for each fuel scenario.

In order to make an approximate comparison between each of the overall EFs used in each study, we have back-calculated them based on the total land conversion and the total GHGs for each of the 10 regions corresponding to the Woods Hole database. The comparison of these EFs is shown in Figure 2-19 for corn ethanol. A “total world emission factor” was calculated for each study based on the total land conversion and the resulting GHGs. Although this method allows for comparison between the Woods Hole and Winrock databases, the LUC EF for Winrock is not a very representative calculation when based on the land conversion reported. The LUC reported is the net change in crop area (including both annual and perennial crops). However, land changes to pasture are also considered when determining the total emissions from each region. Therefore, to determine a more representative overall EF, the net land change including cropland and pasture is considered. This adds additional uncertainty in the comparison between databases. However, the data are still shown since other methods of comparison would require detailed and time-intensive calculations using the results of the publically available models. The apparent emission factor from the FASOM results is also shown for EPA’s analysis for the U.S. Additionally, data from the CARB studies are not sufficient to calculate EFs from each region, so are not presented here.

The EF factors used in the Tyner study are generally slightly lower than those applied in the Searchinger study. Although both studies apply the Woods Hole database, this is expected since Tyner assumes 75% of the carbon in the vegetation is lost upon conversion whereas Searchinger assumes that 100% is lost. Tyner uses higher EFs than Searchinger, however, for China/ India and Pakistan, Europe and Canada. For China/India and Pakistan, Searchinger assumes that only

grasslands are converted, while Tyner’s results predict that some forestland is also converted, leading to a slightly higher EF for the region. The forest carbon stock for the region is assumed to be equivalent to Southeast Asia, which has the highest carbon stocks of the region. The assumption that Tyner makes about land reversion in Europe also results in a higher EF for that region than Searchinger (see Table 2-5). The apparent EF for Canada is higher in Tyner’s report due to the fact that over 60% of the land conversion there is assumed to come from forests, compared to only 20% in the Searchinger study.

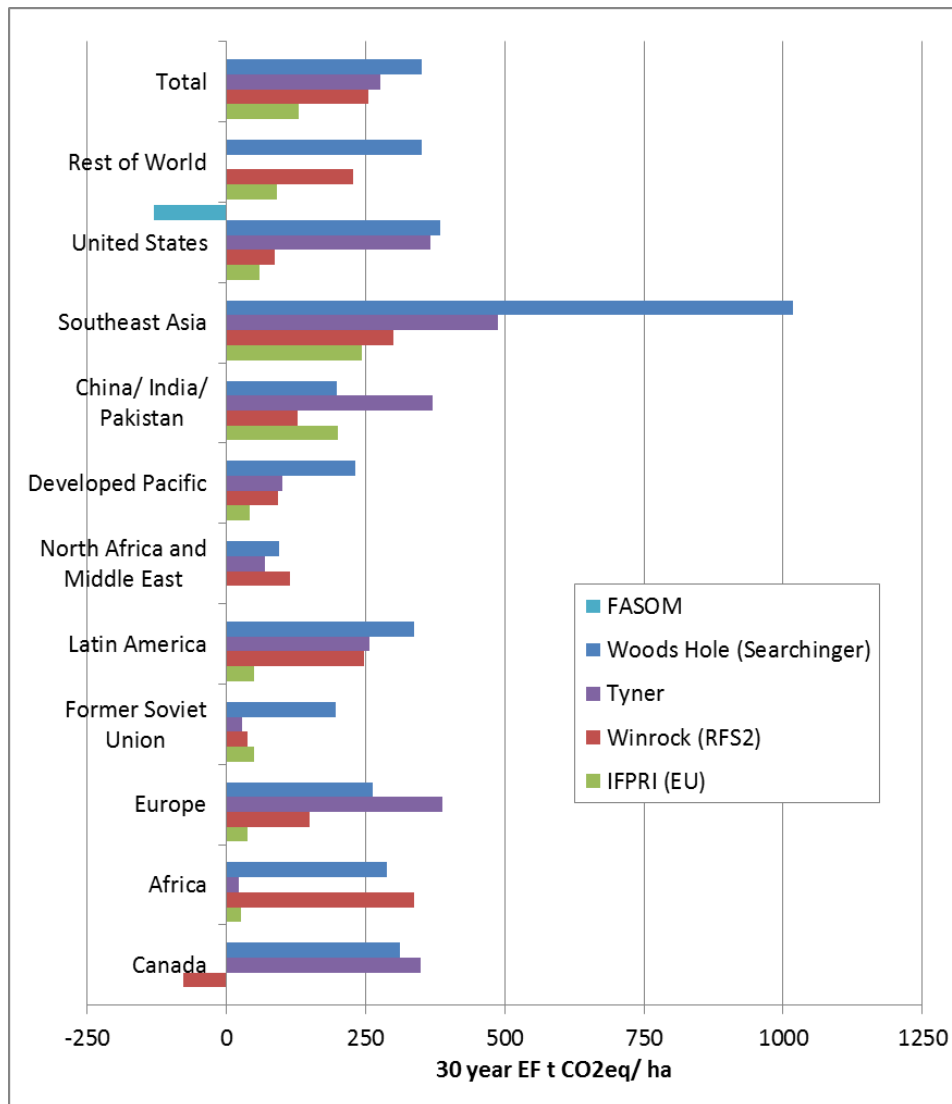


Figure 2-19: Total 30-year emission factors for key studies for corn ethanol, corresponding to Woods Hole regions. Note: The IFPRI study is based on the complete policy, with a blend of fuels. Author’s calculations.

The factors determined from the EPA results are also lower than those used in Searchinger, except for a few cases. The EF calculated for Canada is negative due to movement of land classifications. A larger amount of annual crops is converted to pasture than natural lands converted to pasture, which carries a larger impact to reducing emissions. The calculated EF from the FASOM results is also negative, because of an assumed net land conversion with a

decrease in GHG gases. It is unclear how this result is determined since FASOM endogenously applies the DAYCENT/ CENTURY and FORCARB emission factors.

The factors used in the IFPRI study are consistently smaller than other studies. The data and/or EFs applied are not presented in the study, however, so it is difficult to pinpoint the reasons why they are lower. However, as shown in Figure 2-18, a small percentage of the total land conversion is predicted to occur in forests, which helps to limit the impact. It also should be noted that the time horizon is 20 years rather than 30, so additional GHG occurring in the final 10 years are not considered. However, these emissions are primarily foregone sequestration, which has minimal impact on the final amortized CI value, so amortizing over a shorter time frame should result in a higher emission rate.

The carbon stock data in each of the databases is compared in the next section to illustrate the reasons for the differences in the emission factors.

2.7 COMPARISON OF EMISSION FACTOR DATABASES

The application of the emission factor databases contributes to differences in the total emissions due to ILUC in each model. The total land use estimated from the economic models is tied to emission factors, which provide an estimate of carbon (or CO_{2, eq}) emitted per hectare of land conversion. The main contributors to the emission factors are the release of above and below ground carbon contained in vegetation, soil carbon, and foregone sequestration. Emission factor databases use carbon stock data for each of these contributors.

The EPA RFS2 utilizes the Winrock International database which utilizes carbon stock data for 9 land types over 756 regions to determine a 30-year emission factor for each region (described in Section 2.4.2). In comparison, CARB, Searchinger, and Tyner apply the Woods Hole emission factor database, which is based on research by Houghton using historical carbon trends (described in Section 2.4.1). In the Woods Hole database, Houghton determines emission factors for six different land types over 10 world regions.

Although it is not possible to make a direct comparison between the data used in the databases because of differences in spatial aggregation and weighting schemes, we have developed several figures to compare the carbon stock data from each of the databases. Since it is not possible to provide a spatially weighted average of the Winrock data, in order to present a single figure for comparison, an average of all carbon stock data is given for each administrative unit within the corresponding Woods Hole region. In Figure 2-21 and Figure 2-22, error bars represent the minimum and maximum values given over all the administrative units.

Figure 2-20 provides example EFs from both Winrock and Woods Hole with a breakdown of contributions to the final EF for both conversion of forest to cropland and grasslands to cropland. The carbon released from vegetation is the primary contributor to the EF, particularly when forests are converted. Soil carbon also has a significant impact on the final EF, particularly for grasslands, where the C in vegetation is not as high. When forests are converted, foregone

sequestration also has some impact on the EF, but is generally not considered for other land conversions. In countries with peat soils, emissions from converting those lands can have sizable contributions to the overall EF. The Winrock data applies conditions for peat soils for Indonesia and Malaysia. The EF shown for Indonesia is an average for all regions within that country, where emissions from peat soils range from zero for some regions to 33 tons CO_{2,eq}ha⁻¹yr⁻¹ for regions with high peat areas. Since these emissions are assumed to occur over the entire time horizon (30 years), the contribution from peat soils can have substantial impact in these regions, which far outweigh even the release of C in the vegetation.

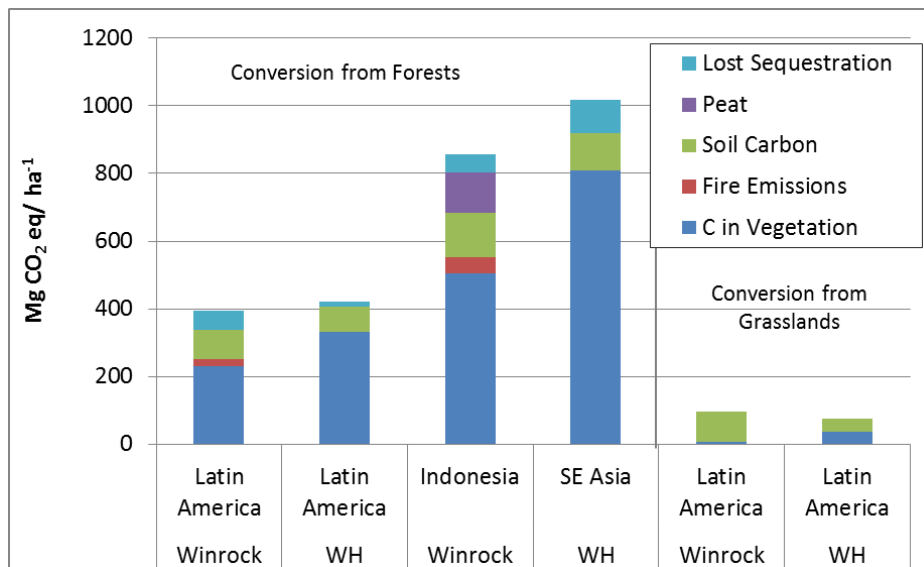


Figure 2-20: Contribution of C sources to EFs from Winrock and Woods Hole for Latin America and Southeast Asia.

Note: Winrock data are the average of all admin units within a WH region. The Woods Hole data are the weighted average of forest or grassland ecosystems within each region. 100% of the C in vegetation and 25% of the soil C is represented in the figure (following Searchinger approach)

Because a direct comparison of the data in the Winrock and Woods Hole databases is not possible, we have aggregated the Winrock administrative units into corresponding Woods Hole regions (As shown in Appendix A) to produce an average value of C-stock data for each region. A more appropriate comparison would be to weight the data by land cover, which could be done using the MODIS satellite data. However, this would require intensive calculations, which is beyond the scope of this work. In order to capture the wide ranges of data for each category in the Winrock database, the average value is presented along with error bars that represent the minimum and maximum stock data.

2.7.1 COMPARISON OF C-STOCK DATA FROM WOODS HOLE AND WINROCK DATABASES

2.7.1.1 Above/ Below Ground Carbon

The carbon stored in the biomass both above and below ground is the key contribution to upfront emissions caused by land-clearing as land use is changed from one classification to another, particularly for land conversion from forests.

Different land types have significantly different carbon stores. For example, forests have significantly greater C-stock than grasslands. The comparison of C-stock data used in Winrock and Woods Hole is shown in Figure 2-21-A for forests and Figure 2-21-B for grasslands. The ranges of data applied for carbon stock of forests are similar in each database, although the resulting Winrock average EF is lower than the Woods Hole EF for most regions. Data from Winrock comes from multiple recent literature and sources (as shown in Figure 2-5). Some of the data are based on more recent research by Houghton than the Woods Hole data, and some are based on IPCC default factors.

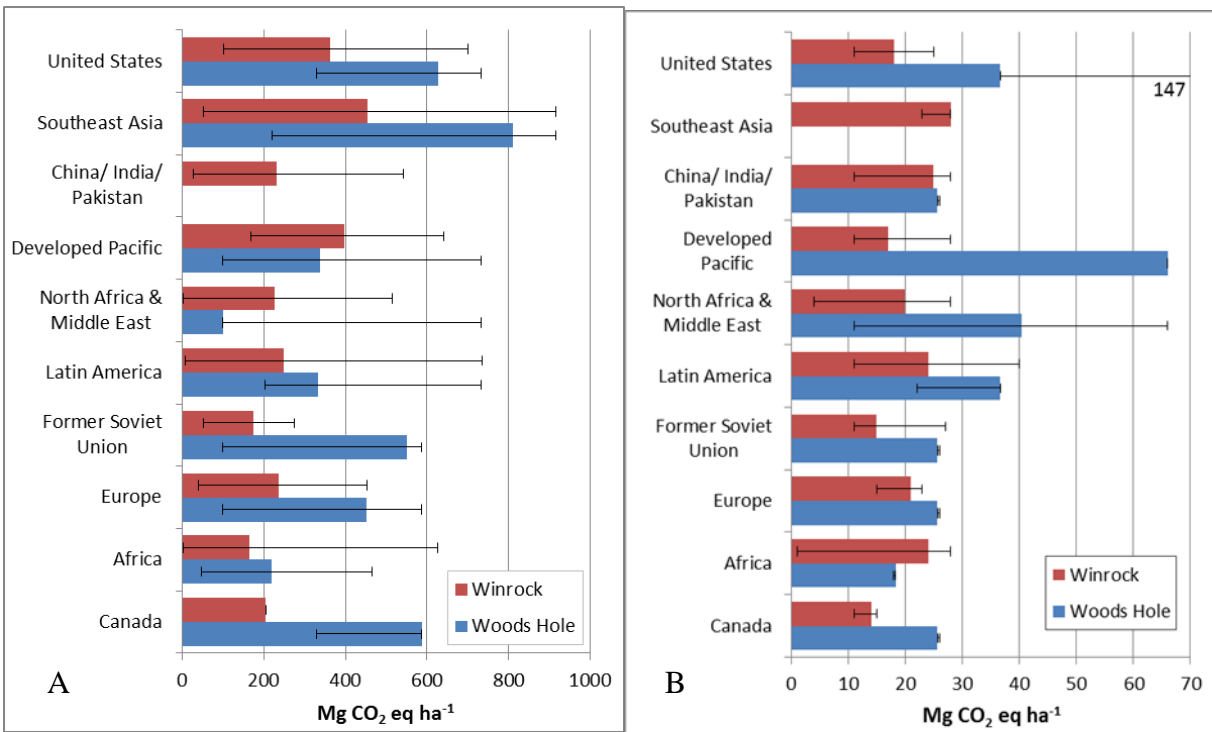


Figure 2-21: Comparison of C stock data for above- and below- ground C in vegetation in Woods Hole regions and corresponding Winrock regions for forestlands (A), and grasslands (B).

Note: The Woods Hole data are weighted averages of ecosystems classified as forests or grasslands within each region. The error bars indicate the minimum and maximum values. The Winrock data are averages of all administrative units within a corresponding Woods Hole Region, with the error bars noting the minimum and maximum C-stocks within the region.

Winrock applies IPCC default factors for grasslands by ecosystem type, as shown in Figure 2-21-B, which also generally results in lower stock values than Woods Hole. Winrock uses additional grassland categories of shrubland and savanna and applies multipliers of 1.8 for savanna and 3.4 for shrubland. There is no difference in classification of these land types in the Woods Hole database.

The accounting of the above and below ground carbon stock data is also done differently for EPA than for CARB, Tyner and Searchinger.

As described in Section 2.4.1, Searchinger assumes that 100% of the carbon in the vegetation is released as a GHG, while CARB and Tyner assume 90% and 75%, respectively. CARB's assumption is based on IPCC 2006 defaults (GPG- Section 5.3.1.2), while Tyner states that they assume 25% of the carbon is stored in wood products that are harvested and used for buildings, furniture and wood.

Included in the Winrock database is a calculation to reduce the vegetation emission by carbon contained in harvested wood products. However, no data are currently applied, so 100% of C-stock in the converted land, less the carbon stock contained in the new land is applied.

2.7.1.2 Soil Carbon

The analysis of soil carbon in the Winrock database is significantly different than in the Woods Hole database. In the Winrock database, the Harmonized World Soil Database (HWSD) is used with soil carbon stocks to a depth of 30 cm. The changes to the soil carbon stock are calculated based on Section 5.3.3.4 of the IPCC[93] as described in Scheme 2-1 and shown below.

$$\Delta C_{soil} = \frac{C_{soil,initial} \cdot (1 - FLU \cdot FI)}{20 \text{ years}} \cdot (1 - \% \text{ peatlands}) \text{ [t CO}_2 \text{ ha}^{-1} \text{ yr}^{-1}]$$

For lands without conversion from peatlands, the equation becomes:

$$C_{soil} = \frac{C_{soil,initial} \cdot (1 - FLU \cdot FI)}{20 \text{ years}}$$

The calculation is based on stock change factors for land use and inputs. The input factor (FI) is set to 1 for all regions, but the land use factor (FLU) is based on IPCC default factors as shown for each region below (Table 2-22). The higher the FLU, the lower the emissions from soil will be. Emissions from soils are assumed to occur over a 20-year period.

In the Woods Hole emission factor database, soil carbon stock data are given based on Houghton's research for carbon fluxes. The data presented are in the top 100 cm of soil, and 25% of the carbon is estimated to be released upon land conversion. (This same assumption is applied for Searchinger, CARB and Tyner work).

A comparison of the carbon stock data is provided in Figure 2-22. Again, the Winrock data are based on an average of all administrative units within the corresponding Woods Hole region. The data shown are the carbon stock data, so naturally, the Woods Hole data would be higher for most regions, since it accounts for 100-cm depth compared to 30-cm depth.

Table 2-22: Land Use Factors for Soil Emissions in Winrock

Region (corresponding to Woods Hole Regions)	Land Use Factor (FLU) range
U.S.	0.8
Southeast Asia	0.5-0.6
China/ India/ Pakistan	0.5-0.7
Developed Pacific	0.5-0.6
North Africa/ Middle East	0.5-0.8
Latin America	0.5-0.8
Former Soviet Union	0.8
Europe	0.7-0.8
Africa	0.5-0.8
Canada	0.8

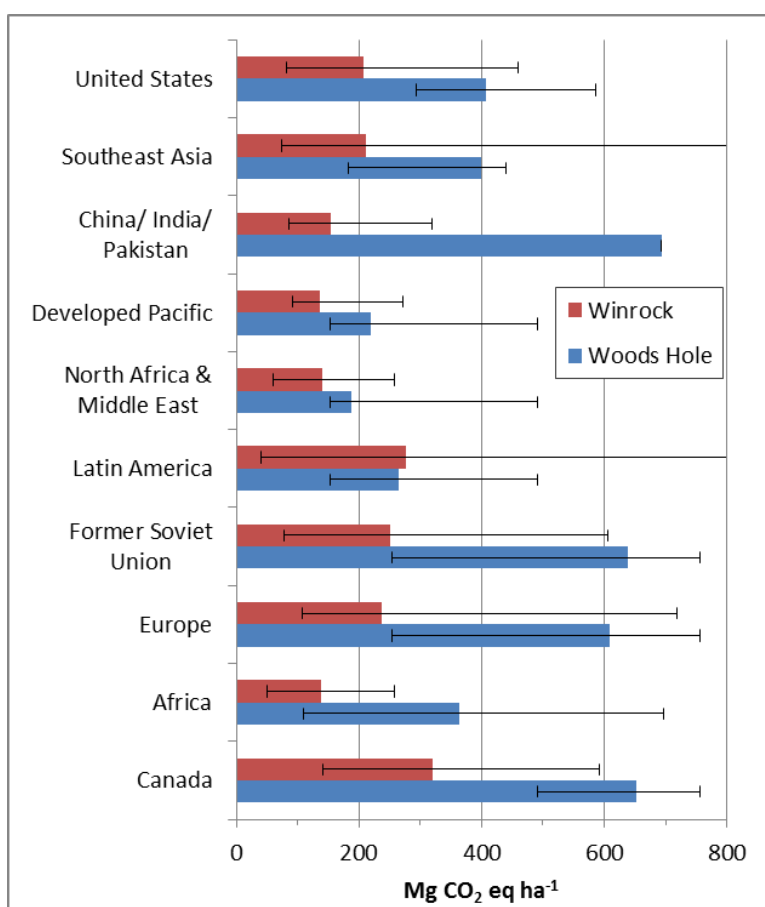


Figure 2-22: Carbon soil stock data from Woods Hole and Winrock.

In the Winrock database, peat emissions are included for Indonesia and Malaysia only. The resulting emissions are assumed to occur over a 30-year time period, which substantially affects the overall EF for regions with high fraction of peat. The Woods Hole database does not include a separate calculation for peat emissions. However, the carbon stock data for Southeast Asia is based on wetlands with high quantities of organic soils.

2.7.1.3 Non-CO₂/ Combustion Emissions

The Winrock analysis includes non-CO₂ emissions produced from lands where fire is used as a means for site clearing and preparation. To define the regions using fire, expert opinion was used to judge which regions commonly use fire for agricultural clearing. [55] Entire countries or continents are flagged as either using fire for land clearing or not. The countries include much of Africa, SE Asia, and much of Latin America (excluding Chile and Argentina).

Fire emissions are only calculated for conversion of natural lands to cropland. A flag in the database indicates whether the fire emissions will be calculated for each administrative unit. The fire emissions are a one-time contribution to the GHG from ILUC, and are calculated as described in Scheme 2-1. The fire combustion factor, and CH₄ and N₂O emission factors used to calculate the fire emissions are given in Table 2-23 for each initial land category. The emission factors for each gas are based on IPCC values. [93] The fire combustion factor for conversion from forests is the lowest at 0.5, which estimates the mass of fuel available for combustion. Russia is the only country that is given a different combustion factor at 0.3. The report on the updates to the Winrock database for the final rule of the RFS2 [55] states that the factors for forests come from the IPCC (Tables 2.5 and 2.6 in [52]) and the remaining factors come from literature [94].

Table 2-23: Fire and combustion factors for land conversion to crops in Winrock database.

Initial Land Type	Fire Combustion Factor	CH ₄ Emission factor	N ₂ O Emission factor
Forest	0.5 (Russia = 0.3)	2.3-6.8	0.2-0.3
Grass	0.8	2.3	0.2
Shrub	0.7	2.3	0.2
Savanna	0.6	2.3	0.2
Wetland	0.7	2.3	0.2
Mixed	0.8	2.3-3.8	0.2

The Woods Hole database does not include a separate calculation for emissions from fire. It is unclear if additional consideration for fire is made within the data themselves. Houghton describes that the structure of the model used to develop the Woods Hole data includes burning to clear land [66], but it is unclear how fire emission rates are included, or if they exclude CH₄ and N₂O. However, the contribution of fire emissions to the overall GHG from land clearing is small.

3 TIME ACCOUNTING PRACTICES

When comparing the life cycle GHG of biofuels to conventional fuels, it is important to consider the time profile associated with each fuel's emission stream. The GHG emissions resulting from production of conventional fuels are primarily associated with the extraction, conversion and combustion of the fuel, and are unlikely to change significantly from year-to-year. Although biofuels also have consistent year-to-year emissions associated with production and use of the fuel, the indirect land use change (ILUC) emissions that are linked to the biofuel follow a different temporal distribution. The ILUC emissions, which include a large up-front GHG release associated with bringing new lands into production and an ongoing release from soil carbon or loss of carbon sequestration possibilities, must be allocated over the entire quantity of fuel produced during the biofuel production period. Therefore, a common metric must be applied that allows the ongoing emissions to be aggregated into a single measure in order to make comparisons between fuels. Many LCA studies that include ILUC use a straight-line amortization method, which spreads out the net emissions occurring during a select time period over the entire time period. The choice of accounting method can have a significant effect on the net GHG impacts. In particular, two important parameters are the time frame considered and the weighting scheme that allows for the comparison of emissions occurring today with those occurring at various points in the future.

Figure 3-1 illustrates the ILUC emissions occurring as a result of expansion of biofuel use. A large release of GHG emissions occurs in year zero from changes in vegetation as a result of land conversion. Additionally, soil carbon emissions continue to be released for approximately 20 years, and foregone sequestration is accounted for through the duration of biofuel production. Three distinct time periods are illustrated in Figure 3-1. The first is the *production period*, which is an estimate of how long the biofuel feedstock will be produced until the fuel is economically displaced or until production is ceased. The production period affects how much biofuel is produced (considering an annual production volume). The *analytical horizon* defines the period of time over which all emissions are accounted for and attributed to the volume of biofuel produced. The analytical time horizon determines how long the biofuel has to "pay back" the ILUC emissions. The analytical horizon can coincide with the production period or extend past it. For cases when it extends beyond the production period, what occurs to the land after biofuel production has ceased may be considered. This period is called the *recovery* or *reversion period*, during which the land could be recovered into a natural state or used for other purposes. What occurs during this recovery or reversion period is dependent on what happens to the land. Inclusion of GHG emissions during this recovery phase has been debated.

The issue of time accounting is complex, and is in essence a question of how to combine one-time changes in carbon storage in soils and plants associated with expansion of biofuel production with a carbon intensity that is based on continuing life cycle inputs. [95] The length of time over which emissions are considered, and the weighting that future emissions are given compared to current emissions, can have considerable impacts. Weighting of emissions over

time is generally done by applying a discount rate, which is used in economics to value investments over time. Applying higher discount rates weight future emissions less than current emissions. Several alternative methods to discounting, such as calculating a fuel warming potential, have also been suggested. Longer time frames and/ or low discount rates favor biofuels in comparison to conventional fuels. There is a general lack of consensus within the scientific community about appropriate time horizons and discounting practices. [10,96,97]

After thorough review and discussion, both the EPA and CARB have currently settled on using a 30-year time horizon with a 0% discount rate. The debate by which each has arrived at these values and alternative methods of time accounting will be discussed in this section.

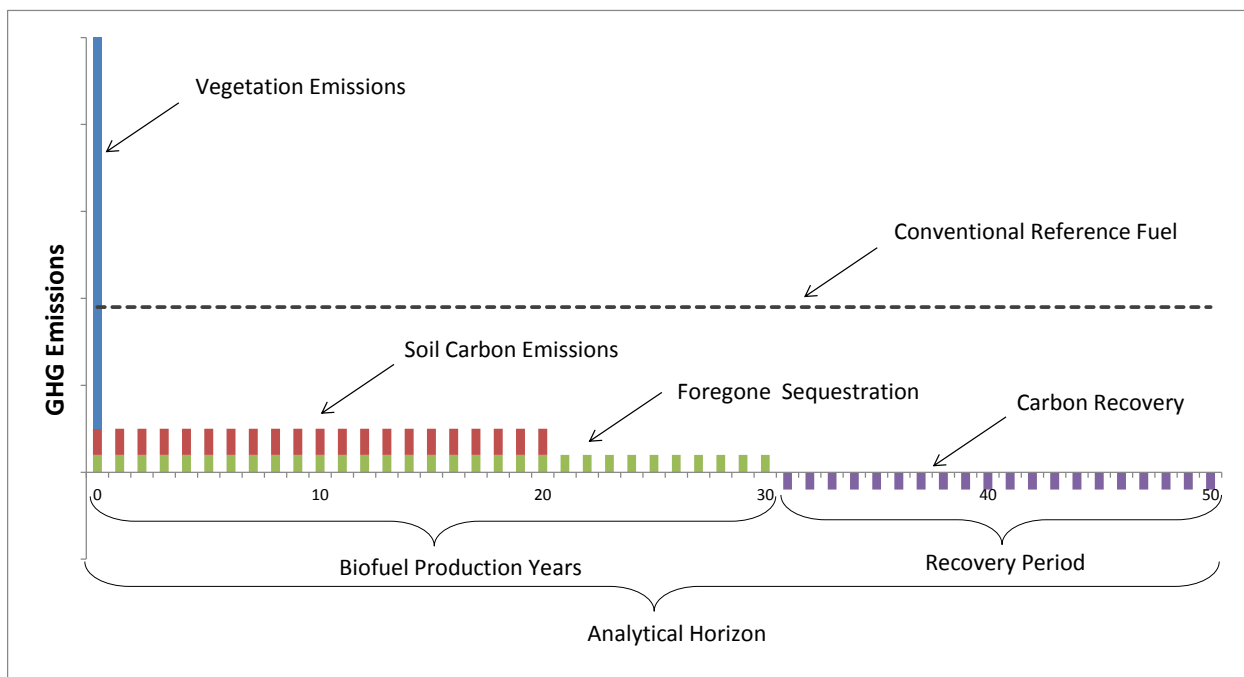


Figure 3-1: Emission flows over time. (Adapted from[95])

3.1 ANNUALIZATION

Because of its simplicity and consistency, EPA, CARB, and EU-RED have adopted the annualization method, in which all indirect emissions occurring over the biofuel production time-period are totaled and divided by the total volume of biofuels produced during the production period. A discount rate can be applied to the emissions to weight near term and future emissions differently. Both the EPA and CARB have settled on a 30-year time period for analysis with a 0% discount rate, while EU applies a 20-year production period. Although the annualization method is simple, it is not without its own inadequacies or areas of controversy. When considering the time profile, two main assumptions have the most significant impact: (1) the analytical horizon considered, and (2) the discount rate applied to future emissions.

3.1.1 ANALYTICAL HORIZON

The selection of the analytical period used to amortize indirect GHG emissions can have considerable impact on the final aggregated CI results for ILUC. If shorter periods are considered, the large upfront emissions occurring during the initial land conversion are apportioned over a smaller time, providing less time for the biofuel to “payback” its carbon debt. Additionally, any emissions, positive or negative, occurring beyond the analytical time horizon are truncated. If a long time horizon is considered, emissions impacts from the large upfront emissions are generally lessened. If the time horizon extends beyond the biofuel production period, there may also be a recovery period that can be considered, further lessening the carbon debt.

The selection of time frame is somewhat arbitrary, and although policies have generally agreed upon a period of 30 years (EU applies a 20-year time frame), there are consequences of selecting both shorter and longer time frames. The EPA gave the following reasons for selecting a 30-year time frame:

“The main reasons for why a short time period is appropriate: this time frame is the average life of a typical biofuel production facility; future emissions are less certain and more difficult to value, so the analysis should be confined insofar as possible to the foreseeable future; and a near-term time horizon is consistent with the latest climate science that indicates that relatively deep reductions of heat-trapping gasses are needed to avoid catastrophic changes due to a warming climate.”

In both the EPA’s draft regulatory impact analysis (RIA) and final RIA, cases were presented for 30-year time frame with 0% discount rate and a 100-year time frame with 2% discount rate [2]. In both cases, the time horizon coincides with the production period to avoid the issue of reversion emissions (discussed in more detail in Section 3.1.3). EPA reviewers suggested time periods ranging from 13 years (which corresponds with the policy time frame to the year 2022) to 100 years. Many agree that a shorter time frame that coincides with the life of a biofuel production facility (20 to 30 years) is more defensible and emissions are more certain than over a longer time frame such as 100 years (Fargione, Heimlich, Martin, Marshall in [10]). However, some (Richards) argued for 100-year time frames to encompass all emissions resulting from the project. A longer time frame introduces the issue of land reversion emissions, if the biofuel production period is shorter than the time frame. In general, the reviewers agreed that consideration of reversion emissions is too uncertain and should be avoided. Based on the review and other comments, the EPA settled on a 30-year time frame for the final rule.

The time accounting methodologies applied in CARB’s LCFS also underwent expert workgroup review, with similar disagreement and general recommendations as those from the EPA. CARB’s time accounting workgroup recommended a short project horizon since a shorter time period promotes fuels with lower upfront LUC costs and earlier benefits, and since it is more difficult to predict future production methods and shifts in fuel usage over the long term.

Some of the advantages and disadvantages discussed for shorter and longer time frames are presented in Table 3-1 below.

Table 3-1: Advantages and Disadvantages for applying short or long time frames in GHG time accounting.

Time Frame	Advantages	Disadvantages
Short Time Frame (20-30 years)	<p>Emphasizes importance of early emissions in the atmosphere.</p> <p>More “conservative” since longer time frames are more uncertain.</p> <p>A shorter time frame may under-predict the actual fuel production period, but then biofuels would outperform whereas an over-prediction might result in irreversible GHG releases.</p>	Truncates potential benefits that occur over time.
Long Time Frame (100 years)	<p>GHGs persist in the atmosphere for long periods; 100 years is similar to GWP accounting.</p> <p>Allows for the consideration of land reversion/land conversion after biofuel production.</p> <p>Long term biofuel production is reasonable to consider because advances in technology and decreases in production costs make it more competitive with respect to conventional fuels.</p> <p>(EPA benefit) RFS does not have a specific end-date.</p> <p>Climate change is a long term problem, allows the opportunity to assess intergenerational issues.</p>	<p>Increases Uncertainty- changes in market conditions could see a decline in biofuel use over a shorter period of time; benefits would never be realized.</p> <p>Reduces the importance of large up-front emissions.</p>

A time period is also applied to estimate and make comparisons between various GHGs in applying the GWP. The most frequently used time period for GWP is 100 years, which is considered a “rolling time horizon,” meaning that the accounting period begins from the emission of the GHG.

3.1.2 DISCOUNT RATE

The continuing existence of GHG in the atmosphere brings up the question of how to rate the relative importance of GHG emissions over time. The IPCC has noted that risks associated with climate change include loss of glaciers and biodiversity.[98] Under such a scenario, if near term emissions aren’t reduced, long term reduction may occur too late to mitigate or reverse these impacts. When considering ILUC emissions occurring over a long period of time, it is therefore important to consider how current emissions may have more or less impact than future emissions. This can be done by applying a discount rate to weight the damage done by emissions in different time periods. Every year that an event is delayed makes it worth less by a

percentage, called the discount rate. By applying a discount rate, near-term emissions are weighted more heavily than future emissions.

The application of a discount rate to ILUC emissions from corn ethanol is shown in Figure 3-2¹¹. When no discount rate is applied (blue bars in Figure 3-2), future emissions have a greater value than when a discount rate is applied (red bars) The net present value (NPV, which is the sum of all emissions over the given time frame, 30 years in this case) of the discounted emissions are less than the NPV of the non-discounted emissions. However, when the NPV of the emissions is annualized to determine an annual net present value (ANPV), they are treated as a mortgage payment on a loan, with the discount rate acting as the interest rate. Therefore, a 0% discount rate means “no interest is paid” so that the ANPV of the ILUC emissions are less than when a discount rate is applied (blue line compared to red line). Therefore, a zero or low discount rate favors biofuels.

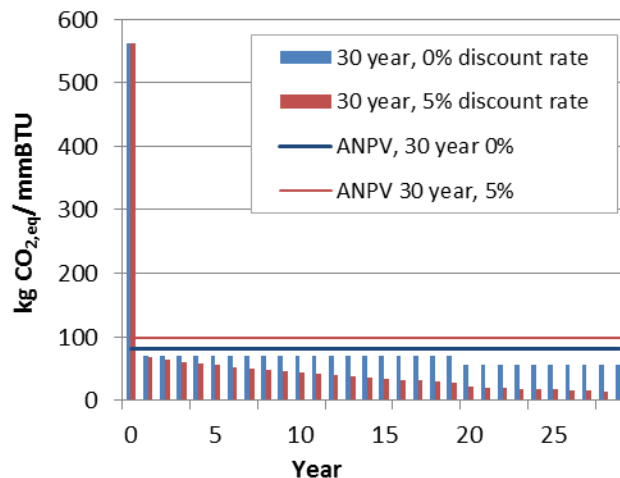


Figure 3-2: ILUC emissions of corn ethanol (EPA analysis) with 0% and 5% discount rates and 30 year time horizon.

Discounting is an economic practice that is used to determine the value of investments over time, and is being applied to physical GHG emissions as a method to compare future versus current emissions. Whether or not to apply a discount rate and what the appropriate discount rate to use have been debated. In the EPA’s Review process for the LCFS, reviewers of the time accounting methodologies had dissenting opinions on the use of a discount rate[10]. Some argued that the use of a discount rate is too uncertain, further complicating the ILUC analysis. Additionally, some argued that discounting is an economic practice, which may not apply to physical phenomena, since a release of a unit of CO₂ years from now may do more or less damage than the same unit discharged today. Instead, GHG emissions should be valued monetarily through a damage factor or social cost before discounting. [99,11,10] However, others argued that a zero discount rate does not give enough emphasis to the importance of reducing near term emissions. Arguments for and against discount rates are given in Table 3-2.

¹¹From EPA analysis of corn ethanol. Results shown are for year 2022 baseline results of a dry mill, natural gas, corn ethanol plant with CHP and DDGS. Excel spreadsheets for corn ethanol LCA results can be found in docket ID number: EPA-HQ-OAR-2005-0161-3173.6 at www.regulations.gov. Docket results were modified to show results for a 5% discount rate.

Table 3-2: Arguments for and against discounting ILUC emissions.

	Arguments for	Arguments against
0% or No discount rate	<ul style="list-style-type: none"> • Simple, reduces uncertainty. • Avoids the issue of intergenerational equity since all benefits and damages are weighted equally for current and future generations. 	<ul style="list-style-type: none"> • Gives no incentive to reduce emissions in the near term since future technology advances will provide better and cheaper opportunities for the same benefit.
Discounting	<ul style="list-style-type: none"> • Weights current emissions heavier than future emissions, since they will exist in the atmosphere longer and likely cause more damage or result in reaching a “tipping point” sooner. • The risks associated with climate change include irreversible damages which increase with increasing atmospheric GHGs. • Any future <i>reductions</i> in emissions should not be valued the same as current emissions since they will have less benefit and will be less likely to reverse damages. 	<ul style="list-style-type: none"> • Intergeneration Equity issue: discounting gives less weight to the well-being of future generations. • Lack of consensus for an appropriate discount rate. • Applies an economic principle to a physical phenomenon, which introduces further uncertainty (Do we really know if emissions will cause more or less damage in the future). • Applying a discount rate increases the uncertainty when determining ILUC emissions.

The appropriate discount rate to use is also heavily debated. The selection of a discount rate requires consideration of multiple additional variables including the rates of carbon accumulation and decay and estimates of marginal damages arising or avoided from atmospheric carbon stocks. [100] The EPA reviewers suggested discount rates ranging from 0 to 7.9%. [10] Discount rates ranging from 2.7 to 7.9% are recommended by the Office of Management and Budget [101]. Since high discount rates imply a low value for future GHG emissions resulting from today’s actions, lower discount rates of around 2-3% are considered more appropriate[102]. Others argue that ILUC emissions are highly uncertain, so applying a discount rate is meaningless.

Some suggest that as carbon stocks in the atmosphere increase, each additional unit released brings us nearer a catastrophic “tipping point”. In this case, each additional unit of carbon will result in more damage which means that a negative discount rate should be used. [100]

Although both the EPA and CARB have currently settled on a 0% discount rate for their analyses, some argue that by rejecting a discount rate, GHG emissions occurring today are the equivalent of those occurring 30 years from now. This methodology does not take into account irreversible impacts that may be caused as a result of higher near-term emissions resulting from LUC. It also implies that owing to technological advances, it will be cheaper to avoid emissions in the future for the same benefit as emissions avoided today. [10,95]

Other methodologies have been discussed to more appropriately discount emissions. O’Hare has proposed relating emissions using cumulative radiative forcing (CRF, discussed below) which

treats emissions similarly as those that are weighted by GWP. [11] Others argue for applying a cost to carbon, which can then be discounted appropriately. [100,103]

3.1.3 LAND REVERSION

The use of biofuels is not expected to continue indefinitely, which will likely result in a subsequent land conversion once the biofuel program ends and/or the biofuel feedstock is no longer grown. This introduces the possibility that the land would either revert to its prior state or be redirected for other uses. When the analytical time frame considered is longer than the project time horizon, what happens to the land post-production needs to be considered.

The possibility of re-vegetation of land after the biofuel program ends may lead to additional carbon sequestration as the native vegetation is re-grown (as illustrated in Figure 3-1). This sequestration could reduce the carbon debt of the biofuel if considered in the ILUC analysis, and some argue that these reversion emissions should be included. Delucchi argues that the end of the biofuels program will be marked by a reversal of the expansion of demand, resulting in some amount of land reversion which should be considered, [96] although these reversion emissions are not likely to entirely offset the initial LUC emissions because of changes and fluctuations in supply and demand over time. Additionally, he argues that these reversion emissions don't have as much value as emissions avoided today, so time accounting practices should include discounting.

Others, however, argue reversion emissions are too uncertain and should not be considered. In the EPA and CARB policy review processes, both work groups reached a general consensus that reversion emissions should not be included. Some argue that the subsequent land use should receive the credit for any carbon sequestration, and would be double counting if it were already accounted for by the previous crop, while others argued that future land use is too uncertain and there is no way to know if the land would actually revert or if it would be kept in crop production. [10,95] In this case, the biofuel could receive a credit that is never realized. Reversion emissions are not included in either the current LCFS or RFS2 methodologies. In RFS2, the analytical horizon is considered to be the same as the production period to avoid the issue of reversion emissions.

3.2 CUMULATIVE RADIATIVE FORCING & FUEL WARMING POTENTIALS

When a GHG is released to the atmosphere, it has a cumulative impact that increases with its time in the atmosphere. Other methodologies of time accounting have been proposed that take into consideration the cumulative effects of GHG. Several methodologies have been proposed that are based on a calculation of the cumulative radiative forcing (CRF) of the ILUC emissions.

CRF has been widely used to estimate the global warming potentials (GWP) of different gases, and attempts to include the cumulative effect of GHGs as they persist in the atmosphere. CRF is a measure of additional warming the atmosphere experiences over a particular time interval due

to the increase of GHGs. The Radiative Forcing (RF) is determined by multiplying the radiative efficiency (a) of a component (i) by the time-dependent decay function of the gas $[C_i(t)]$ as shown on the left hand side of the equation below. The CRF is then determined by integrating the RF over the entire time horizon (TH).

$$GWP_i \equiv \frac{\int_0^{TH} RF_i(t) dt}{\int_0^{TH} RF_r(t) dt} = \frac{\int_0^{TH} a_i \cdot [C_i(t)] dt}{\int_0^{TH} a_r \cdot [C_r(t)] dt} \quad \text{Equation 1 [104]}$$

GWPs are determined on a 20-, 100-, and 500-year time frame for different GHGs by comparing the CRF over each time period to the CRF of the same amount of a reference gas (r), which is typically CO_2 to determine $CO_{2,eq}$. The 100-year GWP is most frequently used in LCA, however, the time frame selected for the GWP is critical due to the differences in residence time of GHGs in the atmosphere. Table 3-3 gives the lifetime, GWP and radiative efficiencies for 3 primary GHGs. Methane has a much shorter lifetime in the atmosphere than does N_2O , so it has a higher GWP when considered on a shorter time frame. When the time horizon considered is shorter than the gas's lifetime, the remaining effects are truncated. The GWP treats all future warming within the time horizon equal and then truncates warming beyond the analytical timeframe.

Table 3-3: Lifetimes, radiative efficiencies and direct GWPs relative to CO_2 . [104] Note: data taken from IPCC/TEAP 2005.

GHG	Formula	Lifetime (years)	Radiative Efficiency	Global Warming Potential for Given Time Horizon		
				20-year	100-year	500-year
Carbon Dioxide	CO_2	1	$1.4 \cdot 10^{-5}$	1	1	1
Methane	CH_4	12	$3.7 \cdot 10^{-4}$	72	25	7.6
Nitrous Oxide	N_2O	114	$3.03 \cdot 10^{-3}$	289	298	153

3.2.1 FUEL WARMING POTENTIAL

O'Hare, et al. have proposed applying the CRF methodology to time accounting of ILUC emissions, which removes consideration of economic discount rates, instead relying on physical science for the calculation. O'Hare applies the CRF approach to calculate a *physical fuel warming potential*, which compares the CRF of a biofuel to the CRF of a reference fuel. [11] The following calculations can be applied using the Biofuel Time-Integrated Model of Emission (BTIME). [105]

The Physical Fuel Warming Potential (FWPp) is the ratio of the CRF associated with a biofuel scenario (CRFb) and a gasoline scenario (CRFg). The FWP is a multiplier for the direct emissions to estimate a fuel warming intensity (FWI), given in $g CO_{2,eq} MJ^{-1}$, that can be

compared between fuels (this is similar to GWP, which is multiplier for each gas to convert a gram of emissions into a gram of CO_{2,eq} emissions).

$$FWP_P = CRF_b / CRF_g \quad \text{Equation 2}$$

This method is similar to GWP except that it compares to fuel production scenarios rather than to GHGs over the same time period. Figure 3-3 illustrates the accumulation of CO₂ in the atmosphere for ethanol versus gasoline. The annual emissions streams over time are shown by the dashed lines for gasoline and ethanol (95 g CO_{2,eq} MJ⁻¹ vs. 60 g CO_{2,eq} MJ⁻¹ direct emissions over 25 years, respectively). The emission stream is converted using the Bern carbon cycle model into additional CO₂ in the atmosphere as shown by the solid lines. Due to the large initial emissions, ethanol production leads to higher CO₂ abundance for the first 20 years. Although a cross-over occurs after around 20 years, the damage caused by the ethanol emissions is greater since they have been in the atmosphere longer. This is illustrated by the cumulative warming effects, captured by the FWP and fuel warming intensity (FWI) metrics shown in Figure 3-4.

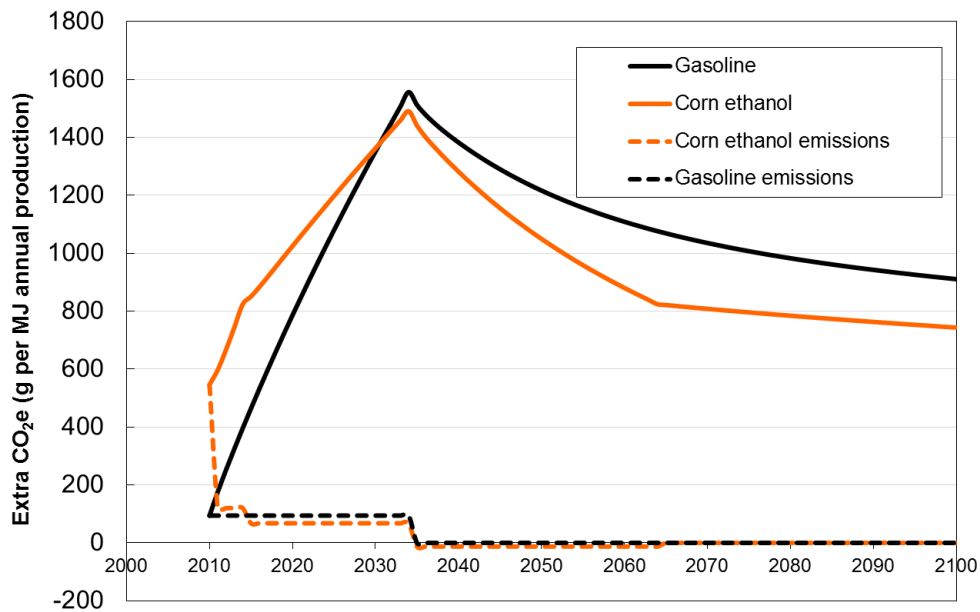


Figure 3-3: CO₂ abundance resulting from ILUC and direct emissions of ethanol (25 years at 60 g CO_{2,eq} MJ⁻¹) and gasoline (25 years at 94 g CO_{2,eq} MJ⁻¹) (From [11,105])

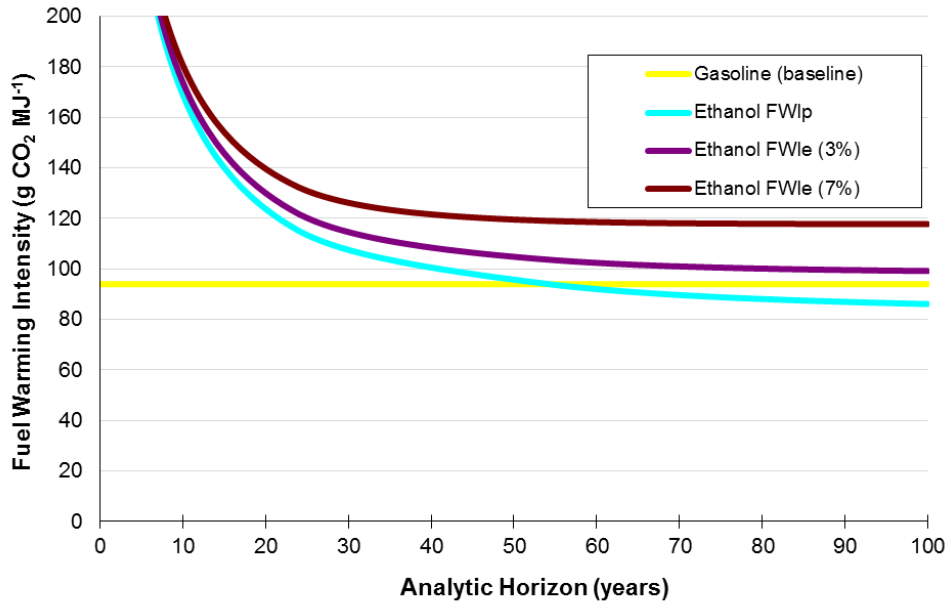


Figure 3-4: Fuel warming intensity (g CO_{2,eq} MJ⁻¹) vs. analytical horizon (From [11,105]).

A discount rate can be applied to the FWP to give an economic Fuel Warming Potential (FWPe). In O'Hare's methodology, the radiative forcing is discounted, and the FWPe is given by the ratio of the net present values:

$$FWP_e = \frac{NPV_b}{NPV_g} \quad \text{Equation 3}$$

There is growing support behind the use of the FWP methodology because it is analogous to the GWP method to convert GHGs into a CO₂-equivalent value and follows the well-known methodology of radiative forcing. It can also be used in conjunction with a discount rate. The FWP method takes into consideration how concentrations of GHGs and warming change over time. However, it does add additional computational complexity because it requires calculation of future GHG concentrations, as well as concentration dependent radiative forcing. Additionally, a damage function needs to be determined. In the ICF review of EPA's time accounting approach, Heimlich suggested the following limitations be addressed before the FWP methodology should be employed [10]:

1. Decay rate for atmospheric CO₂ assumes a constant background atmospheric concentration. In reality, radiative efficiency for a unit of CO₂ decreases non-linearly as atmospheric CO₂ concentration increases, and CO₂ atmospheric residence time increases.
2. FWP assumes that GHG radiative efficiency is constant.
3. FWP only deals with CO₂; it does not include methane or nitrous oxide.

3.2.2 TIME CORRECTION FACTOR

Kendall has proposed using a time correction factor (TCF) that can be used to adjust the value of amortized emissions which also follows the CRF metric [106]. The TCF method is similar to the FWP method, but instead compares the CRF of a pulse of emissions to the CRF of the emission amortized over a set time horizon. The TCF method was developed to address the challenge of representing climate change effects of amortized CO₂ emissions in LCA, which is distinct from the FWP method in that the FWP metric compares biofuels to conventional fuels, which provides a means to discount.

3.3 OTHER METHODOLOGIES

As part of the CARB Expert Work Group (EWG) activities, two additional methodologies were discussed which have not been published in peer-reviewed journals. A summary of the methodologies as they are described and discussed in the EWG reports is given below. [95]

3.3.1 BASELINE TIME ACCOUNTING

Kloverpris and Mueller have introduced a baseline time accounting methodology in which ILUC is measured relative to baseline changes in land use. [12,107] They argue that agricultural lands are expanding in the developing world, but contracting in the developed world. Increased biofuels may cause land to come into use sooner than it otherwise would in the developing world, resulting in more warming, and may cause land in the developed world to stay in production longer which would delay reversion and result in additional GHGs. In the baseline time accounting metric, the GWP over 100 years is used to determine an ILUC factor which is independent of the production period.

Kloverpris and Mueller have expanded this concept into a white paper that gives the full description of the methodology. [95] The members of the EWG subgroup assessing the issue of time accounting generally agreed that more work and description of the baseline time accounting methodology is needed before it should be considered.

3.3.2 SIMPLIFIED TIME ACCOUNTING

The simplified time accounting method discussed in the CARB EWG report is based on the Baseline Time Accounting methodology, avoids assumptions about the production period, and does not require analysis of atmospheric forcing or residence. In the simplified time accounting method, a variable equivalent ILUC discharge (G_{cv}) that can be added to the direct emissions is calculated with the following equation:

$$G_{cv} = G_c - (1-r)G_c = rG_c \quad \text{Equation 4}$$

Where G_c is the ILUC discharge associated with increasing production capacity (in g CO_{2,eq}MJ⁻¹) and r is the discount rate.

Some of the CARB reviewers argued against this methodology, however, since it adds to the uncertainty and does not eliminate the complication of choosing a subjective discount rate.

3.4 SOCIAL COST OF CARBON

Rather than applying a discount rate to a physical carbon unit, it has been suggested that the social cost of carbon can be applied to determine a “damage weighted” carbon content. [100] The social cost of carbon (SCC) is a dollar value assigned to each unit of carbon emissions which reflects the price of damages occurring both today and in the future caused by each additional ton of CO₂ released into the atmosphere. In GHG reduction projects, the SCC is used to measure the financial value of damages avoided, and therefore the benefit of the mitigation project. [103] Therefore, the larger the SCC, the more attractive the project. The SCC is a critical element in the cost-benefit analysis of climate change since current climate policy proposals (e.g. a carbon tax or a cap-and-trade allowance market) are based on the price of carbon emissions. A higher SCC gives emphasis on the risk of catastrophic climate change and provides incentive to reduce emissions.

The SCC is estimated by combining scientific models of global warming with a socio-economic model of the underlying impacts. Models to predict the SCC include DICE, FUND, and PAGE. [108] There are some ethical judgments that must be made to determine a SCC. For example, the loss of an endangered species is difficult to monetize. [108] As such, there is disagreement on how the SCC should be calculated. There are large uncertainties surrounding SCC. One of the primary uncertainties in its determination is the discounting scheme that is applied. Some suggest that a declining discount rate should be used in which the discount factor (or weight that is placed on future emissions) increases over time. In a sensitivity analysis by Guo, applying different discounting schemes grossly affected the SCC, with prices ranging from \$-2.6 to \$226 /tC (in 2005 prices). A negative SCC (which was estimated at a 3% discount rate, the highest evaluated) indicates that near term benefits outweigh future damages because of heavy discounting. The variability reflects the large amounts of uncertainty surrounding the determination of an SCC.

Marshall points out that the SCC can be applied to time accounting for biofuel ILUC to determine a “damage weighted” carbon content that can be compared amongst fuels. The result is a physical discount rate that is much lower than an economic discount rate. [100] To date, however, a social cost has not been included in alternative fuel policies.

4 N₂O EMISSIONS FROM AGRICULTURAL ACTIVITIES

4.1 BACKGROUND/INTRODUCTION

Nitrous oxide (N₂O) is a colorless, non-toxic, non-flammable gas with a slightly sweet odor. It has a variety of small volume uses including anesthetics (laughing gas), aerosol propellant, oxidizer for rocket fuel, and others. N₂O is also an important species in the overall biochemical-geochemical cycling of nitrogen. It is produced naturally in soils by microbial processes of nitrification and denitrification. The oceans are also recognized as a significant natural source of N₂O. In rough terms, approximately 1/3 of global N₂O results from ocean sources, with 2/3 resulting from land sources [53].

Due to its potent greenhouse gas (GHG) behavior, and its influence by human activities, N₂O is considered an important contributor to anthropogenically-induced radiative forcing of climate change. Figure 4-1, taken from the most recent Intergovernmental Panel on Climate Change (IPCC) report, shows the relative importance of N₂O compared to other radiative forcing substances. Because much of this N₂O originates from agricultural activity, it is of considerable interest in life-cycle assessments (LCAs) of biofuels. In this chapter, we discuss several topics related to N₂O from agricultural activities – including formation mechanisms, modeling approaches for determining inventories, and potential mitigation measures.

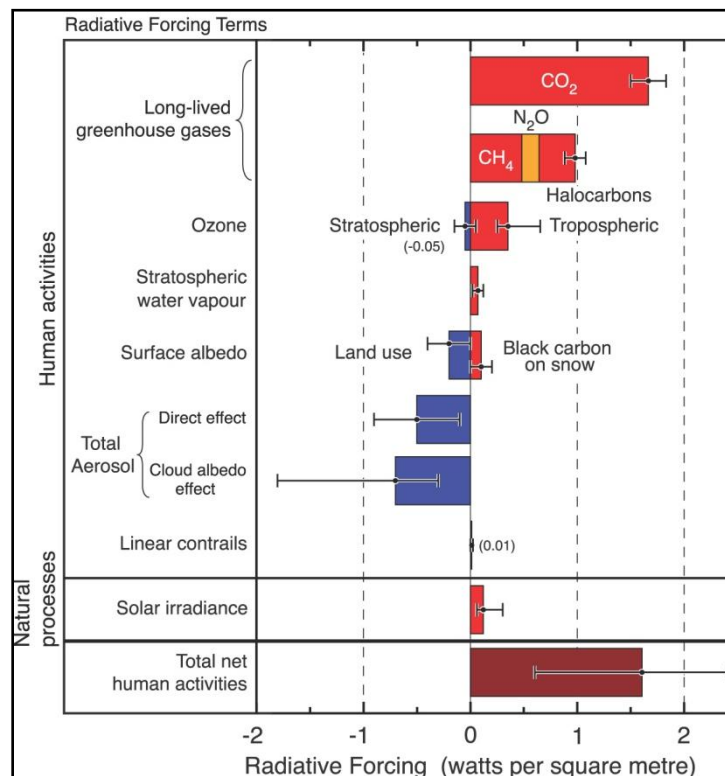


Figure 4-1: Radiative forcing of climate between 1750 and 2005. (Taken from IPCC-2007 [54])

4.2 N₂O OCCURRENCE AND INVENTORIES

The pre-industrial atmospheric concentration of N₂O is estimated to be 270 ppb, whereas today's concentration is approximately 322 ppb [54,13]. The current rate of increase is 0.26% per year. As shown in Figure 4-2, the atmospheric concentration of N₂O has risen sharply during the past century; although the rate of increase is less than that of carbon dioxide (CO₂) or methane (CH₄).

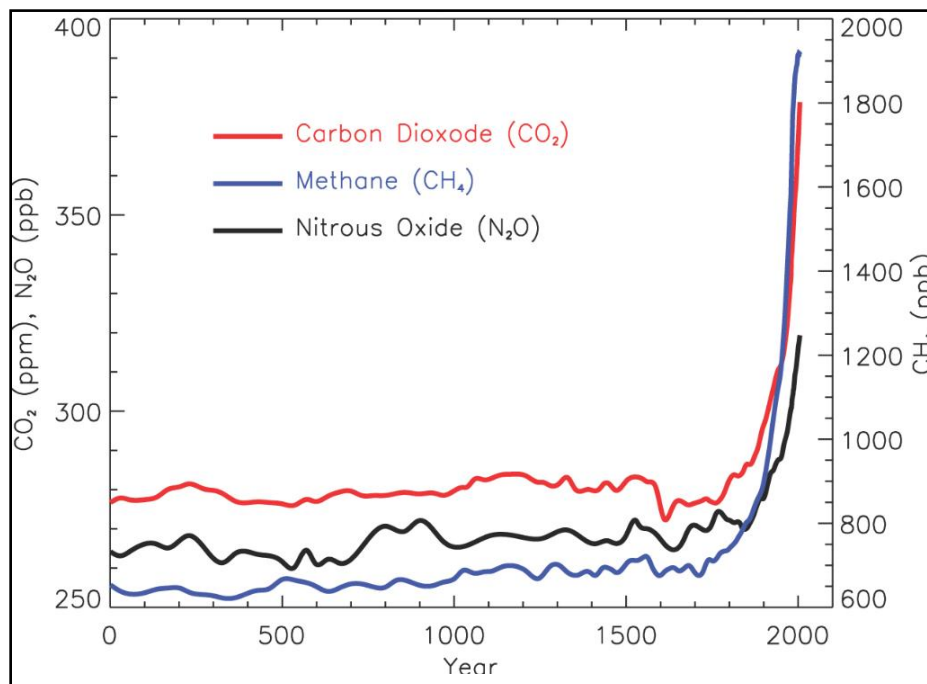


Figure 4-2: Concentrations of long-lived GHGs over the past 2000 years. (Taken from IPCC-2007 [54])

N₂O is removed from the atmosphere by photolytic reactions with ozone in the stratosphere [109]. In fact, N₂O is regarded as an ozone-depleting substance (ODS) of increasing importance, as emissions of chlorofluorocarbons (CFCs) are declining [110]. N₂O is now thought to be the single most important ODS, although it remains unregulated under the Montreal Protocol, which limits other ODSs.

However, of primary concern here is N₂O's global warming potential (GWP), which is much higher than that of CO₂. The exact value of N₂O's GWP is somewhat confusing. In the Second Assessment Report (SAR) from the IPCC (IPCC-1996) a GWP value of 310 was assigned to N₂O (for a 100-year time horizon) [111], meaning that 1 kg of N₂O in the atmosphere has the same radiative forcing effect as 310 kg of CO₂. In IPCC's Third Assessment Report (TAR) (IPCC-2001) the GWP of N₂O was revised to 296 [53]. In the Fourth Assessment Report (AR4) (IPCC-2007) the GWP was further revised to 298 [54].

Most literature reports during the past decade have used either the IPCC-2001 or IPCC-2007 value for N₂O's GWP (296 or 298). However, for official inventory purposes, the U.S. (and other countries) continue to use the IPCC-1996 value of 310 [13]. This is in accordance with GHG reporting standards under the U.N. Framework Convention on Climate Change (UNFCCC; of which the U.S. is a signatory), and is done so that current estimates of GHG emissions are consistent and comparable with previous estimates.

As with all GHGs, N₂O emissions inventories are generally expressed in units of teragrams (Tg) CO_{2,eq.} (1-Tg = 10¹² g = 1 million metric tonnes.) Detailed N₂O emissions inventories for the U.S. have recently been reported by the U.S. EPA [13]. The inventories for three time periods (1990, 2000, and 2009) are provided in Figure 4-3, which shows that agricultural soil management is the dominant source of anthropogenic N₂O emissions, accounting for approximately 60% of the total. Similarly, on a global basis, IPCC estimates that agriculture is responsible for 58% of total N₂O emissions [54]. Figure 4-3 also shows that the 2nd largest contributor to the N₂O inventory, mobile combustion, was reduced substantially between 2000 and 2009. This reduction is attributed primarily to phase-in of more effective emissions control systems on light-duty vehicles.

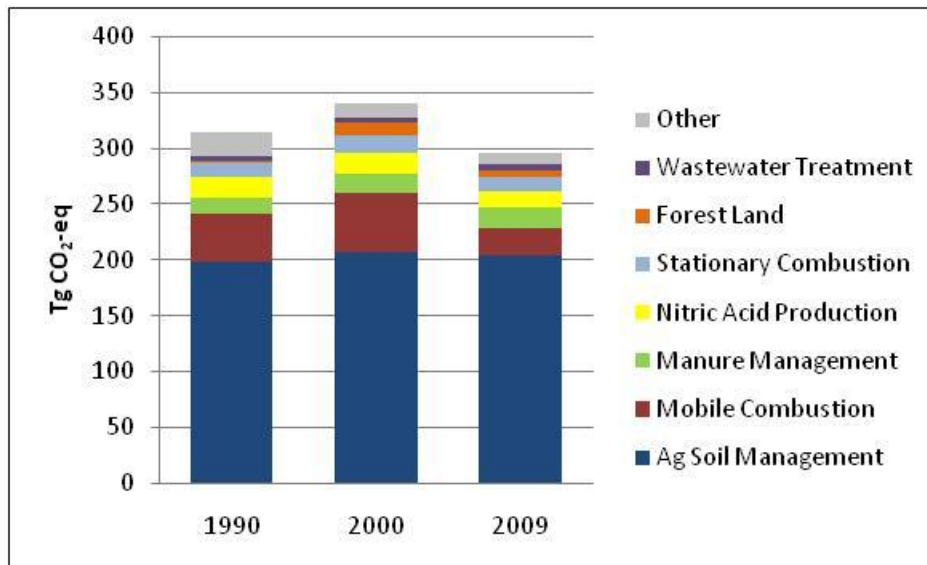


Figure 4-3: Total U.S. Anthropogenic N₂O Emissions Inventories, Tg CO_{2,eq.} (Data from U.S. EPA[13]).

Total U.S. GHG inventories from 1990 and 2009 are presented in Figure 4-4, showing the relative global warming potential (GWP) of the major GHG contributors. This illustrates that N₂O emissions represent only a small fraction of total GWP – 5.1% in 1990; 4.5% in 2009. (U.S. N₂O emissions in the year 2000 are not shown here, but can be interpolated from the 1990 and 2009 data.) On a global basis, N₂O provides a somewhat larger contribution to total GWP than in the U.S. As shown in Figure 4-4, the U.S. EPA estimates that N₂O contributed 7.5% of total global GWP in the year 2000 [112]. It is interesting to note that both globally and in the U.S., methane's contribution to the total GHG inventory is approximately twice that of N₂O's

contribution. However, only a small fraction of this methane is related to non-livestock agricultural activities – the subject of this report.

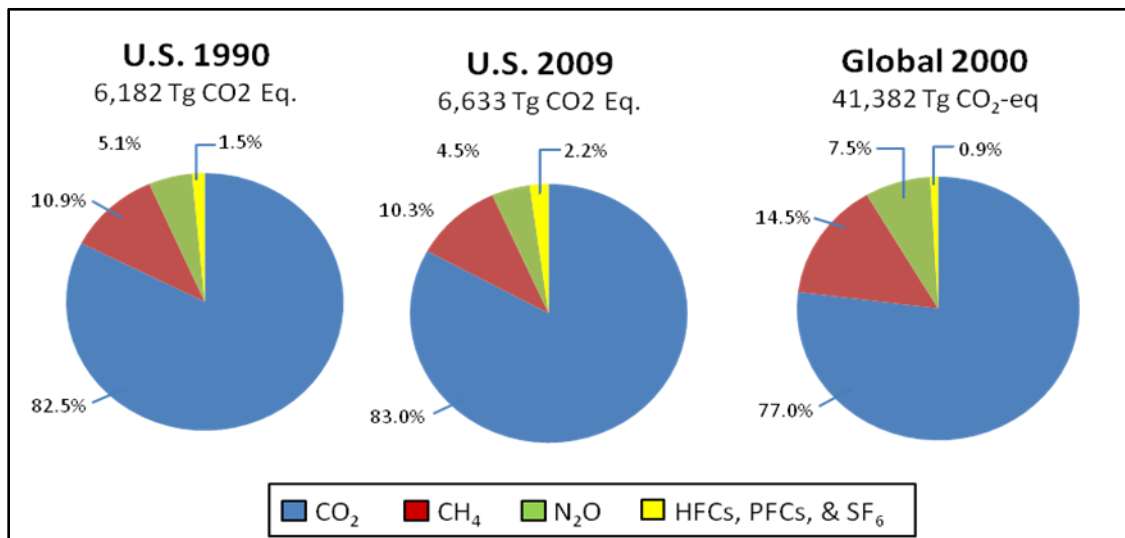


Figure 4-4: Total GHG Inventories, Tg CO_{2,eq}. (a) U.S. 1990; (b) U.S. 2009; (c) Global 2000. (Data from U.S. EPA [13,112])

U.S. emissions inventories are commonly disaggregated by economic sector. Such a breakdown of GHG emissions is provided in Figure 4-5, which shows that overall, the agricultural sector is a rather small contributor to total GHG emissions. (In Figure 4-5, CO₂ emissions from electricity generation are distributed across the relevant economic sectors.) This figure also illustrates that GHG emissions from the agricultural sector in the U.S. have been relatively constant over the past 20-years, whereas emissions from the other sectors have varied significantly. A sharp downturn due to the recent economic situation is particularly evident in the industry and transportation sectors.

As opposed to all other sectors, which are dominated by CO₂ emissions, GHG emissions from the agricultural sector are dominated by N₂O and methane (CH₄). The main sources contributing to these two GHGs in the U.S. in 1990, 2000, and 2009 are shown in Figure 4-6. Field burning of agricultural residues contributes a very small fraction of U.S. N₂O emissions, but is more significant in some other countries. For example, in Australia, it is estimated that prescribed burning of savanna is responsible for approximately 25% of the total agricultural sector’s N₂O emissions [113]. [Not shown in Figure 4-6 are CO₂ emissions attributed to the agricultural sector, which contributes approximately 80-90 Tg in each time period. The USDA also estimates that U.S. agricultural soils provide a small net sink (20-30 Tg of CO₂) [114].]

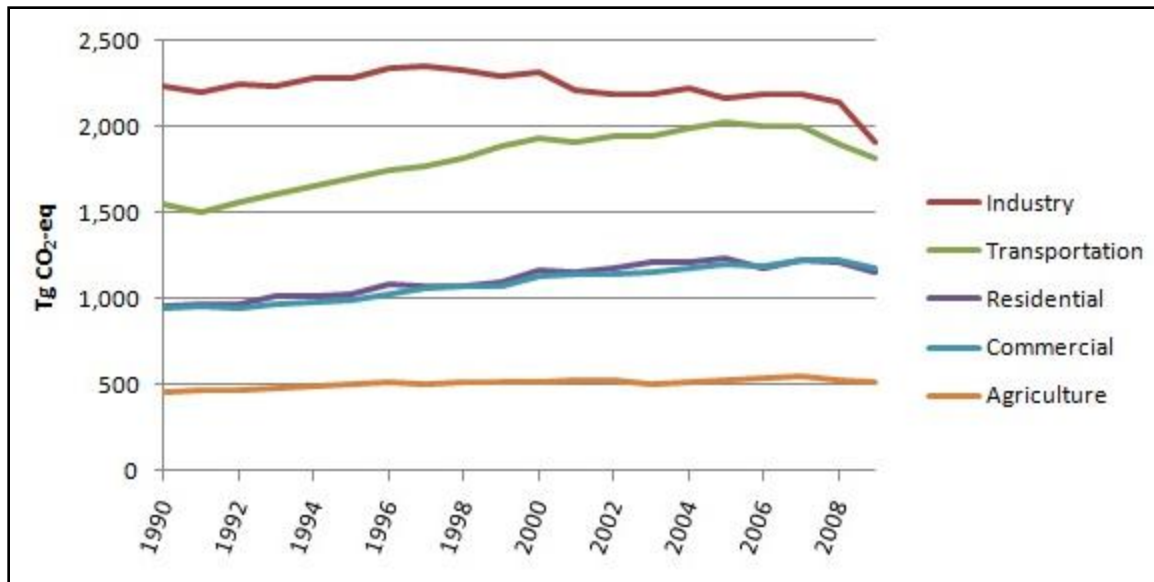


Figure 4-5: U.S. GHG emissions trends. Emissions from electricity generation are distributed to the relevant economic sectors. (Taken from U.S. EPA [13].)

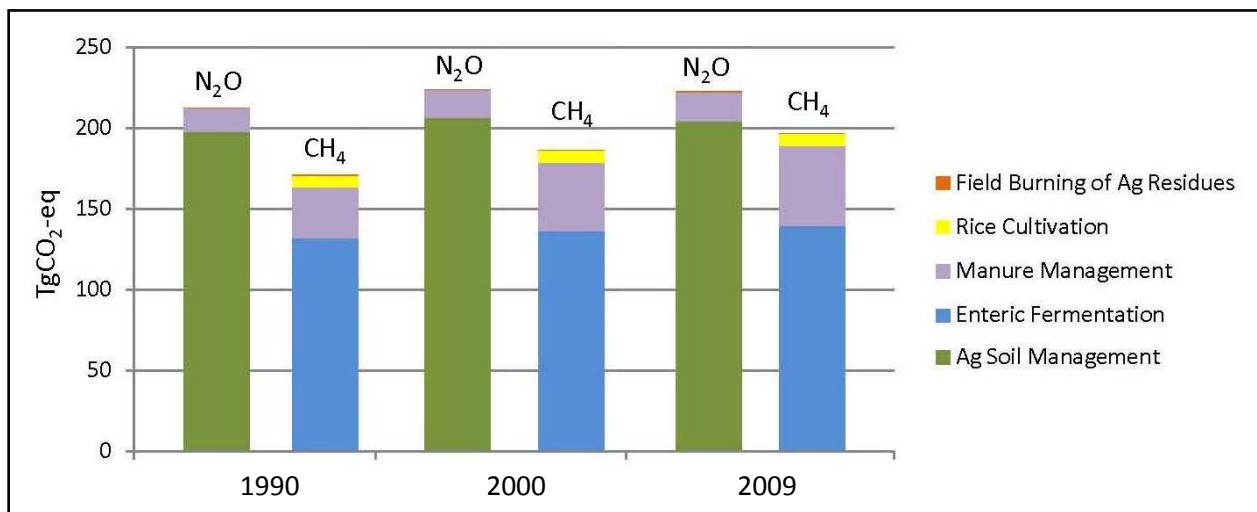


Figure 4-6: Non-CO₂ GHG emissions from the U.S. agricultural sector. (Data from U.S. EPA [112].)

Overall, CH₄ and N₂O have comparable contributions to total agricultural sector GHG emissions in the U.S. However, most of the CH₄ emissions are attributed to enteric fermentation in livestock which is outside the scope of interest for this report. USDA estimates that corn is the leading crop for N₂O emissions, followed by soybeans and wheat [114]. Emissions from corn cropping are high because of the extensive land area used for corn production, and the large amounts of nitrogen (N) fertilizer applied.

On a global basis, the agricultural sector is a larger contributor to total GHG emissions than in the U.S. Global estimates suggest that agriculture is responsible for 32% of total anthropogenic GWP, as opposed to only 8% in the U.S. [13,112]. It is also estimated that agriculture is

responsible for about 80% of global anthropogenic N₂O emissions [115,116], as compared to only about 60% in the U.S. Other differences between U.S. and global agricultural GHG emissions can be seen in Figure 4-7, which shows non-CO₂ GHG inventories projected from 1990 to 2020. (The units used here, Mt CO_{2,eq}, are identical to Tg CO_{2,eq}.) Of major concern is the global increase in non-CO₂ GHG emissions over this 30-year period. This increase is a consequence of producing more food (and higher quality food) to satisfy the growing global population. Also shown in Figure 4-7 is the relatively large contribution of rice cultivation to global agricultural GHG emissions, as compared to the small U.S. contribution (compare Figure 4-6 and Figure 4-7).

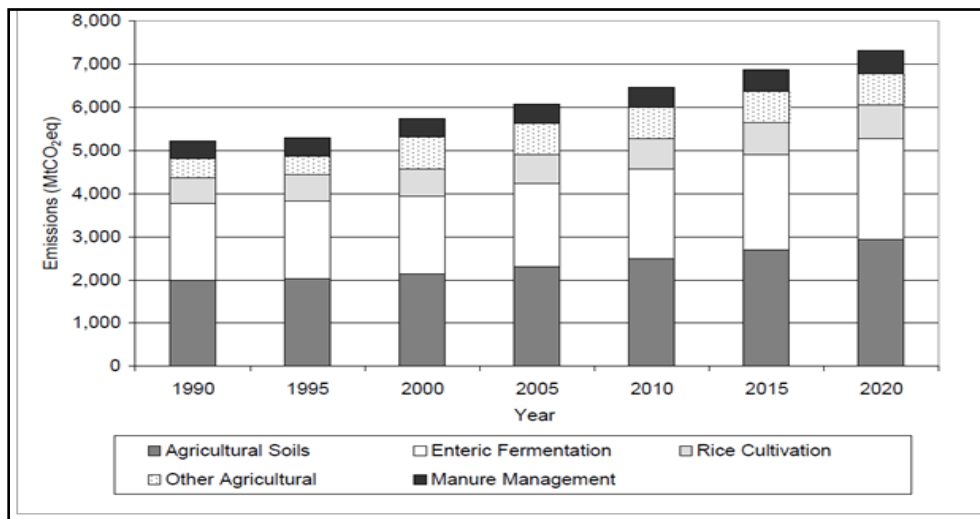


Figure 4-7: Global non-CO₂ GHG's from the Agricultural Sector. (Taken from U.S. EPA [112].)

As shown in Figure 4-7, much of the projected increase in global GHGs from the agricultural sector is attributed to soils. (N₂O formation mechanisms in soils are discussed in a later section.) Figure 4-8 shows where this growth of N₂O emissions from soils is expected to occur, with the majority coming from the developing world, particularly China, Latin America, Africa, and Southeast Asia. N₂O soil emissions from countries comprising the Organization for Economic Cooperation and Development (OECD), which includes the U.S. and Europe, are expected to remain nearly constant.

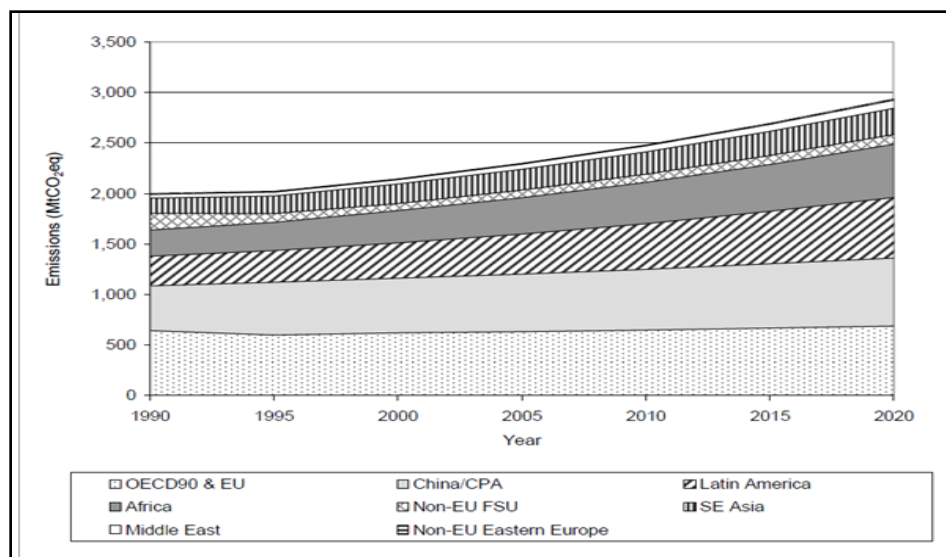


Figure 4-8: N₂O Emissions from agricultural soils. (Taken from U.S. EPA [112].)

In the most recent national GHG inventory, EPA has followed the IPCC-recommended approach for estimating uncertainty. For this purpose, a “Tier 2” analysis was performed, employing the Monte Carlo Stochastic Technique [13]. The overall GHG inventory has relatively low uncertainty, since it is dominated by reasonably well-known CO₂ emissions. However, the N₂O inventory has considerably higher uncertainty, as illustrated below in Table 4-1.

Table 4-1: Estimated Uncertainty in U.S. GHG Inventory (From U.S. EPA [13])

GHG Species	2009 Mean Value, Tg CO _{2,eq}	Standard Deviation, Tg CO _{2,eq}	Relative Std. Deviation, %
CO ₂	5,622.5	97.5	1.73%
CH ₄	702.8	45.3	6.45%
N ₂ O	334.2	42.1	12.60%
PFC, HFC, & SF ₆	143.7	4.8	3.34%
Total	6,803.2	115.0	1.69%

4.3 N₂O FORMATION MECHANISMS

N₂O is an important component in the overall nitrogen cycle by which nitrogenous species are converted among various chemical forms throughout the biosphere. Key processes within the nitrogen cycle include nitrification, denitrification, fixation, and mineralization [117]. A depiction of the nitrogen cycle involving agricultural soils and N₂O emissions is provided in Figure 4-9. As this illustrates, N₂O is emitted directly from soils, but also from numerous indirect sources including reaction of NO_x and NH₃ that are lost from soils by volatilization, nitrogen

species that leach from the soil, decomposition of crop litter and other vegetation, and degradation of human and animal wastes.

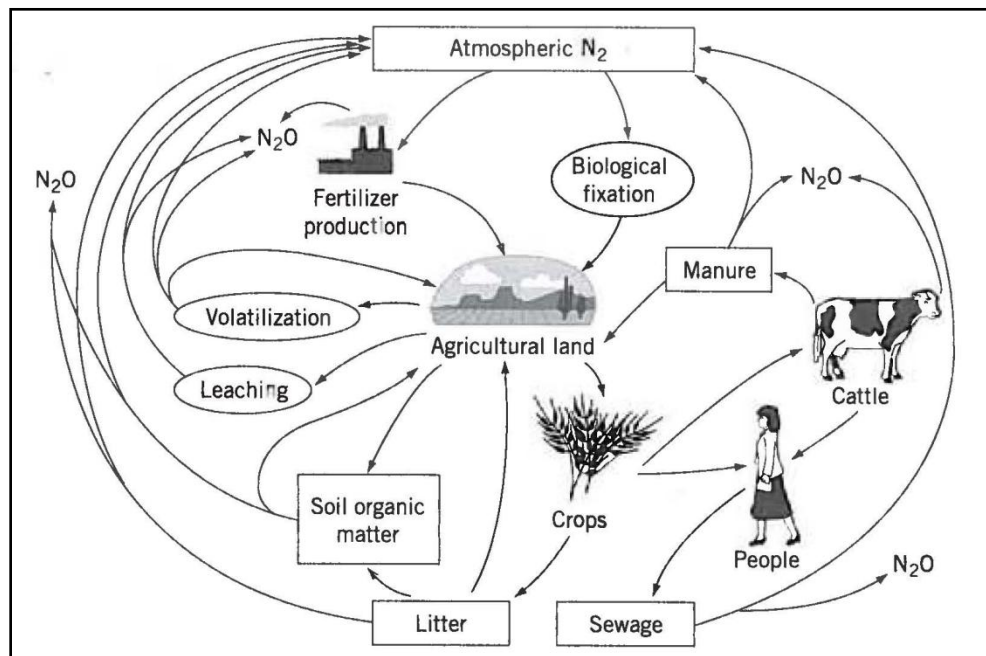
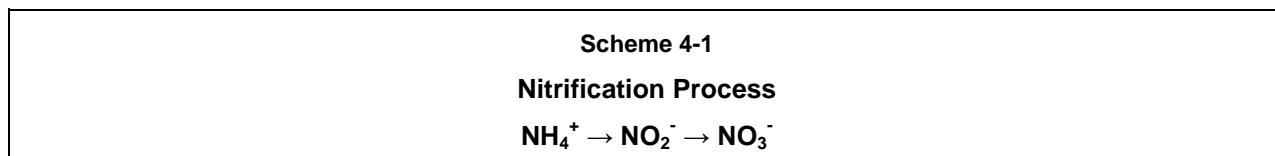


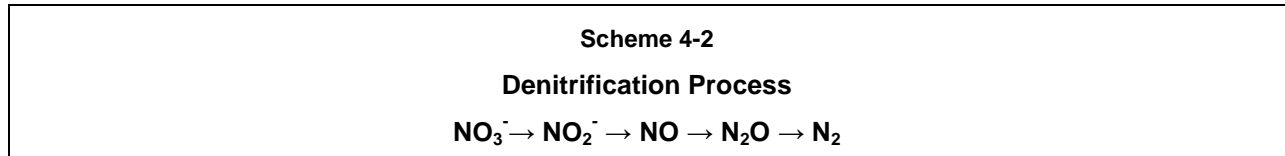
Figure 4-9: Nitrogen cycle of agricultural soils and its relationship to N₂O production. (Taken from Oonk & Kroeze (1998) [118] by permission of John Wiley & Sons, Inc.)

Direct emissions from land are the largest agricultural sources of N₂O. These emissions result from a complex set of microbial soil processes that include both nitrification and denitrification [119,120,121]. As shown in Scheme 4-1, nitrification involves conversion of ammonium (NH₄⁺) to nitrate (NO₃⁻), with nitrite (NO₂⁻) as an intermediate [122]. These oxidative processes occur under aerobic conditions by the action of various soil microorganisms. N₂O is produced by specific bacteria as a minor by-product in the oxidation of nitrite (NO₂⁻) to nitrate (NO₃⁻) [123,124]. Nitrification converts relatively immobile NH₄⁺ to highly mobile NO₃⁻, which is more available for plant uptake, but is also susceptible to leaching from the soil [125,126].



Numerous parameters influence the extent of nitrification within soils, including availability of oxygen, moisture content, soil organic matter (SOM) content, temperature, and pH. However, from a management (and modeling) standpoint, perhaps most critical is the availability of ammonium, which is directly influenced by application of nitrogen fertilizer. Hence the importance of applied N as a model input when estimating N₂O emissions from agricultural activities. (These models are discussed in a later section.)

Denitrification is the process by which NO_3^- is transformed to nitrogen gas (N_2). This transformation occurs through a series of chemically defined steps, as shown in Scheme 4-2 [127,128], with N_2O being produced as an intermediate species [119,120,124]. This reductive transformation proceeds under anaerobic conditions, and involves a number of microbial-induced processes.



Nitrification and denitrification processes can occur simultaneously within soils, creating a complex (and difficult to model) situation. The balance between aerobic and anaerobic conditions is affected by numerous factors, including soil type, tillage practice, moisture level, and others. One particularly important parameter in this balance is the water-filled pore space (WFPS) within the soil. Anaerobic denitrification processes are generally not very significant until the WFPS becomes quite high – at least 60-80%, depending upon soil type. The extent of WFPS changes rapidly with precipitation (or irrigation), which can result in periodic “ N_2O bursts” from the soil, arising from rapid denitrification processes.

Besides the direct emissions of N_2O from soils, there are several indirect processes by which N_2O is emitted into the atmosphere. These include re-deposition of volatilized nitrogenous species, leaching and runoff of nitrate from soils, and sewage treatment processes. Both direct and indirect N_2O formation processes are discussed below in the context of N_2O modeling.

4.4 MODELING APPROACHES FOR AGRICULTURAL N_2O EMISSIONS INVENTORIES

A variety of modeling approaches have been developed and applied to estimate N_2O emissions from agricultural activities. Perhaps most widely used are the approaches developed by IPCC to estimate country-wide N_2O emissions inventories. A different approach -- involving use of a process-based model for determining direct N_2O emissions -- is used by the U.S. EPA. Both of these approaches, and variations of them, are discussed below.

4.4.1 IPCC MODELING APPROACH

The United Nations Framework Convention on Climate Change (UNFCCC) requires that all countries periodically update and publish national inventories of GHGs, using comparable methodologies. By necessity, this requires a fairly simple approach using readily available inputs that can be broadly applied to provide country-level inventories. IPCC’s initial inventory methodology development, called Phase I, was published in the 1995 IPCC Guidelines for National Greenhouse Gas Inventories [129].

4.4.1.1 IPCC 1995 Methodology

The IPCC Phase I effort was based on the state of knowledge of N₂O emissions that existed at that time, as documented in earlier IPCC reports [130] and literature reviews [131,132]. While the complexity of agriculture's influence on N₂O emissions was fully recognized, it was necessary to develop a simplified modeling approach utilizing input variables that were readily available. As described previously, the importance of nitrogen fertilizer inputs upon N₂O emissions was known. In addition, reliable information about land areas used for agriculture and amounts of applied fertilizer was available for many countries using databases of the United Nations Food and Agricultural Organization (FAO). Consequently, a simplified approach of estimating direct N₂O emissions from agricultural cropping lands was developed, based solely upon the level of nitrogen inputs to the soil. A conversion factor of 1.25% ± 1.0% was adopted – meaning that 1.25% of applied nitrogen would eventually be emitted from the soil in the form of N₂O. The derivation of this factor was described by Mosier et al. [131]. It was based upon evaluation of several experimental studies that had been conducted, and was believed to cover more than 90% of the published data [133,134].

The nitrogen inputs considered in the IPCC Phase I approach included synthetic fertilizers, organic nitrogen from manure application, nitrogen remaining in crop residues, and biological nitrogen fixation. However, no clear mechanism existed to estimate nitrogen inputs from either crop residues or N-fixation. Also, no mechanism existed to account for indirect N₂O emissions resulting from soil leaching and runoff. The same direct conversion factor of 1.25% was applied to all soil types, cropping systems, and climate regions – even though it was known that N₂O emissions are affected by changes in these parameters. However, because these relationships are very complex, and insufficient data were available to properly address them, it was expedient to utilize this simple, conversion factor-based estimate for deriving national-level N₂O inventories.

4.4.1.2 IPCC 1997 Approach

Following publication of the IPCC-1995 Guidelines for National Greenhouse Gas Inventories, a Phase II Workgroup was convened to develop an improved methodology for estimating N₂O emissions from agricultural activities. The efforts of this Workgroup are described by Mosier et al. [135,136] and were incorporated into the revised IPCC Guidelines of 1997 [137]. This updated methodology defined and estimated N₂O emissions in three categories: (1) direct emissions from agricultural soils, (2) emissions from animal production, and (3) emissions indirectly induced by agricultural activities. The methodology relates N₂O emissions to the agricultural nitrogen cycle, and to systems into which nitrogen is transported once it leaves the agricultural system. Compared to the previous IPCC approach, the 1997 methodology was much more comprehensive, although it still ignored impacts of climate, soil type, and cropping systems. Further descriptions are provided below for each of the N₂O emissions categories considered by IPCC-1997.

Direct soil emissions

As described above, biogenic N₂O emissions from soil result from nitrification and denitrification processes, with N₂O being produced as an intermediate in both processes. Addition of fertilizer-N stimulates additional N₂O formation, although the effects are highly specific, and vary with soil type, moisture level, temperature, pH, soil carbon availability, and other factors. Another important factor with respect to fertilizer application is loss of some nitrogen by volatilization of certain nitrogenous species – particularly nitric oxide (NO) and ammonia (NH₃). Once these species are volatilized, they are no longer available to participate in the soil production of N₂O through nitrification and denitrification processes. In the IPCC-1997 approach, a distinction was made between synthetic fertilizer and manure application with respect to volatilization of NO and NH₃. For synthetic fertilizers it was assumed that 10% of the applied nitrogen was lost due to volatilization; for manure usage, 20% of applied nitrogen was assumed to be volatilized. For the fertilizer- and manure-derived nitrogen that was not volatilized, a fixed fraction was assumed to result in N₂O emissions. This fraction, defined as emission factor EF₁, was 0.0125 (± 0.01) kg N₂O-N/kg N input – the same factor as was used in IPCC-1995.

Another important soil nitrogen input arises from atmospheric N₂ fixation, which occurs with leguminous crops. This fixed nitrogen can participate in nitrification and denitrification processes in the same way as fertilizer-N, thus providing a source of N₂O. The amount of nitrogen added to the soil by means of N₂ fixation is variable and poorly known. For national inventory purposes, IPCC-1997 assumed that the mass of soil nitrogen from fixation was two times the crop yield mass times the nitrogen content of the crop. Due to lack of other information, a default value for nitrogen content in leguminous crops was set at 3.0%. These seemingly arbitrary values were derived to be representative of the few literature reports available at that time. [135,136]Crop yields are available from the U.N. FAO database for many crops and countries. A fraction of this fixed nitrogen is assumed to produce N₂O emissions in the same way as does fertilizer-applied nitrogen. Thus, the same emission factor, EF₁, (with a default value of 0.0125 kg N₂O-N/kg N input) is applied to fixed nitrogen.

Another direct source of agricultural N₂O emissions is degradation of crop residues. The nitrogen content of the plant residues may be known in specific cases, but default values are used in most cases. For N-fixing crops, it is assumed that crop residues (on a dry mass basis) contain 3.0% nitrogen, while non-N-fixing crop residues are assumed to contain 1.5% nitrogen. The mass of crop residue is assumed to be twice the mass of the edible crop, which is available from FAO databases. Because nitrogen from these crop residues is believed to participate in nitrification and denitrification processes in the same way as fertilizer-applied nitrogen, the same emission factor, EF₁, is employed.

IPCC-1997 also distinguished between N₂O resulting from cultivation of high organic content soils and other soils. In some regions of the world, soils with high organic content (>20% carbon), known as histosols, are being drained and cultivated. (Peat is an example of a histosol

soil.) This can result in very high N₂O emissions due to enhanced mineralization of old, N-rich organic matter [138,139]. Thus a high default emission factor, EF₂, is used for estimating N₂O emissions from such soils. For histosol soils in temperate regions, EF₂ is set at 5 kg N₂O-N/ha-yr; for histosol soils in tropical regions, EF₂ is set at 10 kg N₂O-N/ha-yr. In a simple, mathematical form, the IPCC-1997 method for estimating direct N₂O emissions from agricultural soils is shown below in Scheme 4-3.

Scheme 4-3

IPCC (1997) Method for Direct N₂O Emissions from Agricultural Soils

N₂O_{Direct} = (fertilizer-N + manure-N + fixed-N + crop residue-N) * EF₁ + histosol area * EF₂

Where: Fixed-N is the fraction of nitrogen in N-fixing crops (default of 3.0%) times double the mass of edible crop yield.

Crop residue-N is the fraction of nitrogen in crop residue (default of 3.0% for leguminous crops; 1.5% for other crops) times double the mass of edible crop yield.

The default emission factor EF₁ is 0.0125 (± 0.01) kg N₂O-N/kg N input.

The default emission factor EF₂ is 5 kg N₂O-N/ha-yr for histosol soils in temperate regions, and 10 kg N₂O-N/ha-yr for histosols soils in tropical regions.

Also: The fertilizer and manure nitrogen application levels used in this formula are reduced to correct for the assumed volatilization losses (10% reduction for fertilizer; 20% reduction for manure).

Direct N₂O from animal production activities

Earlier IPCC emissions estimates from agricultural sources did not include N₂O from animal production. However, by the time the IPCC Phase II Workgroup was organized, it was recognized that this could be a significant source that should not be overlooked [135,140,141]. Three potential animal production sources were considered by IPCC-1997: (1) animals themselves, (2) waste from confined animals, and (3) waste from grazing animals.

Direct emissions of N₂O from ruminant animals is known to occur [142]. Although the amount of N₂O emitted in this way is uncertain, it is thought to be quite small – far less than 10 g N₂O-N/kg N feed intake. Therefore, direct animal emissions of N₂O was not included in the IPCC-1997 methodology.

N₂O emissions from animal waste (both confined animals and grazing animals) are significant. Estimates of these emissions are made based upon the amount of nitrogen excreted from different animal types, and emission factors that indicate the amount of N₂O formation per amount of nitrogen excreted. Clearly, this is a complex area, with large uncertainties [136,135]. IPCC-1997 assigned separate default nitrogen excretion factors (kg N/animal-year) for six classes of animals: (1) dairy cattle, (2) non-dairy cattle, (3) poultry, (4) sheep, (5) swine, and (6) other animals. For each animal type, a variety of animal waste management systems (AWMS) was considered, with each AWMS having a defined emission factor, EF₃, expressed in units of g

N₂O-N/kg N excreted. Values of EF₃ ranged from very low (0-2) for anaerobic lagoons and liquid AWMS to very high (5-30) for solid storage and pasture grazing.

The IPCC 1997 method for estimating N₂O emissions from animal production in a given country is shown mathematically in Scheme 4-4.

<p>Scheme 4-4</p> <p>IPCC (1997) Method for Estimating N₂O Emissions from Animal Production</p> $\text{N}_2\text{O}_{\text{Animals}} = \sum \text{N}_{\text{T1}} * \text{N-excretion}_{\text{T1}} * \text{AWMS}_{\text{T1}} * \text{EF}_{3 \text{ AWMS}}$ <p>Where: N_{T1} = number of animals of type 1 N-excretion_{T1} = kg nitrogen excreted per animal per year AWMS_{T1} = fraction of excreted nitrogen managed by AWMS EF_{3 AWMS} = N₂O emission factor for given AWMS</p>

To estimate the total N₂O inventory contribution from animal production in a given country, the individual contributions from each animal type are summed.

Indirect N₂O emissions from agricultural activities

Several pathways for indirect N₂O emissions are related to agricultural activities. The IPCC-1997 methodology explicitly treated three such pathways: (1) atmospheric deposition of NO_x and NH₄, (2) leaching and runoff, and (3) human consumption followed by municipal sewage treatment. Each is discussed below:

As previously mentioned, a fraction of the nitrogen applied to crop land in the form of synthetic fertilizer or manure is assumed to be lost by volatilization of NO and NH₃. It is further assumed that these volatilized species are converted in the atmosphere to oxides of nitrogen (NO_x) and ammonium (NH₄), which are subsequently deposited onto soils and surface waters, and thereby participate in biogenic N₂O formation. There is limited data suggesting that between 0.2% and 1.6% of nitrogen deposited onto soils is eventually emitted as N₂O [135,143]. Based upon this, the IPCC-1997 Workgroup adopted a default emissions factor, EF₄, of 0.01 kg N₂O-N/kg of N volatilized from application of fertilizer and manure. For inventory purposes, all N₂O resulting from deposition is allocated to the country in which the fertilizer and manure application occur, regardless of where the deposition occurs. The IPCC-1997 formula for estimating N₂O emissions from deposition is shown below in Scheme 4-5.

Scheme 4-5

IPCC (1997) Method for Estimating Indirect N₂O Emissions from Atmospheric Deposition

$$N_2O_{\text{Deposition}} = (\text{Fertilizer-N} * 0.1 + \text{Manure-N} * 0.2) * EF_4$$

Where the default value for EF₄ is 0.01 kg N₂O-N/kg of N volatilized

A considerable amount of fertilizer nitrogen applied to agricultural soils can be lost through leaching and runoff. It has been estimated that the fraction of applied nitrogen taken up by the crop ranges from 20% to 70% [136,144]. Much of the remaining nitrogen enters groundwater, rivers, and coastal marine areas, where it participates in nitrification and denitrification processes to produce N₂O. The amount of nitrogen lost due to leaching and runoff is highly variable, and the amount of N₂O that this produces is quite uncertain. Nevertheless, the IPCC-1997 Phase II methodology developed a detailed process for estimating N₂O resulting from leaching and runoff.

The rationale and mechanisms for these estimates are provided in Mosier et al. [135,136]. First, the amount of nitrogen lost due to leaching and runoff is defined to be a fraction of the total applied nitrogen (as fertilizer and manure). While this fraction is believed to range from 0.1 - 0.8 [135,145], IPCC adopted a leach default (N_{Leach}) value of 0.3. Second, different emission factors were defined to estimate the N₂O emissions occurring from nitrification and denitrification in three separate regions following leaching and runoff:

1. Groundwater: EF_{5-g} = 0.015 g N₂O-N/g N_{Leach}
2. Rivers: EF_{5-r} = 0.0075 g N₂O-N/g N_{Leach}
3. Estuaries: EF_{5-e} = 0.0025 g N₂O-N/N_{Leach}

Combining these three hydrologic components gives a total EF₅ value of 0.025 g N₂O-N/g N_{Leach}. The default formula for estimating all N₂O from leaching and runoff is shown below in Scheme 4-6.

Scheme 4-6

IPCC (1997) Method for Estimating Indirect N₂O Emissions from Leaching and Runoff

$$N_2O_{\text{Leach}} = 0.3 * \text{Applied Nitrogen} * EF_5$$

Where: Applied Nitrogen is synthetic fertilizer-N + manure-N

The default value for EF₅ is 0.025 kg N₂O-N/kg N_{LEACH}

The final indirect N₂O pathway addressed by IPCC-1997 involves human consumption of nitrogen-containing foodstuffs and disposition of the sewage nitrogen. To determine the total amount of a country's sewage nitrogen, per-capita protein consumption is used (obtained from FAO data) with the assumption that nitrogen comprises 16% of total protein mass. Land disposal of human sewage is neglected as a source of N₂O, but nitrogen discharges from sewage treatment plants are included. It is assumed that all discharged sewage nitrogen eventually enters rivers and

estuaries, in the same way as nitrogen that is leached from the soil (discussed above). Therefore, N₂O emissions from sewage nitrogen are treated the same way as N₂O from leached nitrogen [135,146], and the same N₂O emission factors are used in both cases. Thus, the emission factor for sewage nitrogen in rivers, EF_{6-r}, was defined as 0.0075 g N₂O-N/g N_{sewage}, and the factor for sewage nitrogen in estuaries, EF_{6-e}, was defined as 0.0025 g N₂O-N/g N_{sewage} – giving a total EF₆ default value of 0.01 g N₂O-N/g N_{sewage}. The formula for total N₂O emissions from human sewage is given below in Scheme 4-7.

<p>Scheme 4-7</p> <p>IPCC (1997) Method for Estimating Indirect N₂O Emissions from Human Sewage</p> $N_{2O_{Sewage}} = N_{Sewage} * EF_6$ <p>Where the default value for EF₆ is 0.01 kg N₂O-N/kg N_{Sewage}</p>
--

Summary of IPCC 1997

The objective of the IPCC-1997 methodology described above was to enable derivation of country-wide estimates of N₂O emissions from agricultural activities, using readily available information sources. This was achieved by determining, and summing together, the N₂O emissions attributed to three separate categories, as shown in Scheme 4-8:

<p>Scheme 4-8</p> <p>IPCC (1997) Method for Estimating N₂O Emissions from all Agricultural Activities</p> $\text{Total Agricultural } N_{2O} = N_{2O_{Direct}} + N_{2O_{Animals}} + N_{2O_{Indirect}}$ <p>Where: N₂O_{Direct} is shown in Scheme 4-3 N₂O_{Animals} is shown in Scheme 4-4 N₂O_{Indirect} is shown in Scheme 4-5 through Scheme 4-7</p>
--

The Phase II IPCC-1997 methodology was used to determine global N₂O emissions from agricultural activities in the year 1989 [135]. This showed nearly identical contributions from each of the three N₂O categories of Direct, Animals, and Indirect (2.1 Tg N₂O-N from each). Further details of this inventory allocation are shown in Figure 4-10.

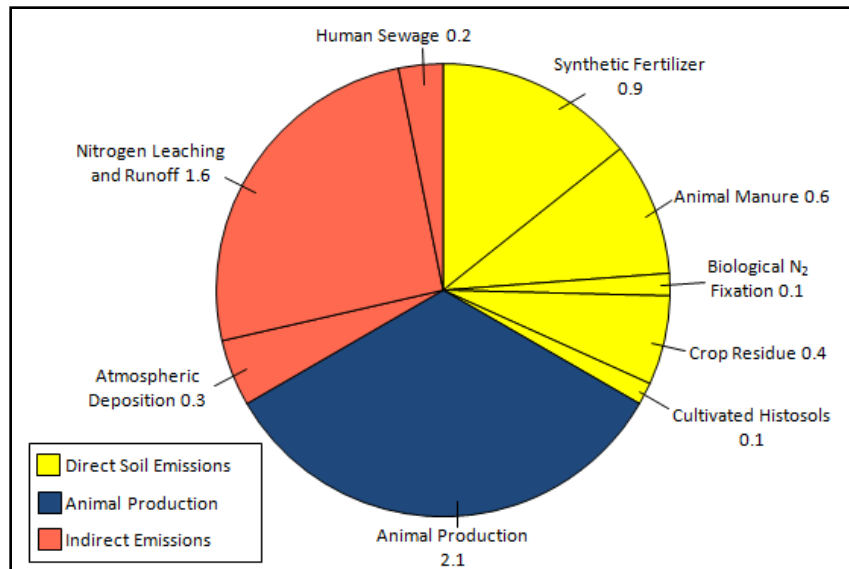


Figure 4-10: Global agriculture-related N₂O emissions in 1989, Tg N₂O-N. Calculated using IPCC 1997 methodology. (Data from Mosier et al.[135].)

This 1989 inventory, when combined with existing estimates of N₂O from natural sources, provided a reasonable balance to the global N₂O budget. This is illustrated in Figure 4-11, which shows the global N₂O budget as computed with the IPCC-1997 Phase II methodology, as well as two earlier IPCC methodologies. With the IPCC-1992 methodology, the global N₂O inventory was significantly underestimated, resulting in a large mis-balance between sources and sinks. Using the 1995 IPCC methodology gave a better balance, with the sinks now only slightly exceeding the sources. Using the 1997 IPCC methodology gave an excellent balance between sources and sinks.

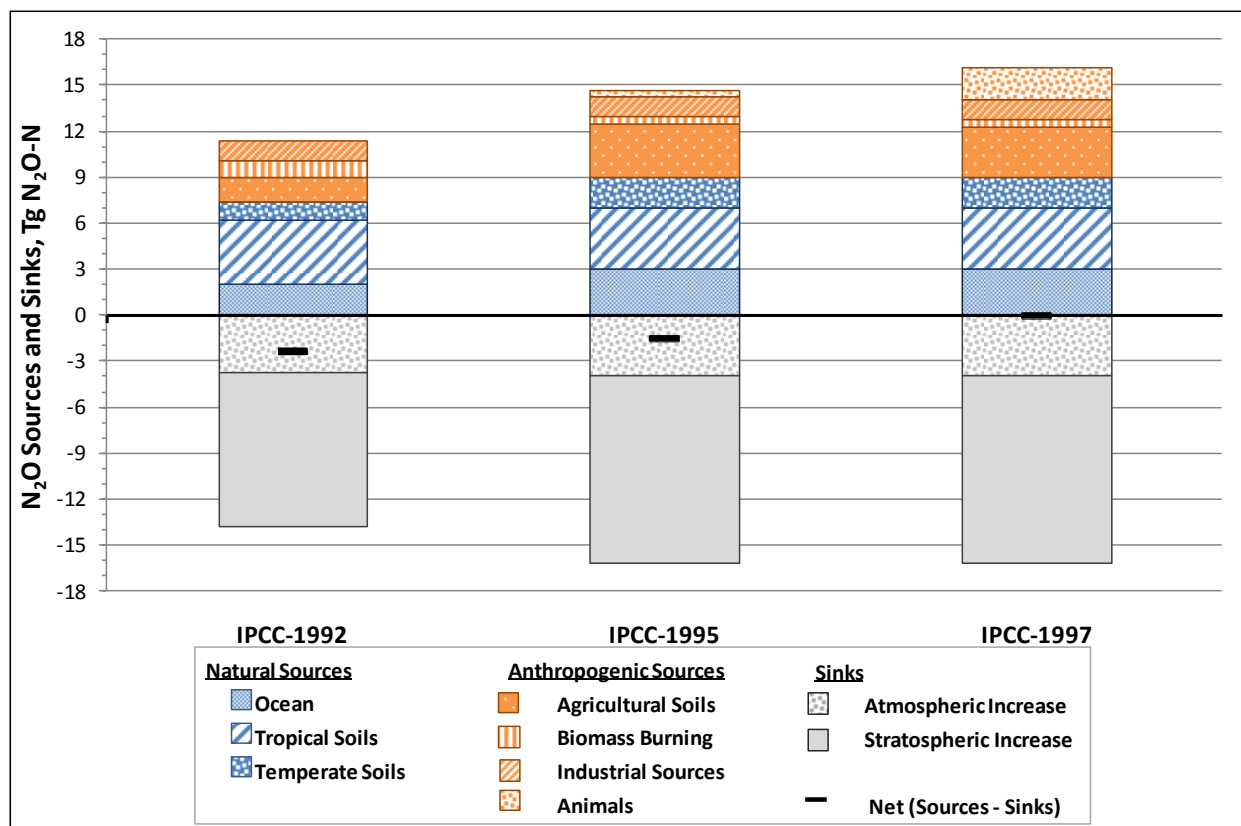


Figure 4-11: Global N₂O budgets derived using different IPCC methodologies. (Data from Mosier et al. [135].)

Providing a good balance between estimated sources and sinks does not guarantee that the N₂O inventory is correct. Given the large number of parameters used in the IPCC methodology, and the large uncertainty associated with many of the model inputs, a rather high total model uncertainty should be expected. This was investigated by Van Aardenne, who used a Monte Carlo sampling technique along with regression and correlation analyses to simulate model outputs while varying 14 model parameters [135,147]. Dutch agriculture nitrogen values were used to run the model. The two parameters that contributed the most to total uncertainty were EF₁ (emission factor for direct soil emissions) and the fraction of nitrogen input that is lost through leaching and runoff. Surprisingly, the total uncertainty was quite small, with a standard deviation of the calculated mean N₂O inventory value of only 20%. This may be because the Netherlands is a small country with little variation in soil type and climate, and relatively well known values for agricultural inputs.

The IPCC-1997 Phase II Work Group also identified a few specific areas where improvements in the N₂O estimation methodology were most needed. It was pointed out that several recent published studies had demonstrated significant N₂O emissions from soils in winter and early spring periods, especially during spring thaw [148,149,150]. Because of this, the IPCC methodology, which ignores spring thaw emissions, may underestimate the true N₂O emissions from agricultural soils. Other issues to address included the following: (1) methodologies to account for effects of crop type, soil type, and climate upon N₂O emissions, (2) better

understanding of soil methane processes, (3) impacts of soil NO_x emissions upon regional ozone concentrations, and (4) effects of mitigation measures to reduce N₂O emissions and increase soil sinks for CH₄.

The Workgroup also stated that to significantly improve inventory methodologies for N₂O from agricultural soils, a process-based model should be utilized. In addition, more appropriate models should be developed for N₂O emissions from animal production, and for nitrogen transformation in aquatic systems. Finally, it was suggested that models regarding soil carbon and soil nitrogen should be integrated, since soil processes involving C and N are inter-related.

4.4.1.3 IPCC 2006 Methodology

In 2006, the IPCC issued a major update to their guidelines for determining national GHG inventories, with Volume 4 addressing inventories in the Agriculture, Forestry and Other Land Use (AFOLU) sector [52]. Chapter 11 of this volume addresses N₂O emissions from managed soils. A concept introduced in the IPCC-2006 guidelines is the hierarchical tiers of methods that range from simple, default emission factors to the use of country-specific data and models. The three tiers of methods are briefly summarized below:

- Tier 1 methods are designed to be the simplest to use, for which standard equations and default parameter values are applied (for example, the default values for EF₁ – EF₆ as described above under the IPCC-1997 methodology).
- Tier 2 methods utilize the same methodological approach as Tier 1, but apply emissions and stock change factors that are based on country- or region-specific data for the most important land-use or livestock categories. Higher temporal and spatial resolution and more disaggregated activity data are typically employed in Tier 2 methods.
- Tier 3 methods employ models and inventory measurement systems driven by high-resolution activity data and disaggregation at sub-national levels. These higher order methods are tailored to address specific national circumstances, and generally provide GHG estimates of greater certainty than lower tiers.

As with the earlier methodology, IPCC-2006 estimated N₂O emissions from managed soils as the sum of direct and indirect processes. However, in this updated methodology, N₂O emissions from animal production are not treated as a separate source, but are allocated between the direct and indirect sources. A schematic showing the overall sources and pathways of nitrogen that contribute to N₂O under the IPCC-2006 methodology is provided in Figure 4-12.

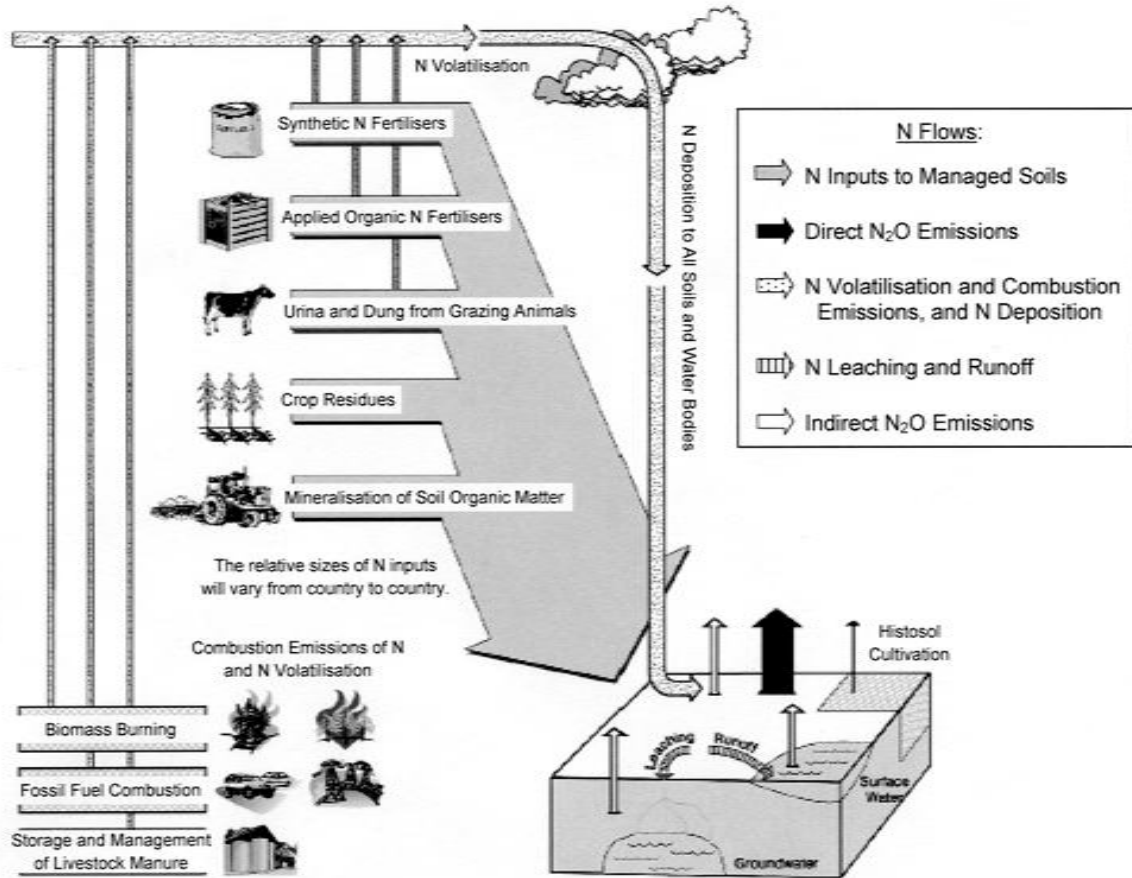


Figure 4-12: Schematic diagram illustrating sources and pathways of N that result in direct and indirect N₂O emissions from soils and waters. (Taken from IPCC 2006 [52])

Direct N₂O Emissions

In the earlier IPCC-1997 methodology, direct emissions from conventional agricultural soils were determined from various nitrogen inputs multiplied by an emission factor, EF_1 . To this was added the N₂O contribution from cultivation of highly organic soils (histosols), which was defined as the area of histosol cultivation times an emission factor, EF_2 (see Scheme 4-3). In the IPCC-2006 Tier 1 methodology, a similar approach was taken, although now the direct N₂O emissions are defined as the sum of three terms, as shown in Scheme 4-9.

Scheme 4-9

IPCC (2006) Method for Estimating Direct N₂O Emissions

$$N_2O-N_{\text{direct}} = N_2O-N_{N\text{-inputs}} + N_2O-N_{OS} + N_2O-N_{PRP}$$

Where: $N_2O-N_{N\text{-inputs}}$ = direct N₂O-N emissions from nitrogen inputs to managed soils; kg N₂O-N/year
 N_2O-N_{OS} = direct N₂O-N emissions from managed organic soils; kg N₂O-N/year
 N_2O-N_{PRP} = direct N₂O-N emissions from animal waste deposited on grazed pasture, range and paddock; kg N₂O-N/year

As shown in Scheme 4-9, N₂O in the IPCC-2006 methodology is estimated in units of nitrogen mass, not N₂O mass, as was done in IPCC-1997. To convert to N₂O mass, the N₂O-N amounts must be multiplied by the factor 44/28. In the Tier 1 method, each of the three direct N₂O-N terms shown in Scheme 4-9 is computed from a combination of factors, as described below:

- $N_2O-N_{N\text{-inputs}}$ is the sum of nitrogen inputs from synthetic fertilizer, animal manure and sewage sludge, crop residues, and mineralized soil – all multiplied by a single emission factor, EF_1 . This emission factor is the same for all crop types, except for rice grown in flooded fields, in which case a different factor, EF_{1FR} is used. The value of EF_1 was changed to 1.0%, compared to 1.25% in the IPCC-1997 methodology. This was due to new analyses of experimental data which drew upon a larger body of measurements than were available previously [151,152,153,154,155]. A nitrogen input term for atmospheric nitrogen fixation was removed as a direct source of N₂O in the IPCC-2006 methodology, due to lack of evidence that this is a significant process [156]. On the other hand, a term was added to account for mineralization of nitrogen contained in soil organic matter (SOM). Thus, the total $N_2O-N_{N\text{-input}}$ term can be expressed as shown in Scheme 4-10.

Scheme 4-10

IPCC (2006) Method for Estimating Direct N₂O Emissions from Soil N Inputs

$$\text{N}_2\text{O-N}_{\text{N-input}} = (\text{F}_{\text{SN}} + \text{F}_{\text{ON}} + \text{F}_{\text{CR}} + \text{F}_{\text{SOM}}) * \text{EF}_1$$

Where: F_{SN} is the annual amount of synthetic fertilizer-nitrogen applied to soils. Unlike previously, this term is no longer adjusted for the assumed amounts of NO and NH₃ volatilization after application to the soil.

F_{ON} is the annual amount of organic fertilizer-nitrogen applied to soils. This includes applied manure, sewage sludge, compost, and other organic amendments.

F_{CR} is the annual amount of nitrogen in crop residues – including both above-ground and below-ground residues – that is returned to the soil. The amount of crop residue, and the nitrogen content of this residue, varies with crop type. The IPCC- 2006 guidelines include default factors for 24 different crop types. To develop a national inventory, the residue-N values are first computed for each crop, then summed over all crops. An additional term within F_{CR} is used to account for nitrogen remaining on the soil after burning of crop residues.

F_{SOM} is the annual amount of nitrogen associated with soil organic matter (SOM) that is mineralized (converted to NH₄ and NO₃) as a consequence of land use change or management practice. Organic carbon and nitrogen are intimately linked in SOM. When soil carbon is lost through oxidation as a result of land use or management change, the organic nitrogen is mineralized, thus becoming available for conversion to N₂O [157]. IPCC-2006 provides guidance to compute this soil nitrogen input term for various soils and land use types.

- N₂O-N_{OS} is the sum of numerous terms, each of which is the land area of a particular histosol soil times an emission factor, EF₂, specific for that soil type. The various histosol soils include temperate and tropical, with sub-classifications within each category. The values of EF₂ for these histosol classifications are given in Table 4-2, along with the comparable values used in the IPCC-1997 methodology.
- N₂O-N_{PRP} is determined by multiplying the annual amount of animal waste nitrogen deposited by grazing, times an emission factor, EF₃, for a specific animal type. In IPCC-1997, six different classes of animals (and six different EF_{3's}) were used; in the updated IPCC-2006 methodology, only two sets of animals (and two EF_{3's}) are considered:
 - EF_{3CPP} pertains to cattle, poultry, and pigs
 - EF_{3SO} pertains to sheep and other animals

The values for these EF₃ factors are shown in Table 4-2. In the IPCC-1997 methodology, different EF₃ factors were assigned for different animal waste management systems (AWMS). For grazing activities with no AWMS (such as pasture, range, and paddock) an emissions factor of 0.02 kg N₂O-N/kg N excreted was used – with no distinction among animal types. The same emission factor of 0.02 is used for most animals in the updated IPCC-2006 methodology, while the factor for sheep is only half as large, at 0.01.

The default emission factor values shown in Table 4-2 apply to the IPCC Tier 1 method. If more detailed emission factors and activity data are available to a particular country, further disaggregation of the N₂O-N direct terms in Scheme 4-9 can be performed. This so-called Tier 2 method utilizes the same computational framework as in Tier 1, but introduces greater regional specificity due to improved knowledge of nitrogen sources, crop types, crop management, land use, climate, soil type, or other condition-specific emission factors.

Table 4-2: Default Emission Factors to Estimate Direct N₂O Emissions from Managed Soils

Emission Factor	IPCC-2006 Defaults		IPCC-1997 Defaults	
	Value	Uncertainty	Value	Uncertainty
EF ₁ – Nitrogen from synthetic fertilizer, organic amendments, crop residues, and N mineralization [kg N ₂ O-N/kg N]	0.01	0.003 - 0.03	0.0125	0.0025-0.0225
EF _{1FR} – same nitrogen additions as with EF ₁ , but from flooded rice fields [kg N ₂ O-N/kg N]	0.003	0.000-0.006	-	-
EF _{2CG,Temp} – temperate histosol soils used for crops and grassland [kg N ₂ O-N/ha]	8	2 - 24	5	2 - 15
EF _{2CG,Trop} – tropical histosol soils used for crops and grasslands [kg N ₂ O-N/ha]	16	5 - 48	10	2 - 15
EF _{2F,Temp,Org,R} – temperate, nutrient rich histosol soils with boreal forests [kg N ₂ O-N/ha]	0.06	0.16 - 2.4	-	-
EF _{2F,Temp,Org,P} – temperate, nutrient poor histosol soils with boreal forests [kg N ₂ O-N/ha]	0.1	0.02 - 0.3	-	-
EF _{2F,Trop} – tropical histosol soils with forests [kg N ₂ O-N/ha]	8	0 - 24	-	-
EF _{3PRP, CPP} – N inputs to soil from grazing cattle, poultry, and pigs [kg N ₂ O-N/kg N]	0.02	0.007 - 0.06	0.02	0.005 - 0.030
EF _{3PRP, SO} – N inputs to soil from grazing sheep and other animals [kg N ₂ O-N/kg N]	0.01	0.003 - 0.03	0.02	0.005 - 0.030

IPCC Tier 3 inventory methods are very different, being based upon modeling and measurement studies, rather than use of default emission factors. Such modeling relates N₂O emissions to specific physical and chemical processes that occur in a particular situation. A considerably larger amount of data inputs are required to run such process models. These models should only be used when sufficient inputs are available, and after model validation has been demonstrated by experimental measurement. Further discussion of N₂O emission models is provided in a later section of this report.

Indirect N₂O Emissions

IPCC-2006 methodology considers two pathways for indirect emissions of N₂O: (1) volatilization of NH₃ and NO_x, and subsequent re-deposition of nitrogen species to soils and waters, and (2) leaching and runoff of nitrogen (mainly NO₃⁻) from managed soils. These two indirect pathways are discussed separately below.

The Tier 1 method for determining indirect N₂O emissions resulting from atmospheric deposition is represented in Scheme 4-11.

Scheme 4-11

IPCC (2006) Tier 1 Method for Estimating Indirect N₂O Emissions from Atmospheric Deposition

$$N_2O_{ATD-N} = [(F_{SN} * \text{Frac}_{GASF}) + ((F_{ON} + F_{PRP}) * \text{Frac}_{GASM})] * EF_4$$

Where: N₂O_{ATD-N} is the annual N₂O-N produced from atmospheric deposition of N volatilized from managed soils; (kg N₂O-N/yr)

F_{SN} is the annual amount of synthetic fertilizer-nitrogen applied to soils; (kg N/yr)

Frac_{GASF} is the fraction of synthetic fertilizer that volatilizes as NH₃ and NO_x; (kg N volatilized/kg N applied)

F_{ON} is the annual amount of organic fertilizer-N applied to soils. This includes applied manure, sewage sludge, compost, and other organic amendments; (kg N/yr)

F_{PRP} is the annual amount of animal waste deposited by grazing animals on pasture, range, and paddock; (kg N/yr)

Frac_{GASM} is the fraction of organic N materials (F_{ON}) that volatilizes as NH₃ and NO_x; (kg N volatilized/kg N applied or deposited)

EF₄ is the emission factor for N₂O emissions from atmospheric deposition of N on soils and water surfaces; (kg N₂O-N/(kg NH₃-N + NO_x-N volatilized)

The Tier 1 default values for EF₄, volatilization fraction, and leaching fraction are shown in Table 4-3. The default EF₄ value is 0.010 kg N₂O-N/kg N volatilized – the same value as used in IPCC-1997. However, the uncertainty range in IPCC-2006 is wider, because of recent experimental studies showing that in certain environments with high rates of nitrogen deposition, the N₂O emission rates are substantially higher than previously reported [158,159,160]. The Frac_{GASF} and Frac_{GASM} default values are also the same as in IPCC-1997, although uncertainty ranges have been added in IPCC-2006 (see Table 4-3). As was the case with IPCC-1997, for national inventory purposes all indirect N₂O emissions from deposition sources are attributed to the country where the volatilization occurred, not the country where deposition occurred.

The Tier 1 method for determining indirect N₂O emissions resulting from leaching and runoff is represented in Scheme 4-12.

Scheme 4-12

IPCC (2006) Tier 1 Method for Estimating Indirect N₂O Emissions from Leaching and Runoff

$$N_2O_{L-N} = (F_{SN} + F_{ON} + F_{PRP} + F_{CR} + F_{SOM}) * \text{Frac}_{LEACH-(H)} * EF_5$$

Where: N₂O_{L-N} is the annual N₂O-N produced from leaching and runoff of N additions to managed soils in regions where leaching/runoff occurs; (kg N₂O-N/yr)

F_{SN} is the annual amount of synthetic fertilizer-nitrogen applied to soils in regions where leaching/runoff occurs; (kg N/yr)

F_{ON} is the annual amount of organic-N (from manure, sewage sludge, compost, and other materials) applied to soils in regions where leaching/runoff occurs; (kg N/yr)

F_{PRP} is the annual amount of animal waste deposited by grazing animals on pasture, range, and paddock in regions where leaching/runoff occurs; (kg N/yr)

F_{CR} is the amount of N in crop residues (above- and below-ground) returned to soils annually in regions where leaching/runoff occurs; (kg N/yr)

F_{SOM} is the amount of N mineralized in soils (associated with loss of soil C due to changes in land use or management) in regions where leaching/runoff occurs; (kg N/yr)

Frac_{LEACH-(H)} is the fraction of all N added to managed soils in regions where leaching/runoff occurs that is lost through leaching and runoff; (kg N₂O-N/kg of N addition)

EF₅ is the emission factor for N₂O emissions from N leaching and runoff; (kg N₂O-N/(kg N leached and runoff))

The Tier 1 default value for EF₅ is 0.0075 kg N₂O-N/kg N in leach/runoff. This is considerably lower than the IPCC-1997 value of 0.025. Experimental results that support this reduction in EF₅ were recently published by Reay et al. [161] In both IPCC-1997 and IPCC-2006 the EF₅ emission factor is the sum of three separate factors: (1) EF_{5g} for groundwater, (2) EF_{5r} for rivers, and (3) EF_{5e} for estuaries. In IPCC-2006, all three of these have default values of 0.0025; in IPCC-1997, the factor for EF_{5g} was 0.015 and EF_{5r} was 0.0075.

The default Frac_{LEACH} term has changed significantly from the previous IPCC methodology. In IPCC 1997, Frac_{LEACH} had a value of 0.3 (30% of applied nitrogen was lost by leaching and runoff) for all soil conditions. In IPCC-2006, this term has been changed to Frac_{LEACH-(H)}. The value of this term is still 0.3, but it now applies only to soils in which the water-holding capacity is exceeded as a result of rainfall and/or irrigation. The IPCC-2006 guidelines include a method for determining when such conditions are reached.

As with the direct N₂O emissions, the methodology for determining indirect N₂O can advance to Tier 2 by utilizing more detailed, regional-specific inputs for emission factors, volatilization factors, and leaching factors. Tier 3 methods for determining indirect N₂O emissions inventories would be based on modeling and measurements.

Table 4-3: Default Emissions, Volatilization and Leaching Factors for Indirect Soil N₂O Emissions

Factor	IPCC-2006 Defaults		IPCC-1997 Defaults	
	Value	Uncertainty	Value	Uncertainty
EF ₄ – Nitrogen volatilization and re-deposition [kg N ₂ O-N/kg NH ₃ -N + NO _x -N volatilized]	0.010	0.002 - 0.05	0.01	0.002 - 0.02
EF ₅ – leaching and runoff [kg N ₂ O-N/kg N leached/runoff]	0.0075	0.0005-0.025	0.025	0.002 - 0.12
Fra _{C_{GAS}F} – volatilization from synthetic fertilizer [(kg NH ₃ -N + NO _x -N)/kg N applied]	0.10	0.03 – 0.3	0.1	-
Fra _{C_{GAS}M} – volatilization from organic N applied and deposited [(kg NH ₃ -N + NO _x -N)/kg N applied]	0.20	0.05 – 0.5	0.2	-
Fra _{C_{LEACH}(H)} – N losses by leaching/runoff for regions where soil water-holding capacity is exceeded [(kg N)/(kg N applied and deposited)]	0.30	0.1 – 0.8	0.3	-

Summary of IPCC 2006 Methodology

While largely based on the same structural and operational foundation as the earlier methodology for determining N₂O emission inventories, the IPCC-2006 approach introduced several improvements. Some changes were due to on-going research efforts, which led to updated default values for certain emission factors or activity use factors. Other changes were more fundamental – such as considering nitrogen leaching from soils only in cases where the soil water-holding capacity is exceeded. Thus, it would appear that even when using the simple default value-based Tier 1 approach, the IPCC-2006 method would provide more reliable results than the IPCC-1997 method. However, we are not aware of any systematic study to confirm this expectation.

Further improvements in reliability would be expected by using an IPCC-2006 Tier 2 method. Presumably, information sources that are specific to a particular country (or region within a country) would be more reliable than the general default values used in Tier 1. Rochette et al. developed and applied Tier 2 methodology for determining the national N₂O emission inventory for Canada [162,163]. Regional-specific conditions (precipitation, soil texture, spring thaw, etc.) were considered in developing emission factor adjustments that were then applied on an eco-district scale. Total agriculture-related N₂O emissions between 1990 and 2005 were estimated to average 58.1 Gg N₂O-N/year, with 68% attributed to direct emissions from soils, 15% attributed to direct emissions from animal waste management, and 17% attributed to indirect emissions. (1 Gg = 10⁹ g, = 0.001 Tg.) The authors concluded that compared to IPCC Tier 1, application of this Tier 2 methodology yielded more accurate estimates of national emissions, as well as a better description of N₂O spatial and temporal patterns.

Application of a Tier 3, process model-based method for determining N₂O emissions inventories may be expected to provide the most reliable results – provided sufficient inputs of high quality are available to run the model. Numerous studies have compared N₂O emissions determined by process model-based methods and emission factor-based methods. Some of these comparisons

are discussed in the next section, in which the structure and use of process-based models are presented.

4.4.1.4 Comparison of IPCC Estimates with Field Measurements

Although it is desirable to compare IPCC N₂O emissions estimates with actual field measurements, there are several factors which make this difficult and highly uncertain. Many of these factors are related to differences in temporal and spatial scales. The IPCC methodology is intended to estimate annual average N₂O emissions on a large spatial scale – typically country-wide. In contrast, field measurements of necessity are focused on smaller regions, and usually shorter time frames, but with higher temporal resolution. The development and application of automated flux chambers has enabled more rapid and reliable field measurements of N₂O, providing multiple measurements throughout a 24-hour period, without disturbing the soil being sampled [164,165,166]. An example of such high resolution measurements is provided in Figure 4-13.

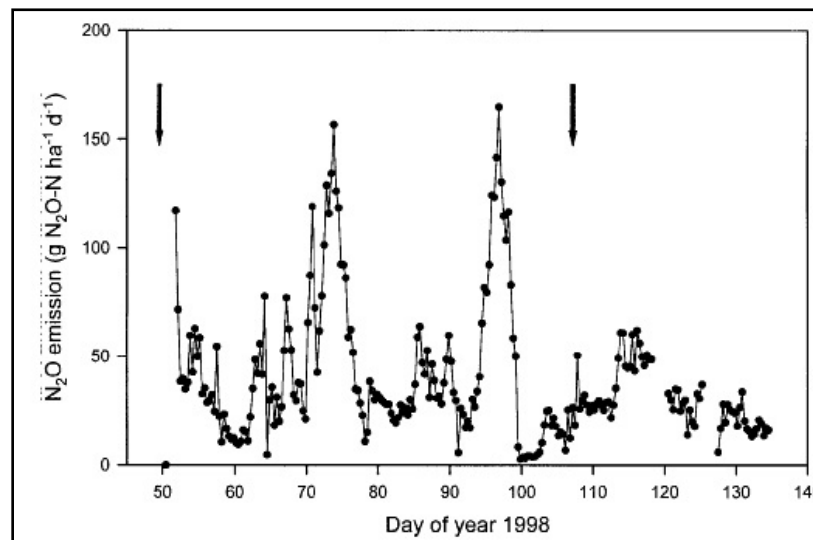


Figure 4-13: Measurement of N₂O fluxes on a near-continuous basis. Arrows indicate dates of N fertilization. (Taken from Smith & Dobbie (2001) [164] by permission of John Wiley and Sons.)

While these high resolution measurements are very useful in providing greater temporal “fine structure” of N₂O emissions, spatial variability may be more important in understanding total N₂O emissions [164,166,167]. Even within a single field under identical agricultural activity, variations in soil type and water content result in significant differences in N₂O emissions. Also, recent studies have shown that N₂O emissions are affected not only by the total amount of applied fertilizer, but also by the form of the nitrogen (ammonia, urea, and other forms) [168,169] and the application technique [170,171]. Additionally, N₂O emissions are influenced by land topography (slope) [172] and degree of compaction [173], due to the impact of these factors on soil structure and water content.

In some agricultural regions, the springtime thaw of soils has been recognized as a significant contributor to the total annual emissions of N₂O [148,174,175]. Johnson et al. showed that up to

65% of the total N₂O annual flux in the U.S. cornbelt occurs during spring thaw [174]. It is generally believed that this “spring burst” is due to both release of N₂O trapped in the frozen soil, and to enhanced formation due to increased nutrient availability in the spring. However, Wagner-Riddle recently showed that most of this spring burst is due to newly produced N₂O in the soil surface layer (primarily by denitrification processes), not due to release of trapped N₂O [175].

Given these many factors that influence N₂O emissions, but are not accounted for in the simple IPCC Tier 1 methodology, comparison between IPCC estimates and field measurements would not necessarily be expected to provide good agreement in specific cases. However, it should be remembered that the IPCC default emission factor, EF₁, for direct emissions of N₂O was derived from analysis of numerous field studies [151,152,153,154,155]. (Only measurements of direct soil N₂O emissions can be compared with IPCC estimates, as indirect emissions occur elsewhere.) Also, although the IPCC default factor is often referred to as a single value (i.e. EF₁ in IPCC-2006 is 1.0% of applied nitrogen), this value has considerable uncertainty, with a stated range of 0.3% - 3.0% (see Table 4-2).

Since establishment of the IPCC-2006 default N₂O emissions factor, several experimental studies have been reported in which measured values were compared with IPCC default values.

Hyvönen et al. measured N₂O fluxes from a peat extraction site in Finland that was used to cultivate Reed Canary Grass [176]. According to IPCC, considerable N₂O emissions are expected from cultivation of histosol soils (such as peat). The IPCC-2006 default emissions factor for background N₂O from temperate histosol soils used for crops and grasslands is 8 kg N₂O-N/ha (see Table 4-2). However, over a 4-year measurement period, these researchers obtained an average value of only 0.56 kg N₂O-N/ha – far below the IPCC default value. Van Beek et al. also measured N₂O fluxes from fertilized and unfertilized grasslands on peat soils in the Netherlands [177]. Over a 2-year period, they found background N₂O emissions in the range of 0.2 - 7.6 kg N₂O-N/ha, with the result depending upon the wetness of the fields. These authors suggested that the IPCC methodology for peat soils could be improved by including a factor to account for annual average groundwater level.

Chirinda et al. measured direct N₂O emissions under several cropping systems on two soils in Denmark [178]. They determined annual N₂O emission values that corresponded to 0.5-0.8% of applied fertilizer nitrogen. This range is slightly below the IPCC default EF₁ value of 1.0%, but clearly within the established uncertainty range. Barton et al. measured N₂O fluxes from canola croplands in semi-arid regions of Australia [179]. They found very low N₂O levels, corresponding to 0.06% of applied fertilizer nitrogen – a value below the lower uncertainty range of EF₁ established by IPCC.

Jiang et al. investigated use of several different fertilizer types on corn and wheat crops in China (especially slow-release nitrogen compounds) [168]. N₂O emissions were found to vary significantly with both crop type and fertilizer type, but were generally lower than predicted using the IPCC default EF₁ value by a factor of 2-4. Finally, Vilain et al. investigated the effects of topography and slope position on N₂O emissions in the Seine River basin of France [172].

They found that N₂O emission levels varied across the regions of shoulder, backslope, footslope, and riparian zones; and that this variation was largely explainable by differences in WFPS (water-filled pore space) and soil NO₃⁻ concentrations across the topography. Measured annual average N₂O emissions across the landscape ranged from 0.6% to 2.2% of applied nitrogen fertilizer, which is within the IPCC-2006 default range.

Crutzen et al. have taken a very different approach in comparing N₂O measurements with IPCC estimates [30]. Their top-down analysis is based on global atmospheric budgets of N₂O. Using known atmospheric removal rates and a fixed pre-industrial N₂O mixing ratio of 270 ppb, these authors determined the amount of anthropogenic N₂O required to explain the current atmospheric mixing ratio. After subtracting estimated industrial sources, the remainder was defined to be agricultural sources of N₂O. It was then determined that 3-5% of all nitrogen inputs to the terrestrial biosphere (whether by chemical, biological, or atmospheric mechanisms) were emitted as N₂O. It was pointed out that this range of 3-5% greatly exceeded the IPCC-2006 direct N₂O default value of 1.0% (or about 1.3% when including indirect N₂O sources).

This discrepancy between the Crutzen top-down and IPCC bottom-up inventory results is not as large as it initially appears. For example, N₂O emissions associated with confined animal production are known to be large and variable – depending upon the type of animal waste management system (AWMS) being used. In IPCC-2006, however, this source of N₂O is not included in the agricultural category. Other sources possibly mis-classified as agriculture-related by the Crutzen “remainder calculation” include biomass combustion and mobile sources [180,181] Also, very recently, Destouni and Darracq identified an additional indirect N₂O source that has been neglected by IPCC, but included implicitly in Crutzen’s top-down method [182]. This N₂O source results from conversion of leached nitrate in the sub-surface water system. The IPCC method does consider the impacts of leached nitrate, but only in surface water systems, not sub-surface. Based upon modeling of a Swedish drainage basin, these authors concluded that leaching-derived N₂O emissions are of similar magnitude in the surface and sub-surface water systems. In summary, the approach taken by Crutzen et al. appears to over-estimate the amount of N₂O that originates from agricultural activities.

4.4.2 PROCESS-BASED MODELS FOR ESTIMATING N₂O EMISSIONS

While expedient for estimating country-level N₂O emissions inventories using readily available information sources, the IPCC emission factor (EF) approach is unable to address numerous processes known to be important in affecting nitrification-denitrification mechanisms and N₂O production [183,184,135]. For example, the IPCC-EF approach considers all agricultural systems to be the same throughout the world. It does not take account of differences in crops, soils, climate, and agricultural management practices – all of which are known to be important. Furthermore, IPCC-EF assumes that all cropped systems are in steady-state, with the entire N cycle occurring within a single calendar year. Clearly, this is an erroneous assumption, as nitrogen can be stored in the plant/soil system for longer periods of time, and participate in N₂O-forming processes after a lag period of over 1-year [185,186].

Process-based biogeochemical models are used to simulate fluxes of C and N among the atmosphere, vegetation, and soil; and determine global budgets for these species. Historically, these models were developed and applied to address critical agricultural concerns such as plant growth, crop yield, and soil organic matter (SOM) as functions of soil texture, temperature, precipitation, nutrient supply, tillage practices, and other parameters. More recently, these models have been adapted for use in estimating GHG emissions (including N₂O) from agricultural activities.

In contrast to simple, empirical models (such as IPCC Tier 1), process-based models simulate the biological, chemical, and physical processes that control C and N flows. These more complex models require detailed parameterization and extensive computation. Numerous biogeochemical models have been developed and applied to estimate GHG emissions from agricultural activities. Recently, the Technical Working Group on Agricultural Greenhouse Gases (T-AGG) issued a report describing three models commonly used in the U.S.: (1) CENTURY/DAYCENT, (2) DNDC (De-Nitrification De-Composition), and (3) EPIC/APEX [187]. These models were compared with respect to data input requirements, agricultural management practices included, crop types included, and other aspects. While these models are quite similar overall, a large number of subtle differences are identified. It was concluded that the primary limitations of these models are gaps in research and data, both of which are being filled over time.

Other process-based models have been developed and applied to estimate N₂O emissions in various agricultural situations around the world. Examples reported in the literature include the Nitrous Oxide Emission (NOE) model [188,189,173,190], NGAS [188], and SWAP-ANIMO [191]. A recent review paper summarizes the structure and attributes of these and other N₂O simulation models [192]. However, for the purposes of this report, we focus on the CENTURY/DAYCENT modeling approach, as this is utilized by EPA and USDA in determining GHG emissions inventories associated with agricultural activities in the U.S.

4.4.2.1 Development of DAYCENT

One of the most widely used process models for simulating C and N fluxes was developed in the early 1990's and is called CENTURY. This ecosystem model provides annual output predictions of crop yield on a monthly time step [193,194]. Such low temporal resolution is sufficient for simulating the long-term changes (~100 years; hence the name CENTURY) in SOM, plant productivity, and other agricultural parameters in response to changes in climate, land use, and atmospheric CO₂ concentrations. However, to accurately simulate trace gas fluxes (such as N₂O) in soils requires much finer time resolution, since large changes in these fluxes result from short-time events (hours – days) such as precipitation and snow melt. As an illustration of this, Figure 4-13 shows actual field measurements of N₂O from agricultural soil on an 8-hour basis. Clearly, a model with a monthly time step would be unable to represent the highly variable N₂O flux shown in this figure.

To provide improved temporal resolution, a daily time-stamp version of the CENTURY Model was developed. This daily model, called DAYCENT, has sufficient specificity to enable modeling of N₂O production and emissions from soils [195,196]. DAYCENT contains sub-models for plant productivity, decomposition of dead plant material and SOM, soil water and temperature dynamics, and trace gas fluxes – including N₂O [184,195]. The N sub-model simulates N₂O, NO_x, and N₂ gaseous emissions from soils resulting from nitrification and denitrification processes [197,198].

DAYCENT assumes that releases of these nitrogen-containing gases from soils due to nitrification are proportional to the nitrification rates. These rates are controlled by soil NH₄⁺ concentration, water content, temperature, pH, and soil texture [197,199]. Additional parameters and assumptions regarding DAYCENT's treatment of nitrification are given in Scheme 4-13.

The denitrification sub-model of DAYCENT first calculates total N gas flux from denitrification (N₂ + N₂O) and then uses a N₂/N₂O ratio function to infer separate N₂ and N₂O emissions [184,198,199]. Denitrification is controlled by labile soil carbon availability, soil NO₃⁻ concentration, and O₂ availability. Additional parameters and assumptions regarding DAYCENT's treatment of denitrification are given in Scheme 4-13.

Scheme 4-13

DAYCENT N Gas Sub-Model Parameters and Assumptions

Nitrification Process:

- Nitrification rate increases with soil temperature (T_{soil}) until T_{soil} reaches the average high temperature for the warmest month of the year.
- Nitrification is limited by moisture stress on microbial activity when the water-filled pore space (WFPS) is low.
- Nitrification is limited by O₂ availability when WFPS is high.
- Peak nitrification rates typically occur when soil water content is ~50% WFPS; with finer-textured soils, peak nitrification rates occur at higher WFPS.

Denitrification Process:

- Modeled soil heterotrophic respiration is used as a proxy for labile soil C availability.
- O₂ availability is a function of WFPS and O₂ demand.
- O₂ demand is a function of simulated heterotrophic CO₂ respiration and soil diffusivity.
- Gas diffusivity is a function of soil WFPS, bulk density, and field capacity.

The DAYCENT model predicts that O₂ is readily available, and that little denitrification can occur in coarse-textured soils unless WFPS exceeds about 80%. However, in finer-textured soils (having lower gas diffusivity), denitrification can occur at WFPS values as low as 60%. Also, some N₂O produced by denitrification can undergo further reduction to N₂ before diffusing from

the soil surface. DAYCENT utilizes a soil gas diffusivity function to determine the residence time of N₂O in the soil, and hence the fraction that is converted to N₂ before diffusing out.

DAYCENT model inputs include daily maximum and minimum air temperatures, daily precipitation, soil texture class, vegetation type, cultivation schedules, amount and timing of nutrient amendments, and others. The model then computes N₂O and N₂ emissions from nitrification and denitrification in each of several soil layers on a daily time step basis. Simulated daily values of soil NH₄⁺, NO₃⁻, CO₂, water content, and temperature are used in this computation. The computed N gas values are then summed over all soil layers to determine the total N₂O and N₂ emissions for the soil profile.

NO_x emissions from soils are computed as a function of total N₂O emissions. The NO_x/N₂O ratio is low (~1) when gas diffusivity (and hence O₂ availability) is low; but this ratio increases to a maximum of 20 as gas diffusivity increases. (With highly aerated soils, nitrification dominates over denitrification.) The computed base NO_x emission rate is then modified by a “pulse multiplier” to account for periodic bursts of NO_x resulting from precipitation events (as illustrated in Figure 4-13). A pulse multiplier sub-model is used to account for the amount of precipitation and the number of days since the previous precipitation event [184,200].

4.4.2.2 Validation of DAYCENT

Numerous field experiments have been conducted to develop and improve inputs to parameterize the DAYCENT model, and to validate the model’s performance. Much of this model validation work has been conducted and/or coordinated by groups of scientists from USDA and Colorado State University (CSU) [201,202,203,183,184,204]. CSU also maintains a website that offers descriptions of DAYCENT’s development and usage, provides downloads for running the model, and lists literature references for more information [62].

Another recent report by Jarecki et al. showed that DAYCENT simulations of N₂O emissions from a corn field in Iowa agreed reasonably well with daily flux measurements when integrated over a year, although significant differences were observed on individual days [205]. Other comparisons of DAYCENT and IPCC estimates of N₂O emissions in specific cases are provided in later sections of this report.

4.4.3 U.S. APPROACH FOR AGRICULTURAL N₂O EMISSIONS INVENTORIES

USDA and EPA are the two primary U.S. agencies involved in determining and updating GHG emissions from agricultural activities. Recent reports from both agencies outline and document the methods by which agricultural-related N₂O emissions are estimated [13,206,114].

The U.S. has adopted an IPCC Tier 3 approach to N₂O inventories, using the DAYCENT process-based model for direct N₂O from soils, while utilizing simpler emission factor (EF) estimates in other parts of the inventory process. Specifically, DAYCENT is used to simulate fluxes of N₂O between mineral agricultural soils and the atmosphere for major crop types – including corn, soybeans, wheat, alfalfa, cotton, and sorghum. (These crops represent

approximately 86% of total cropland in the U.S.) The IPCC Tier 1 methodology is used to estimate direct N₂O emissions from non-major crops on mineral soils (barley, oats, tobacco, sugarcane, sugar beets, sunflower, rice, peanuts, and others) as well as direct emissions from cultivation of organic cropland soils (histosols).

The underlying model data for the DAYCENT emissions estimates include global data sets of weather, soils, cropland area, and native vegetation. Daily weather data (precipitation, maximum temperature, and minimum temperature) are obtained from the National Oceanic and Atmospheric Administration (NOAA) National Center for Environmental Prediction (NCEP). Soils data include texture percentages of clay, sand, and silt as determined from national soil surveys [207]. Land management data (e.g. timing of planting, harvesting, and intensity of cultivation) are obtained from the Agricultural Sector Model (ASM) [208]. Cropland area data are obtained from the USDA's National Agriculture Statistics Service NASS [209].

DAYCENT simulations are conducted for each major crop at the county scale throughout the U.S. These simulated direct N₂O emissions cannot be partitioned into the IPCC-recommended categories (i.e. synthetic fertilizer, organic fertilizer, sewage sludge, and crop residues) because in DAYCENT, once nitrogen enters the plant/soil system, the model cannot distinguish the original source of the nitrogen from which the N₂O emissions are derived. To approximate emissions by IPCC activity categories, the total simulated amount of N₂O emissions are simply apportioned according to the amount of N added to the soil from each source. However, this approach is quite uncertain because it assumes that all N made available in soil has an equal probability of being released as N₂O, regardless of its source, which is unlikely to be the case [210].

Nitrogen losses from soils due to volatilization and leaching/runoff are calculated within DAYCENT for all major crops. However, the model does not simulate the transport and subsequent off-site conversion of these nitrogen species to N₂O. Consequently, the amount of indirect N₂O resulting from re-deposition of volatilized N is determined using the IPCC-2006 default emission factor (EF₄; 1.0% of N volatilized). Similarly, the amount of indirect N₂O resulting from leaching/runoff of NO₃⁻ is determined using the IPCC-2006 default factor (EF₅; 0.75% of N leached/runoff). For minor crops, both the amount of N volatilized or leached/runoff, and the fraction of this N that is converted to N₂O are determined using the IPCC-2006 Tier 1 method. As with IPCC, the U.S. approach assigns all indirect N₂O emissions to the original source of the nitrogen, regardless of the final location where N₂O occurs.

4.4.4 COMPARISON OF DAYCENT AND IPCC N₂O ESTIMATES

In their description of the U.S. GHG inventory process, EPA presented a comparison of direct N₂O emission estimates provided by DAYCENT and the IPCC-2006 Tier 1 approach [13]. Published field measurement studies from 12 North American sites were considered (11 in the U.S.; 1 in Canada). These represented numerous combinations of crop type, fertilizer treatment, and cultivation practices. All N₂O emission values were expressed on a common basis of g N₂O-

N/ha-day. The results are shown in Figure 4-14, which is taken directly from the EPA document. This figure shows that in nearly every case, the DAYCENT estimates were closer to measured values than were the IPCC estimates. It was pointed out that in general, the IPCC Tier 1 methodology tends to over-estimate emissions when the observed values are low, and underestimate emissions when the observed values are high. In comparison, the DAYCENT estimates are less biased. The improved performance of DAYCENT is expected, because this model accounts for site-specific factors (such as weather, soil type, and crop type) that influence N₂O emissions, while the IPCC methodology does not.

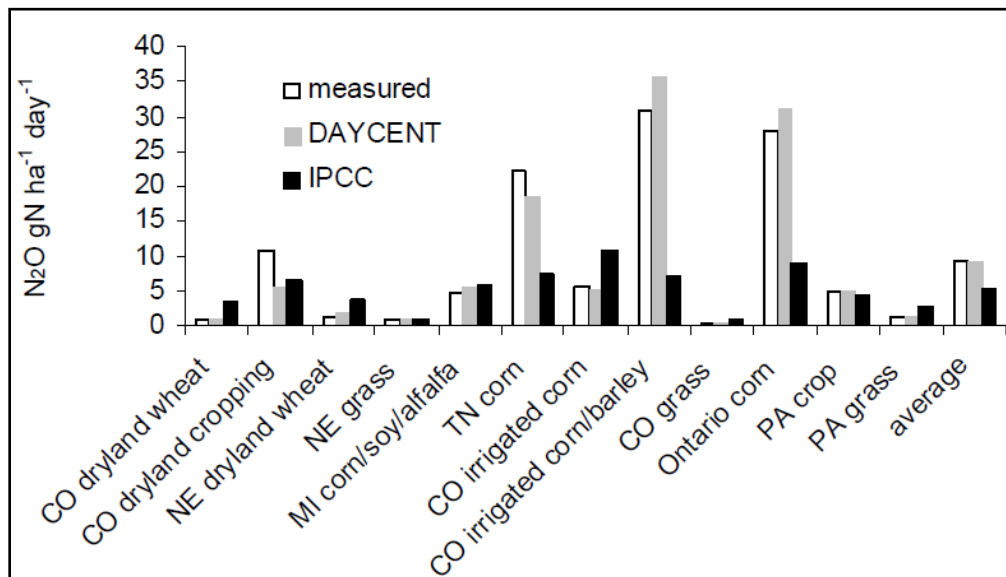


Figure 4-14: Comparison of direct soil N₂O emission estimates from DAYCENT and IPCC (2006). (Taken from U.S.EPA [13])

A detailed comparison of DAYCENT and IPCC-1997 estimates of N₂O emissions under different cropping conditions and geographic locations within the U.S. was published by Del Grosso et al. in 2005 [183]. Both direct soil N₂O and indirect N₂O (from volatilization/deposition and leaching) were estimated by the two methodologies. Major results from this study are represented graphically in Figure 4-15. At the national scale, DAYCENT simulation of total N₂O emissions was about 25% lower than estimates derived using the IPCC-1997 method. Both methods computed highest N₂O emissions in the central region, followed by northwest, southwest, southeast, and northeast. This ordering followed the relative sizes of these regions, as measured by cultivated acres. Within each of the five geographic regions, DAYCENT simulated lower direct N₂O emissions and higher indirect emissions. Due to the dominance of the direct fraction, total N₂O emissions were lower with DAYCENT compared to IPCC-1997. [Note: this difference between the DAYCENT and IPCC values would be smaller if the most recent IPCC method were used (IPCC-2006), due to reduction of the EF₁ default emission factor from 1.25% to 1.00%.]

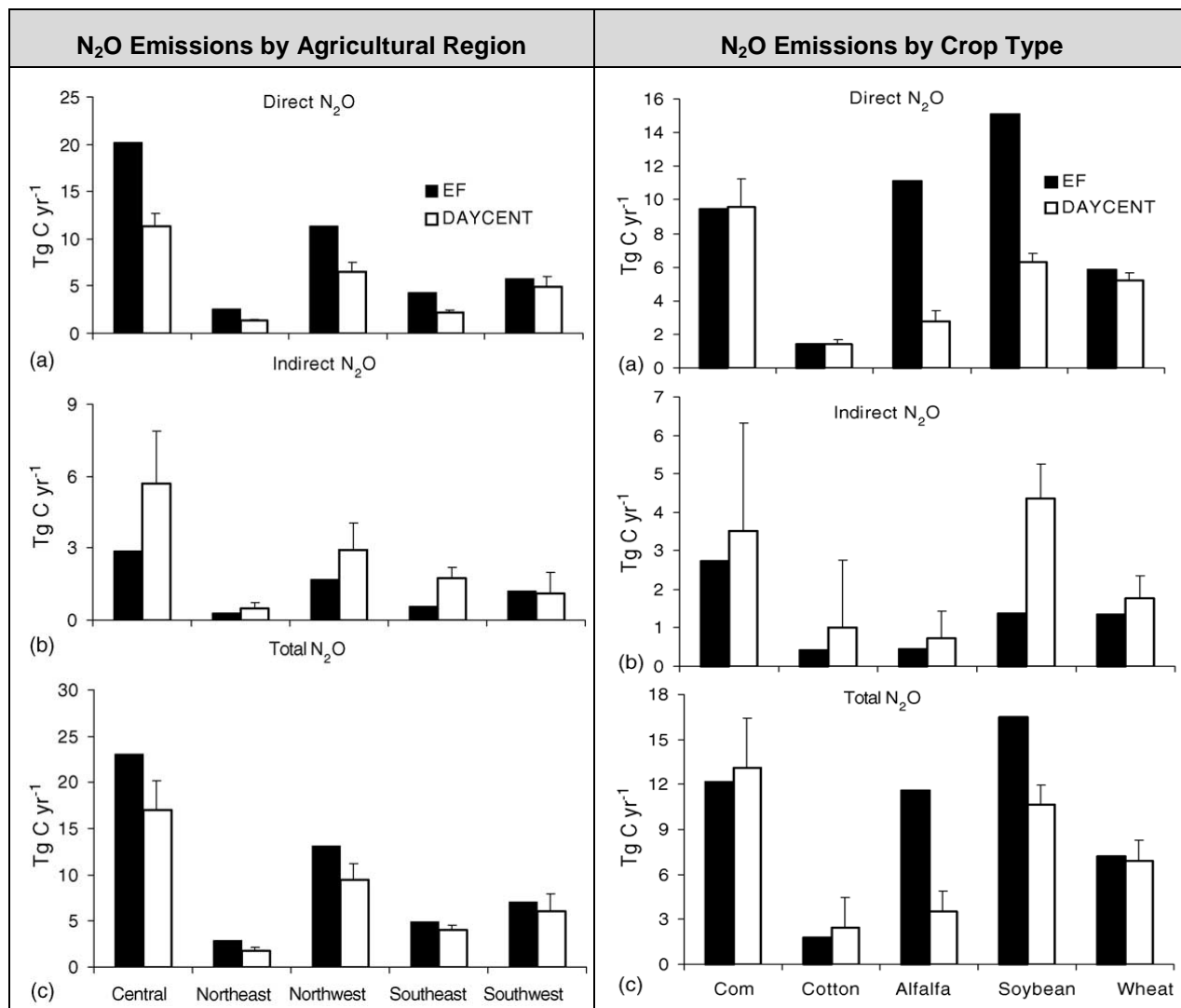


Figure 4-15: Comparison of DAYCENT and IPCC (1997) estimates of N₂O emissions from major crops and agricultural regions in the U.S. Results are 10-year mean and standard deviation in units of CO₂-C_{eq}. (Taken from Del Grosso et al. [183]. Used by permission of Elsevier.)

Figure 4-15 also compares DAYCENT- and IPCC-predicted N₂O emissions by crop type. These results highlight certain differences in the methodologies. For example, direct N₂O emissions estimates are in close agreement for corn, cotton, and wheat; but not for the two nitrogen-fixing crops: alfalfa and soybeans. (These and other similar experimental data are reasons why the IPCC-2006 methodology eliminated atmospheric nitrogen fixation as a direct source of N₂O.) On the other hand, estimated indirect N₂O emissions are higher with DAYCENT, especially for soybeans. In part, this is due to assumed leaching of fixed nitrogen in DAYCENT, while this component is not included in IPCC-1997.

4.5 EFFECTS OF N₂O EMISSIONS ON LIFE-CYCLE GHG EMISSIONS OF BIOFUELS

As described in earlier sections of this report, life-cycle assessments (LCAs) are commonly employed to estimate and compare the carbon intensity (CI) of various biofuel pathways. Due to the importance of agricultural activities in producing feedstocks for 1st generation biofuels (ethanol and biodiesel), accurate assessments of N₂O emissions and their impacts are critical (See Figure 2-1).

4.5.1 CARB/ GREET APPROACH

In their recent assessment of life-cycle GHG emissions for biofuels, the California Air Resources Board (CARB) utilized the GREET model, developed by Argonne National Laboratory. (A California modification, called Ca-GREET, was actually used by CARB.) This model accounts for agricultural N₂O emissions (both direct and indirect) using simple, default emission factors as recommended in the IPCC-2006 Tier 1 approach. The total default N₂O emission factor used in GREET is 0.0133 kg N₂O-N/kg applied N. This factor represents the sum of three separate factors, as shown in Table 4-4.

Table 4-4: Default N₂O Emission Factors used in GREET

N ₂ O Emissions Component	Factor, kg N ₂ O-N/kg soil-N inputs	Uncertainty, kg N ₂ O-N/kg soil-N inputs
Direct N ₂ O from soil	0.0100	0.0030 – 0.0300
Indirect N ₂ O from volatilized and re-deposited N	0.0010	0.0001 – 0.0055
Indirect N ₂ O from nitrate leaching and runoff	0.0023	0.0004 – 0.0088
Total	0.0133	0.0058 – 0.0348 *

*Total estimated range is derived assuming the individual IPCC ranges are log normal. Standard propagation of error routines are applied to lower and upper standard deviations[181].

The GREET methodology considers only direct N₂O from managed mineral soils, not N₂O from high organic histosol soils or from animal waste deposited on grazed pastures, range, and paddock. In other words, GREET only utilizes the first of three terms shown in Scheme 4-9 for computing N₂O-N_{direct} emissions. Also, under the direct N₂O-N_{N-inputs} term, GREET includes nitrogen from application of synthetic fertilizer (F_{SN}) and nitrogen from crop residue (F_{CR}), but not nitrogen from organic fertilizer (F_{ON}) or nitrogen from mineralization of organic matter (F_{SOM}) (see Scheme 4-10).[211]

For indirect N₂O emissions resulting from volatilization and re-deposition, GREET considers only synthetic fertilizers with an assumed volatilization fraction of 10%. Other terms involving organic fertilizers and animal wastes are not included (see Scheme 4-11).

For indirect N₂O emissions resulting from leaching and runoff, the GREET approach is not entirely clear. Again, only nitrogen inputs from synthetic fertilizer are included—not organic

fertilizers, animal waste, or soil organic mineralization. However, simple application of the IPCC default leaching fraction of 0.3 and the default leaching emission factor of 0.0075 would provide a total factor of 0.0025. The slightly reduced factor of 0.0023 shown in Table 4-4 suggests that at least in some applications, GREET may use slightly different factors.

The estimated contribution of N₂O emissions to the total life-cycle GHG impacts of a biofuel can be very significant. For example, in the CARB pathway for corn ethanol produced in a dry mill process, the total life-cycle GHG carbon intensity (CI) value is 67.6 g CO_{2,eq}MJ⁻¹[81]. Of this total, 15.9 g CO_{2,eq}MJ⁻¹(23.5%) is attributed to agricultural N₂O emissions. This is shown in Figure 4-16 along with similar assessments of N₂O's contribution to the CI of sugarcane ethanol and soy biodiesel.

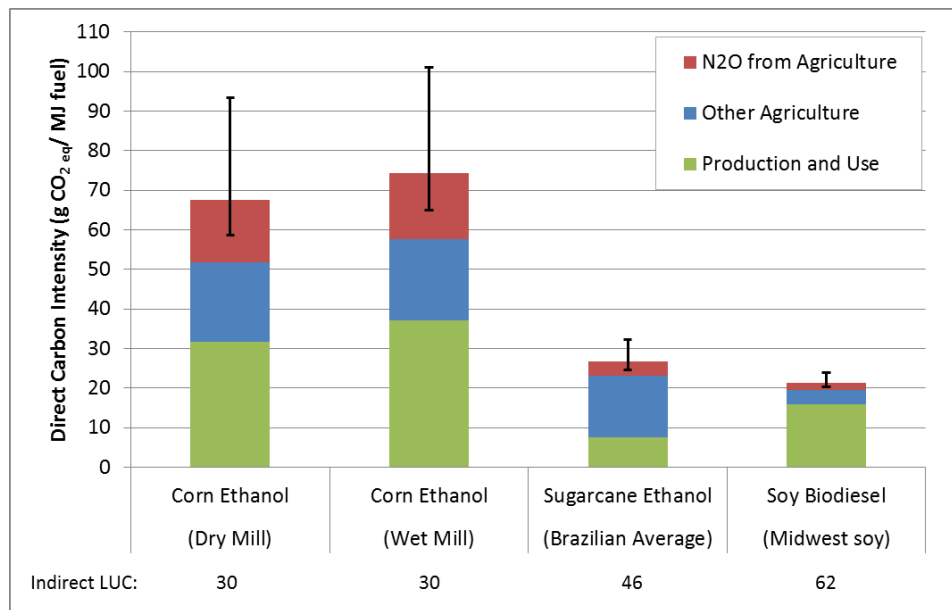


Figure 4-16: CARB's assessment of N₂O's contribution to direct CI of biofuels. [81,82,79]

4.5.2 EPA'S APPROACH IN THE RFS2

In their assessment of N₂O emissions from adoption of RFS2, EPA combines estimates from FASOM for the U.S. and FAPRI for international emissions. FASOM emissions are based the DAYCENT model with regionally specific detail for crop type, moisture conditions, and other parameters. International emissions are based on the FAPRI analysis of crops and FAO estimates of fertilizer inputs. The treatment is similar to GREET although the parameters for fertilizer application and crop residue are likely different.

Figure 4-17 shows EPA's estimates of N₂O emissions from various feedstocks as presented in the regulatory impact analysis. [2] These estimates are generated from the FASOM model which uses DAYCENT estimates of N₂O emissions. Note the differences among feedstocks between the portion of emissions associated with fertilizer and crop residue. Crops such as switchgrass, which are largely removed from the field are assumed to leave no residue, while corn and soybeans leave more significant residues. The level of N₂O emissions are consistent with a

paper by Colorado State University, developers of DAYCENT, which show N₂O emissions ranging from 1,000 to 2,000 g CO_{2,eq} ha⁻¹. [212]

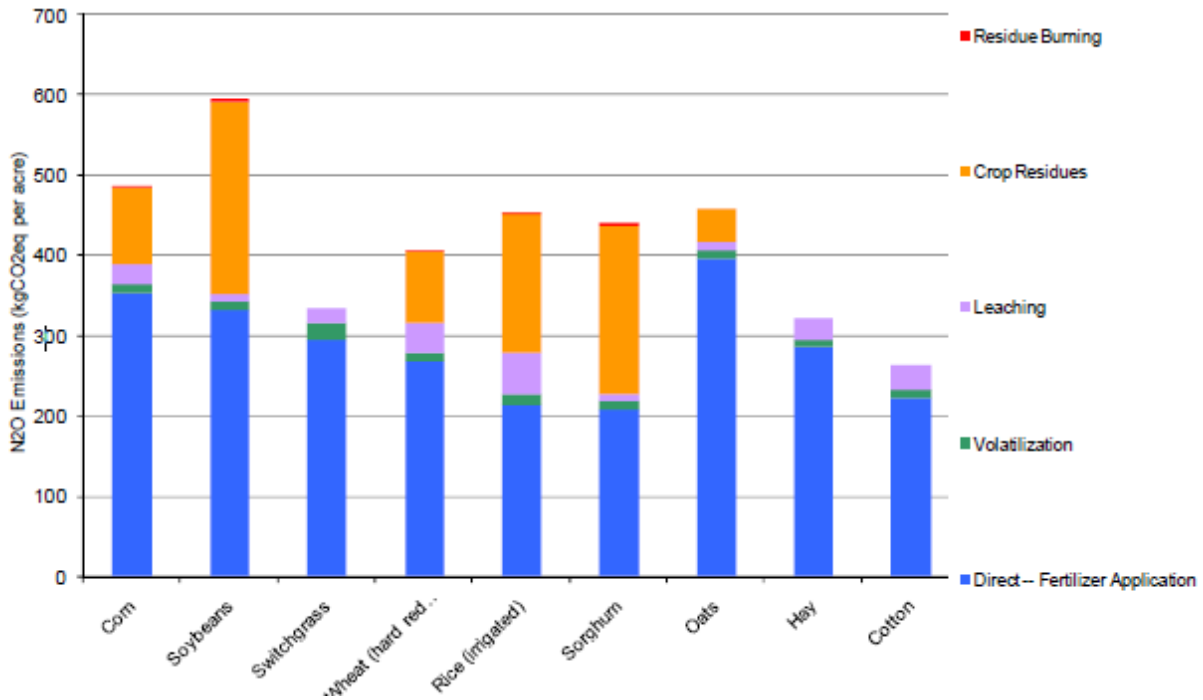


Figure 4-17: Annual N₂O emission rates from the RFS2 Analysis. [2]

4.5.3 JRC/ BIOGRACE APPROACH IN EU- RENEWABLE ENERGY DIRECTIVE

The JRC report on the life cycle of fuels serves as a scientific evaluation of the range of fuel options and examines a range of inputs and allocation procedures. To model N₂O emissions from agriculture, the study used results from a database-calculation model developed from a project estimating GHG emissions for all of Europe by the Soils and Waste Unit at the Institute for Environment and Sustainability at EC's Joint Research Center at Ispra. [19]GHG emissions for Europe were calculated day-by-day using the soil chemistry model and data segregated by crop type to give EU-averaged N₂O emissions for each crop. The model was built on the soil chemistry model DNDC (DeNitrification DeComposition) [213] JRC uses daily weather data, manure rates, fertilizer rates from crop and soils characteristics, and country-based correction factor inputs. However, the IPCC default emission factor approach for indirect emissions from leached Nitrogen was used.

The BioGrace model was developed for certification under the Renewable Energy Directive (RED).[214] The tool was used to provide default values for 22 fuel pathways in the Annex V of the RED, and is used by fuel developers to perform LCA analysis for certification. [215]The model follows the approach laid out in the JRC report. BioGrace is configured with a series of

workbooks for many feedstocks and fuel pathways. The N₂O emissions produced in the field are represented as inputs (default values) in kg/ha. The origin of the BioGrace defaults is the JRC analysis, so they are also based on the same nitrogen model approach.

4.5.4 COMPARISON OF N₂O ESTIMATES FROM DIFFERENT MODELING SYSTEMS

The N₂O estimates from different modeling systems can be compared using several metrics. However, comparing N₂O contributions on a g/MJ of fuel basis is challenging because some modeling systems (such as FAPRI) incorporate yield improvements into the total demand for crops to create a biofuel feedstock.

Figure 4-18 compares the overall N₂O emissions from different studies on a g CO_{2,eq} acre⁻¹ basis. Results from GREET are computed using fertilizer and crop residue values with default conversion factors. The RFS2 results are from the domestic analysis using FASOM as reported in the RIA [2] and shown in Figure 4-17. Additionally, results from the JRC (Joint Research Center) and the Biograce model are shown. Note that version of the JRC study and Biograce that were examined do not have an analysis for corn ethanol.

The figure illustrates some significant differences between the model approaches. The N₂O emissions from all of the crops vary over a significant range (except for rapeseed). The differences may be due in part to assumed fertilizer application rates for corn. In the case of soybeans, the effects of nitrogen fixation and crop residues are significant. Atmospheric nitrogen fixation in soybeans is an important process, resulting in over 100 pounds of nitrogen per acre (around 230 kg CO_{2,eq} acre⁻¹ as shown by the orange bar in Figure 4-17). Much of the fixed nitrogen is absorbed in the soybean crop itself, and thus is accounted for as part of the component of crop residue. However, other nitrogen may be incorporated directly into the soil, not in the plant itself. GREET does not include a term for this nitrogen fixation process, while FASOM (through the DAYCENT model) does. The potential for N₂O generation (both direct and indirect) from this fixed soil nitrogen is significant and uncertain.

Since the default inputs for the Biograce model are based on the JRC study, not surprisingly, the N₂O emissions from wheat and rapeseed are similar.

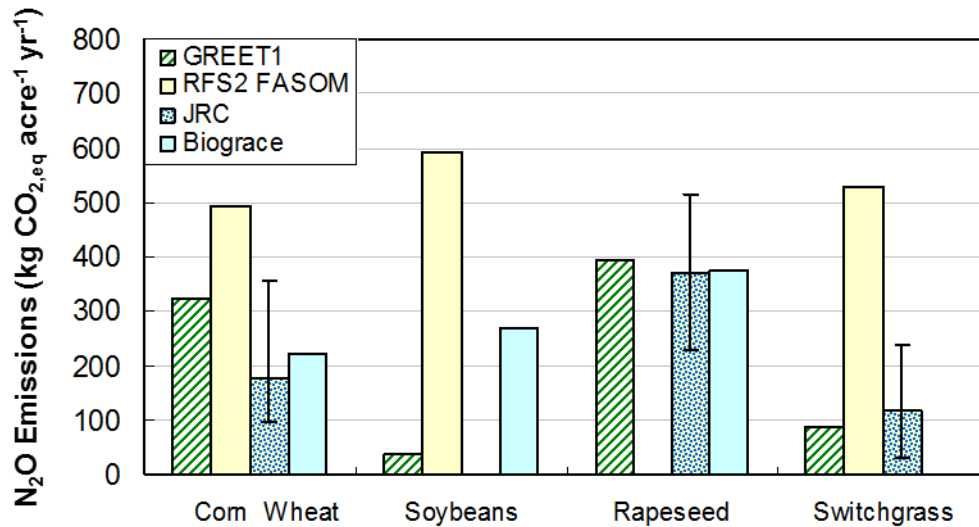


Figure 4-18: Comparison of Annual N₂O emissions from LCA modeling systems.

4.5.5 OTHER CONSIDERATIONS

Adler et al. utilized an LCA approach to evaluate GHG impact of several bioenergy cropping systems [216]. The DAYCENT model was used to assess biomass yields and GHG fluxes for corn, soybeans, alfalfa, hybrid poplar, reed canarygrass, and switchgrass as bioenergy crops in Pennsylvania. All cropping systems provided net GHG sinks, mainly due to displaced fossil fuel by the biofuels produced from these biosources. N₂O emissions (both direct and indirect) were the largest GHG sources in all cropping systems. Compared to the other crops, switchgrass and hybrid poplar had the lowest N₂O emissions (mainly due to low fertilizer inputs), and consequently, provided the greatest GHG benefits.

Reijnders and Huijbregts investigated LCA of biodiesel fuel produced from European rapeseed and Brazilian soybeans [217]. They concluded that total GHG emissions were higher in the biofuel cases than with conventional fossil diesel. A significant contributor to this was the assumed high N₂O emissions from agricultural activities. Based on the reports by Crutzen et al. [30], these authors assumed a wide range of 1.5-5.0% conversion of applied N to N₂O. The overall high uncertainty in their GHG assessments (10-30%) was driven mainly by this large range of N₂O emission factors.

In the report by Crutzen et al., the effects of N₂O on GWP of three biofuels were estimated: (1) biodiesel from rapeseed, (2) ethanol from corn, and (3) ethanol from sugar cane. This work did not involve a formal LCA study. Instead the nitrogen content within the biomass feedstocks themselves was used as a proxy for the amount of nitrogen that must eventually be replenished in the soil. Thus, crops containing higher N content (such as rapeseed) require more nitrogen inputs – and hence are assumed to be responsible for more N₂O emissions – than crops with low nitrogen content (such as sugar cane). Using the high range of N₂O conversion factors (3-5%) determined by their top-down inventory method, Crutzen et al. then computed the N₂O emissions

resulting from each of these three biofuels. The increase in GWP resulting from these emissions were compared to the GWP decrease resulting from displacement of fossil fuels with biofuels using a factor called “relative warming.” (This factor is the ratio between “climate warming” from N₂O and “climate cooling” from displaced fossil fuels.) For ethanol from sugar cane, the computed relative warming values are 0.5-0.9, meaning that GWP benefits are realized over the range of N₂O emission factors used. For biodiesel from rapeseed, the relative warming values are 1.0-1.7, meaning that GWP dis-benefits are realized over the range of N₂O emission factors. Ethanol from corn had intermediate relative warming values of 0.9-1.5.

Crutzen et al. suggested that greater GWP benefits would result from use of low-nitrogen containing perennial grass biofuel feedstocks such as switchgrass and miscanthus. (In fact, Davis et al. recently reported use of DAYCENT modeling to show significantly reduced N₂O emissions from these grasses as compared to corn [218].) Crutzen also assumed a global nitrogen fertilizer uptake efficiency of 40%, and showed that increasing this efficiency to 60% would substantially improve the GWP benefits of biofuels. Other assumptions and simplifications by Crutzen are discussed by Mortimer et al. who offer this assessment of the approach: “All-in-all, one layer of dubious assumptions is added on top of further layers of assumptions and combined with unreliable data to form firm and radical conclusions about the potential of biofuels to reduce GHG emissions” [181].

In a more thorough study, Smeets et al. investigated the contribution of N₂O to life-cycle GHG impacts of 1st generation biofuels from various sources [219]. In particular, ethanol from corn, wheat, sugar cane, and sugar beets was considered; as well as biodiesel from soybeans, rapeseed, and palm oil. Two levels of crop management were considered: (1) conventional management as of the year 2000, and (2) optimized management, which included higher crop yields, optimized fertilizer and water regimes, and use of nitrification inhibitors to reduce N₂O emissions. N₂O emission rates for each crop/fuel system were based upon a modified IPCC-2006 Tier 1 approach for the geographic regions of interest. In most scenarios investigated, optimized agricultural management reduced N₂O emissions/mass of crop by 20-80%. LCA modeling results showed that the impact of N₂O emissions on total GHG varied widely among different crops, regions, and land reference systems chosen. A good summary of the results from several scenarios is presented in Figure 4-19, which shows both N₂O mass emissions and the percent change in total GHGs compared to fossil fuel usage. On both bases, the benefit of optimized management (OM) compared to conventional management (CM) can be seen. The authors concluded that N₂O emissions typically contribute between 10% and 80% of the total life-cycle GHG emissions due to biofuels; and that the crop type, climate, and choice of reference land use system are key factors when calculating N₂O emissions due to crop production. While the overall GHG benefits of some scenarios were uncertain, clear benefits were seen in nearly all cases involving ethanol from sugar cane, ethanol from sugar beets, and biodiesel from palm oil.

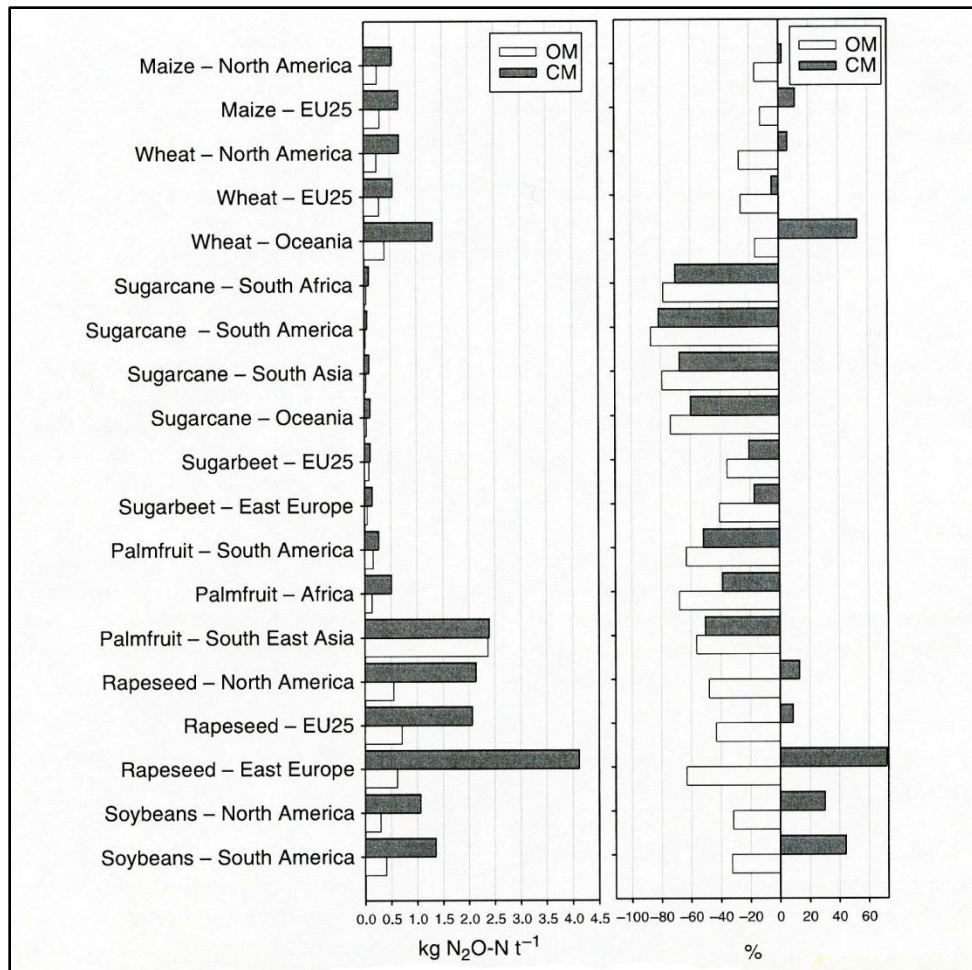


Figure 4-19: Impact of crop management system on emissions of N_2O per unit crop and on the change in GHG emissions compared with fossil fuels. OM is optimized management, CM is conventional management. (Taken from Smeets et al. [219]. Used by permission of publisher)

4.6 MITIGATION OF N_2O EMISSIONS

It has been recognized for some time that specific agricultural management practices can be employed to reduce N_2O emissions from soils. Wagner-Riddle and Thurtell reported that the spring thaw N_2O burst from cropland soils in Ontario, Canada was exacerbated by manure application or alfalfa incorporation in the fall, but was reduced by use of over-wintering crops[148].

McSwiney and Robertson demonstrated a non-linear relationship between fertilizer nitrogen application and N_2O emissions from corn fields in Michigan [220]. Linear N_2O increases were observed until a threshold fertilizer level was reached, after which the increase in N_2O was much higher. These authors suggested that avoiding excessive fertilizer application would be an effective N_2O mitigation measure. DeAngelo et al. reported that avoidance of excessive fertilizer use could be the most cost-effective agricultural N_2O mitigation measure [221].

Drury et al. demonstrated the effects of rotational cropping on N₂O emissions from fields in Ontario, Canada [222]. They pointed out that the crop residue being decomposed and supplying nutrients to the soil is usually from a different crop than what is currently being grown. Monoculture of corn was found to give much higher annualized N₂O emissions than monoculture of wheat or soybeans. This was due both to the higher fertilizer requirements for the corn being grown, and retention of high-N corn residue from the previous years in the soil. Rotational cropping of wheat or soybeans with corn substantially reduced the overall N₂O emissions. Similar N₂O reduction benefits of corn rotational cropping practices have been reported in other studies [169,223].

The type of fertilizer being used also has been shown to affect N₂O emissions. Venterea et al. demonstrated reduced N₂O from Minnesota corn cropping systems when using urea as compared to anhydrous ammonia [169]. There has also been considerable interest in use of fertilizer formulations that include nitrification inhibitors to reduce N₂O emissions [224,225,226]. In addition, application of time-release fertilizers – and application of smaller but more frequent dosages of fertilizer – have been shown to reduce N₂O emissions [114].

No-till cultivation has received considerable attention as a possible means of reducing overall GHG emissions from agricultural activities – mainly due to lower CO₂ emissions. However, the effects of no-till upon N₂O are less clear, and vary considerably from case-to-case. Several studies have reported increased N₂O emissions from application of no-till cultivation [227,157,228]; others have reported decreases [184,204,229,223]; and some report no effect. Six et al. recently evaluated numerous published studies regarding the effect of no-till upon total GHG emissions [230]. They determined that N₂O fluxes increased during the first 10-years of no-till cultivation, but eventually decreased after many years.

Another potential mitigation measure involves application of biochar to soils [231]. It is postulated that both biological and soil physical mechanisms could be responsible for the reductions in N₂O observed following application of biochar. Others have suggested that the copper-based de-nitrification enzyme responsible for reducing N₂O to N₂ in soils could be manipulated to promote greater conversion of N₂O, thereby reducing its emissions from soil [232]. Broader discussions of a range of N₂O mitigation measures from agricultural management strategies are provided by Snyder et al. [126], IPCC [233], and the Technical Working Group on Agricultural Greenhouse Gases (T-AGG) [234].

5 SUMMARY AND RECOMMENDATIONS

Life cycle assessments are being used in policy as a method to determine the relative GHG benefits of alternative fuels as compared to conventional petroleum fuels. However, there are still several aspects of biofuel LCA that contain large uncertainties, particularly agricultural emissions of N₂O and GHG emissions arising from indirect land use changes. In this work, we have investigated approaches taken to modeling these two controversial areas of LCA.

5.1 INDIRECT LAND USE CHANGES

Modeling ILUC is complex and is outside the scope of a conventional LCA model. The determination of ILUC requires linking agro-economic models, which determine the amount and type of land use changes occurring in response to increased biofuel use, to emission factor databases, which contain carbon-stock data to calculate the resulting GHG flux from converting these lands. Because of the complexity and lack of means for verification, the issue of ILUC is highly uncertain. Assessments of a carbon intensity of ILUC range from 18 to 106 g CO_{2,eq} MJ⁻¹ fuel for corn ethanol over a 30 year period. [5,1] Regardless, policies are adopting ILUC into LCA calculations so as not to ignore such a potentially significant impact.

It is therefore important to understand how ILUC is modeled, which assumptions introduce the most uncertainties, and which carry the most impact. The primary influences in ILUC are the determination of the amount, location and type of land converted, and the emission factors applied to the land. In this work, we have compared the modeling approaches used in policy such as the EPA's Renewable Fuel Standard (RFS2) and California's Low Carbon Fuel Standard (LCFS), with other significant studies such as Searchinger [1,6] and Tyner [5].

Comparisons of the differences from the overall LCA results, the results from the agro-economic models, and the emission factor databases are highlighted below.

Discussion of Overall LCA results

- Searchinger was one of the first to introduce the potentially significant impacts of ILUC to GHG of biofuels, and has predicted some of the highest carbon intensity values. [1] His work was based on land use modeling by FAPRI-CARD [91], and linked to the Woods Hole emission factor database. Since then, agro-economic models have utilized updated databases to better predict the LUC response to biofuels policy, and overall estimates of LUC-induced GHG emissions have decreased. [57,60,64,90]
- Many studies have relied on the Woods Hole database to determine the GHG emission factors resulting from LUC predicted by agro-economic models. [3,5]. This database is coarse, breaking down the world into only 10 regions. The EPA has applied a more spatially explicit approach, and has applied the Winrock database, which has carbon stock data for over 750 regions worldwide. [2,73] We attempted to compare these databases to determine which data and assumptions have the largest influence on results.

However, the databases are not directly comparable due to differences in methodologies and application, as well as differences in spatial data. Comparison of the databases would be possible through further manipulation of the Winrock data into corresponding regions of the Woods Hole database.

- In all LCA studies investigated, predicted GHG emissions are larger for soy biodiesel than corn-ethanol. Low yields of soy oil and high demands for vegetable oils which must be replaced require more land extension, particularly in Latin America and Southeast Asia

Discussion of Land Use Change Results from Agro-economic models

LUC results are not consistent between reports, or even within reports. The major differences in LUC results are due to differences in agro-economic models used. CARB uses the GTAP model, while EPA uses two different models: FASOM is used to predict domestic LUC while FAPRI is used to predict international LUC. Different models predict different amounts of land use change in different locations, as well as different types of land conversion.

- The GTAP model predicts land conversion between forests, pasture and cropland for 19 different world regions. Both Tyner and CARB use the GTAP model.[3,5] However, recent publications from Tyner include major revisions to the GTAP model which improve the analysis of biofuels and result in lower LUC. The total land conversion predicted by Tyner is only half that predicted by CARB although more of the conversion occurs in forests (32% compared to 22%).
- FAPRI predicts land conversion of cropland (including perennial and annual crops) and pasture. A net zero land approach is taken, so the makeup of any land requirements not met through conversion between these categories is met through “natural lands”. Natural lands are made up of forests, shrublands, grasslands, and other land types, each of which has its own emission factors. FAPRI predicts land conversions for 54 regions.
- FASOM predicts cropland conversion within the U.S., calculating the LUC and resulting emissions endogenously. It is therefore difficult to fully understand and evaluate the LUC and GHG emissions, and is not possible to compare the EFs from other databases. The EPA results show a FASOM prediction of negative emissions from LUC for both corn ethanol and soy biodiesel, although the reasons for this are not clear.
- The total ILUC estimated in the EPA report is from expansion of cropland [2]. In the FAPRI analysis for international ILUC, cropland includes annual and perennial crops. Total LUC results from FAPRI include changes to pastureland, which are also used to estimate the resulting GHGs. FASOM, however, only reports increases in cropland, so it is unclear how changes in pasture or other land types affect the final ILUC- GHG result. However, it seems likely additional LUC not reported is used to estimate GHGs since results for cropland increases total 1.4 million acres, yet GHGs are reduced by 4 g CO_{2,eq}MJ⁻¹ in the corn ethanol case. The changes in pasture land are also used to estimate

other emissions in the “direct” categories. This adds additional uncertainty about double counting emissions.

- In the EPA modeling approach, the boundaries between the CI values reported are not clear, making it difficult to understand which of the impacts are direct and which are indirect.
- The CARB analysis is the least transparent. Very coarse results are given, so it is difficult to compare the LUC results.

Comparison of Emission Factor Databases.

The methods and approaches used by CARB and EPA are not directly comparable and introduce further questions.

- C-stock data in the Winrock database are given for over 750 administrative units world wide. The data are used to calculate emission factors for 44 conversion and reversion classifications. The EFs are then weighted into regional EFs for several different land conversion classifications using MODIS satellite data. A single weighted EF for each region in the FAPRI database is not provided.
- The Woods Hole database provides emission factors for 10 regions. In the CARB analysis, the emission factors are weighted into conversion from forest and pasture based on historical land use change data.
- More spatially explicit data adds complexity, but improves reliability of results. Most researchers believe the regions used in the Woods Hole database are too coarse. CARB is currently developing a more spatially explicit database for use in the LCFS. The data are from similar sources as Winrock (such as the World Harmonized Soils Database- WHSD).
- Soil carbon analysis is different between the two studies so is not directly comparable. The Woods Hole database provides data for the top 1 m of soil, and assumes that 25% is released following conversion to cropland. The Winrock database applies the WHSD for the top 30 cm of soil. The amount lost is variable by region and soil type, ranging from 20% to 50%, and is accounted over 20 years.
- Carbon stock for vegetation are comparable between databases in that the ranges are similar. However, the Winrock database applies lower average C-stock data for above and below ground biomass. The calculations for emissions from above- and below-ground biomass are treated differently between EPA and CARB. EPA assumes that all C-stock will be lost upon conversion, although a calculation for harvested wood products is included (but no data are). CARB assumes that 10% of the carbon in vegetation is not converted, following IPCC recommendations.

Additional considerations: The impacts of global biofuel policies should be modeled

Although the EU has not yet adopted the inclusion of ILUC in its policy, it is beginning to look at its potential effects. [8,27,89,88] In policy-related studies, the impacts of the full policy are modeled, and fuels are broken out separately. However, it is reasonable to assume that each individual study might project LUC on the same lands. For example, in the EU policy, a mandate of 5.6% biofuel use by 2020 means that additional ethanol will have to be imported from Brazil. The U.S. policy requiring additional ethanol by 2020 is also projected to demand land in Brazil. This might result in a “competition” for the new lands from each of the policies, which could cause additional expansion into lower quality, more marginal lands, resulting in lower yields and greater GHG emissions.

5.2 TIME ACCOUNTING

Although there has been a general consensus among policy makers in the approach taken for time accounting, the topic has been heavily debated within the scientific community. The annualization approach adopted by the EPA, CARB, and the was chosen primarily out of simplicity, since the application of complex models adds further uncertainty to a topic which is already highly uncertain. Both EPA and CARB have selected a time horizon of 30 years, while the EU has elected to allocate over 20 years.

Numerous other methodologies have been proposed, and calculation methods within the annualization methodology have been debated. Support is garnering behind the fuel warming potential (FWP) methodology for time accounting since it follows similar metrics to those already used to determine GWPs of different GHGs. However, it is unlikely that policies will adopt a different method in the near term, particularly since CI values predicted using the current annualization methods have already been adopted into regulation.

5.3 AGRICULTURAL EMISSIONS

N₂O is a potent GHG that contributes significantly to the total anthropogenic GWP. N₂O is emitted directly from soils, through microbially-induced nitrification and denitrification processes. In addition, indirect N₂O emissions result from deposition of nitrogenous species previously volatilized from soils, and from leaching/runoff of nitrogen from soils and into waterways. A complete understanding of a biofuel’s GHG impacts requires accurate accounting of N₂O emissions from all these pathways.

IPCC methodology for N₂O modeling

- IPCC methodologies have evolved over the past 15 years. Current guidance describes a set of three Tiers for developing N₂O emissions inventories, with the choice of tier to be used depending upon the availability and reliability of data input sources.
- IPCC’s most simplified approach, called Tier 1, computes N₂O emissions as the sum of three main components: (1) direct emissions from soils, (2) indirect emissions resulting

from deposition of previously volatilized soil nitrogen, and (3) indirect emissions resulting from leaching and/or runoff of nitrogen from soils.

- The IPCC Tier 1 method utilizes default emission factors and default values for fraction of soil nitrogen that is volatilized, and fraction of soil nitrogen lost by runoff and/or leaching. While these values are based upon assessments of experimental data, they have very large uncertainty ranges.
- IPCC Tier 2 utilizes the same methodological approach as Tier 1, but applies emissions and stock change factors that are based on regionally-specific data, rather than universal defaults. A Tier 2 N₂O inventory typically has higher temporal and spatial resolution compared to a Tier 1 inventory.
- IPCC Tier 3 employs process-based methodologies for determining N₂O emissions inventories. The current U.S. agricultural GHG inventory utilizes a Tier 3 approach for estimating direct N₂O emissions from major crops.
- Use of the GREET Model to estimate a biofuel's carbon intensity (CI) generally involves application of an IPCC Tier 1 approach for determining agricultural N₂O emissions.

Process-based methodology for N₂O modeling

- Process-based biogeochemical models simulate fluxes of nitrogen among the atmosphere, vegetation, and soil. These models represent the physical, chemical, and biological processes that influence N₂O formation.
- In development of the current U.S. agricultural GHG inventory, U.S. EPA and USDA have employed a process-based model, called DAYCENT, to estimate N₂O emissions.
- DAYCENT (and all other process-based models) require extensive data inputs to accurately simulate N₂O emissions. These inputs include crop type, soil type, nitrogen input, temperature, precipitation, pH, and others.
- Limited experimental data suggests that agricultural N₂O emissions are estimated more accurately when using DAYCENT than when using an IPCC Tier 1 method.

Mitigation of N₂O emissions

- Specific agricultural practices have been shown to mitigate N₂O emissions. These include adjustments to the timing, type, and amount of fertilizer application. The impacts of no-till cultivation upon N₂O emissions are unclear.
- An IPCC Tier 1 method for estimating N₂O emissions does not account for any variations in agricultural practices (other than fertilizer amount).

5.4 RECOMMENDATIONS FOR FUTURE WORK

1. Further understanding of the differences in assumptions and inputs of economic models is needed.

The agro-economic models are used to determine key factors for estimating land use change emissions, including how much LUC is occurring, where it is occurring, and which types of land are being converted. Further investigation of how different economic models measure and predict LUC is needed to understand how assumptions and inputs can affect the results.

2. Analysis of Developing Policies

CARB is updating its methodologies to develop more spatially explicit EF databases that can be used directly with the GTAP model. Additionally, it is incorporating updates to the GTAP model, which tend to predict lower amounts of LUC than originally estimated. [5,60] Revisions to ILUC modeling approaches should be completed and considered by the Board by mid-2012. Changes to the GTAP model and their effects on results should be understood. Updates to the carbon-stock databases should be compared to those used by the EPA.

Additionally, the EU has taken a “wait and see” approach in response to ILUC. Developments in international fuel policies should be monitored.

3. Improved Transparency, Harmonization and Uncertainty Analysis

Different modeling systems, approaches, and data sets have arisen to address different scientific and regulatory needs. Given this situation, it seems unlikely that harmonization can be achieved, although greater consistency of certain modeling approaches and data sets is certainly desirable. For example, classification of land conversion types can result in significant differences to GHG emissions estimates from ILUC. Additionally, carbon stock data from existing databases such as Woods Hole and Winrock are difficult to compare without careful manipulation of data. However, improved transparency should be a goal in every case. This can be achieved by providing sufficient details regarding methodologies, datasets, assumptions and results. Related to the transparency, a quantitative assessment of model uncertainty (including ILUC uncertainty) should be provided.

4. Treatment of agricultural N₂O emissions in LCA of biofuels

Use of the GREET Model in biofuel LCA studies generally involves application of IPCC Tier 1 recommended emission factors for agriculturally-related N₂O emissions. However, derivation of the emission factors actually applied in GREET is generally not clearly explained, and distinctions between direct and indirect emissions are not always apparent. Future studies should more clearly explain the derivation of all factors being used. Additionally, the full uncertainty range of the IPCC-recommended default factors should be used in sensitivity studies to better understand the possible range of contributions that agricultural N₂O emissions can have to a biofuel’s CI value.

5. Application of process-based N₂O emissions model

The contribution of N₂O emissions to a biofuel's CI value is generally estimated using simplistic default emission factors, which do not account for crop type, soil type, climate, cropping practices, or other factors known to influence N₂O emissions. Efforts should be made to couple a process-based N₂O emissions model, such as DAYCENT, with GREET, to provide more reliable estimates of the N₂O emissions attributable to growth of feedstocks for biofuels. In addition, more rigorous comparisons should be made between N₂O determined by DAYCENT and determined by IPCC Tier 1.

6 REFERENCES

1. Searchinger, T., R. Heimlich, R.A. Houghton, F. Dong, A. Elobeid, J. Fabiosa, S. Tokgoz, D. Hayes, and T.H. Yu; Use of U.S. croplands for biofuels increases greenhouse gases through emissions from land-use change. *Science*, 319, 1238-1240. 2008.
2. U.S.EPA; Renewable Fuel Standard Program (RFS2) Regulatory Impact Analysis. EPA-420-R-10-006, 2010.
3. California Air Resources Board; California Low Carbon Fuel Standard Program. *California Environmental Protection Agency, Air Resources Board*, 2009.
4. Unnasch, S., B. Riffel, S. Sanchez, L. Waterland, and L. Life Cycle Associates; Review of Transportation Fuel Life Cycle Analysis. CRC E-88 Final Report, 2011.
5. Tyner, W.E., F. Taheripour, Q. Zhuang, D. Birur, and U. Baldos; Land Use Changes and Consequent CO2 Emissions due to U.S. Corn Ethanol Production: A Comprehensive Analysis. Final Report, 2010.
6. Searchinger, T. and Heimlich, R.; Estimating Greenhouse Gas Emissions from Soy-based US Biodiesel when Factoring In Emissions from Land Use Change. *The Lifecycle Carbon Footprint of Biofuels*, 35-45. Presented at Biofuels Food and Feed Tradeoffs. Miami Beach, FL; Jan. 29, 2008
7. California Air Resources Board, Low Carbon Fuel Standard, Carbon Intensity Look-Up Tables. 2009. Retrieved from: <http://www.arb.ca.gov/fuels/lcfs/lcfs.htm>
8. Al-Riffai, P., B. Dimaranan, and D. Laborde; Global Trade and Environmental Impact Study of the EU Biofuels Mandate. Final Report, 2010.
9. Houghton, R.A.; Revised Estimates of the Annual Net Flux of Carbon to the Atmosphere from Changes in Land Use and Land Management 1850 - 2000. *Tellus*, 55B, 378-390. 2003.
10. ICF International; Lifecycle Greenhouse Gas Emissions due to Increased Biofuel Production: Methods and Approaches to Account for Lifecycle Greenhouse Gas Emissions from Biofuels Production Over Time. Peer Review Report, 2009.
11. O'Hare, M., R.J. Plevin, J.I. Martin, A.D. Jones, A. Kendall, and E. Hopson; Proper Accounting for Time Increases Crop-based Biofuels' Greenhouse Gas Deficit Versus Petroleum. *Environmental Research Letters*, 4, 1-7. 2009.
12. Kloverpris, J. H. and Mueller, S.; Improved Time Accounting in the Estimation of GHG Emissions from Indirect Land Use Change. IEA Bioenergy Task 38 Conference. Brussels, Belgium; Mar. 9, 2010
13. U.S.EPA; Inventory of U.S. Greenhouse Gas Emissions and Sinks: 1990 - 2009. EPA 430-R-11-005, 2011.
14. UK Department of Transport; UK Policy, Renewable Transport Fuel Obligation. 2005.

15. European Union; Directive 2003/30/EC of the European Parliament and of the Council of 8 May 2003 on the promotion of the use of biofuels or other renewable fuels for transport. *Official Journal of the European Union*,(17.5.2003), L 123/42-L 123/46. 2003.
16. Janulis, P.; Reduction of energy consumption in biodiesel fuel life cycle. *Renewable Energy*, 29,(6), 861-871. 2004.
17. S&T2 Consultants Inc., Cheminfo Services Inc., H. MacLean, and Fugacity Technology; Sensitivity Analysis of Biodiesel LCA Models to Determine Assumptions With the Greatest Influence on Outputs. 2008.
18. Sheehan, J., V. Camobreco, J. Duffield, M.S. Graboski, and H. Shapouri; A life cycle inventory of biodiesel and petroleum diesel for use in an urban bus. NREL/SR-580-24089, 1998.
19. Edwards, R., J.F. Larive, V. Mahieu, and P. Rouveirolles; Well-to-Wheels Analysis of Future Automotive Fuels and Powertrains in the European Context. Version 3.1, 2008.
20. Bernesson, S., D. Nilsson, and P.-A. Hansson; A limited LCA comparing large- and small-scale production of rape methyl ester (RME) under Swedish conditions. *Biomass & Bioenergy*, 26, 545-559. 2004.
21. Broch, A., S.K. Hoekman, A. Gertler, C. Robbins, and M. Natarajan; Biodistillate Transportation Fuels 3. - Life-Cycle Impacts. *SAE Technical Paper Series*, SAE 2009-01-2768, 2009.
22. Kalnes, T., T. Marker, and D.R. Shonnard; Green diesel: A second generation biofuel. *International Journal of Chemical Reactor Engineering*, 5, Article A48- 2007.
23. Niederl, A. and M. Narodoslawsky; Ecological evaluation of processes based on by-products or waste from agriculture: Life cycle assessment of biodiesel from tallow and used vegetable oil. *Feedstocks for the Future: Renewables for the Production of Chemicals and Materials*, 921, 239-252. 2006.
24. Guinee, J.B. and R. Heijungs; Calculating the influence of alternative allocation scenarios in fossil fuel chains. *International Journal of Life Cycle Assessment*, 12,(3), 173-180. 2007.
25. Bernesson, S., D. Nilsson, and P.-A. Hansson; A limited LCA comparing large- and small-scale production of rape methyl ester (RME) under Swedish conditions. *Biomass & Bioenergy*, 26, 545-559. 2004.
26. Wang, M., H. Huo, and S. Arora; Methods of dealing with co-products of biofuels in life-cycle analysis and consequent results within the U.S. context. *Energy Policy*, 39,(10), 5726-5736. 2011.
27. DG Energy; The impact of land use change on greenhouse gas emissions from biofuels and bioliquids: Literature review. 2010.
28. Delucchi, M. A.; Important Issues in Lifecycle Analysis of CO₂-Equivalent Greenhouse-Gas. Measuring and Modeling the Lifecycle GHG Impacts of Transportation Fuels. U.C. Berkeley, CA; July 1, 2008

29. Wang, M.; Life cycle analysis practicality. Measuring and Modeling Lifecycle GHG Impacts of Transportation Fuels. U.C. Berkeley, CA; July 1, 2008
30. Crutzen, P.J., A.R. Mosier, K.A. Smith, and W. Winiwarter; N₂O Release from Agro-biofuel Production Negates Global Warming Reduction by Replacing Fossil Fuels. *Atmospheric Chemistry and Physics Discussions*, 7,(4), 11191-111205. 2007.
31. Erickson, B. and Biotechnology Industry Organization; Proposed Regulations to Implement the Low Carbon Fuel Standard. Comments of Biotechnology Industry Organization. To California EPA- ARB, 2009.
32. Mathews, J. and H. Tan; Biofuels and indirect land use change effects: the debate continues. *Biofuels Bioproducts & Biorefining*, 3,(3), 305-317. 2009.
33. Simmons, B.S., H.W. Blanch, and B.E. Dale; RE: Call for Third Party Analysis of Indirect Land Use Change and Indirect Effects in Support of the CA LCFS. 2009.
34. Zilberman, D., G. Hochman, and D. Rajagopal; Indirect Land Use: One Consideration Too Many in Biofuel Regulation. *Agriculture and Resources Economics*, 13,(4), 2010.
35. Liska, A.J. and R.K. Perrin; Indirect Land Use Emissions in the Life Cycle of Biofuels: Regulations vs. Science. *Biofuels Bioproducts & Biorefining*, 3,(3), 318-328. 2009.
36. Kim, S. and B. Dale; Indirect Land Use Change for Biofuels: Testing Predictions and Improving Analytical Methods. *Biomass and Bioenergy*, 35,(7), 3235-3240. 2011.
37. Matson, P.; Letter to CARB to include use of ILUC. Apr.2009
38. Grace, J.; Understanding and managing the global carbon cycle. *Journal of Ecology*, 92,(2), 189-202. 2004.
39. Brown, S and Masera, O.; Supplementary methods and good practice guides arising from the Kyoto Protocol, section 4.3 LULUCF projects. In: *Good Practice Guidance for Land Use, Land-Use Change and Forestry, Intergovernmental Panel on Climate Change National Greenhouse Gas Inventories Program*. Penman, J., Gytartsky, M., Hiraishi, T., Krug, T., Kruger, D., Pipatti, R., Buendia, L., Miwa, K., Ngara, T., Tanabe, K., and Wagner, F., Kanagawa: Institute for Global Environmental Strategies (IGES).: 4.89-4.120, 2003.
40. Dale, V.H., K.L. Kline, J. Wiens, and J. Fargione; Biofuels: Implications for Land Use and Biodiversity. *Biofuels and Sustainability Reports*, 2010.
41. Kim, H., S. Kim, and B.E. Dale; Biofuels, Land Use Change, and Greenhouse Gas Emissions: Some Unexplored Variables. *Environ.Sci.Technol.*, 43,(3), 961-967. 2009.
42. Post, W.M. and K.C. Kwon; Soil carbon sequestration and land-use change: processes and potential. *Global Change Biology*, 6,(3), 317-327. 2000.
43. DeLucia, E.H.; Biofuel Crops, Soil Carbon and Land Use Change. Presented at CRC Workshop on Life Cycle Analysis of Biofuels. Argonne, Ill. Oct. 2009. 2009.

44. Houghton, R. and J. Hackler; Emissions of carbon from land use change in sub-Saharan Africa. *Journal of Geophysical Research-Biogeosciences*, 111,(G02003), 1-12. 2006.
45. Wilhelm, W., J.M. Johnson, D.L. Karlen, and D.T. Lightle; Corn stover to sustain soil organic carbon further constrains Biomass supply. *Agronomy Journal*, 99,(6), 1665-1667. 2007.
46. Cruse, R. and C. Herndl; Balancing corn stover harvest for biofuels with soil and water conservation. *Journal of Soil and Water Conservation*, 64,(4), 286-291. 2009.
47. Guo, L.B. and R.M. Gifford; Soil carbon stocks and land use change: a meta analysis. *Global Change Biology*, 8, 345-360. 2002.
48. Gibbs, H.K., S. Brown, J.O. Niles, and J.A. Foley; Monitoring and estimating tropical forest carbon stocks: making REDD a reality. *Environmental Research Letters*, 2,(4), 045023- 2007.
49. Gnansounou, E., L. Panichelli, A. Dauriat, and J. Villegas; Accounting for indirect land-use changes in GHG balances of biofuels: Review of current approaches. Working Paper Ref: 437.101, 2008.
50. IPCC; *Good Practice Guidance for Land Use, Land Use Change and Forestry, Chapters 3 and 4*. Penman, J., Gytarsky, M, Hiraishi, T., Krug, T., Kruger, D., Pipatti, R., Buendia, L., Miwa, K., Ngara, T., Tanabe, K., and Wagner, F., 2003.
51. IPCC; IPCC 2000. Good Practice Guidance and Uncertainty Management in National Greenhouse Gas Inventories. 2000.
52. IPCC; IPCC (2006) Guidelines for National Greenhouse Gas Inventories. Vol. 4: Agriculture, Forestry, and Other Land Use. 2006.
53. IPCC; IPCC (2001). Climate Change 2001: The Scientific Basis. 2001.
54. IPCC; IPCC (2007). Climate Change 2007: The Physical Science Basis. Contribution of Working Group I to the Fourth Assessment Report of the IPCC. 2007.
55. Harris, N., S. Grimland, and S. Brown; Land Use Change and Emission Factors: Updates since the RFS Proposed Rule. Report Submitted to the EPA, 2009.
56. Kloverpris, J., H. Wenzel, and P.H. Nielsen; Life cycle inventory modeling of land use induced by crop consumption. Part 1: Conceptual analysis and methodological proposal. *International Journal of Life Cycle Assessment*, 12,(1), 13-21. 2008.
57. Taheripour, F., D. Birur, T.W. Hertel, and W.E. Tyner; Introducing Liquid Biofuels into the GTAP Data Base. GTAP Research Memorandum No. 11, 2008.
58. Gibbs, H.K., J. Sheehan, and R. Nelson; Land Cover Types Subworkgroup. Low Carbon Fuel Standard (LCFS) Indirect Land Use Change Expert Workgroup. A Report to the California Air Resources Board. 2010.
59. Roundtable on Sustainable Biofuels; Direct and Indirect Land Use Change: Expert Advisory Group and Working Group on GHGs. 2008.

60. Golub, A. A., Taheripour, F., and Tyner, W. E.; Calculation of Indirect Land Use Change (ILUC) Values for Low Carbon Fuel Standard (LCFS) Fuel Pathways. CARB LCFS Public Meeting. Sacramento, CA; Sept. 14, 2011
61. Beach, R. and B. McCarl; U.S. Agricultural and Forestry Impacts of the Energy Independence and Security Act: FASOM Results and Model Description. Final Report prepared for U.S. EPA, 2010.
62. Colorado State University; DAYCENT website. 2011. Retrieved from: <http://www.nrel.colostate.edu/projects/daycent/index.html>
63. Heath, L.S., R.A. Birdsey, and D.W. Williams; Methodology for estimating soil carbon for the forest carbon budget model of the United States, 2001. *Environmental Pollution*, 116, 373-380. 2002.
64. CARD Staff.; An Analysis of EPA Renewable Fuel Scenarios with the FAPRI-CARD International Models. Technical Report to EPA, 2009.
65. Houghton, R.A.; Aboveground forest biomass and the global carbon balance. *Global Change Biology*, 11,(6), 945-958. 2005.
66. Houghton, R.A.; The Annual Net Flux of Carbon to the Atmosphere from Changes in Land Use 1850-1990. *Tellus*, 51B, 298-313. 1999.
67. California Air Resources Board, Emission Factor Tables (GTAP, Woods Hole). 2009. Retrieved from: www.arb.ca.gov/fuels/lcfs/ef_tables.xls
68. Houghton, R.A. and J.L. Hackler; Carbon Flux to the Atmosphere from Land Use Changes: 1850-1990. ORNL/CDIAC-131 NPD-050/R1, 2001.
69. Schlesinger, W. H.; Changes in soil carbon storage and associated properties with disturbance and recovery. In: *The changing carbon cycle: a global analysis*. Trabalka, J. R. and Reichle, D. E., New York: Springer-Verlag.: 194-220, 1986.
70. Davidson, E.A. and A.L. Ackerman; Changes in soil carbon inventories following cultivation of perviously untilled soils. *Biogeochemistry*, 20, 161-193. 1993.
71. Detwiler, R.P.; Land use change and the global carbon cycle: the role of tropical soils. *Biogeochemistry*, 2, 67-93- 1986.
72. Murty, D.; Does Conversion of Forest to Agricultural Land Change Soil Carbon and Nitrogen? A Review of the Literature. *Global Change Biology*, 8, 105-123. 2002.
73. Winrock International, Harris, NL, Grimland, S., and Brown, S, Winrock Emission Factor Database. 2010. Retrieved from: www.regulations.gov EPA-HQ-OAR-2005-0161-3163
74. ICF International; Stochastic Analysis of Biofuel-Induced Land Use Change GHG Emissions Impacts. Submitted to US EPA, 2009.
75. ICF International, Stochastic Land Use Change Model Database. 2009. Retrieved from: www.regulations.gov EPA-HQ-OAR-2005-0161-3152

76. Curtis, J. and J. Duffy; California EPA Air Resources Board: Low Carbon Fuel Standard; Release of the Expert Workgroup Final Reports- ARB Staff Cover Report. 2011.
77. California EPA Air Resources Board Stationary Source Division; Staff Report: Initial Statement of Reasons Proposed Regulation to Implement the Low Carbon Fuel Standard Volume 1. 2009.
78. California EPA Air Resources Board Stationary Source Division; Staff Report: Initial Statement of Reasons Proposed Regulation to Implement the Low Carbon Fuel Standard Volume II Appendices. 2009.
79. Prabhu, A., C. Pham, A. Glabe, and J. Duffy; Detailed California-Modified GREET Pathway for Conversion of Midwest Soybeans to Biodiesel (Fatty Acid Methyl Esters-FAME). Version 3.0, 2009.
80. Prabhu, A., C. Pham, and A. Glabe; Detailed California-Modified GREET Pathway for Conversion of Midwest Soybeans to Renewable Diesel. Version 3.0, 2009.
81. Prabhu, A., C. Pham, A. Glabe, and J. Duffy; Detailed California-Modified GREET Pathway for Corn Ethanol Version 2.1. Draft - for Review, 2009.
82. Prabhu, A., C. Pham, and A. Glabe; Detailed California-Modified GREET Pathways for Brazilian Sugarcane Ethanol: Average Brazilian Ethanol, with Mechanized Harvesting and Electricity Co-product Credit, With Electricity Co-product Credit Version 2.3. Preliminary draft distributed for public comment, 2009.
83. California Air Resources Board; Attachment 2: Land Use Change Effects for Soy Biodiesel and Renewable Diesel. 2010.
84. Hertel, T.W., A.A. Golub, A.D. Jones, M. O'Hare, R. Plevin, and D.M. Kammen; Effects of US Maize Ethanol on Global Land Use and Greenhouse Gas Emissions: Estimating Market-mediated Responses. *BioScience*, 60,(3), 223-231. 2010.
85. CARB and Duffy, Jim; California Air Resources Board- Low Carbon Fuel Standard LUC Workshop. CARB LCFS Public Meeting. Sept. 14, 2011
86. Gibbs, H. and Yui, S.; Updating GTAP's Soil and Biomass Carbon Stock Estimates. CARB LCFS Public Meeting. Sept. 14, 2011
87. Plevin, R.; Updated ILUC Emission Factor. CARB LCFS Public Workshop. Sept. 14, 2011
88. Edwards, R., D. Mulligan, and D. Margaroni; Indirect Land Use Change from Increased Biofuels Demand. Comparison of Models and Results for Marginal Biofuels Production from Different Feedstocks. Final report of the contract n. 070307/2008/517067/3, 2010.
89. Blanco Fonseca, M., A. Burrell, H. Gay, M. Henseler, A. Kavallari, R. M'Barek, I. Perez-Dominguez, and A. Tonini; Impacts of the EU biofuel target on agricultural markets and land use: a comparative modelling assessment. EUR 24449 EN - 2010, 2011.

90. Dumortier, J., D.J. Hayes, M. Carriquiry, F. Dong, X. Du, A. Elobeid, J.F. Fabiosa, and S. Tokgoz; Sensitivity of Carbon Emission Estimates from Indirect Land-Use Change. Report No. 09-WP 493, 2009.
91. Tokgoz, S., A. Elobeid, J. Fabiosa, D.J. Hayes, B.A. Babcock, and T.H. Yu; Emerging Biofuels: Outlook of Effects on US Grain, Oilseed, and Livestock Markets. CARD Staff Report. 07-SR 101, 2007.
92. Taheripour, F., T.W. Hertel, W.E. Tyner, I.D. Bedoya, and J.A. Bittle; Biofuels and their By-Products: Global Economic and Environmental Implications. Final Report, 2010.
93. Harris, N., S. Grimland, and S. Brown; GHG Emission Factors for Different Land-Use Transitions in Selected Countries of the World. Report Submitted to the EPA. 2008.
94. DeCastro, E.A. and J.B. Kauffman; A vegetation gradient of above ground biomass, root and consumption by fire. *Journal of Tropical Ecology*, 14,(3), 263-283. 1998.
95. Martin, J., Klooverpris, J. H., Kline, K., Mueller, S., and O'Hare, M.; White Paper: Time Accounting Subgroup. Seventh Low Carbon Fuel Standard Expert Workgroup. Sacramento, CA and Davis, CA; Oct. 14, 2010
96. Delucchi, M.; A Conceptual Framework for Estimating Bioenergy-Related Land-Use Change and Its Impacts over Time. UCD-ITS-RR-09-45, 2009.
97. Martin, J. and E. Hopson; Memo to EPA from Union of Concerned Scientists Re: Treatment of Time in Life Cycle Accounting. 2009.
98. Schneider, S. H., Semenov, S., Patwardhan, A., Burton, I., Magadza, C. H. D., Oppenheimer, M., Pittock, A. B., Rahman, A., Smith, J. B., Suarez, A., and Yamin, F.; Assessing key vulnerabilities and the risk from climate change. In: *Climate Change 2007: Impacts, Adaptation and Vulnerability. Contribution of Working Group II to the Fourth Assessment Report of the IPCC*. Parry, M. L., Canziani, O. F., Palutikof, J. P., van der Linden, P. J., and Hanson, C. E., Cambridge, UK: Cambridge University Press.: 779-810, 2007.
99. Marshall, L. and A. Kelly; The Time Value of Carbon and Carbon Storage: Clarifying the Terms and the Policy Implications of the Debate. WRI Working Paper, 2010.
100. Marshall, L.; Biofuels and the Time Value of Carbon: Recommendations for GHG Accounting Protocols. *WRI Working Paper*, 2009.
101. Office of Management and Budget; Circular A-4. Sept.2003
102. Federal Register Volume 74, Number 99 Rules and Regulations. Section VI: Impacts of the Program on Greenhouse Gas Emissions, 2009.
103. Guo, J., C.J. Hepburn, R.S.J. Tol, and D. Anthoff; Discounting and the Social Cost of Carbon: A Closer Look at Uncertainty. *Environmental Science & Policy* 2, 9, 205-216. 2006.
104. Forster, P., Ramaswamy, V., Artaxo, P., Berntsen, T., Betts, R., Fahey, D. W., Haywood, J., Lean, J., Lowe, D. C., Myhre, G., Nganga, J., Prinn, R., Raga.G., Schulz, M., and Van Dorland, R.; Changes in

- Atmospheric Constituents and in Radiative Forcing. In: *Climate Change 2007: The Physical Science Basis. Contribution of Working Group I to the Fourth Assessment Report of the Intergovernmental Panel on Climate Change*. Solomon, S., Qin, D., Manning, M., Chen, Z., Marquis, M., Averyt, K. B., Tignor, M., and Miller, H. L., Cambridge, United Kingdom and New York, NY, USA: Cambridge University Press.: 129, 2007.
105. Hopson, E., Jones, A., Kendall, A., Martin, J., O'Hare, M., and Plevin, R., Biofuel Time-Integrated Model of Emissions (BTIME). 2009. Retrieved from:
 106. Kendall, A., B. Chang, and B. Sharpe; Accounting for Time-Dependent Effects in Biofuels Life Cycle Greenhouse Gas Emissions Calculations. *Environ.Sci.Technol.*, 43, 7142-7147. 2009.
 107. Kloverpris, J.H. and K. Baltzer; Life Cycle Inventory Modelling of Land Use Induced by Crop Consumption Part 2: Example of Wheat Consumption in Brazil, China, Denmark and the USA. *International Journal of Life Cycle Assessment*, 15, 90-103. 2010.
 108. Ackerman, F. and E.A. Stanton; The Social Cost of Carbon: A Report for the Economics for Equity and the Environmental Network. 2010.
 109. Crutzen, P. J.; Atmospheric chemical processes of the oxides of nitrogen, including nitrous oxide. In: *Denitrification, Nitrification and Atmospheric N2O*. Delwiche, C. C., New York: John Wiley and Sons.: 17-44, 1981.
 110. Ravishankara, A.R., J.S. Daniel, and R.W. Portmann; Nitrous Oxide (N2O): The Dominant Ozone-Depleting Substance Emitted in the 21st Century. *Science*, 326,(5949), 123-125. 2009.
 111. IPCC; IPCC (1996). *Climate Change 1995: The Science of Climate Change*. 1996.
 112. U.S.EPA; Global Anthropogenic Non-CO2 Greenhouse Gas Emissions: 1990-2020. 430-R-06-003, 2006.
 113. Dalal, R.C., W. Wang, G.P. Robertson, and W.J. Parton; Nitrous Oxide Emission from Australian Agricultural Lands and Mitigation Options: A Review. *Australian Journal of Soil Research*, 41, 165-195. 2003.
 114. Del Grosso, S.J., M. Walsh, J. Duffield, L. Heath, S. Ogle, J. Smith, and T. Wirth; U.S. Agriculture and Forestry Greenhouse Gas Inventory: 1990-2005. Technical Bulletin No. 1921, 2008.
 115. Isermann, K.; Agriculture's Share in the Emission of Trace Gases Affecting the Climate and Some Cause-Oriented Proposals for Sufficiently Reducing this Share. *Environmental Pollution*, 83, 95-111. 1994.
 116. Kroeze, C., A. Mosier, and L. Bouwman; Closing the Global N2O Budget: A Retrospective Analysis 1500 - 1994. *Global Biogeochemical Cycles*, 13,(1), 1-8. 1999.
 117. Delwiche, C. C.; The nitrogen cycle and nitrous oxide. In: *Denitrification, Nitrification, and Atmospheric Nitrous Oxide*. Delwiche, C. C., New York: Wiley.: 1-15, 1981.

118. Oonk, H. and Kroeze, C.; Nitrous Oxide (N₂O), Emissions and Control. In: *Encyclopedia of environmental analysis and remediation*. Meyers, R. A., London: John Wiley and Sons.: 3035-3053, 1998.
119. Firestone, M. K.; Soil nitrogen budgets. In: *Nitrogen in Agricultural Soils*. Stevenson, F. J., Madison, WI: Crop Science Society of America.: 289-326, 1982.
120. Firestone, M. K. and Davidson, E. A.; Microbiological basis of NO and N₂O production and consumption in soil. In: *Trace Gas Exchange between Terrestrial Ecosystems and the Atmosphere*. Andreae, M. D. and Schimel, D. S, Berlin: Wiley.: 7-22, 1989.
121. Conrad, R.; Soil Microorganisms as Controllers of Atmospheric Trace Gases (H₂, CO, CH₄, and NO). *Microbiological Review*, 60, 609-640. 1996.
122. Bremner, J. M. and Blackmer, A. M.; Terrestrial nitrification as a source of atmospheric nitrous oxide. In: *Denitrification, Nitrification, and Atmospheric Nitrous Oxide*. Delwiche, C. C., New York: Wiley.: 151-170, 1981.
123. Paul, E. A. and Clark, F. E.; Ammonification and nitrification. In: *Soil Microbiology and Biochemistry*. Paul, E. A. and Clark, F. E., Academic Press.: 181-197, 1996.
124. Robertson, G. P. and Groffman, P. M.; Nitrogen transformation. In: *Soil Microbiology, Biochemistry, and Ecology*. Paul, E. A., New York: Springer.: 341-364, 2007.
125. Norton, J. M.; Nitrification in agricultural soils. In: *Nitrogen in Agricultural Systems. Agronomy Monograph 49*. Schepers, J. S. and Raun, W. R., Madison, WI: American Society of Agronomy, Crop Science Society of America.: 173-199, 2008.
126. Snyder, C.S., T.W. Bruulsema, T.L. Jensen, and P.E. Fixen; Review of Greenhouse Gas Emissions from Crop Production Systems and Fertilizer Management Effects. *Agriculture Ecosystems & Environment*, 133, 247-266. 2009.
127. Payne, W. J.; The status of nitric oxide and nitrous oxide as intermediates in denitrification. In: *Denitrification, Nitrification, and Atmospheric Nitrous Oxide*. Delwiche, C. C., New York: Wiley.: 85-103, 1981.
128. Paul, E. A. and Clark, F. E.; The fate of nitrate. In: *Soil Microbiology and Biochemistry*. Paul, E. A. and Clark, F. E., Academic Press.: 199-214, 1996.
129. IPCC; IPCC Guidelines for National Greenhouse Gas Inventories. 1995.
130. Houghton, J.T. and B.A. Callander; Climate Change (1992). Supplementary Report to the IPCC Scientific Assessment Published for the IPCC. 1992.
131. Mosier, A.R., J.M. Duxbury, J.R. Freney, O. Heinemeyer, and K. Minami; Nitrous oxide emissions from agricultural fields: Assessment, measurement and mitigation. *Plant and Soil*, 181,(1), 95-108. 1996.

132. Mosier, A.R.; Nitrous-Oxide Emissions from Agricultural Soils. *Fertilizer Research*, 37,(3), 191-200. 1994.
133. Cole, V., Cerri, C., Minami, K., Mosier, A., Rosenberg, N., and Sauerbeck, D.; Agricultural Options for Mitigation of Greenhouse Gas Emissions. In: *Climate Change 1995. Impacts, Adaptations and Mitigation of Climate Change: Scientific-Technical Analyses*. Watson, R. T., Zinyowera, M. C., and Moss, R. H., Cambridge University Press.: 745-771, 1996.
134. Bouwman, A.F.; Direct emission of nitrous oxide from agricultural soils. *Nutrient Cycling in Agroecosystems*, 46,(1), 53-70. 1996.
135. Mosier, A., C. Kroeze, C. Nevison, O. Oenema, S. Seitzinger, and O. van Cleemput; Closing the Global N₂O Budget: Nitrous Oxide Emissions Through the Agricultural Nitrogen Cycle. *Nutrient Cycling in Agroecosystems*, 52, 225-248. 1998.
136. Mosier, A., C. Kroeze, C. Nevison, O. Oenema, S. Seitzinger, and O. van Cleemput; An Overview of the Revised 1996 IPCC Guidelines for National Greenhouse Gas Inventory Methodology for Nitrous Oxide from Agriculture. *Environmental Science & Policy* 2, 325-333. 1999.
137. IPCC; IPCC Guidelines for National Greenhouse Gas Inventories. Chapter 4. Agriculture: nitrous oxide from agricultural soils and manure management. 1997.
138. Koops, J.G., M.L. vanBeusichem, and O. Oenema; Nitrogen loss from grassland on peat soils through nitrous oxide production. *Plant and Soil*, 188,(1), 119-130. 1997.
139. Koops, J.G., O. Oenema, and M.L. vanBeusichem; Denitrification in the top and sub soil of grassland on peat soils. *Plant and Soil*, 184,(1), 1-10. 1996.
140. Jarvis, S.C. and B.F. Pain; Greenhouse-Gas Emissions from Intensive Livestock Systems - Their Estimation and Technologies for Reduction. *Climatic Change*, 27,(1), 27-38. 1994.
141. Flessa, H., P. Dorsch, F. Beese, H. Konig, and A.F. Bouwman; Influence of cattle wastes on nitrous oxide and methane fluxes in pasture land. *Journal of Environmental Quality*, 25,(6), 1366-1370. 1996.
142. Kaspar, H.F. and J.M. Tiedje; Dissimilatory Reduction of Nitrate and Nitrite in the Bovine Rumen - Nitrous-Oxide Production and Effect of Acetylene. *Applied and Environmental Microbiology*, 41,(3), 705-709. 1981.
143. Bowden, R.D., J.M. Melillo, P.A. Steudler, and J.D. Aber; Effects of Nitrogen Additions on Annual Nitrous-Oxide Fluxes from Temperate Forest Soils in the Northeastern United-States. *Journal of Geophysical Research-Atmospheres*, 96,(D5), 9321-9328. 1991.
144. Meisinger, J. J and Randall, G. W.; Estimating nitrogen budgets for soil-crop systems. In: *Managing Nitrogen for Groundwater Quality and Farm Profitability*. Follett, R. F., Keeney, D. R., and Cruse, R. M., Madison, WI: Soil Science Society of America.: 85-124, 1991.

145. Kroeze, C. and S.P. Seitzinger; Nitrogen inputs to rivers, estuaries and continental shelves and related nitrous oxide emissions in 1990 and 2050: a global model. *Nutrient Cycling in Agroecosystems*, 52,(2-3), 195-212. 1998.
146. Seitzinger, S.P. and C. Kroeze; Global distribution of nitrous oxide production and N inputs in freshwater and coastal marine ecosystems. *Global Biogeochemical Cycles*, 12,(1), 93-113. 1998.
147. Van Aardenne, J.A.; Uncertainty and sensitivity analysis of an IPCC/OECD model for estimating N₂O emissions from agricultural soils. 1996.
148. Wagner-Riddle, C. and G.W. Thurtell; Nitrous Oxide Emissions from Agricultural Fields During Winter and Spring Thaw as Affected by Management Practices. *Nutrient Cycling in Agroecosystems*, 52, 151-163. 1998.
149. van Bochove, E., H.G. Jones, P. Pelletier, and D. Prevoist; Emission of N₂O from agricultural soil under snow cover. A significant part of N budget. *Hydrological Processes*, 10, 1545-1549. 1996.
150. Flessa, H., P. Dorsch, and F. Beese; Seasonal-Variation of N₂O and CH₄ Fluxes in Differently Managed Arable Soils in Southern Germany. *Journal of Geophysical Research-Atmospheres*, 100,(D11), 23115-23124. 1995.
151. Bouwman, A.F., L.J.M. Boumans, and N.H. Batjes; Modeling global annual N₂O and NO emissions from fertilized fields. *Global Biogeochemical Cycles*, 16,(4), 1080-1090. 2002.
152. Bouwman, A.F., L.J.M. Boumans, and N.H. Batjes; Emissions of N₂O and NO from fertilized fields: Summary of available measurement data. *Global Biogeochemical Cycles*, 16,(4), 6-1-6-13. 2002.
153. Stehfest, E. and L. Bouwman; N₂O and NO emission from agricultural fields and soils under natural vegetation: summarizing available measurement data and modeling of global annual emissions. *Nutrient Cycling in Agroecosystems*, 74,(3), 207-228. 2006.
154. Novoa, R.S. and H.R. Tejeda; Evaluation of the N₂O emissions from N in plant residues as affected by environmental and management factors. *Nutrient Cycling in Agroecosystems*, 75,(1-3), 29-46. 2006.
155. Laegreid, M. and A.H. Aastveit; Nitrous Oxide Emissions from Field-applied Fertilizers. *Plant Production*, 81, 122-134. 2002.
156. Rochette, P. and H.H. Janzen; Towards a Revised Coefficient for Estimating N₂O Emissions from Legumes. *Nutrient Cycling in Agroecosystems*, 73, 171-179. 2005.
157. Smith, K.A. and F. Conen; Impacts of Land Management on Fluxes of Trace Greenhouse Gases. *Soil Use and Management*, 20, 255-263. 2004.
158. ButterbachBahl, K., R. Gasche, L. Breuer, and H. Papen; Fluxes of NO and N₂O from temperate forest soils: impact of forest type, N deposition and of liming on the NO and N₂O emissions. *Nutrient Cycling in Agroecosystems*, 48,(1-2), 79-90. 1997.

159. Brumme, R., W. Borken, and S. Finke; Hierarchical control on nitrous oxide emission in forest ecosystems. *Global Biogeochemical Cycles*, 13,(4), 1137-1148. 1999.
160. van der Gon, H.D. and A. Bleeker; Indirect N₂O emission due to atmospheric N deposition for the Netherlands. *Atmos. Environ.*, 39,(32), 5827-5838. 2005.
161. Reay, D.S., A.C. Edwards, and K.A. Smith; Importance of indirect nitrous oxide emissions at the field, farm and catchment scale. *Agriculture Ecosystems & Environment*, 133,(3-4), 163-169. 2009.
162. Rochette, P., D.E. Worth, R.L. Lemke, B.G. McConkey, D.J. Pennock, C. Wagner-Riddle, and R.L. Desjardins; Estimation of N₂O emissions from agricultural soils in Canada. I. Development of a country-specific methodology. *Canadian Journal of Soil Science*, 88,(5), 641-654. 2008.
163. Rochette, P., D.E. Worth, E.C. Huffman, J.A. Brierley, B.G. McConkey, J. Yang, J.J. Hutchinson, R.L. Desjardins, R. Lemke, and S. Gameda; Estimation of N₂O Emissions from Agricultural Soils In Canada. II. 1990-2005 Inventory. *Canadian Journal of Soil Science*, 88,(5), 655-669. 2008.
164. Smith, K.A. and K.E. Dobbie; The Impact of Sampling Frequency and Sampling Times on Chamber-Based Measurements of N₂O Emissions from Fertilized Soils. *Global Change Biology*, 7, 933-945. 2001.
165. Parkin, T.B.; Effect of Sampling Frequency on Estimates of Cumulative Nitrous Oxide Emissions. *Journal of Environmental Quality*, 37, 1390-1395. 2008.
166. Laville, P., S. Lehuger, B. Loubet, F. Chaumartin, and P. Cellier; Effect of Management, Climate and Soil Conditions on N₂O and NO Emissions from an Arable Crop Rotation Using High Temporal Resolution Measurements. *Agricultural and Forest Meteorology*, 151, 228-240. 2011.
167. Ambus, P. and S. Christensen; Measurement of N₂O Emission from a Fertilized Grassland: An Analysis of Spatial Variability. *Journal of Geophysical Research*, 99,(D8), 16549-16555. 1994.
168. Jiang, J., Z. Hu, W. Sun, and Y. Huang; Nitrous Oxide Emissions from Chinese Cropland Fertilized with a Range of Slow-release Nitrogen Compounds. *Agriculture Ecosystems & Environment*, 135, 216-225. 2010.
169. Venterea, R.T., M.S. Dolan, and T.E. Ochsner; Urea Decreases Nitrous Oxide Emissions Compared with Anhydrous Ammonia in a Minnesota Corn Cropping System. *Soil Science Society of America Journal*, 74,(2), 407-418. 2010.
170. Lovanh, N., J. Warren, and K. Sistani; Determination of Ammonia and Greenhouse Gas Emissions from Land Application of Swine Slurry: A Comparison of Three Application Methods. *Bioresource Technology*, 101, 1662-1667. 2010.
171. Agnew, J., C. Lague, J. Schoenau, and R. Farrell; Greenhouse Gas Emissions Measured 24 Hours After Surface and Subsurface Application of Different Manure Types. *Transactions of the ASABE*, 53,(5), 1689-1701. 2010.

172. Vilain, G., J. Garnier, G. Tallec, and P. Cellier; Effect of Slope Position and Land Use on Nitrous Oxide (N₂O) Emissions (Seine Basin, France). *Agricultural and Forest Meteorology*, 150, 1192-1202. 2010.
173. Bessou, C., B. Mary, J. Leonard, M. Roussel, E. Grehan, and B. Gabrielle; Modelling Soil Compaction Impacts on Nitrous Oxide Emissions in Arable Fields. *European Journal of Soil Science*, 61, 348-363. 2010.
174. Johnson, J.M.F., D. Archer, and N. Barbour; Greenhouse Gas Emission from Contrasting Management Scenarios in the Northern Corn Belt. *Soil Science Society of America Journal*, 74,(2), 396-406. 2010.
175. Wagner-Riddle, C., Q.C. Hu, E. van Bochove, and S. Jayasundara; Linking Nitrous Oxide Flux During Spring Thaw to Nitrate Denitrification in the Soil Profile. *Soil Science Society of America Journal*, 72,(4), 908-916. 2008.
176. Hyvonen, N.P., J.T. Huttunen, N.J. Shurpali, N.M. Tavi, M.E. Repo, and P.J. Martikainen; Fluxes of Nitrous Oxide and Methane on an Abandoned Peat Extraction Site: Effect of Reed Canary Grass Cultivation. *Bioresource Technology*, 100, 4723-4730. 2009.
177. van Beek, C.L., M. Pleijter, and P.J. Kuikman; Nitrous Oxide Emissions from Fertilized and Unfertilized Grasslands on Peat Soil. *Nutrient Cycling in Agroecosystems*, 89,(3), 453-461. 2011.
178. Chirinda, N., M.S. Carter, K.R. Albert, P. Ambus, J.E. Olesen, J.R. Porter, and S.O. Petersen; Emissions of Nitrous Oxide from Arable Organic and Conventional Cropping Systems on Two Soil Types. *Agriculture Ecosystems & Environment*, 136, 199-208. 2010.
179. Barton, L., D.V. Murphy, R. Kiese, and K. Butterbach-Bahl; Soil Nitrous Oxide and Methane Fluxes are Low from a Bioenergy Crop (Canola) Grown in a Semi-arid Climate. *Global Change Biology Bioenergy*, 2, 1-15. 2010.
180. Yeh, S., H.K. Gibbs, S. Mueller, R. Nelson, and D. O'Connor; Low Carbon Fuel Standard (LCFS) Indirect Land Use Change. Carbon Emission Factors Subworkgroup. A Report to the California Air Resources Board. 2010.
181. Mortimer, N.D., A. Ashley, A. Evans, A.J. Hunter, and V.L. Shaw; Support for the Review of the Indirect Effects of Biofuels. Final Version, 2008.
182. Destouni, G. and A. Darracq; Nutrient cycling and N₂O emissions in a changing climate: the subsurface water system role. *Environmental Research Letters*, 4,(3), 2009.
183. Del Grosso, S.J., A.R. Mosier, W.J. Parton, and D.S. Ojima; DAYCENT Model Analysis of Past and Contemporary Soil N₂O and Net Greenhouse Gas Flux for Major Crops in the USA. *Soil & Tillage Research*, 83, 9-24. 2005.
184. Del Grosso, S. J., Parton, W. J., Mosier, A. R., Hartman, M. D., Brenner, J., Ojima, D. S., and Schimel, D. S.; Simulated Interaction of Carbon Dynamics and Nitrogen Trace Gas Fluxes Using the DAYCENT Model. In: *Modeling Carbon and Nitrogen Dynamics for Soil Management*. Shaffer, M. J., Ma, L., and Hansen, S., Boca Raton: Lewis Publishers.: 303-332, 2001.

185. Follett, R. F.; Chapter 2: Nitrogen transformation and transport processes. In: *Nitrogen in the Environment: Sources, Problems and Management.*: 17-44, 2001.
186. Bakken, L.R. and M.A. Bleken; Temporal aspects of N-enrichment and emission of N₂O to the atmosphere. *Nutrient Cycling in Agroecosystems*, 52,(2-3), 107-121. 1998.
187. Olander, L.P., K. Haugen-Kozyra, S. Del Grosso, C. Izaurralde, D. Malin, K. Paustian, and W. Salas; Using Biogeochemical Process Models to Quantify Greenhouse Gas Mitigation from Agricultural Management Projects. Technical Working Group on Agricultural Greenhouse Gases (T-AGG) Supplemental Report Report NI R 11-03, 2011.
188. Hergoualc'h, K., J.M. Harmand, P. Cannavo, U. Skiba, R. Oliver, and C. Henault; The Utility of Process-based Models for Simulating N₂O Emissions from Soils: A Case Study Based on Costa Rican Coffee Plantations. *Soil Biology & Biochemistry*, 41, 2343-2355. 2009.
189. Metay, A., L. Chapuis-Lardy, A. Findeling, R. Oliver, J.A.A. Moreira, and C. Feller; Simulating N₂O Fluxes from a Brazilian Cropped Soil with Contrasted Tillage Practices. *Agriculture Ecosystems & Environment*, 140, 255-263. 2011.
190. Henault, C., F. Bizouard, P. Laville, B. Gabrielle, B. Nicoullaud, J.C. Germon, and P. Cellier; Predicting in situ Soil N₂O Emission Using NOE Algorithm and Soil Database. *Global Change Biology*, 11, 115-127. 2005.
191. Stolk, P.C., R.F.A. Hendriks, C.M.J. Jacobs, J. Duyzer, E.J. Moors, J.W. van Groenigen, P.S. Kroon, A.P. Schrier-Uijl, E.M. Veenendaal, and P. Kabat; Simulation of Daily Nitrous Oxide Emissions from Managed Peat Soils. *Vadose Zone Journal*, 10, 156-168. 2011.
192. Chen, D.L., Y. Li, P. Grace, and A.R. Mosier; N(2)O emissions from agricultural lands: a synthesis of simulation approaches. *Plant and Soil*, 309,(1-2), 169-189. 2008.
193. Parton, W. J., Ojima, D. S., Cole, C. V., and Schimel, D. S; A general model for soil organic matter dynamics: sensitivity to litter chemistry, texture and management. In: *Quantitative Modeling of Soil Forming Processes*. Bryant, R. B. and Arnold, R. W., Madison, WI: Soil Sci. Soc. Am.: 147-167, 1994.
194. Parton, W.J. and P.E. Rasmussen; Long-Term Effects of Crop Management in Wheat-Fallow .2. Century Model Simulations. *Soil Science Society of America Journal*, 58,(2), 530-536. 1994.
195. Parton, W.J., M. Hartman, D. Ojima, and D. Schimel; DAYCENT and its land surface submodel: description and testing. *Global and Planetary Change*, 19,(1-4), 35-48. 1998.
196. Kelly, R.H., W.J. Parton, M.D. Hartman, L.K. Stretch, D.S. Ojima, and D.S. Schimel; Intra-annual and interannual variability of ecosystem processes in shortgrass steppe. *Journal of Geophysical Research-Atmospheres*, 105,(D15), 20093-20100. 2000.
197. Parton, W.J., E.A. Holland, S.J. Del Grosso, M.D. Hartman, R.E. Martin, A.R. Mosier, D.S. Ojima, and D.S. Schimel; Generalized model for NO(x) and N(2)O emissions from soils. *Journal of Geophysical Research-Atmospheres*, 106,(D15), 17403-17419. 2001.

198. Del Grosso, S. J., Parton, W. J., Mosier, A. R., Ojima, D. S., and Hartman, M. D.; Interaction of Soil Carbon Sequestration and N₂O Flux with Different Land Use Practices. In: *Non-CO₂ Greenhouse Gases: Scientific Understanding, Control and Implementation*. van Ham, J., Kluwer Academic.: 303-311, 2000.
199. Parton, W.J., A.R. Mosier, D.S. Ojima, D.W. Valentine, D.S. Schimel, K. Weier, and A.E. Kulmala; Generalized model for N₂ and N₂O production from nitrification and denitrification. *Global Biogeochemical Cycles*, 10,(3), 401-412. 1996.
200. Yienger, J.J. and H. Levy; Empirical-Model of Global Soil-Biogenic NO_x Emissions. *Journal of Geophysical Research-Atmospheres*, 100,(D6), 11447-11464. 1995.
201. Frohling, S.E., A.R. Mosier, D.S. Ojima, C. Li, W.J. Parton, C.S. Potter, E. Priesack, R. Stenger, C. Haberbosch, P. Dorsch, H. Flessa, and K.A. Smith; Comparison of N₂O emissions from soils at three temperate agricultural sites: simulations of year-round measurements by four models. *Nutrient Cycling in Agroecosystems*, 52,(2-3), 77-105. 1998.
202. Mosier, A.R., W.D. Guenzi, and E.E. Schweizer; Soil Losses of Dinitrogen and Nitrous-Oxide from Irrigated Crops in Northeastern Colorado. *Soil Science Society of America Journal*, 50,(2), 344-348. 1986.
203. Mosier, A.R., W.J. Parton, D.W. Valentine, D.S. Ojima, D.S. Schimel, and J.A. Delgado; CH₄ and N₂O fluxes in the Colorado shortgrass steppe .1. Impact of landscape and nitrogen addition. *Global Biogeochemical Cycles*, 10,(3), 387-399. 1996.
204. Del Grosso, S.J., A.D. Halvorson, and W.J. Parton; Testing DAYCENT Model Simulations of Corn Yields and Nitrous Oxide Emissions in Irrigated Tillage Systems in Colorado. *Journal of Environmental Quality*, 37, 1383-1389. 2008.
205. Jarecki, M.K., T.B. Parkin, A.S.K. Chan, J.L. Hatfield, and R. Jones; Comparison of DAYCENT-simulated and Measured Nitrous Oxide Emissions from a Corn Field. *Journal of Environmental Quality*, 37,(5), 1685-1690. 2008.
206. U.S.EPA; Global Mitigation of Non-CO₂ Greenhouse Gases. EPA 430-R-06-005, 2006.
207. Soil Survey Staff-Natural Resources Conservation Service; State Soil Geographic (STATSGO) Database for State. 2005.
208. McCarl, B.A., C.C. Chang, J.D. Atwood, and W.I. Nayda; Documentation of ASM: The U.S. Agricultural Sector Model. Technical Report TR-93, 1993.
209. USDA National Agricultural Statistics Service; Crop Production 2009 Summary. 2010.
210. Delgado, J.A., S.J. Del Grosso, and S.M. Ogle; N-15 Isotopic Crop Residue Cycling Studies and Modeling Suggest that IPCC Methodologies to Assess Residue Contributions to N₂O-N Emissions Should be Reevaluated. *Nutrient Cycling in Agroecosystems*, 86, 383-390. 2010.
211. Huo, H., M. Wang, C. Bloyd, and V. Putsche; Life-Cycle Assessment of Energy and Greenhouse Gas Effects of Soybean-Derived Biodiesel and Renewable Fuels. ANL/ESD/08-2, 2008.

212. Ogle, S., Del Grosso, S., Adler, P. R., and Parton, W.; Soil Nitrous Oxide Emissions with Crop Production for Biofuel: Implications for Greenhouse Gas Mitigation. *The Lifecycle Carbon Footprint of Biofuels*, 11-18. Presented at Biofuels, Food and Feed Tradeoffs. Miami Beach, FL; Jan. 29, 2008
213. University of New Hampshire, DeNitrification- DeComposition (DNDC) Model. 2003. Retrieved from: www.dndc.sr.unh.edu
214. Intelligent Energy Europe, Biograce- Harmonized Calculations of Biofuel Greenhouse Gas Emissions in Europe. 2010. Retrieved from: www.biograce.net
215. European Union; Directive 2009/28/EC of the European Parliament and of the Council of 23 April 2009 on the promotion of the use of energy from renewable sources and amending and subsequently repealing Directives 2001/77/EC and 2003/30/EC. *Official Journal of the European Union*, 5.06.2009, 2009.
216. Adler, P.R., S.J.D. Grosso, and W.J. Parton; Life-Cycle Assessment of Net Greenhouse-gas Flux for Bioenergy Cropping Systems. *Ecological Applications*, 17,(3), 675-691. 2007.
217. Reijnders, L. and M.A.J. Huijbregts; Biogenic greenhouse gas emissions linked to the life cycles of biodiesel derived from European rapeseed and Brazilian soybeans. *Journal of Cleaner Production*, 16, 1943-1948. 2008.
218. Davis, S.C., W.J. Parton, F.G. Dohleman, C.M. Smith, S. Del Grosso, A.D. Kent, and E.H. DeLucia; Comparative Biogeochemical Cycles of Bioenergy Crops Reveal Nitrogen-Fixation and Low Greenhouse Gas Emissions in a *Miscanthus x giganteus* Agro-Ecosystem. *Ecosystems*, 13, 144-156. 2010.
219. Smeets, E.M.W., L.F. Bouwman, E. Stehfest, D.P. van Vuuren, and A. Posthuma; Contribution of N₂O to the Greenhouse Gas Balance of First-generation Biofuels. *Global Change Biology*, 15, 1-23. 2009.
220. McSwiney, C.P. and G.P. Robertson; Nonlinear Response of N₂O Flux to Incremental Fertilizer Addition in a Continuous Maize (*Zea mays* L.) Cropping System. *Global Change Biology*, 11, 1712-1719. 2005.
221. DeAngelo, B.J., F.C. de la Chesnaye, R.H. Beach, A. Sommer, and B.C. Murray; Methane and Nitrous Oxide Mitigation in Agriculture. *Energy Journal*,(Special Issue #3), 89-108. 2006.
222. Drury, C.F., X.M. Yang, W.D. Reynolds, and N.B. McLaughlin; Nitrous Oxide and Carbon Dioxide Emissions from Monoculture and Rotational Cropping of Corn, Soybean and Winter Wheat. *Canadian Journal of Soil Science*, 88, 163-174. 2008.
223. Omonode, R.A., D.R. Smith, A. Gal, and T.J. Vyn; Soil Nitrous Oxide Emissions in Corn following Three Decades of Tillage and Rotation Treatments. *Soil Science Society of America Journal*, 75,(1), 152-163. 2011.
224. McTaggart, I.P., H. Clayton, J. Parker, L. Swan, and K.A. Smith; Nitrous oxide emissions from grassland and spring barley, following N fertiliser application with and without nitrification inhibitors. *Biology and Fertility of Soils*, 25,(3), 261-268. 1997.

225. Weiske, A., G. Benckiser, T. Herbert, and J.C.G. Ottow; Influence of the nitrification inhibitor 3,4-dimethylpyrazole phosphate (DMPP) in comparison to dicyandiamide (DCD) on nitrous oxide emissions, carbon dioxide fluxes and methane oxidation during 3 years of repeated application in field experiments. *Biology and Fertility of Soils*, 34,(2), 109-117. 2001.
226. Weiske, A., G. Benckiser, and J.C.G. Ottow; Effect of the new nitrification inhibitor DMPP in comparison to DCD on nitrous oxide (N₂O) emissions and methane (CH₄) oxidation during 3 years of repeated applications in field experiments. *Nutrient Cycling in Agroecosystems*, 60,(1-3), 57-64. 2001.
227. MacKenzie, A.F., M.X. Fan, and F. Cadrin; Nitrous oxide emission as affected by tillage, corn-soybean-alfalfa rotations and nitrogen fertilization. *Canadian Journal of Soil Science*, 77,(2), 145-152. 1997.
228. Ball, B.C., A. Scott, and J.P. Parker; Field N₂O, CO₂ and CH₄ fluxes in relation to tillage, compaction and soil quality in Scotland. *Soil & Tillage Research*, 53,(1), 29-39. 1999.
229. Hellebrand, H.J., V. Scholz, and J. Kern; Fertiliser induced nitrous oxide emissions during energy crop cultivation on loamy sand soils. *Atmos. Environ.*, 42,(36), 8403-8411. 2008.
230. Six, J., S.M. Ogle, F.J. Breidt, R.T. Conant, A.R. Mosiers, and K. Paustian; The Potential to Mitigate Global Warming with No-tillage Management is Only Realized When Practised in the Long Term. *Global Change Biology*, 10, 155-160. 2004.
231. Van Zwieten, L., Singh, B., Joseph, S., Kimber, S., Cowie, A., and Chan, K. Y.; Biochar and Emissions of Non-CO₂ Greenhouse Gases from Soil. In: *Biochar for Environmental Management - Science and Technology*. Lehmann, J and Joseph, S., Sterling, VA: Earthscan.: 227-249, 2009.
232. Richardson, D., H. Felgate, N. Watmough, A. Thomson, and E. Baggs; Mitigating Release of the Potent Greenhouse Gas N₂O from the Nitrogen Cycle - Could Enzymic Regulation Hold the Key? *Trends in Biotechnology*, 27,(7), 388-397. 2009.
233. Smith, P., D. Martino, Z. Cai, D. Gwary, H. Janzen, P. Kumar, B. McCarl, S. Ogle, F. O'Mara, C. Rice, B. Scholes, and O. Sirotenko; Agriculture. In *Climate Change 2007; Mitigation. Contribution of Working Group III to the Fourth Assessment Report of the IPCC*. 2007.
234. Eagle, A.J., L.R. Henry, L.P. Olander, K. Haugen-Kozyra, N. Millar, and G.P. Robertson; Greenhouse Gas Mitigation Potential of Agricultural Land Management in the United States. A Synthesis of the Literature. *Technical Working Group on Agricultural Greenhouse Gases (T-AGG) Report*, 2011.

A. APPENDIX A: REGION CORRELATION FOR WINROCK, FAPRI AND WOOD'S HOLE

Winrock Country	Winrock- Admin Unit	Corresponding FAPRI Region	Corresponding Woods Hole Region
Afghanistan		Other Asia	N. Africa/ Middle East
Albania		Other Eastern Europe	Soviet Union
Algeria		Algeria	N. Africa/ Middle East
Andorra		Rest of World	Rest of World
Angola		Other Africa	Africa
Argentina	Buenos Aires	Argentina	Latin America
Argentina	Catamarca	Argentina	Latin America
Argentina	Chaco	Argentina	Latin America
Argentina	Chubut	Argentina	Latin America
Argentina	Ciudad de Buenos Aires	Argentina	Latin America
Argentina	Corrientes	Argentina	Latin America
Argentina	Formosa	Argentina	Latin America
Argentina	Jujuy	Argentina	Latin America
Argentina	La Pampa	Argentina	Latin America
Argentina	La Rioja	Argentina	Latin America
Argentina	Mendoza	Argentina	Latin America
Argentina	Misiones	Argentina	Latin America
Argentina	Salta	Argentina	Latin America
Argentina	San Juan	Argentina	Latin America
Argentina	San Luis	Argentina	Latin America
Argentina	Santa Cruz	Argentina	Latin America
Argentina	Santa Fe	Argentina	Latin America
Argentina	Santiago del Estero	Argentina	Latin America
Argentina	Tierra del Fuego	Argentina	Latin America
Argentina	Cordoba	Argentina	Latin America
Argentina	Entre Rios	Argentina	Latin America
Argentina	Neuquen	Argentina	Latin America
Argentina	Rio Negro	Argentina	Latin America
Argentina	Tucuman	Argentina	Latin America
Armenia		Other CIS	Soviet Union
Australia	Australian Capital Territory	Australia	Developed Pacific
Australia	New South Wales	Australia	Developed Pacific
Australia	Northern Territory	Australia	Developed Pacific
Australia	Queensland	Australia	Developed Pacific
Australia	South Australia	Australia	Developed Pacific
Australia	Tasmania	Australia	Developed Pacific
Australia	Victoria	Australia	Developed Pacific
Australia	Western Australia	Australia	Developed Pacific
Azerbaijan		Other CIS	Soviet Union
Bangladesh		Bangladesh	Southeast Asia
Belarus		Other CIS	Soviet Union
Belize		Rest of World	Rest of World
Benin		Western Africa	Africa
Bhutan		Other Asia	Southeast Asia
Bolivia		Other Latin America	Latin America
Bosnia and Herzegovina		Other Eastern Europe	Soviet Union
Botswana		Other Africa	Africa
Brazil: Amazon Biome	Acre	Brazil: Amazon Biome	Latin America
Brazil: Northeast Coast	Alagoas	Brazil: Northeast Coast	Latin America
Brazil: Amazon Biome	Amapa	Brazil: Amazon Biome	Latin America
Brazil: Amazon Biome	Amazonas	Brazil: Amazon Biome	Latin America
Brazil: North-Northeast Cerrados	Bahia	Brazil: North-Northeast Cerrados	Latin America
Brazil: Northeast Coast	Ceara	Brazil: Northeast Coast	Latin America
Brazil: Central-West Cerrados	Distrito Federal	Brazil: Central-West Cerrados	Latin America
Brazil: Southeast	Espirito Santo	Brazil: Southeast	Latin America
Brazil: Central-West Cerrados	Goiias	Brazil: Central-West Cerrados	Latin America
Brazil: North-Northeast Cerrados	Maranhao	Brazil: North-Northeast Cerrados	Latin America
Brazil: Amazon Biome	Mato Grosso A	Brazil: Amazon Biome	Latin America
Brazil: Central-West Cerrados	Mato Grosso CW	Brazil: Central-West Cerrados	Latin America
Brazil: Central-West Cerrados	Mato Grosso do Sul	Brazil: Central-West Cerrados	Latin America
Brazil: Southeast	Minas Gerais	Brazil: Southeast	Latin America

Winrock Country	Winrock- Admin Unit	Corresponding FAPRI Region	Corresponding Woods Hole Region
Brazil: Amazon Biome	Para	Brazil: Amazon Biome	Latin America
Brazil: Northeast Coast	Paraiba	Brazil: Northeast Coast	Latin America
Brazil: Southeast	Parana SE	#N/A	Latin America
Brazil: South	Parana S	Brazil: South	Latin America
Brazil: Northeast Coast	Pernambuco	Brazil: Northeast Coast	Latin America
Brazil: North-Northeast Cerrados	Piaui	Brazil: North-Northeast Cerrados	Latin America
Brazil: Southeast	Rio de Janeiro	Brazil: Southeast	Latin America
Brazil: Northeast Coast	Rio Grande do Norte	Brazil: Northeast Coast	Latin America
Brazil: South	Rio Grande do Sul	Brazil: South	Latin America
Brazil: Amazon Biome	Rondonia	Brazil: Amazon Biome	Latin America
Brazil: Amazon Biome	Roraima	Brazil: Amazon Biome	Latin America
Brazil: South	Santa Catarina	Brazil: South	Latin America
Brazil: Southeast	Sao Paulo	Brazil: Southeast	Latin America
Brazil: Northeast Coast	Sergipe	Brazil: Northeast Coast	Latin America
Brazil: North-Northeast Cerrados	Tocantins	Brazil: North-Northeast Cerrados	Latin America
Brunei Darussalam		Rest of World	Rest of World
Burkina Faso		Other Africa	Africa
Burundi		Other Africa	Africa
Cambodia		Rest of World	Rest of World
Cameroon		Other Africa	Africa
Canada	Alberta	Canada	Canada
Canada	British Columbia	Canada	Canada
Canada	Manitoba	Canada	Canada
Canada	New Brunswick	Canada	Canada
Canada	Newfoundland and Labrador	Canada	Canada
Canada	Northwest Territories	Canada	Canada
Canada	Nova Scotia	Canada	Canada
Canada	Nunavut	Canada	Canada
Canada	Ontario	Canada	Canada
Canada	Prince Edward Island	Canada	Canada
Canada	Saskatchewan	Canada	Canada
Canada	Yukon	Canada	Canada
Canada	Quebec	Canada	Canada
Central African Republic		Other Africa	Africa
Chad		Other Africa	Africa
Chile		Other Latin America	Latin America
China	Anhui	China	China/ India/ Pakistan
China	Beijing	China	China/ India/ Pakistan
China	Chongqing	China	China/ India/ Pakistan
China	Fujian	China	China/ India/ Pakistan
China	Gansu	China	China/ India/ Pakistan
China	Guangdong	China	China/ India/ Pakistan
China	Guangxi	China	China/ India/ Pakistan
China	Guizhou	China	China/ India/ Pakistan
China	Hainan	China	China/ India/ Pakistan
China	Hebei	China	China/ India/ Pakistan
China	Heilongjiang	China	China/ India/ Pakistan
China	Henan	China	China/ India/ Pakistan
China	Hubei	China	China/ India/ Pakistan
China	Hunan	China	China/ India/ Pakistan
China	Jiangsu	China	China/ India/ Pakistan
China	Jiangxi	China	China/ India/ Pakistan
China	Jilin	China	China/ India/ Pakistan
China	Liaoning	China	China/ India/ Pakistan
China	Nei Mongol	China	China/ India/ Pakistan
China	Ningxia Hui	China	China/ India/ Pakistan
China	Qinghai	China	China/ India/ Pakistan
China	Shaanxi	China	China/ India/ Pakistan
China	Shandong	China	China/ India/ Pakistan
China	Shanghai	China	China/ India/ Pakistan
China	Shanxi	China	China/ India/ Pakistan
China	Sichuan	China	China/ India/ Pakistan
China	Tianjin	China	China/ India/ Pakistan
China	Xinjiang Uygur	China	China/ India/ Pakistan
China	Xizang	China	China/ India/ Pakistan
China	Yunnan	China	China/ India/ Pakistan
China	Zhejiang	China	China/ India/ Pakistan
Colombia		Colombia	Latin America
Costa Rica		Other Latin America	Latin America
Cote d'Ivoire		Ivory Coast	Africa

Winrock Country	Winrock- Admin Unit	Corresponding FAPRI Region	Corresponding Woods Hole Region
Croatia		Other Eastern Europe	Soviet Union
Cuba		Cuba	Latin America
Democratic Republic of the Congo		Other Africa	Africa
Dominican Republic		Other Latin America	Latin America
Ecuador		Other Latin America	Latin America
Egypt		Egypt	N. Africa/ Middle East
El Salvador		Other Latin America	Latin America
Equatorial Guinea		Rest of World	Rest of World
Eritrea		Rest of World	Rest of World
Ethiopia		Other Africa	Africa
EU	Austria	EU	Europe
EU	Belgie	EU	Europe
EU	Bulgaria	EU	Europe
EU	Cyprus	EU	Europe
EU	Czech Republic	EU	Europe
EU	Denmark	EU	Europe
EU	Germany	EU	Europe
EU	Spain	EU	Europe
EU	Estonia	EU	Europe
EU	Finland	EU	Europe
EU	France	EU	Europe
EU	Greece	EU	Europe
EU	Hungary	EU	Europe
EU	Ireland	EU	Europe
EU	Italy	EU	Europe
EU	Latvia	EU	Europe
EU	Lithuania	EU	Europe
EU	Luxembourg	EU	Europe
EU	Netherlands	EU	Europe
EU	Poland	EU	Europe
EU	Portugal	EU	Europe
EU	Slovenia	EU	Europe
EU	Romania	EU	Europe
EU	Slovakia	EU	Europe
EU	Sweden	EU	Europe
EU	United Kingdom	EU	Europe
Gabon		Other Africa	Africa
Gambia		Rest of World	Rest of World
Ghana		Other Africa	Africa
Guatemala		Guatemala	Latin America
Guinea		Other Africa	Africa
Guinea-Bissau		Rest of World	Rest of World
Guyana		Other Latin America	Latin America
Guyane		Rest of World	Rest of World
Haiti		Other Latin America	Latin America
Honduras		Other Latin America	Latin America
Iceland		EU	Europe
India	Andaman and Nicobar	India	China/ India/ Pakistan
India	Andhra Pradesh	India	China/ India/ Pakistan
India	Arunachal Pradesh	India	China/ India/ Pakistan
India	Assam	India	China/ India/ Pakistan
India	Bihar	India	China/ India/ Pakistan
India	Chandigarh	India	China/ India/ Pakistan
India	Chhattisgarh	India	China/ India/ Pakistan
India	Dadra and Nagar Haveli	India	China/ India/ Pakistan
India	Daman and Diu	India	China/ India/ Pakistan
India	Delhi	India	China/ India/ Pakistan
India	Goa	India	China/ India/ Pakistan
India	Gujarat	India	China/ India/ Pakistan
India	Haryana	India	China/ India/ Pakistan
India	Himachal Pradesh	India	China/ India/ Pakistan
India	Jammu and Kashmir	India	China/ India/ Pakistan
India	Jharkhand	India	China/ India/ Pakistan
India	Karnataka	India	China/ India/ Pakistan
India	Kerala	India	China/ India/ Pakistan
India	Lakshadweep	India	China/ India/ Pakistan
India	Madhya Pradesh	India	China/ India/ Pakistan
India	Maharashtra	India	China/ India/ Pakistan
India	Manipur	India	China/ India/ Pakistan
India	Meghalaya	India	China/ India/ Pakistan

Winrock Country	Winrock- Admin Unit	Corresponding FAPRI Region	Corresponding Woods Hole Region
India	Mizoram	India	China/ India/ Pakistan
India	Nagaland	India	China/ India/ Pakistan
India	Orissa	India	China/ India/ Pakistan
India	Puducherry	India	China/ India/ Pakistan
India	Punjab	India	China/ India/ Pakistan
India	Rajasthan	India	China/ India/ Pakistan
India	Sikkim	India	China/ India/ Pakistan
India	Tamil Nadu	India	China/ India/ Pakistan
India	Tripura	India	China/ India/ Pakistan
India	Uttar Pradesh	India	China/ India/ Pakistan
India	Uttaranchal	India	China/ India/ Pakistan
India	West Bengal	India	China/ India/ Pakistan
Indonesia	Aceh	Indonesia	Southeast Asia
Indonesia	Bali	Indonesia	Southeast Asia
Indonesia	Bangka-Belitung	Indonesia	Southeast Asia
Indonesia	Banten	Indonesia	Southeast Asia
Indonesia	Bengkulu	Indonesia	Southeast Asia
Indonesia	Gorontalo	Indonesia	Southeast Asia
Indonesia	Irian Jaya Barat	Indonesia	Southeast Asia
Indonesia	Jakarta Raya	Indonesia	Southeast Asia
Indonesia	Jambi	Indonesia	Southeast Asia
Indonesia	Jawa Barat	Indonesia	Southeast Asia
Indonesia	Jawa Tengah	Indonesia	Southeast Asia
Indonesia	Jawa Timur	Indonesia	Southeast Asia
Indonesia	Kalimantan Barat	Indonesia	Southeast Asia
Indonesia	Kalimantan Selatan	Indonesia	Southeast Asia
Indonesia	Kalimantan Tengah	Indonesia	Southeast Asia
Indonesia	Kalimantan Timur	Indonesia	Southeast Asia
Indonesia	Kepulauan Riau	Indonesia	Southeast Asia
Indonesia	Lampung	Indonesia	Southeast Asia
Indonesia	Maluku	Indonesia	Southeast Asia
Indonesia	Nusa Tenggara Barat	Indonesia	Southeast Asia
Indonesia	Nusa Tenggara Timur	Indonesia	Southeast Asia
Indonesia	Papua	Indonesia	Southeast Asia
Indonesia	Riau	Indonesia	Southeast Asia
Indonesia	Sulawesi Barat	Indonesia	Southeast Asia
Indonesia	Sulawesi Selatan	Indonesia	Southeast Asia
Indonesia	Sulawesi Tengah	Indonesia	Southeast Asia
Indonesia	Sulawesi Tenggara	Indonesia	Southeast Asia
Indonesia	Sulawesi Utara	Indonesia	Southeast Asia
Indonesia	Sumatera Barat	Indonesia	Southeast Asia
Indonesia	Sumatera Selatan	Indonesia	Southeast Asia
Indonesia	Sumatera Utara	Indonesia	Southeast Asia
Indonesia	Yogyakarta	Indonesia	Southeast Asia
Iran	Ardebil	Iran	N. Africa/ Middle East
Iran	Bushehr	Iran	N. Africa/ Middle East
Iran	Chahar Mahall and Bakhtiari	Iran	N. Africa/ Middle East
Iran	East Azarbaijan	Iran	N. Africa/ Middle East
Iran	Esfahan	Iran	N. Africa/ Middle East
Iran	Fars	Iran	N. Africa/ Middle East
Iran	Gilan	Iran	N. Africa/ Middle East
Iran	Golestan	Iran	N. Africa/ Middle East
Iran	Hamadan	Iran	N. Africa/ Middle East
Iran	Hormozgan	Iran	N. Africa/ Middle East
Iran	Ilam	Iran	N. Africa/ Middle East
Iran	Kerman	Iran	N. Africa/ Middle East
Iran	Kermanshah	Iran	N. Africa/ Middle East
Iran	Khuzestan	Iran	N. Africa/ Middle East
Iran	Kohgiluyeh and Buyer Ahmad	Iran	N. Africa/ Middle East
Iran	Kordestan	Iran	N. Africa/ Middle East
Iran	Lorestan	Iran	N. Africa/ Middle East
Iran	Markazi	Iran	N. Africa/ Middle East
Iran	Mazandaran	Iran	N. Africa/ Middle East
Iran	North Khorasan	Iran	N. Africa/ Middle East
Iran	Qazvin	Iran	N. Africa/ Middle East
Iran	Qom	Iran	N. Africa/ Middle East
Iran	Razavi Khorasan	Iran	N. Africa/ Middle East
Iran	Semnan	Iran	N. Africa/ Middle East
Iran	Sistan and Baluchestan	Iran	N. Africa/ Middle East
Iran	South Khorasan	Iran	N. Africa/ Middle East

Winrock Country	Winrock- Admin Unit	Corresponding FAPRI Region	Corresponding Woods Hole Region
Iran	Tehran	Iran	N. Africa/ Middle East
Iran	West Azarbajian	Iran	N. Africa/ Middle East
Iran	Yazd	Iran	N. Africa/ Middle East
Iran	Zanjan	Iran	N. Africa/ Middle East
Iraq		Iraq	N. Africa/ Middle East
Israel		Other Middle East	N. Africa/ Middle East
Japan		Japan	Southeast Asia
Kazakhstan		Other CIS	Soviet Union
Kenya		Other Africa	Africa
Kosova		Rest of World	Rest of World
Kyrgyzstan		Other CIS	Soviet Union
Laos		Rest of World	Rest of World
Lebanon		Other Middle East	N. Africa/ Middle East
Lesotho		Other Africa	Africa
Liberia		Other Africa	Africa
Libya		Other Africa	Africa
Liechtenstein		EU	Europe
Macedonia		Other Eastern Europe	Soviet Union
Madagascar		Other Africa	Africa
Malawi		Rest of World	Rest of World
Malaysia	Johor	Malaysia	Southeast Asia
Malaysia	Kedah	Malaysia	Southeast Asia
Malaysia	Kelantan	Malaysia	Southeast Asia
Malaysia	Melaka	Malaysia	Southeast Asia
Malaysia	Negeri Sembilan	Malaysia	Southeast Asia
Malaysia	Pahang	Malaysia	Southeast Asia
Malaysia	Perak	Malaysia	Southeast Asia
Malaysia	Perlis	Malaysia	Southeast Asia
Malaysia	Pulau Pinang	Malaysia	Southeast Asia
Malaysia	Sabah	Malaysia	Southeast Asia
Malaysia	Sarawak	Malaysia	Southeast Asia
Malaysia	Selangor	Malaysia	Southeast Asia
Malaysia	Trengganu	Malaysia	Southeast Asia
Mali		Other Africa	Africa
Mauritania		Other Africa	Africa
Mexico	Aguascalientes	Mexico	Latin America
Mexico	Baja California	Mexico	Latin America
Mexico	Baja California Sur	Mexico	Latin America
Mexico	Campeche	Mexico	Latin America
Mexico	Chiapas	Mexico	Latin America
Mexico	Chihuahua	Mexico	Latin America
Mexico	Coahuila	Mexico	Latin America
Mexico	Colima	Mexico	Latin America
Mexico	Distrito Federal	Mexico	Latin America
Mexico	Durango	Mexico	Latin America
Mexico	Guanajuato	Mexico	Latin America
Mexico	Guerrero	Mexico	Latin America
Mexico	Hidalgo	Mexico	Latin America
Mexico	Jalisco	Mexico	Latin America
Mexico	Morelos	Mexico	Latin America
Mexico	Nayarit	Mexico	Latin America
Mexico	Oaxaca	Mexico	Latin America
Mexico	Puebla	Mexico	Latin America
Mexico	Quintana Roo	Mexico	Latin America
Mexico	Sinaloa	Mexico	Latin America
Mexico	Sonora	Mexico	Latin America
Mexico	Tabasco	Mexico	Latin America
Mexico	Tamaulipas	Mexico	Latin America
Mexico	Tlaxcala	Mexico	Latin America
Mexico	Veracruz	Mexico	Latin America
Mexico	Zacatecas	Mexico	Latin America
Mexico	Michoacan	Mexico	Latin America
Mexico	Mexico	Mexico	Latin America
Mexico	Nuevo Leon	Mexico	Latin America
Mexico	Queretaro	Mexico	Latin America
Mexico	San Luis Potosi	Mexico	Latin America
Mexico	Yucatan	Mexico	Latin America
Moldova		Other CIS	Soviet Union
Mongolia		Other Asia	Southeast Asia
Montenegro		Rest of World	Rest of World

Winrock Country	Winrock- Admin Unit	Corresponding FAPRI Region	Corresponding Woods Hole Region
Morocco		Morocco	N. Africa/ Middle East
Mozambique		Other Africa	Africa
Myanmar		Myanmar	Southeast Asia
Namibia		Rest of World	Rest of World
Nepal		Other Asia	Southeast Asia
New Zealand		New Zealand	Developed Pacific
Nicaragua		Other Latin America	Latin America
Niger		Other Africa	Africa
Nigeria	Abia	Nigeria	N. Africa/ Middle East
Nigeria	Adamawa	Nigeria	N. Africa/ Middle East
Nigeria	Akwa Ibom	Nigeria	N. Africa/ Middle East
Nigeria	Anambra	Nigeria	N. Africa/ Middle East
Nigeria	Bauchi	Nigeria	N. Africa/ Middle East
Nigeria	Bayelsa	Nigeria	N. Africa/ Middle East
Nigeria	Benue	Nigeria	N. Africa/ Middle East
Nigeria	Borno	Nigeria	N. Africa/ Middle East
Nigeria	Cross River	Nigeria	N. Africa/ Middle East
Nigeria	Delta	Nigeria	N. Africa/ Middle East
Nigeria	Ebonyi	Nigeria	N. Africa/ Middle East
Nigeria	Edo	Nigeria	N. Africa/ Middle East
Nigeria	Ekiti	Nigeria	N. Africa/ Middle East
Nigeria	Enugu	Nigeria	N. Africa/ Middle East
Nigeria	Federal Capital Territory	Nigeria	N. Africa/ Middle East
Nigeria	Gombe	Nigeria	N. Africa/ Middle East
Nigeria	Imo	Nigeria	N. Africa/ Middle East
Nigeria	Jigawa	Nigeria	N. Africa/ Middle East
Nigeria	Kaduna	Nigeria	N. Africa/ Middle East
Nigeria	Kano	Nigeria	N. Africa/ Middle East
Nigeria	Katsina	Nigeria	N. Africa/ Middle East
Nigeria	Kebbi	Nigeria	N. Africa/ Middle East
Nigeria	Kogi	Nigeria	N. Africa/ Middle East
Nigeria	Kwara	Nigeria	N. Africa/ Middle East
Nigeria	Lagos	Nigeria	N. Africa/ Middle East
Nigeria	Nassarawa	Nigeria	N. Africa/ Middle East
Nigeria	Niger	Nigeria	N. Africa/ Middle East
Nigeria	Ogun	Nigeria	N. Africa/ Middle East
Nigeria	Ondo	Nigeria	N. Africa/ Middle East
Nigeria	Osun	Nigeria	N. Africa/ Middle East
Nigeria	Oyo	Nigeria	N. Africa/ Middle East
Nigeria	Plateau	Nigeria	N. Africa/ Middle East
Nigeria	Rivers	Nigeria	N. Africa/ Middle East
Nigeria	Sokoto	Nigeria	N. Africa/ Middle East
Nigeria	Taraba	Nigeria	N. Africa/ Middle East
Nigeria	Yobe	Nigeria	N. Africa/ Middle East
Nigeria	Zamfara	Nigeria	N. Africa/ Middle East
North Korea		Other Asia	Southeast Asia
Norway		EU	Europe
Oman		Rest of World	Rest of World
Pakistan		Pakistan	China/ India/ Pakistan
Panama		Other Latin America	Latin America
Papua New Guinea		Rest of World	Rest of World
Paraguay	Neembucu	Paraguay	Latin America
Paraguay	Alto Paraguay	Paraguay	Latin America
Paraguay	Amambay	Paraguay	Latin America
Paraguay	Caaguaz-	Paraguay	Latin America
Paraguay	Canindey-	Paraguay	Latin America
Paraguay	Central	Paraguay	Latin America
Paraguay	Cordillera	Paraguay	Latin America
Paraguay	Itap-a	Paraguay	Latin America
Paraguay	Misiones	Paraguay	Latin America
Paraguay	Presidente Hayes	Paraguay	Latin America
Paraguay	San Pedro	Paraguay	Latin America
Paraguay	Alto Parana	Paraguay	Latin America
Paraguay	Asuncion	Paraguay	Latin America
Paraguay	Boqueron	Paraguay	Latin America
Paraguay	Caazapa	Paraguay	Latin America
Paraguay	Concepcion	Paraguay	Latin America
Paraguay	Guaira	Paraguay	Latin America
Paraguay	Paraguari	Paraguay	Latin America
Peru		Peru	Latin America

Winrock Country	Winrock- Admin Unit	Corresponding FAPRI Region	Corresponding Woods Hole Region
Philippines	Abra	Philippines	Southeast Asia
Philippines	Agusan del Norte	Philippines	Southeast Asia
Philippines	Agusan del Sur	Philippines	Southeast Asia
Philippines	Aklan	Philippines	Southeast Asia
Philippines	Albay	Philippines	Southeast Asia
Philippines	Antique	Philippines	Southeast Asia
Philippines	Apayao	Philippines	Southeast Asia
Philippines	Aurora	Philippines	Southeast Asia
Philippines	Basilan	Philippines	Southeast Asia
Philippines	Bataan	Philippines	Southeast Asia
Philippines	Batanes	Philippines	Southeast Asia
Philippines	Batangas	Philippines	Southeast Asia
Philippines	Benguet	Philippines	Southeast Asia
Philippines	Biliran	Philippines	Southeast Asia
Philippines	Bohol	Philippines	Southeast Asia
Philippines	Bukidnon	Philippines	Southeast Asia
Philippines	Bulacan	Philippines	Southeast Asia
Philippines	Cagayan	Philippines	Southeast Asia
Philippines	Camarines Norte	Philippines	Southeast Asia
Philippines	Camarines Sur	Philippines	Southeast Asia
Philippines	Camiguin	Philippines	Southeast Asia
Philippines	Capiz	Philippines	Southeast Asia
Philippines	Catanduanes	Philippines	Southeast Asia
Philippines	Cavite	Philippines	Southeast Asia
Philippines	Cebu	Philippines	Southeast Asia
Philippines	Compostela Valley	Philippines	Southeast Asia
Philippines	Davao del Norte	Philippines	Southeast Asia
Philippines	Davao del Sur	Philippines	Southeast Asia
Philippines	Davao Oriental	Philippines	Southeast Asia
Philippines	Dinagat Islands	Philippines	Southeast Asia
Philippines	Eastern Samar	Philippines	Southeast Asia
Philippines	Guimaras	Philippines	Southeast Asia
Philippines	Ifugao	Philippines	Southeast Asia
Philippines	Ilocos Norte	Philippines	Southeast Asia
Philippines	Ilocos Sur	Philippines	Southeast Asia
Philippines	Iloilo	Philippines	Southeast Asia
Philippines	Isabela	Philippines	Southeast Asia
Philippines	Kalinga	Philippines	Southeast Asia
Philippines	La Union	Philippines	Southeast Asia
Philippines	Laguna	Philippines	Southeast Asia
Philippines	Lanao del Norte	Philippines	Southeast Asia
Philippines	Lanao del Sur	Philippines	Southeast Asia
Philippines	Leyte	Philippines	Southeast Asia
Philippines	Maguindanao	Philippines	Southeast Asia
Philippines	Marinduque	Philippines	Southeast Asia
Philippines	Masbate	Philippines	Southeast Asia
Philippines	Metropolitan Manila	Philippines	Southeast Asia
Philippines	Misamis Occidental	Philippines	Southeast Asia
Philippines	Misamis Oriental	Philippines	Southeast Asia
Philippines	Mountain Province	Philippines	Southeast Asia
Philippines	Negros Occidental	Philippines	Southeast Asia
Philippines	Negros Oriental	Philippines	Southeast Asia
Philippines	North Cotabato	Philippines	Southeast Asia
Philippines	Northern Samar	Philippines	Southeast Asia
Philippines	Nueva Ecija	Philippines	Southeast Asia
Philippines	Nueva Vizcaya	Philippines	Southeast Asia
Philippines	Occidental Mindoro	Philippines	Southeast Asia
Philippines	Oriental Mindoro	Philippines	Southeast Asia
Philippines	Palawan	Philippines	Southeast Asia
Philippines	Pampanga	Philippines	Southeast Asia
Philippines	Pangasinan	Philippines	Southeast Asia
Philippines	Quezon	Philippines	Southeast Asia
Philippines	Quirino	Philippines	Southeast Asia
Philippines	Rizal	Philippines	Southeast Asia
Philippines	Romblon	Philippines	Southeast Asia
Philippines	Samar	Philippines	Southeast Asia
Philippines	Sarangani	Philippines	Southeast Asia
Philippines	Shariff Kabunsuan	Philippines	Southeast Asia
Philippines	Siquijor	Philippines	Southeast Asia
Philippines	Sorsogon	Philippines	Southeast Asia

Winrock Country	Winrock- Admin Unit	Corresponding FAPRI Region	Corresponding Woods Hole Region
Philippines	South Cotabato	Philippines	Southeast Asia
Philippines	Southern Leyte	Philippines	Southeast Asia
Philippines	Sultan Kudarat	Philippines	Southeast Asia
Philippines	Sulu	Philippines	Southeast Asia
Philippines	Surigao del Norte	Philippines	Southeast Asia
Philippines	Surigao del Sur	Philippines	Southeast Asia
Philippines	Tarlac	Philippines	Southeast Asia
Philippines	Tawi-Tawi	Philippines	Southeast Asia
Philippines	Zambales	Philippines	Southeast Asia
Philippines	Zamboanga del Norte	Philippines	Southeast Asia
Philippines	Zamboanga del Sur	Philippines	Southeast Asia
Philippines	Zamboanga Sibugay	Philippines	Southeast Asia
Republic of Congo		Other Africa	Africa
Russia	Adygey	Russia	Soviet Union
Russia	Aga Buryat	Russia	Soviet Union
Russia	Altay	Russia	Soviet Union
Russia	Amur	Russia	Soviet Union
Russia	Arkhangel'sk	Russia	Soviet Union
Russia	Astrakhan'	Russia	Soviet Union
Russia	Bashkortostan	Russia	Soviet Union
Russia	Belgorod	Russia	Soviet Union
Russia	Bryansk	Russia	Soviet Union
Russia	Buryat	Russia	Soviet Union
Russia	Chechnya	Russia	Soviet Union
Russia	Chelyabinsk	Russia	Soviet Union
Russia	Chita	Russia	Soviet Union
Russia	Chukot	Russia	Soviet Union
Russia	Chuvash	Russia	Soviet Union
Russia	City of St. Petersburg	Russia	Soviet Union
Russia	Dagestan	Russia	Soviet Union
Russia	Evenk	Russia	Soviet Union
Russia	Gorno-Altay	Russia	Soviet Union
Russia	Ingush	Russia	Soviet Union
Russia	Irkutsk	Russia	Soviet Union
Russia	Ivanovo	Russia	Soviet Union
Russia	Kabardin-Balkar	Russia	Soviet Union
Russia	Kaliningrad	Russia	Soviet Union
Russia	Kalmyk	Russia	Soviet Union
Russia	Kaluga	Russia	Soviet Union
Russia	Kamchatka	Russia	Soviet Union
Russia	Karachay-Cherkess	Russia	Soviet Union
Russia	Karelia	Russia	Soviet Union
Russia	Kemerovo	Russia	Soviet Union
Russia	Khabarovsk	Russia	Soviet Union
Russia	Khakass	Russia	Soviet Union
Russia	Khanty-Mansiy	Russia	Soviet Union
Russia	Kirov	Russia	Soviet Union
Russia	Komi	Russia	Soviet Union
Russia	Komi-Permyak	Russia	Soviet Union
Russia	Koryak	Russia	Soviet Union
Russia	Kostroma	Russia	Soviet Union
Russia	Krasnodar	Russia	Soviet Union
Russia	Krasnoyarsk	Russia	Soviet Union
Russia	Kurgan	Russia	Soviet Union
Russia	Kursk	Russia	Soviet Union
Russia	Leningrad	Russia	Soviet Union
Russia	Lipetsk	Russia	Soviet Union
Russia	Maga Buryatdan	Russia	Soviet Union
Russia	Mariy-El	Russia	Soviet Union
Russia	Mordovia	Russia	Soviet Union
Russia	Moskva	Russia	Soviet Union
Russia	Murmansk	Russia	Soviet Union
Russia	Nenets	Russia	Soviet Union
Russia	Nizhegorod	Russia	Soviet Union
Russia	North Ossetia	Russia	Soviet Union
Russia	Novgorod	Russia	Soviet Union
Russia	Novosibirsk	Russia	Soviet Union
Russia	Omsk	Russia	Soviet Union
Russia	Orel	Russia	Soviet Union
Russia	Orenburg	Russia	Soviet Union

Winrock Country	Winrock- Admin Unit	Corresponding FAPRI Region	Corresponding Woods Hole Region
Russia	Penza	Russia	Soviet Union
Russia	Perm'	Russia	Soviet Union
Russia	Primor'ye	Russia	Soviet Union
Russia	Pskov	Russia	Soviet Union
Russia	Rostov	Russia	Soviet Union
Russia	Ryazan'	Russia	Soviet Union
Russia	Sakha	Russia	Soviet Union
Russia	Sakhalin	Russia	Soviet Union
Russia	Samara	Russia	Soviet Union
Russia	Saratov	Russia	Soviet Union
Russia	Smolensk	Russia	Soviet Union
Russia	Stavropol'	Russia	Soviet Union
Russia	Sverdlovsk	Russia	Soviet Union
Russia	Tambov	Russia	Soviet Union
Russia	Tatarstan	Russia	Soviet Union
Russia	Taymyr	Russia	Soviet Union
Russia	Tomsk	Russia	Soviet Union
Russia	Tula	Russia	Soviet Union
Russia	Tuva	Russia	Soviet Union
Russia	Tver'	Russia	Soviet Union
Russia	Tyumen'	Russia	Soviet Union
Russia	Udmurt	Russia	Soviet Union
Russia	Ul'yanovsk	Russia	Soviet Union
Russia	Ust-Orda Buryat	Russia	Soviet Union
Russia	Vladimir	Russia	Soviet Union
Russia	Volgograd	Russia	Soviet Union
Russia	Vologda	Russia	Soviet Union
Russia	Voronezh	Russia	Soviet Union
Russia	Yamal-Nenets	Russia	Soviet Union
Russia	Yaroslavl'	Russia	Soviet Union
Russia	Yevrey	Russia	Soviet Union
Rwanda		Rest of World	Rest of World
Saudi Arabia		Other Middle East	N. Africa/ Middle East
Senegal		Other Africa	Africa
Serbia		Rest of World	Rest of World
Sierra Leone		Other Africa	Africa
Singapore		Other Asia	Southeast Asia
Somalia		Other Africa	Africa
South Africa	Eastern Cape	South Africa	Africa
South Africa	Gauteng	South Africa	Africa
South Africa	KwaZulu-Natal	South Africa	Africa
South Africa	Limpopo	South Africa	Africa
South Africa	Mpumalanga	South Africa	Africa
South Africa	North West	South Africa	Africa
South Africa	Northern Cape	South Africa	Africa
South Africa	Orange Free State	South Africa	Africa
South Africa	Western Cape	South Africa	Africa
South Korea		South Korea	Southeast Asia
Sri Lanka		Other Asia	Southeast Asia
Sudan		Other Africa	Africa
Suriname		Rest of World	Rest of World
Swaziland		Rest of World	Rest of World
Switzerland		EU	Europe
Syria		Other Middle East	N. Africa/ Middle East
Taiwan		Taiwan	Southeast Asia
Tajikistan		Other CIS	Soviet Union
Tanzania		Other Africa	Africa
Thailand	Amnat Charoen	Thailand	Southeast Asia
Thailand	Ang Thong	Thailand	Southeast Asia
Thailand	Bangkok Metropolis	Thailand	Southeast Asia
Thailand	Buri Ram	Thailand	Southeast Asia
Thailand	Chachoengsao	Thailand	Southeast Asia
Thailand	Chai Nat	Thailand	Southeast Asia
Thailand	Chaiyaphum	Thailand	Southeast Asia
Thailand	Chanthaburi	Thailand	Southeast Asia
Thailand	Chiang Mai	Thailand	Southeast Asia
Thailand	Chiang Rai	Thailand	Southeast Asia
Thailand	Chon Buri	Thailand	Southeast Asia
Thailand	Chumphon	Thailand	Southeast Asia
Thailand	Kalasin	Thailand	Southeast Asia

Winrock Country	Winrock- Admin Unit	Corresponding FAPRI Region	Corresponding Woods Hole Region
Thailand	Kamphaeng Phet	Thailand	Southeast Asia
Thailand	Kanchanaburi	Thailand	Southeast Asia
Thailand	Khon Kaen	Thailand	Southeast Asia
Thailand	Krabi	Thailand	Southeast Asia
Thailand	Lampang	Thailand	Southeast Asia
Thailand	Lamphun	Thailand	Southeast Asia
Thailand	Loei	Thailand	Southeast Asia
Thailand	Lop Buri	Thailand	Southeast Asia
Thailand	Mae Hong Son	Thailand	Southeast Asia
Thailand	Maha Sarakham	Thailand	Southeast Asia
Thailand	Mukdahan	Thailand	Southeast Asia
Thailand	Nakhon Nayok	Thailand	Southeast Asia
Thailand	Nakhon Pathom	Thailand	Southeast Asia
Thailand	Nakhon Phanom	Thailand	Southeast Asia
Thailand	Nakhon Ratchasima	Thailand	Southeast Asia
Thailand	Nakhon Sawan	Thailand	Southeast Asia
Thailand	Nakhon Si Thammarat	Thailand	Southeast Asia
Thailand	Nan	Thailand	Southeast Asia
Thailand	Narathiwat	Thailand	Southeast Asia
Thailand	Nong Bua Lam Phu	Thailand	Southeast Asia
Thailand	Nong Khai	Thailand	Southeast Asia
Thailand	Nonthaburi	Thailand	Southeast Asia
Thailand	Pathum Thani	Thailand	Southeast Asia
Thailand	Pattani	Thailand	Southeast Asia
Thailand	Phangnga	Thailand	Southeast Asia
Thailand	Phatthalung	Thailand	Southeast Asia
Thailand	Phayao	Thailand	Southeast Asia
Thailand	Phetchabun	Thailand	Southeast Asia
Thailand	Phetchaburi	Thailand	Southeast Asia
Thailand	Phichit	Thailand	Southeast Asia
Thailand	Phitsanulok	Thailand	Southeast Asia
Thailand	Phra Nakhon Si Ayutthaya	Thailand	Southeast Asia
Thailand	Phrae	Thailand	Southeast Asia
Thailand	Phuket	Thailand	Southeast Asia
Thailand	Prachin Buri	Thailand	Southeast Asia
Thailand	Prachuap Khiri Khan	Thailand	Southeast Asia
Thailand	Ranong	Thailand	Southeast Asia
Thailand	Ratchaburi	Thailand	Southeast Asia
Thailand	Rayong	Thailand	Southeast Asia
Thailand	Roi Et	Thailand	Southeast Asia
Thailand	Sa Kaeo	Thailand	Southeast Asia
Thailand	Sakon Nakhon	Thailand	Southeast Asia
Thailand	Samut Prakan	Thailand	Southeast Asia
Thailand	Samut Sakhon	Thailand	Southeast Asia
Thailand	Samut Songkhram	Thailand	Southeast Asia
Thailand	Saraburi	Thailand	Southeast Asia
Thailand	Satun	Thailand	Southeast Asia
Thailand	Si Sa Ket	Thailand	Southeast Asia
Thailand	Sing Buri	Thailand	Southeast Asia
Thailand	Songkhla	Thailand	Southeast Asia
Thailand	Sukhothai	Thailand	Southeast Asia
Thailand	Suphan Buri	Thailand	Southeast Asia
Thailand	Surat Thani	Thailand	Southeast Asia
Thailand	Surin	Thailand	Southeast Asia
Thailand	Tak	Thailand	Southeast Asia
Thailand	Trang	Thailand	Southeast Asia
Thailand	Trat	Thailand	Southeast Asia
Thailand	Ubon Ratchathani	Thailand	Southeast Asia
Thailand	Udon Thani	Thailand	Southeast Asia
Thailand	Uthai Thani	Thailand	Southeast Asia
Thailand	Uttaradit	Thailand	Southeast Asia
Thailand	Yala	Thailand	Southeast Asia
Thailand	Yasothon	Thailand	Southeast Asia
Timor-Leste		Rest of World	Rest of World
Togo		Other Africa	Africa
Trinidad and Tobago		Other Latin America	Latin America
Tunisia		Tunisia	Africa
Turkey		Turkey	N. Africa/ Middle East
Turkmenistan		Other CIS	Soviet Union
Uganda		Rest of World	Rest of World

Winrock Country	Winrock- Admin Unit	Corresponding FAPRI Region	Corresponding Woods Hole Region
Ukraine		Ukraine	Soviet Union
United Arab Emirates		Rest of World	Rest of World
United States	Alabama	US	US
United States	Arizona	US	US
United States	Arkansas	US	US
United States	California	US	US
United States	Colorado	US	US
United States	Connecticut	US	US
United States	Delaware	US	US
United States	District of Columbia	US	US
United States	Florida	US	US
United States	Georgia	US	US
United States	Idaho	US	US
United States	Illinois	US	US
United States	Indiana	US	US
United States	Iowa	US	US
United States	Kansas	US	US
United States	Kentucky	US	US
United States	Louisiana	US	US
United States	Maine	US	US
United States	Maryland	US	US
United States	Massachusetts	US	US
United States	Michigan	US	US
United States	Minnesota	US	US
United States	Mississippi	US	US
United States	Missouri	US	US
United States	Montana	US	US
United States	Nebraska	US	US
United States	Nevada	US	US
United States	New Hampshire	US	US
United States	New Jersey	US	US
United States	New Mexico	US	US
United States	New York	US	US
United States	North Carolina	US	US
United States	North Dakota	US	US
United States	Ohio	US	US
United States	Oklahoma	US	US
United States	Oregon	US	US
United States	Pennsylvania	US	US
United States	Rhode Island	US	US
United States	South Carolina	US	US
United States	South Dakota	US	US
United States	Tennessee	US	US
United States	Texas	US	US
United States	Utah	US	US
United States	Vermont	US	US
United States	Virginia	US	US
United States	Washington	US	US
United States	West Virginia	US	US
United States	Wisconsin	US	US
United States	Wyoming	US	US
Uruguay		Uruguay	Latin America
Uzbekistan		Uzbekistan	Soviet Union
Venezuela		Venezuela	Latin America
Vietnam	Central Highlands	Vietnam	Southeast Asia
Vietnam	Mekong River Delta	Vietnam	Southeast Asia
Vietnam	North Central Coast	Vietnam	Southeast Asia
Vietnam	North East	Vietnam	Southeast Asia
Vietnam	North West	Vietnam	Southeast Asia
Vietnam	Red River Delta	Vietnam	Southeast Asia
Vietnam	South Central Coast	Vietnam	Southeast Asia
Vietnam	South East	Vietnam	Southeast Asia
Yemen		Other Middle East	N. Africa/ Middle East
Zambia		Other Africa	Africa
Zimbabwe		Other Africa	Africa